UNIVERSIDAD COMPLUTENSE DE MADRID

FACULTAD DE FARMACIA
Departamento de Química Farmacéutica

TESIS DOCTORAL

Bioisosterism and conformational restriction: ligand-based design in the development of nicotinic ligands and melatonin analogues with neurogenic properties

MEMORIA PARA OPTAR AL GRADO DE DOCTOR

PRESENTADA POR

Mario de la Fuente Revenga

Directora

María Isabel Rodríguez Franco

Madrid, 2014

BIOISOSTERISMO Y RESTRICCIÓN CONFORMACIONAL: DISEÑO BASADO EN EL LIGANDO APLICADO AL ESTUDIO DE LA SELECTIVIDAD EN RECEPTORES NICOTÍNICOS Y AL DESARROLLO DE ANÁLOGOS DE MELATONINA CON PROPIEDADES NEUROGÉNICAS

PhD thesis

Mario de la Fuente Revenga

IQM-CSIC

Madrid, 2014

Universidad Complutense de Madrid

Facultad de Farmacia

Departamento de Química Farmacéutica

Bioisosterism and conformational restriction: Ligand-based design in the development of nicotinic ligands and melatonin analogues with neurogenic properties

PhD student

Mario de la Fuente Revenga

Supervisor

María Isabel Rodríguez Franco, PhD. Research Scientist.

Instituto de Química Médica,

Consejo Superior de Investigaciones Científicas (IQM, CSIC)

C/Juan de la Cierva 3, 28006. Madrid

Spain

Faculty of Health and Medical Sciences,

University of Copenhagen

Scientific stay

(April – October 2011, March – June 2012)

Supervisor

Bente Frølund, PhD. Associate Professor.

Department of Drug Design and Pharmacology

Faculty of Health and Medical Sciences

Medicinal Chemistry Research,

University of Copenhagen

Jagtvej 162, 2100 Copenhagen Ø

Denmark

INDEX

Prologue 1

Chapter 1. Design, synthesis and pharmacological characterization of novel melatonin analogues based on the bioisosteric replacement of its *N*-acetyl moiety for azoles and retroamides 3

Introduction 3

Approach 9

Chemistry 10

Synthesis of retroamides and oxazoles 10

Synthesis of 1,2,4- and 1,3,4-oxadiazoles 12

Synthesis of 4-alkyl-1,2,4-triazol-5-(thio)ones and 2-amino-1,3,4-thiadiazol 14

Synthesis of 1,3,4-oxadiazol-2-(thio)ones 17

NMR studies on the tautomerism of hydrogen-bearing azoles 17

Pharmacology 22

Radioligand binding studies on melatonin receptors MT_1 and MT_2 22

Functional studies on melatonin receptors MT_1 and MT_2 ... 25

Thermodynamic solubility studies ... 27

Discussion ... 29

Conclusions ... 36

Experimental section ... 38

Bibliography ... 58

Chapter 2. Neurogenesis studies on melatonin analogues ... 67

Introduction ... 67

Results ... 69

In vitro neural differentiation and maturation in the presence of different melatonin analogues ... 69

In vivo neural differentiation and maturation after chronic treatment with **1.21** ... 79

Discussion ... 82

Conclusions ... 88

Experimental section ... 90

Bibliography ... 94

Chapter 3. Pinoline pharmacological characterization and development of rigid melatonin-pinoline hybrids with neurogenic potential ... 99

Introduction ... 99

Approach ... 103

Chemistry ... 105

Pharmacology ... 108

Serotonin receptors and transporter 108
Inhibition of monoamine-oxidase A and B 111
Affinity and intrinsic activity at melatonin receptors 112
Blood-brain barrier permeability 113
In vitro antioxidant potential 113
Neurogenesis studies *in vitro* 115
Discussion 121
Conclusions 130
Experimental section 132
Bibliography 140

Chapter 4. Conformationally restrained carbamoylcholine analogues and bioisosteres. Design, synthesis and pharmacology at nicotinic acetylcholine receptors (nAChRs) 149

Introduction 149
Approach 154
Chemistry 156
Synthesis of restricted analogues of DMABC (**4.1**) 156
Synthesis of oxadiazole-containing DMABC (**4.1**) analogues 163
Pharmacology 164
Binding at recombinant nAChRs 164
Functional characterization at recombinant nAChRs 167
Molecular modelling. Docking studies 169
Conclusions 173

Experimental section 174

Bibliography 201

Epilogue 207

Concluding remarks 207

Bibliograpy 217

Abstract 219

Resumen 225

Prologue

This thesis consists of four different chapters. Each chapter is written in a full-paper style. When data from a previous chapter has been used, it appears mentioned in the text. All chapters share and differ in the approaches and the systems to which they are addressed. Two different traditional medicinal chemistry approaches, bioisosterism and conformational restriction, have provided novel ligands for two different systems, melatoninergic and cholinergic system. Preliminar studies on their pharmacological mechanism and potential as novel tools for neurodegenerative diseases have been initiated for some of them. Since each chapter contains its own introduction, specific approach, methodologies, results, discussion and conclusions, in the epilogue of this thesis work general concluding remarks are made in order to provide a general overview of the whole work.

Chapter 1

Design, synthesis and pharmacological characterization of novel melatonin analogues based on the bioisosteric replacement of its *N*-acetyl moiety for azoles and retroamides

Introduction

Melatonin receptors MT_1 and MT_2 lack a crystalized structure that would permit the characterization of the tertiary structure of these G protein-coupled receptors (GPCRs) and of the pattern of interactions undertaken with their ligands. The structural knowledge gained along the years emerges from homology models based on other crystalized transmembrane-receptors structure and site directed-mutagenesis studies. Unlike other GPCRs that lack a crystal structure, melatonergic receptors MT_1 and MT_2 have some additional limitations: lack of a reliable template to build the homologous constructs, and the elusive ligand-receptor interactions[1,2]. Rhodopsin and more recently aminergic GPCRs are the most common templates used in melatonin receptor homology modeling[3]. However, sequence alignments are rather poor,

providing structural models whose reliability has still to be proven. The low identity of the sequences increases the degree of speculation, and the poor usefulness of these models for drug design purposes[4]. Additionally, the nature of the endogenous ligand limits the identification of important ligand-receptor interactions. Melatonin lacks a charged group at physiological pH that would facilitate the identification of ionic interactions, like in the case of its parent amino-compound, the neurotransmitter serotonin[1]. As abovementioned, mutagenesis studies have provided some insights into the putative binding mode of melatonin[5]. In the case of MT_1 receptor three amino acids have been identified as key contacts for ligand binding Ser110, Ser114 and His195[6,7]. In the case of MT_2 several amino acids were identified as important for molecular recognition: Asn175, Val204, Asn268, Leu272, Ala275, Val291, Leu295, Tyr298 and Tyr188[8,9]. In the case of MT_2, consistent with the physicochemical properties of the natural ligand, the number and the lipophilicity of the amino acids involved in melatonin binding suggest the presence of a network of contacts characterized by the lack of strong polar interactions. This structural feature complicates the identification of an unambiguous binding pose for melatonin or synthetic analogues. Therefore, till now, structure-based design has not been a suitable approach for the design of novel melatonin ligands.

Ligand-based drug design has been widely exploited and has provided two marketed drugs: agomelatine (Valdoxan®) for major depression and ramelteon (Rozerem®) for sleeping disorders, and other ligands are in development stages[10]. Subtle and major changes on melatonin structure have provided a plethora of ligands, in many cases able to beat the picomolar affinity of melatonin for its receptors, and several pharmacophoric models have been proposed[4,11,12]. Among the different pharmacophores there is a wide consensus on the necessity of the oxygen of the methoxy group for agonists, attached to an aromatic or heteroaromatic core connected to the acetamido side chain. Suppression of the methoxy group generally leads to an

inversion of the activity profile, like the antagonist luzindole (figure 1). This methylether has also been bioisosterically replaced for bromine (**1.1**)[13], and its oxygen employed as the anchoring point for the linker in MT_1-selective dimers and related structures (1.**2**)[14]. With respect to the indole nucleus, there are numerous successful examples of scaffold hopping of the aromatic core that demonstrate that the hydrogen held in position N1 of melatonin is not necessary for melatonergic receptor recognition[15,16]. The exploitation of a putative lipophilic pocket close to the binding site of melatonin has also been a successful approach, especially in the development of nonselective and MT_2-selective ligands[17]. This approach has provided synthetic ligands like the antagonist luzindole or the radioligand 2-[^{125}I]iodomelatonin, which have been key pharmacological tools in the understanding of the melatonergic system[18–20]. Both the replacement of the indole ring for other aromatic and more lipophilic heterocycles or carbocycles, and the exploitation of this putative non-polar cavity have proven to be successful approaches. Nevertheless its application represents an increase in the overall lipophilicity of the potential drug candidates, what can in turn bring associated certain limitations in their development in more advanced stages. A high lipophilicity translates into poor water solubility what limits the pharmacokinetic properties of the developmental molecule. A gain in lipophilicity generally leads also to an increase of the hydrophobic effect, a non-specific component of the binding thermodynamics[21]. This effect might in turn translate into off-target binding and increased likeliness of adverse interactions like hERG inhibition or toxicity associated to its metabolism and/or accumulation[22–24]. Therefore, at early development stages it is more desirable to exploit the ligand-receptor specific polar interactions in order to optimize the specific intermolecular contacts that have a greater enthalpic contribution to the free energy of the binding (i.e. hydrogen bonds, multipolar interactions, cation-π)[21]. Melatonin has good water solubility but limited oral bioavailability. Attempts to introduce polar groups on the indole ring or on the scaffold of

other melatonergic ligands invariably led to a decrease of receptor binding affinity[25,26].

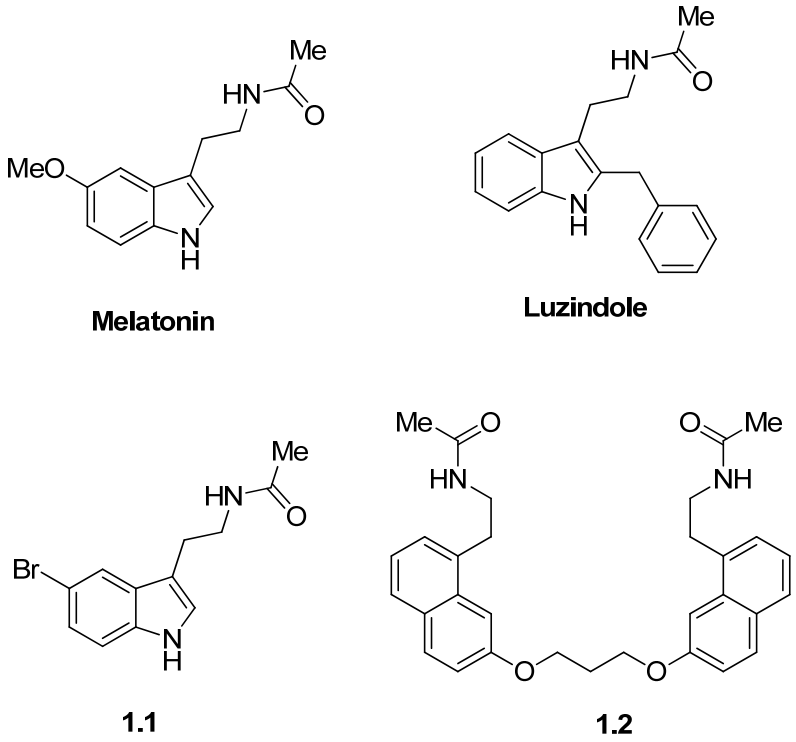

Figure 1. Selected melatonergic ligands.

In the case of the acetamido moiety, the design and synthesis of melatonergic ligands also tend to be very conservative maintaining this group unmodified, with the exception of few bioisosteric replacements and elongation of the acyl group[27]. Bioisosterism is a classic ligand-based drug design strategy founded on the assumption that distinct molecular structures can be recognized in a similar manner by biological systems regardless of their structural or physicochemical similarity[28]. That is, bioisosterism is not defined by structural or physicochemical features, but by the ability of the bioisostere to mimic the biochemical recognition in a certain biological context. The mimicry does not imply that identical properties are retained by the

bioisosteres, conversely they normally modulate the properties of the original pattern. This approach is commonly used in the practice of medicinal chemistry in the development of new drug candidates and pharmacological tools[29–31]. The structural and physicochemical changes present in bioisosteres can translate into changes in pharmacological and pharmacodynamic properties such as selectivity, metabolic stability, permeability, solubility, synthetic ease, etc. and also permit acquiring additional intellectual property.

Modifications performed on the acetamido group of melatonin were discouraging since its replacement by other moieties generally led to loss in binding affinity and potency at MT_1 and MT_2. As abovementioned, there are few reported cases of bioisosterism applied to the carbonyl of acetamido group of melatonin maintaining the 5-methoxytryptamine skeleton intact. Fewer exist in which the whole moiety has been bioisosterically replaced (figure 2). In 1998 Leclerc et al. synthesized a melatonin bioisostere in which the acetamido moiety was replaced by ethylurea (**1.3**). This compound proved to be a full melatonergic agonist in ovine pars tuberalis cells, showing a biphasic binding curve (pK_{i1}, 11.50; pK_{i2}, 7.92)[27]. Compound **ML-23** is reported to be a melatonin antagonist able to displace 2-[^{125}I]-iodomelatonin in prostate (IC_{50}, 0.14 nM)[32] that has been proposed for the treatment of Parkinson disease[33]. Another compound that is currently being studied for several disorders is **NeuP11**. In both **NeuP11** and compound **1.4** the amine group is acylated with an unusual aromatic acid, maintaining good MT_1 and MT_2 binding affinities[34–36]. More recently Rami et al. in 2013, described the use of 5-membered ring heterocycles as bioisosteres of the acetamido group (**1.5**) and of the carbonyl group (**1.6**, **1.7**) of agomelatine. The maintenance of the acetamido portion in melatonergic ligands is also justified by its relative metabolic stability; the main metabolic hotspots of melatonin are position 6 and demethylation at position 5, being deacetylation a minor metabolic event[38,39].

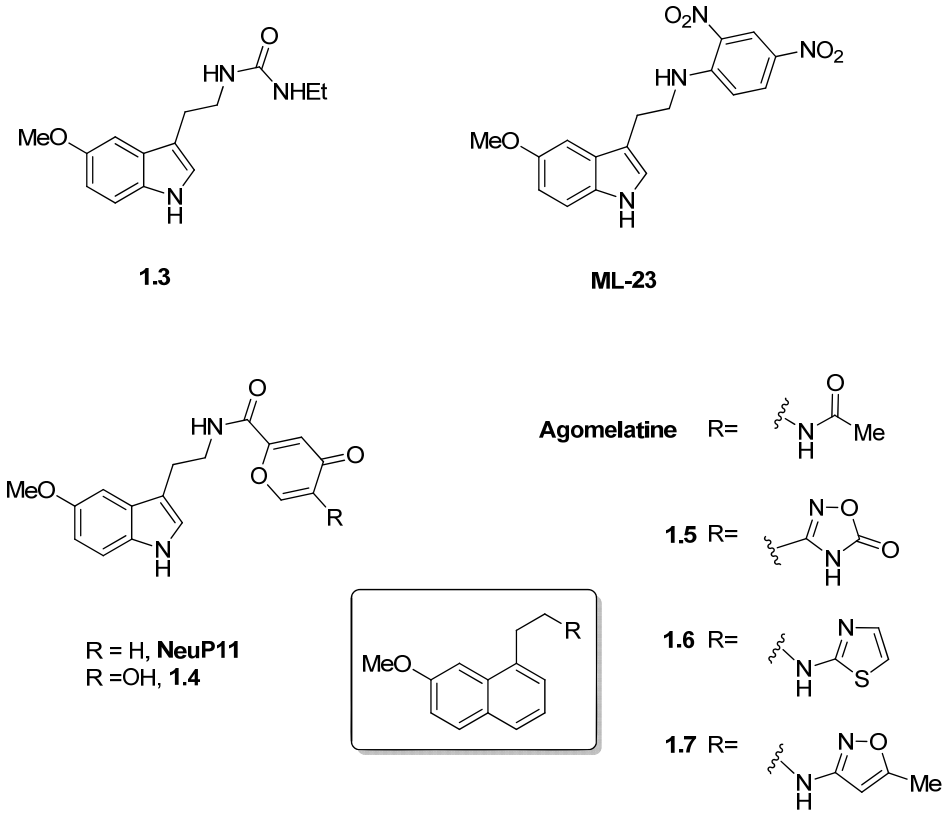

Cpd.	MT_1 K_i (nM)	MT_2 K_i (nM)
NeuP11[34]	22	34
1.4[34]	13	7
1.5[37]	80	25
1.6[37]	34	12
1.7[37]	48	20

Figure 2. Melatonin analogues in which the *N*-acetyl group has been totally or partially replaced and their reported binding affinities.

Approach

Bioisosteric replacement of the acetamide could represent an interesting tool in the biostructural understanding of the not so well-known properties (size, shape, electronic distribution, lipophilicity) of the melatonin binding pocket where the acetamido portion is accommodated within the receptors. Herein, we have bioisosterically replaced the acetamido fragment of melatonin with a series of reversed amides and heteroaromatic azoles (figure 3). We have included in this study the hallucinogenic natural occurring alkaloid *N,N*-dimethyl-5-methoxytryptamine (**1.36**) to evaluate how this serotonin analogue behaves within the orthosteric locus of melatonin receptors[40]. The bioisosterism of amides has been widely studied in the development of peptidomimetics, and its substitution for heterocycles is common[41,42]. In order to establish a structure-activity relationship study of different azolic bioisosteres we have utilized common and well established peptidic bond bioisosteres: oxazole, 1,2,4-oxadiazole and 1,3,4-oxadiazole[43], as well as some other relatively acidic azoles bearing a hydrogen that could intervene in a captodative hydrogen bond: 1,3,4-oxadiazol-(thio)ones, 1,3,4-triazol-(thio)ones and a 1,3,4-aminothiazole. The thermodynamic solubility at pH 7.4 of those compounds showing significant binding on melatonin receptors and representative of each family of compounds was determined and it was taken as an indirect evaluation of their hydrophilicity. For those azolic compounds bearing an acidic proton the solubility was also determined at different pH values in order to indirectly confirm their acidic character[44].

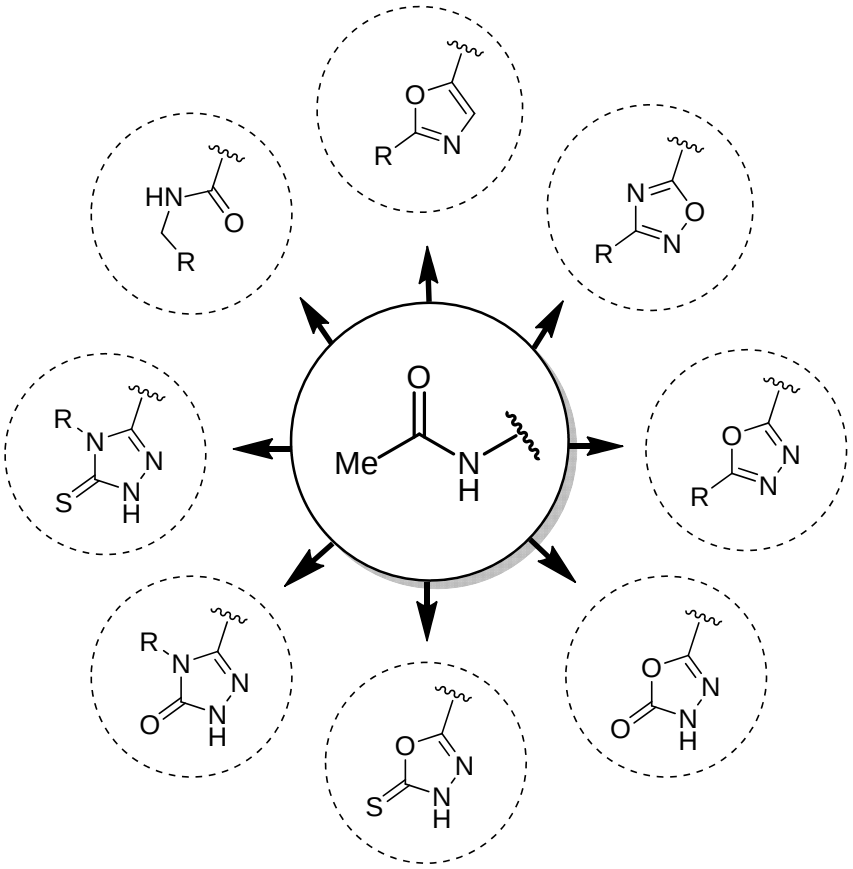

Figure 3. Illustration of the different replacements of the acetamido moiety of melatonin carried out in this work.

Chemistry

Synthesis of retroamides and oxazoles

Indoleamides **1.8 - 1.11,** and were synthesized starting from the corresponding acids activated with carbonyldiimidazole (CDI) and propargylamine or allylamine (scheme 1). Subsequently propargyl amides **1.8** and **1.9** underwent gold(III) catalyzed cycloisomerization affording the corresponding oxazoles **1.12** and **1.13**[45,46].

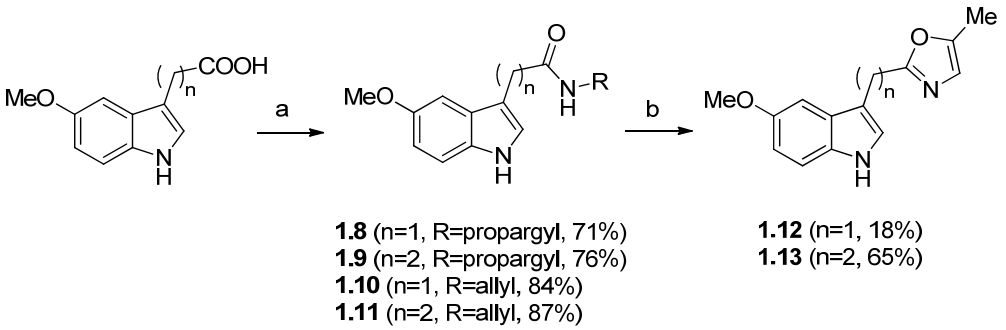

Scheme 1. *Reagents and conditions*. (a) CDI, CH_2Cl_2, propargylamine or allylamine, rt; (b) $AuCl_3$, DCM, N_2, rt.

According to the mechanism proposed by Yao et al., gold (III) coordinates the terminal alkyne that suffers the attack of the amide oxygen on its enol form to give the oxazole and thus, the catalyst is regenerated (scheme 2)[47].

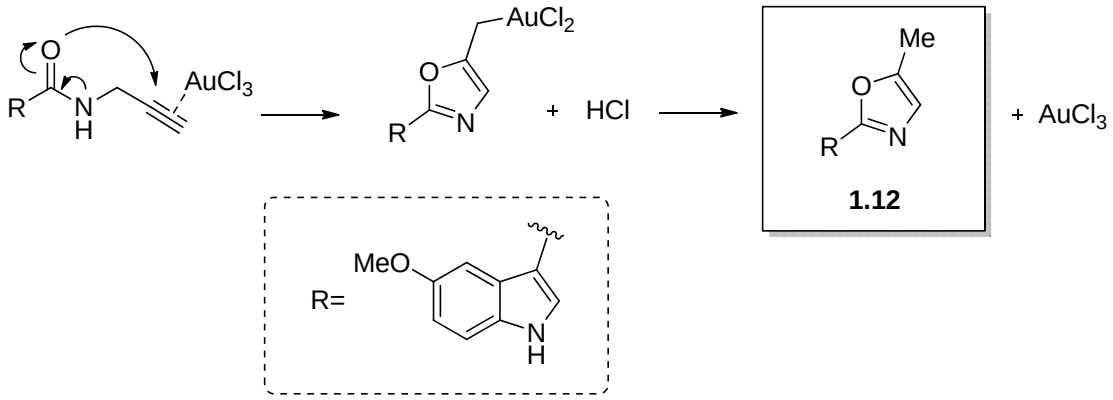

Scheme 2. Adapted mechanism from Yao et al.[47] for the synthesis of **1.12**.

Ester **1.14** was obtained by acid catalyzed Fischer esterification from 2-(5-methoxyindol-3-yl)acetic acid. Ester **1.15** was obtained via Michael addition of the electron-rich heteroaromatic 5-methoxyindole over ethylacrylate catalyzed by anhydrous zirconium (IV) chloride in good yield (scheme 3)[48].

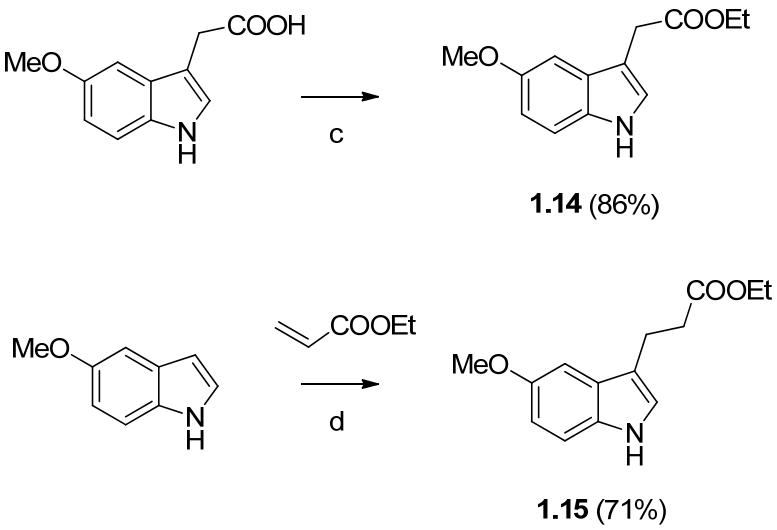

Scheme 3. *Reagents and conditions*. (c) H_2SO_4 (cat.), EtOH, reflux; (d) ethylacrylate, $ZrCl_4$ (anh.), CH_2Cl_2, N_2, rt.

Synthesis of 1,2,4- and 1,3,4-oxadiazoles

1,2,4-oxadiazoles **1.16** and **1.17** were prepared directly from the corresponding esters **1.14** and **1.15** by cyclocondensation with acetamidoxime in fair yields(scheme 4)[49]. To obtain 1,3,4-oxadiazole isomers, esters **1.14** and **1.15** were subjected to microwave-promoted hydrazinolysis yielding hydrazides **1.18** and **1.19** in quantitative yields. The hydrazides were subjected to condensation with the corresponding orthoester in acidic medium to afford 1,3,4-oxadiazoles **1.20 - 1.22** (scheme 4).

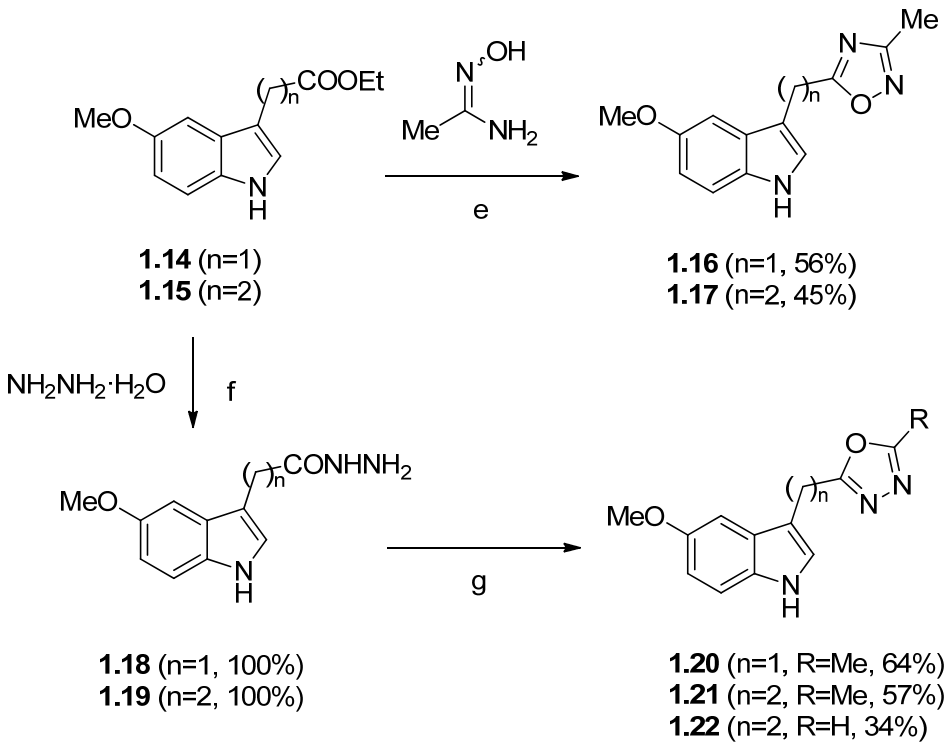

Scheme 4. *Reagents and conditions*. (e) acetamidoxime, NaH, THF, mol. sieves, 80ºC; (f) hidrazine hydrate, 150°C (mw), 45 min; (g) orthoester, AcOH (cat.), 125°C (mw), 1h.

The synthesis of 1,3,4-oxadiazoles from hydrazides and orthoesters was performed with acid catalysis, which increases the electrophilic potential of the orthoester favoring the attack of the nucleophilic hydrazide. The subsequent elimination of an alcohol molecule yields the corresponding 1,3,4-oxadiazole. An adapted mechanism leading to **1.20** from **1.18** is shown in scheme 5.

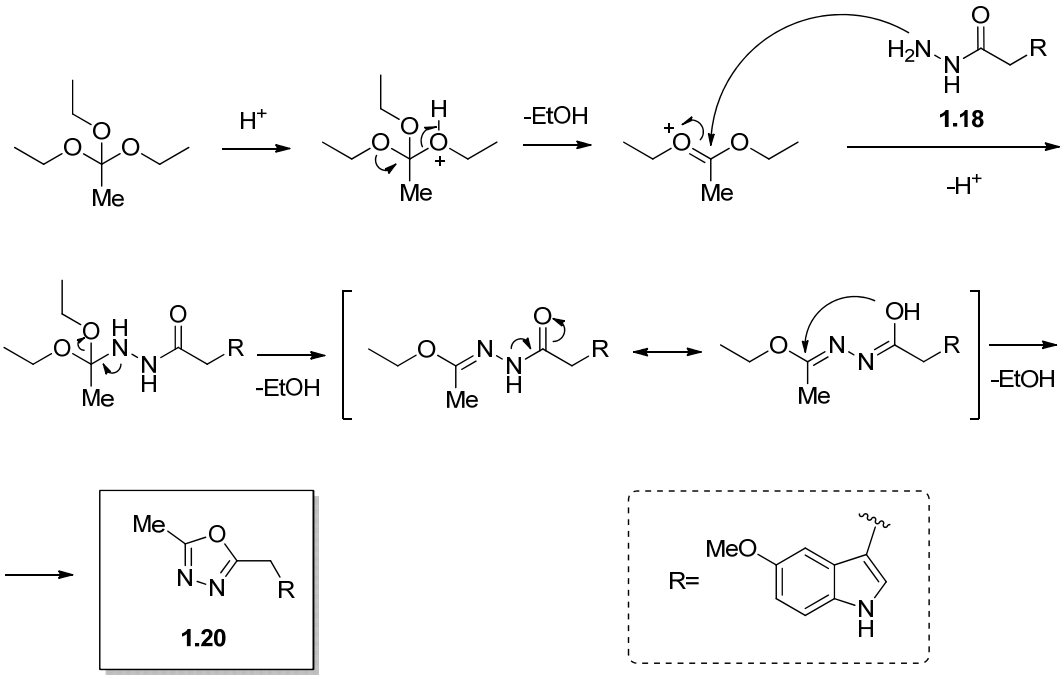

Scheme 5. Proposed mechanism for the acid-catalysed cyclocondensation of hydrazides with ethylorthoacetate to form 1,3,4-oxadiazoles adapted to the preparation of **1.20**.

Synthesis of 4-alkyl-1,2,4-triazol-5-(thio)ones and 2-amino-1,3,4-thiadiazol

Reaction of hydrazides **1.18** and **1.19** with methylisocyanate or ethylisothiocyanate afforded the corresponding acylsemicarbazides **1.23** and **1.26,** or acylthiosemicarbazides **1.27** and **1.28,** that underwent microwave-induced cyclocondensation in basic medium to give 4-methyl-1,2,4-triazol-5-ones **1.25** and **1.26,** and 4-ethyl-1,2,4-triazol-5-thiones **1.29** and **1.30** in good and very good yields, respectively (scheme 6). There are several reports in the literature employing different methods for the synthesis of 2-amino-1,3,4-oxadiazoles and 2-amino-1,3,4-thiadiazoles from acylsemicarbazides and acylsemithiocarbazides. After different failed attempts with sulfuric acid[50] and P^{v}-reagent[43], only in the case of acylsemithiocarbazide **1.27** successful

cyclization to 2-amino-1,3,4-thiadiazole **1.31** was achieved with phosphorus oxychloride at room temperature in fair yield.

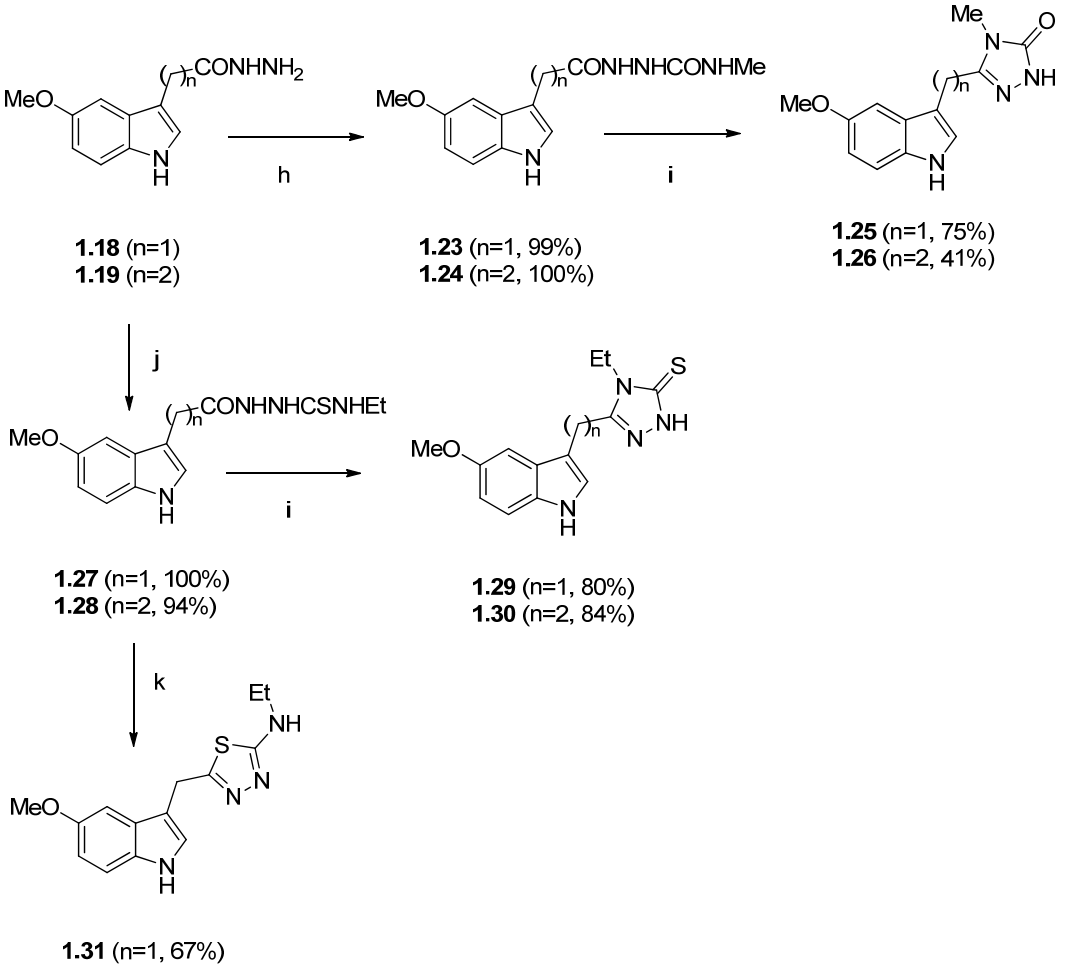

Scheme 6. *Reagents and conditions*. (h) MeNCO, EtOH, rt; (i) NaOH (aq.), EtOH, 100ºC (mw), 15 min; (j) EtSCN, EtOH, rt; (k) $POCl_3$, rt.

Since two different azoles can be obtained from the same intermediate in different conditions, two mechanisms are proposed for the synthesis of **1.30** and **1.31** from **1.27.** In basic medium, a proton is cleaved from the acylsemithiocarbazide, and the formed anion is stabilized by resonance. Sulfur anion promotes the intramolecular attack of the imine nitrogen over the

carbonyl forming a triazolidin-thione that evolves to **1.30** by elimination of a water molecule (scheme 7A). In the second case, phosphoryl oxychloride coordinates to the acetylsemithiocarbazide oxygen on its enol form. Direct attack of sulfur on its thioenol form gives **1.31** (scheme 7B).

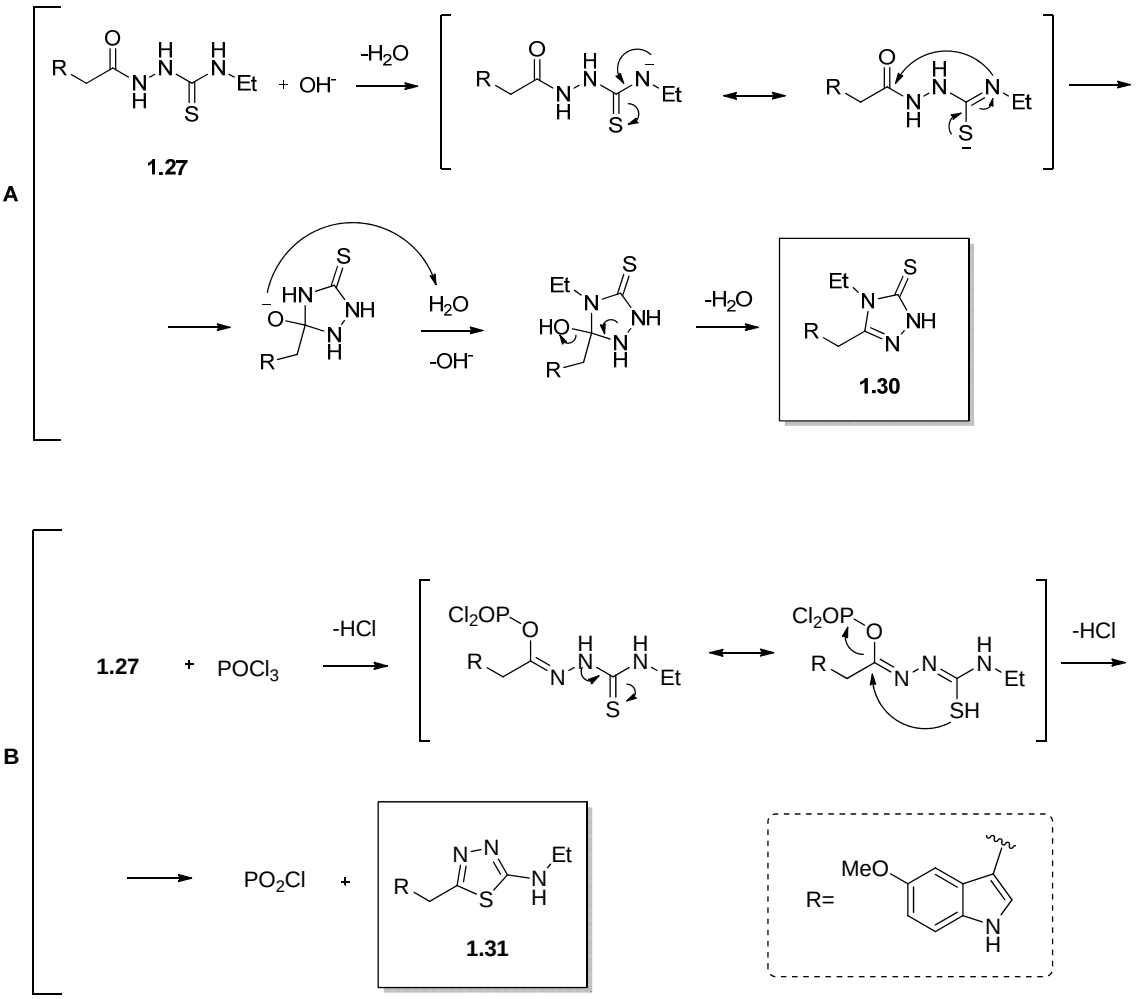

Scheme 7. Suggested mechanism for the cyclocondensation of **1.27** (A) in basic medium and (B) in acid medium (phosphorus oxychloride).

Synthesis of 1,3,4-oxadiazol-2-(thio)ones

When microwave-heated in the presence carbonyldiimidazole and triethylamine hydrazides **1.18** and **1.19** afforded the corresponding 1,3,4-oxadiazole-2-ones **1.32** and **1.33**. In basic medium, with carbon disulfide, 1,3,4-oxadiazole-2-thiones **1.34** and **1.35** were obtained. (scheme 8)

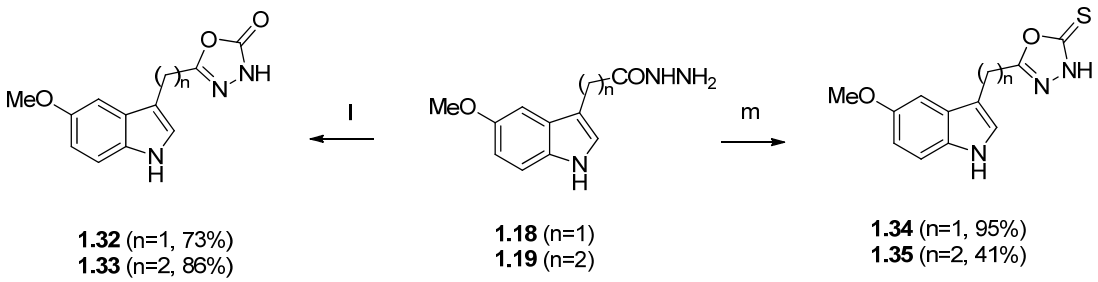

1.32 (n=1, 73%)
1.33 (n=2, 86%)

1.18 (n=1)
1.19 (n=2)

1.34 (n=1, 95%)
1.35 (n=2, 41%)

Scheme 8. *Reagents and conditions*. (l) CDI, TEA, THF, 100ºC (mw), 10 min; (m) CS_2, EtOH, KOH (aq.). 150ºC (mw), 10 min.

NMR studies on the tautomerism of hydrogen-bearing azoles

Compounds like **1.32** among others in this work can exist in two possible tautomeric forms as shown on figure 4[51].

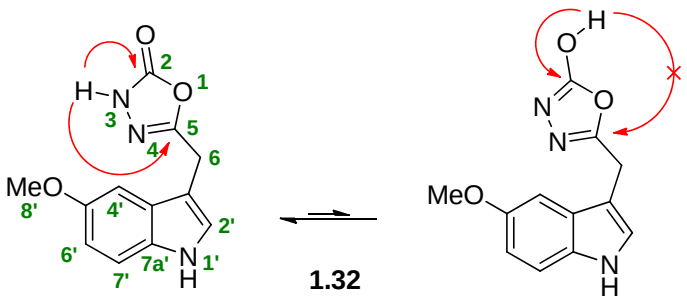

Figure 4. Possible tautomers of **1.32.**

The unequivocal attribution of proton signals of **1.32** was done with the ^{1}H-NMR spectrum aided by the COSY correlations. The observed ^{1}H-^{13}C HSQC cross-peaks allowed the identification of all hydrogenated carbons. ^{1}H-^{13}C HMBC spectrum permitted the characterization of the quaternary carbons and confirmed the assignation. In the 150-160 ppm field of the ^{13}C spectrum, three quaternary carbons are found (figure 5). One matched to C-5′ of the indole and the other two to the azole ring. The HMBC correlation between H-8′ and C-5′ (3.73 ppm, 153.25 ppm) allowed the identification of the indole carbon C-5′ (153.18 ppm). The HMBC correlation observed between H-6 and C-5 (3.96 ppm, 156.55 ppm) allows the assignation of C-5 (156.46 ppm), and consequently of C-2 (155.07 ppm). In the ^{1}H-NMR, only two protons are found in the higher field: the indole H-1′ (10.89 ppm) and the azole hydrogen (12.08 ppm). The correlation found on ^{1}H-^{13}C HMBC between the latter, not only with C-2 (12.11 ppm, 155.12 ppm), but also with C-5 (12.11 ppm, 156.55 ppm) allowed us to conclude that this hydrogen is in fact held over nitrogen the N3 (H-3, 12.08 ppm) thus, permitting the unequivocal assignation of the compound (see experimental section), and confirming that the only tautomer observed in DMSO solution was the *keto*-form: the oxadiazolone (figure 4).

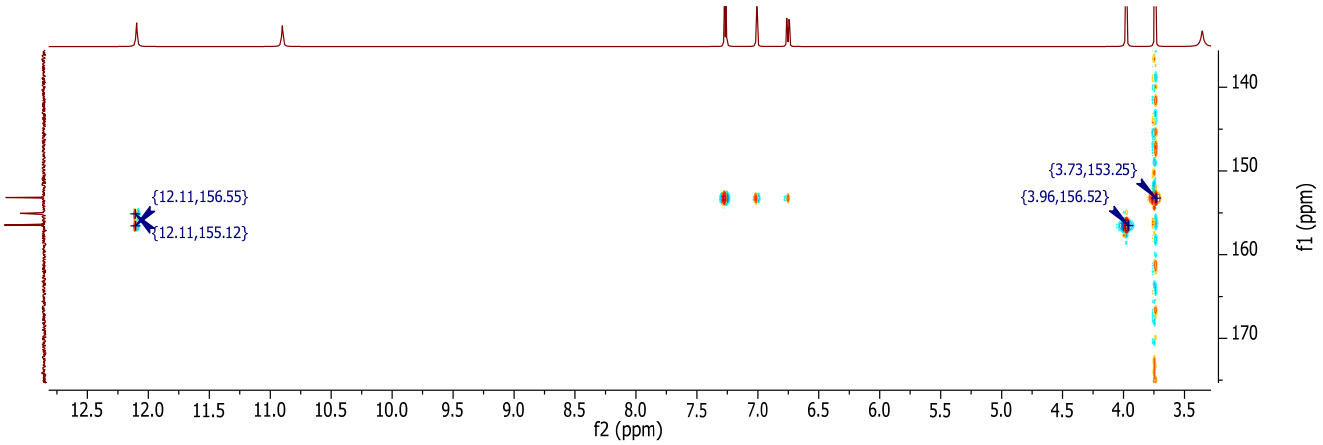

Figure 5. **1.32** selected observed ^{1}H-^{13}C HMBC correlations. ^{13}C-NMR spectra of **1.32** in the vertical axis (f1, ppm) and ^{1}H-NMR spectra in the horizontal axis (f2, ppm).

This assignment was further confirmed in the ^{1}H-^{15}N HMBC correlation. Two secondary nitrogens are observed in the bidimensional spectrum, N-1′ (-244.60 ppm) and N-3 (-224.46 ppm), as they showed satellital signals around their corresponding hydrogens H-1′ (10.91 ppm, -244.60 ppm) and H-3 (12.10 ppm, -224.46 ppm). Moreover a correlation could be observed between H-2′ and N-1′ (7.27 ppm, -244.60 ppm). The correlation between H-3 and N-4 (12.09 ppm - 437.65 ppm) allowed the identification of N-4, the tertiary nitrogen in the oxadiazolone ring, and confirmed the proposed structure (figure 6).

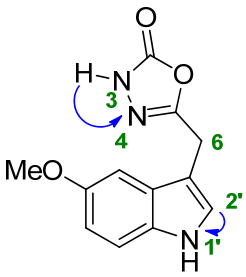

1.32

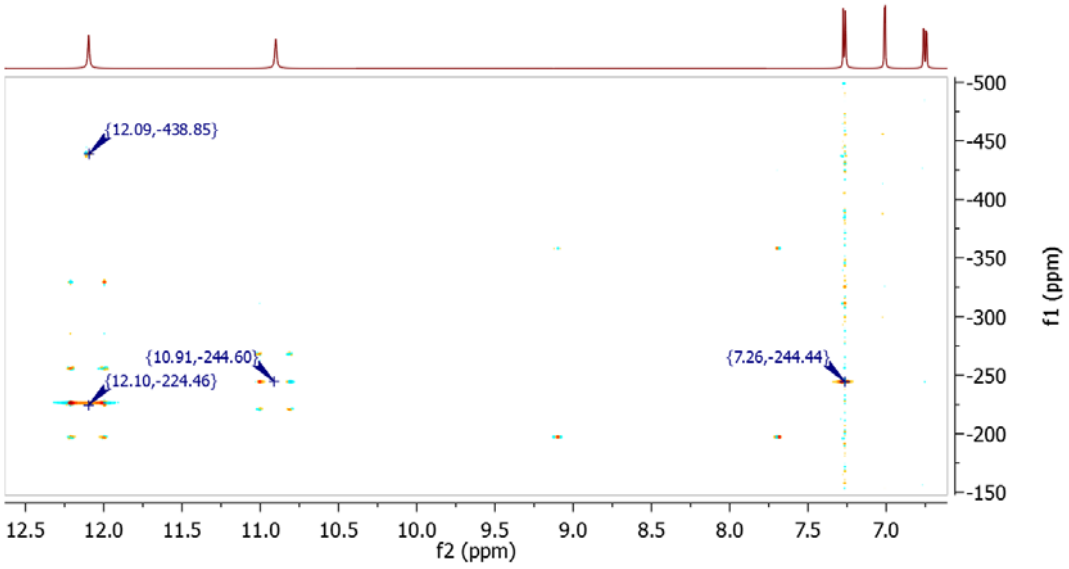

Figure 6. Observed ^{1}H-^{15}N HMBC correlations of **1.32.** ^{15}N-NMR spectra of **1.32** in the vertical axis (f1, ppm) and ^{1}H-NMR spectra in the horizontal axis (f2, ppm).

Since ^{1}H-^{13}C HMBC experiment was sufficient for the identification of the major tautomer in DMSO solution, this experiment was performed with all synthesized compounds in the oxadiazolone, oxadiazolthione and triazolone series. In all cases the *keto*-tautomer was the only species observed in DMSO-d_6.

In the particular case of **1.31** the COSY experiment was sufficient for the characterization of the 2-amino-1,3,4-thiadiazole ring. The protons held on C-2 (H-2, 3.17 ppm) couple with the one held on the nitrogen N-3 (H3, 7.39 ppm) (figure 7).

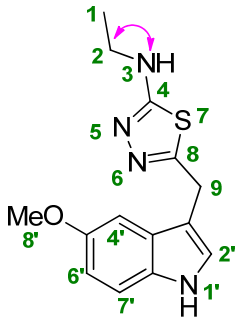

1.31

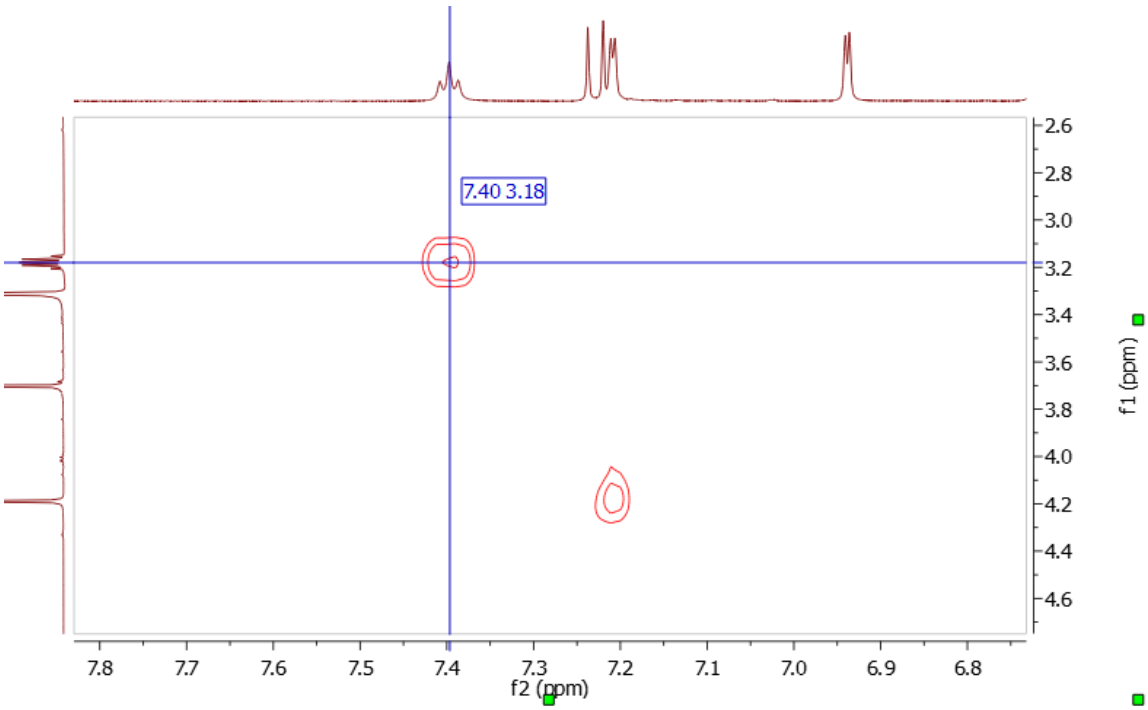

Figure 7. Observed COSY correlation between H2 and H3 of **1.31.** ^{1}H-NMR spectrum of **1.31** in the vertical axis (f1, ppm) and in the horizontal axis (f2, ppm).

Only these two examples are given to exemplify the characterization of these series of compounds. The 5-methoxyindole pattern was easily identified for all derivatives both in ^{1}H-NMR and ^{13}C-NMR spectra. The identification of the methylene or ethylene linker was straightforward in the lower field of both spectra. The ^{1}H-^{13}C HMBC correlation between the hydrogens of the linker and the quaternary carbons of the different azoles permitted their unequivocal assignation.

Pharmacology

Radioligand binding studies on melatonin receptors MT_1 and MT_2

The binding affinities of the newly synthesized compounds are reported in table 1. Retroamides with unsaturated side chains showed the highest affinity of all families of compounds, with K_is in the nano and sub-nanomolar range. The alkenyl or alkynyl substitution does not seem to significantly affect the potency of the compounds; conversely, the length of the spacer does. Ethylene spacer is preferred in both cases (**1.9** and **1.11**) and compound **1.11** displays only 3-fold lower binding affinity at MT_2 receptors than melatonin

Oxadiazole-bearing compounds affinity is clearly more favored by a methylene (**1.16** and **1.20**) than an ethylene spacer (**1.17**, **1.21**). Removal of the methyl substituent in the case of 1,3,4-oxadiazoles slightly favors affinity (**1.22**). The isomery of the oxadiazole does not seem relevant in the case of methylene-oxadiazoles (**1.16**, **1.20**). Oxazoles **1.12** and **1.13** do not seem to match the oxadiazole profile and show significantly lower binding affinities.

1,3,4-triazolones and –thiones are the most penalized derivatives together with oxazoles and 1,3,4-oxadiazolthiones. Only those bearing a methylene spacer (**1.25** and **1.29**) have an affinity constant <1 µM at the MT_2 subtype.

1,3,4-Oxadiazolones and –thiones display the most dramatic drop in binding affinity. The 1,3,4-oxadiazolthione ring is clearly detrimental; only compound **1.34** shows some affinity for MT_2. Conversely, the ethylene-1,3,4-oxadiazolone **1.33** is the compound with the highest affinity for both MT_1 and MT_2 of all synthesized azolic compounds.

The compound with the most marked selectivity profile together with rather good binding potency for the MT_2 subtype is 2-amino-1,3,4-thiadiazole (**1.31**). Unfortunately the synthesis of other amino-azoles was not accomplished and a complete SAR study could not be done. Unexpectedly equipotent at MT_2 is the dimethylamino derivative **1.36**, but with a less marked selectivity profile (10-fold).

Table 1. Radioligand displacement binding studies at MT_1 and MT_2 receptors. (K_i ,nM).

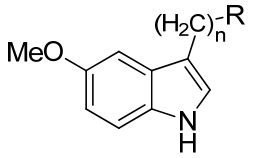

General formula

Cpd.	n	R	MT_1	MT_2	Ratio (MT_1/MT_2)[a]
Mel.	2	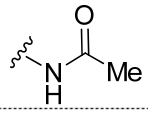	0.091±0.005	0.15±0.07	0.6
1.8	1	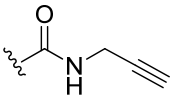	14±4	3.8±0.5	3.6
1.9	2		5.0±0.9	1.0±0.6	5
1.10	1	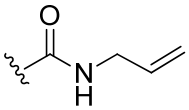	17±0.7	4.9±4	3.5
1.11	2		2.5±0.2	0.45±0.08	5.5
1.12	1	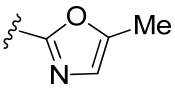	280±20	>10000	-
1.13	2		>10000	498±11	-
1.16	1	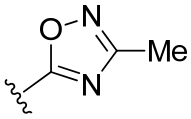	170±15	44±3	3.9
1.17	2		>10000	>10000	-
1.20	1	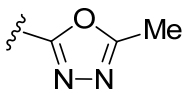	210±10	16±3	10
1.21	2		709±10	190±8	3.6
1.22	2	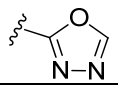	570±10	68±15	8.6

[a] Ratio calculated only for compounds with K_i < 100 nM for either of the subtypes.

Table 1. (cont.)

1.25	1	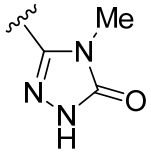	>10000	560±60	-
1.26	2		>10000	>10000	-
1.29	1	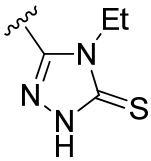	>10000	220±50	-
1.30	2		>10000	>10000	-
1.31	1	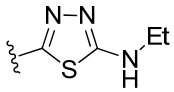	>10000	17±3	>500
1.32	1	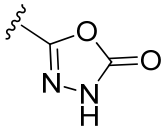	>10000	160±50	-
1.33	2		35±1	4±0.5	10
1.34	1	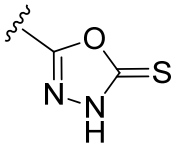	>10000	535±30	-
1.35	2		>10000	530±50	-
1.36	2	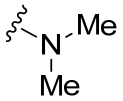	210±10	16±0.5	10

[a] Ratio calculated only for compounds with K_i < 100 nM for either of the subtypes.

Functional studies on melatonin receptors MT_1 and MT_2

Only compounds showing significant affinity for either receptor were functionally characterized in the [^{35}S]GTPγS binding assay. Results are summarized in table 2.

Retroamides resulted the most potent compounds. The length of the spacer determined the profile. Compounds **1.8** and **1.11** with the methylene spacer were partial agonists, whereas those bearing an ethylene, **1.9** and **1.11**, resulted full agonists, but significantly less potent than melatonin.

The tested azole-containing compounds showed a very similar behavior. Weak partial agonist at the MT_2, and little or no effect at the MT_1. Only compounds **1.20** and **1.33** showed an EC_{50} in the 10^{-8} range.

1.36 resulted nearly equipotent at both receptor subtypes but with higher efficacy at the MT_1 receptor than at the MT_2.

Table 2. Functional studies at MT_1 and MT_2 of selected compounds

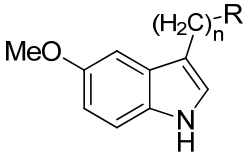

General formula

			MT_1		MT_2	
Cpd.	n	R	EC_{50} (nM)	E_{max}	EC_{50} (nM)	E_{max}
Mel.	2	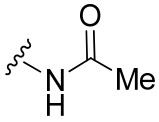	0.098 ±0.003	100%	0.069 ±0.003	100%
1.8	1	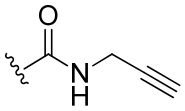	289±13	67±8%	81±3	82±5%
1.9	2		38±3	106±9%	3±0.3	99±9%
1.10	1	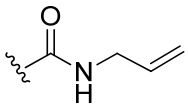	525±307	64±4%	132±70	70±8%
1.11	2		204±54	92±2%	11±9	88±4%
1.12	1	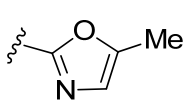	-	-	989±23	23±4%
1.13	2		-	-	503±5	32±1%

Table 2. (cont.)

1.16	1	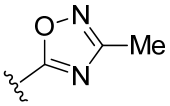	711±23	16±2%	295±13	48±2%
1.17	2		-	-	-	-
1.20	1	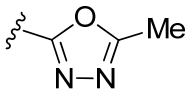	>10uM	-	71±28	24±3%
1.21	2		961±16	19±6%	881±23	32±4%
1.22	2	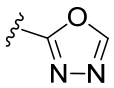	>10uM	-	457±141	25±2%
1.25	1	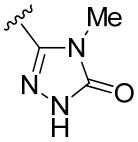	-	-	>10uM	-
1.26	2		-	-	-	-
1.29	1	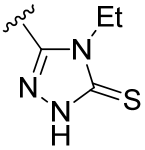	-	-	>10uM	-
1.30	2		-	-	-	-
1.31	1	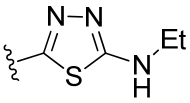	-	-	110±25	35±7%
1.32	1	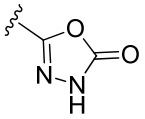	>10uM	-	>10uM	-
1.33	2		326±30	26±4%	29±3	29±3%
1.34	1	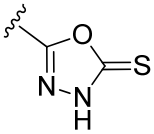	>10uM	-	>10uM	-
1.35	2		-	-	1096±316	32±9%
1.36	2	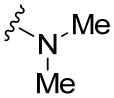	257±98	62±3%	112±110	28±3%

Thermodynamic solubility studies

The thermodynamic solubility of representatives of each family of azoles was determined in buffer at pH 7.4 (table 3). For comparison purposes

the solubility of agomelatine and melatonin at pH 7.4 were also determined. Melatonin was the most soluble compound at physiologic pH. No significant differences were found between 1,2,3-oxadiazole **1.16** and 1,3,4-oxadiazole **1.20** at pH 7.4 showing a solubility similar to that of agomelatine. Additionally, for those compounds bearing acid azoles and **1.31**, their solubility was also determined at pH 5.5 and pH 9.3 as an indirect estimation of their acid-basic properties (figure 8). The solubility of **1.33**, **1.34**, **1.24** and **1.30** showed a clear dependence on the pH, peaking at basic pH. It is especially notable in the case of **1.33** and **1.34**, what evidences the acidic nature of the compounds. The sulfur substitution in **1.35**, compared to **1.33**, improves the pH-dependent increase in solubility. Derivative **1.31** also showed a mild pH dependence of its solubility, higher at acidic pH, supporting its weak basic nature[52].

Table 3. Thermodynamic solubility of selected compounds.

	Thermodynamic solubility (μM)		
Cpd.	pH 5.5	pH 7.4	pH 9.3
Melatonin	nd	6640±25	nd
Agomelatine	nd	804±24	nd
1.16	nd	1165±23	nd
1.20	nd	970±8	nd
1.26	860±13	1104±17	1408±30
1.30	131±1	137±1	208±2
1.31	1718±85	1417±77	1437±78
1.33	1406±1	2100±20	7920±30
1.34	907±5	3460±200	18660±40

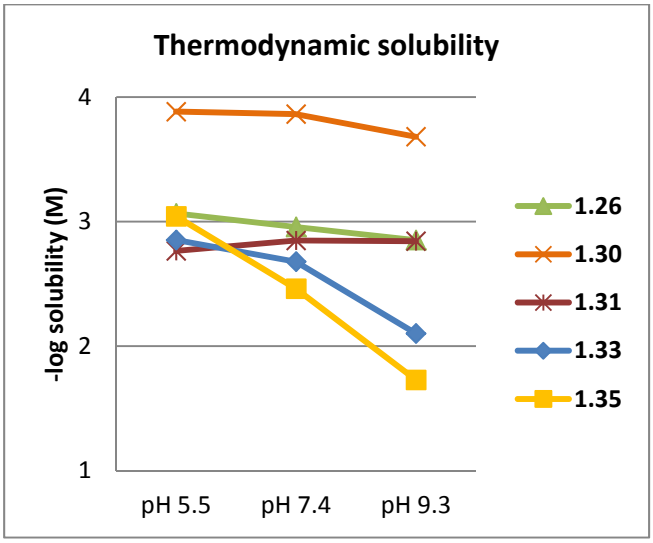

Figure 8. Solubility of azole melatonergic ligands at different pH values.

Discussion

Inverted amides have already been reported as a class of melatonin receptor ligands, for example on the naphthalene scaffold of agomelatine, but not yet on the classical 5-methoxyindole scaffold[27,53]. Binding data obtained are consistent with literature ones; the two most potent compounds within the series are inverted amides with an ethylene spacer, **1.9** and **1.11**. Both compounds retain good binding affinity, particularly for the MT_2 subtype. This could be due to their ability to arrange their pharmacophoric groups in a way resembling that of melatonin in its bioactive conformation (figure 9)[11,54]. This hypothesis is also supported by their full agonistic properties.

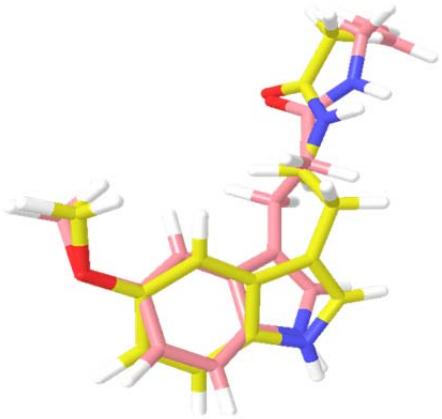

Figure 9. Superposition of melatonin (yellow carbons) in its putative bioactive conformation[11] and **1.11** (pink carbons).

Binding potency of azole derivatives more affected by the length of the spacer being the differences 10-fold or higher in the case of active compounds. The preferred spacer depends on the nature of the azole attached to it. In the case of the oxazoles the low affinity displayed does not allow to draw any conclusions even if the spacer seems to determine the preferred receptor subtype. In the case of 1,2,4- and 1,3,4-oxadiazole matching pairs the methylene spacer is clearly preferred (**1.16-1.17**, **1.20-1.21**). Superposition of **1.16** and **1.20** with the active bioconformation of melatonin reveals that the nitrogen atom of the oxadiazoles can be superposed on the amide oxygen of melatonin (figure 10). Following this hypothesis, the lack of affinity of oxazole **1.12** could be attributed to the absence of the second nitrogen atom present in the oxadiazole ring.

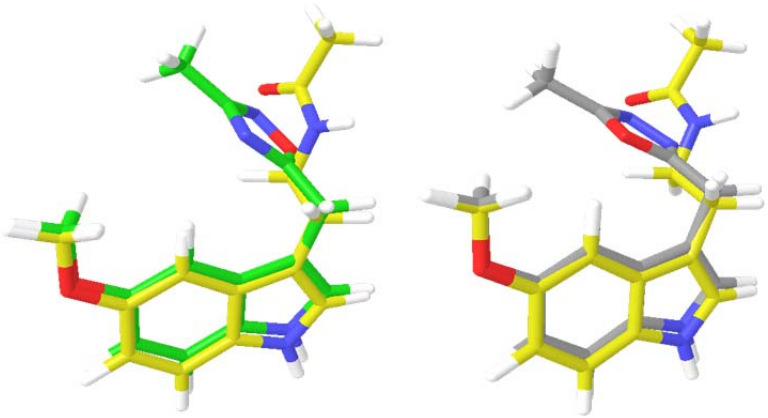

Figure 10. **1.16** (green carbons) and **1.20** (gray carbons) superposed on melatonin (yellow carbons).

Compound **1.22**, the nor-isomer of **1.21** shows the same selectivity and potency as **1.20**, whereas **1.21** is penalized in its binding to MT_2. This penalty is probably attributable to steric clashes in the region where the amide of melatonin is accommodated. With the nitrogen closer to the ethylene spacer (nitrogen in position 4) mimicking the carbonyl group of melatonin, the methyl group attached to the heterocycle would point out beyond the methyl end of melatonin (figure 11).

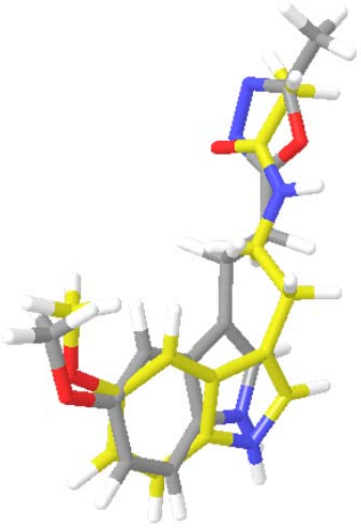

Figure 11. **1.21** (gray carbons) superposed on melatonin (yellow carbons).

With regard on the oxadiazole ring isomerism, the comparison between the isomer pairs **1.20-1.16** and **1.21-1.17,** assuming that each pair would bind in a similar pose, demonstrates that the 1,3,4-oxadiazole ring is slightly preferred by the melatonergic system in terms of potency. The isomerism of the oxadiazole does not seem to make a difference in the selectivity; the same subtle MT_2 preference was observed in the azolic compounds described by Rami et al[37]. The carbonyl group of melatonin is putatively involved in a hydrogen bond as acceptor; this is especially relevant in the case of the MT_2 subtype. Moreover the NH group is not essential in this receptor subtype[55,56]. Therefore the contribution of the carbonyl to the binding to MT_2 should be of great relevance. Assuming that an imine-like nitrogen within the oxadiazole ring substitutes for the carbonyl group of melatonin, the hydrogen bond donor properties of the heterocycle shall be of relevance for MT_2 recognition. Previous studies on both oxadiazole isomers revealed that 1,3,4-oxadiazole nitrogens calculated hydrogen bond acceptor properties are greater than those of 1,2,4-oxadiazoles[43]. Even if the contribution of this

calculated difference is limited it could explain the MT_2 preference towards 1,3,4-oxadiazoles.

In the case of acidic azoles, the affinity constants of the compounds with a methylene linker **1.32**, **1.34**, **1.25**, **1.29** are all within the $2 \cdot 10^{-7}$ - $6 \cdot 10^{-7}$ M range for the MT_2 receptor, regardless of the azole or the bulk of the substituents in it. Conversely, their ethylene counterparts (**1.35**, **1.26**, **1.30**) show virtually no affinity at all for either receptor subtype, with the remarkable exception of **1.33** that turned out to be the most potent compound in the whole series of azoles. The 1,3,4-oxadiazolone ring of **1.33** can exist in two different tautomer forms (exemplified in figure 4 for **1.32**). Even if its NMR-characterization in DMSO shows a single species, the *keto* form, the presence of an equilibrium in physiological medium cannot be excluded. Moreover, the acidic nature of the heterocycle further confirmed by its differential solubility at different pHs could also imply the existence of equilibrium with the conjugated base in aqueous media. Melatonin solubility is reported to be around 430 µM in water[57]. In our experiment the solubility of melatonin was found to reach the mM range (6.64 mM) in buffer solution at pH 7.4. The solubility of **1.33** at pH 7.4 is lower, but within the same concentration range as melatonin. The bioisosteric replacement of the *N*-acetyl group of melatonin for 1,3,4-oxadiazolone represents a lower drop (~3-fold) in solubility than the indole-naftalene scaffold hopping (8-fold) what suggest a comparable degree of hydrophilicity of the 1,3,4-oxadiazolone ring and the acetamide at physiological pH. It is not possible to determine the exact contribution of the combination of hydrophilicity, acidity and plausible tautomerism to the binding of the compound since it adds a great degree of complexity to the interpretation of putative interactions within an already elusive binding pocket. Nevertheless, superimposition of **1.33** to the putative bioactive conformation of melatonin suggests that the nitrogen of the heterocycle closer to the ethylene spacer (the nitrogen in position 4), can

mimic the carbonyl of the amide group of melatonin (figure 12). Compounds **1.35**, **1.26** and **1.30** could be superimposed to the structure of melatonin in a similar manner; nevertheless none of them display any affinity for either MT_1 or MT_2. In the case of **1.34**, the sulfur atom that replaces for the carbonyl-like oxygen of **1.33** not only represents an additional bulk in the molecule, but also the acidity and the putative tautomeric equilibrium in aqueous media could be affected, and in turn be responsible for its lack of affinity. The same applies for compounds **1.26** and **1.30,** in which not only the nature of the azole is different, but also the substituent attached to it also represents a greater bulk more likely to be impeded by steric clashes within the receptor binding site.

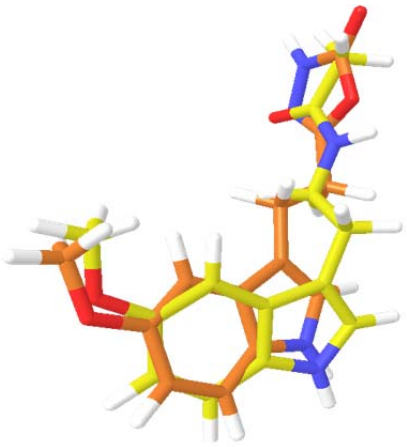

Figure 12. **1.33** (orange carbons) in its keto form superposed to melatonin (yellow carbons).

The promising profile of the slightly basic compound **1.31** encouraged us to try to broaden up the family of amino-thiadiazoles and amino-oxadiazoles, but unfortunately the synthetic approaches have failed with the exception of **1.31**. This compound showed the highest selectivity towards the MT_2 receptor of all compounds included in this work. Its binding affinity

constant for the MT_2 is similar to that of methylene-oxadiazoles **1.20** and **1.16,** with virtually no affinity for the MT_1. This selectivity could be attributed to the ability of the MT_2 receptor only to accommodate the ethylamino chain of **1.31** within the binding pocket.

Compound **1.36** shows a milder selectivity for the MT_2 than **1.31.** The pK_a of its non-methoxylated analogue is 8.68, what translates into a protonated state at physiological pH[58]. Therefore **1.36** should be mostly on its protonated state upon binding to melatonin receptors. MT_1 and MT_2 receptor models suggest the presence of a tyrosine residue (Tyr 298) on the transmembrane domain 7 that might be involved in a cation-π interaction with the protonated ending of the molecule[17]. The differential selectivity could be attributed to the ease of accommodating the bulky dimethylammonium group. The 2-[^{125}I]iodomelatonin displacement of **1.36** together with other basic tryptamines were already tested in hamster brain membranes[59]. The ability of **1.36** to displace the radioligand from brain binding sites was found to be 134-fold less than melatonin, and comparable to that of bufotenin (*N,N*-dimethyl-5-hydroxytryptamine) or 5-methoxytryptamine. In our case a similar decrease in affinity was found at the MT_2 subtype (100-fold). Besides its well-known agonistic properties at 5-HT receptors[60,61], this methoxylated tryptamine is also able to partially activate both melatonin receptors, being 2-fold more efficient at MT_1. Provided the hypothermic effect elicited by melatonin[62], this finding, arises question on whether the hypothermia observed in rats pretreated with a 5-HT_{2A} antagonists, could be mediated not only via 5-HT_{1A}, but also via melatonergic receptors[40].

In contrast to the differences found in the binding affinity of all tested compounds bearing a five-membered ring, their functional profile is markedly similar and appears unaffected by the nature of the azole employed to replace for the acetamido chain of melatonin. Whilst the potency varies depending on the compound, they all retain the mild MT_2 subtype preference, and are

partial agonists with an E_{max} that barely goes above the 30% relative to melatonin at either receptor subtype. This class of compounds, upon binding to MT_2, presumably fit their heterocyclic substituent in the pocket where the amide of melatonin is placed as depicted above (exemplified for **1.20** and **1.33** in figures 10 and 12)**.** Nevertheless the relatively low binding affinity of these compounds suggests that either the accommodation of the azole ring in the region occupied by the acetyl group of melatonin is hampered by some steric clash, or that this accommodation is secondary to some alteration in the proper arrangement of the 5-methoxyindol-3-ylalkyl portion, possible impeding the conformational changes that lead to receptor activation, resulting in the observed partial agonism.

Conclusions

We have synthesized and characterized different retroamides, azoles, and the hallucinogenic alkaloid 5-methoxy-*N,N*-dimethyltryptamine at the melatonin receptors MT_1 and MT_2. This study allowed us to broaden up the spectrum of moieties with varying electronic configurations, molecular volume, and H-bond capability that can totally or partially replace for the *N*-acetyl group of melatonin, especially at MT_2 receptors. The most conservative approach, the retroamide replacement, has proven to be the best approach being all the synthesized analogues potent at either melatonin receptor subtype. In the case of oxadiazoles, both 1,3,4- and 1,2,4-isomers are able to substitute for the acetamide moiety, retaining the ability to bind the melatonergic receptors. Bigger differences within the series can be observed in the case of azoles able to intervene as hydrogen bond donors, being all its representatives devoid of significant affinity with the exception of **1.33** and **1.31.** Unfortunately the synthetic efforts employed to broaden up the amino-(oxa/thia)diazole family failed, but its only member selectivity profile appears

promising. Derivative **1.33** represents a good starting point for further SAR studies that could help in the understanding of molecular recognition exerted by the melatonin receptors MT_1 and MT_2.

In this work we have been very conservative in keeping the 5-methoxyindole moiety so as to maintain the *N*-acetyl chain as the only source of structural diversity among the synthesized ligands, and the sole point of comparison to the natural ligand, melatonin. Additional melatonin-binding sites and receptors have been identified[63]. As abovementioned the polar nitrogen in position N1 can be suppressed without negatively-affecting the affinity of the ligands for the melatonergic receptors MT_1 and MT_2. Nevertheless, this hydrogen could potentially be essential in the recognition of melatonin by other systems not yet fully characterized but responsible for the pleiotropic actions of the pineal neurohormone. In this respect, the bioisosteres synthesized in this work could expand the scope of bioisosterism application to other not-so-well characterized systems.

Our results highlight once more the importance of the acetamido moiety of melatonergic ligands in the activation of melatonin receptors, and opens the door for development of novel ligands with different pharmacological profiles by modulation of the interaction with the locus where the acetamido moiety of melatonin is accommodated in melatonin receptors. We have demonstrated how the replacement of the acetamido moiety for certain azoles can modulate the activation of the receptor yielding compounds with different pharmacological profiles. Integration of the acetamide bioisosteric groups developed in this work in other validated aromatic or heteroaromatic scaffolds could open up a plethora of possibilities in the development of new melatonergic ligands of MT_1 and specially MT_2 receptors.

Experimental section

Chemistry. **General Methods.** Reagents and solvents were purchased from common commercial suppliers and were used without further purification. Analytical thin-layer chromatography (TLC) was carried out using Merck silica gel 60 F254 plates, and the compounds were visualized under UV-light (λ = 254 or 365 nm) and/or stained with phosphomolybdic acid 10% wt. in ethanol. Automatized chromatographic separation was carried out in a IsoleraOne (Biotage) using different silica Si50 cartridges from Agilent Technologies. High-performance liquid chromatography was performed on a Waters analytical HPLC-MS (Alliance Watters 2690) equipped with a SunFire C_{18} 4.6 x 50 mm column, a UV photodiode array detector (λ = 214–274 nm) and cuadrupole mass spectrometer (Micromass ZQ). HPLC analyses were used to confirm the purity of all compounds (>95%) and were performed on Waters 6000 equipment, at a flow rate of 1.0 mL/min, with a UV photodiode array detector (λ = 214–274 nm), and using a Delta Pak C_{18} 5 μm, 300 Å column. The elution was performed in a gradient mixture of MeCN/water.

Melting points (uncorrected) were determined in a MP70 apparatus (Mettler Toledo). ^{1}H NMR and ^{13}C NMR spectra were recorded in $CDCl_3$ or DMSO-d_6 solutions using the following NMR spectrometers: Varian INOVA-300, Varian INOVA-400, Varian Mercury-400 or Varian Unity-500. Chemical shifts are reported in δ scale (ppm) relative to internal Me_4Si. *J* values are given in hertz, and spin multiplicities are expressed as s (singlet), d (doublet), t (triplet), q (quartet), or m (multiplet). Mass spectra (MS) were obtained by electron spray ionization (ESI) in positive mode using a Hewlett-Packard MSD 1100 spectrometer. Elemental analyses were carried out in a Perkin-Elmer 240C equipment in the Centro de Química Orgánica 'Manuel Lora-Tamayo' (CSIC) and the results are within ± 0.4% of the theoretical values.

Synthesis of amides. General procedure.

The corresponding acid (1 mmol) is dissolved in dry acetonitrile (MeCN, 20 mL). Carbonyldiimidazole (CDI, 1.2 mmol) and a catalytic amount of dimethylaminopyridine (DMAP, 0.01 mmol) are then added. After stirring for 2h at 50ºC, the corresponding unsaturated amine is added to the solution. After stirring for 2 additional hours at room temperature (r.t.) the solvent is evaporated. The resulting crude is resuspended in HCl 1M (20 mL), and the suspension extracted with ethyl acetate (EtOAc, 3 x 20 mL). The combined organic layers were washed with NaOH 2M (3 x 20 mL), dried over anhydrous $MgSO_4$, and concentrated in vacuo to yield the corresponding amide.

***N*-propargyl-2-(5-methoxy-1*H*-indol-3-yl)-acetamide (1.8).**

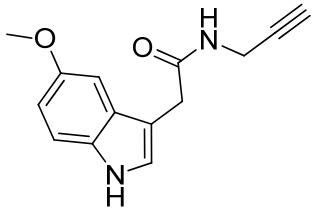

According to the general procedure for the preparation of amides, from 2-(5-methoxy-1*H*-indol-3-yl)acetic acid (200 mg, 1 mmol) and propargylamine (0.64 mL, 1 mmol), **1.8** (146 mg, 61%) was obtained as a white solid of mp: 117 – 118ºC. ^{1}H NMR (300 MHz, $CDCl_3$) δ 8.35 (s, 1H), 7.25 (d, *J* = 8.8 1H), 7.17 – 7.05 (m, 2H), 6.85 (dd, *J* = 8.7, 2.5 Hz, 1H), 6.66 (s, 1H), 4.21 (s, 2H), 3.85 (s, 3H), 2.26 (s, 3H). ^{13}C NMR (75 MHz, $CDCl_3$) δ 161.52, 155.48, 144.90, 133.81, 128.38, 129.21, 124.04, 112.82, 112.72, 109.16, 106.68, 56.87, 28.43, 13.14. HRMS (ESI$^+$): *m/z* calcd for $C_{14}H_{14}N_2O_2$ $(M)^+$ 242.1055, found 242.1063. HPLC purity 100% (230 to 400 nm).

***N*-propargyl-3-(5-methoxy-1*H*-indol-3-yl)-propanamide (1.9).**

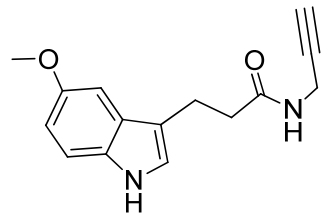

According to the general procedure for the preparation of amides, from 3-(5-methoxy-1*H*-indol-3-yl)propanoic acid (192 mg, 1 mmol) and propargylamine (0.71 mL, 1.1 mmol), **1.9** (160 mg, 65%) was obtained as a white solid of mp: 118 – 119°C. ^{1}H NMR (300 MHz, DMSO) δ 10.57 (s, 1H), 8.29 (s, 1H), 7.18 (d, *J* = 8.7 Hz, 1H), 7.02 (s, 1H), 6.97 (s, 1H), 6.68 (d, *J* = 8.6 Hz, 1H), 3.90 – 3.80 (m, 2H), 3.74 (s, 3H), 3.09 – 3.07 (t, *J* = 2.7 Hz , 1H), 2.85 (t, *J* = 7.7 Hz, 2H), 2.42 (t, *J* = 6.8 Hz, 2H). ^{13}C NMR (75 MHz, Acetone-d_6) δ 173.16, 155.26, 133.31, 129.32, 124.06, 115.76, 113.29, 112.93, 101.79, 82.19, 72.44, 56.54, 37.93, 29.38, 22.53. HRMS (ESI$^+$): *m/z* calcd for $C_{15}H_{16}N_2O_2$ $(M)^+$ 256.1212, found 256.1202. HPLC purity 97% (230 to 400 nm).

***N*-allyl-2-(5-methoxy-1*H*-indol-3-yl)acetamide (1.10).**

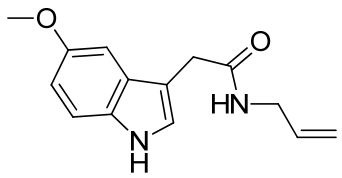

According to the general procedure for the preparation of amides, from 2-(5-methoxy-1*H*-indol-3-yl)acetic acid (168 mg, 0.84 mmol) and allylamine (92 µL, 1.26 mmol), **1.10** (178 mg, 86%) was obtained as a yellow oil that crystalised upon standing. Mp: 92 – 93°C. ^{1}H NMR (300 MHz, DMSO) δ 10.71 – 10.66 (s, 1H), 8.05 – 7.97 (m, 1H), 7.24 – 7.19 (d, *J* = 8.7 Hz, 1H), 7.14 – 7.12 (d, *J* = 2.2 Hz, 1H), 7.07 – 7.04 (d, *J* = 2.3 Hz, 1H), 6.74 – 6.67 (dd, *J* = 8.7, 2.4 Hz, 1H), 5.85 – 5.70 (ddt, *J* = 17.1, 10.3, 5.2 Hz, 1H), 5.12 – 5.05 (dd, *J* = 17.2, 1.8 Hz, 1H), 5.03 – 4.97 (dd, *J* = 10.3, 1.7 Hz, 1H), 3.74 – 3.72 (s, 3H), 3.71 – 3.66 (m, 2H), 3.48 – 3.48 (s, 2H). ^{13}C NMR (75 MHz, DMSO) δ 170.51, 152.96, 135.49, 131.21, 127.49, 124.42, 114.85, 111.90, 111.04, 108.61, 100.53, 55.30, 40.90, 32.70.HRMS (ESI$^+$): *m/z* calcd for $C_{14}H_{16}N_2O_2$ $(M)^+$ 244.1212, found 244.1202. HPLC purity 100% (230 to 400 nm).

***N*-allyl-3-(5-methoxy-1*H*-indol-3-yl)propanamide (1.11).**

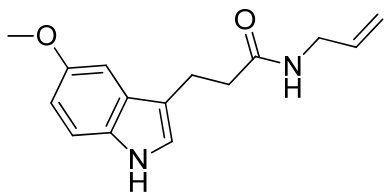

According to the general procedure for the preparation of amides, from 3-(5-methoxy-1*H*-indol-3-yl)propanoic acid (80 mg, 0.36 mmol) and allylamine (40 µL, 0.54 mmol), **1.11** (81 mg, 87%) was obtained as a brownish solid of mp: 173 – 174°C. ^{1}H NMR (300 MHz, DMSO) δ 10.62 – 10.54 (s, 1H), 8.03 – 7.93 (t, *J* = 5.5 Hz, 1H), 7.22 – 7.16 (d, *J* = 8.7 Hz, 1H), 7.05 – 7.01 (d, *J* = 2.3 Hz, 1H), 6.99 – 6.97 (d, *J* = 2.4 Hz, 1H), 6.72 – 6.66 (dd, *J* = 8.7, 2.4 Hz, 1H), 5.83 – 5.69 (ddt, *J* = 17.2, 10.3, 5.2 Hz, 1H), 5.11 – 4.98 (m, 2H), 3.76 – 3.74 (s, 3H), 3.71 – 3.65 (tt, *J* = 5.6, 1.7 Hz, 2H), 2.92 – 2.83 (t, *J* = 7.7 Hz, 2H), 2.48 – 2.41 (t, *J* = 7.7 Hz, 2H). ^{13}C NMR (75 MHz, DMSO) δ 172.08, 153.25, 135.87, 131.72, 127.66, 123.14, 115.30, 113.98, 112.25, 111.34, 100.62, 55.72, 41.18, 36.48, 21.44. HRMS (ESI^{+}): *m/z* calcd for $C_{15}H_{18}N_2O_2$ $(M)^{+}$ 258.1368, found 258.1370. HPLC purity 100% (230 to 400 nm).

Synthesis of oxazoles.

5-((5-methoxy-1*H*-indol-3-yl)methyl)-2-methyloxazole (1.12).

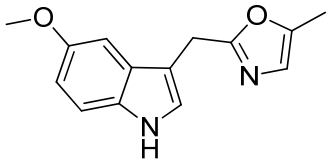

To a solution of **1.8** (100 mg, 0.41 mmol) in 10 mL of dry dichloromethane was added gold(III) chloride (12 mg, 0.041 mmol). The resulting mixture was stirred at r.t. under inert atmosphere for 18 h. After this time, triethylamine (TEA, 0.5 mL) was added and the reaction mixture was filtered over a short plug of silica gel eluting with EtOAc. The solvent was evaporated and the resulting oil chromatographed on silica (gradient Hexane: EtOAc) to afford **1.12** (18 mg, 18%) as a coloured solid of mp: 106 – 108°C. ^{1}H NMR (300 MHz, $CDCl_3$) δ 8.35

(s, 1H), 7.25 (d, *J* = 8.8 1H), 7.17 – 7.05 (m, 2H), 6.85 (dd, *J* = 8.7, 2.5 Hz, 1H), 6.66 (s, 1H), 4.21 (s, 2H), 3.85 (s, 3H), 2.26 (s, 3H). ^{13}C NMR (75 MHz, $CDCl_3$) δ 161.52, 155.48, 144.90, 133.81, 128.38, 129.21, 124.04, 112.82, 112.72, 109.16, 106.68, 56.87, 28.43, 13.14. HRMS (ESI^+): *m/z* calcd for $C_{14}H_{14}N_2O_2$ $(M)^+$ 242.1055, found 242.1055. HPLC purity 100% (230 to 400 nm).

5-(2-(5-methoxy-1H-indol-3-yl)ethyl)-2-methyloxazole (1.13).

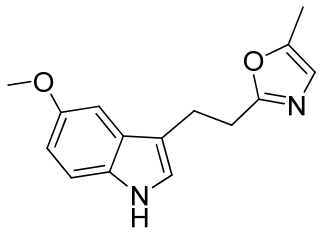

Starting from **1.9** (30 mg, 0.11 mmol), the compound was synthesized according to the procedure described for **1.8,** and thus **1.13** (11 mg, 38%) obtained as a light brown solid of mp: 100 – 105ºC. ^{1}H NMR (300 MHz, $CDCl_3$) δ 7.94 (s, 1H), 7.25 (d, *J* = 8.8 Hz, 1H), 7.03 (d, *J* = 2.3 Hz, 1H), 7.00 (s, 1H), 6.86 (dd, *J* = 8.8, 2.4 Hz, 1H), 6.64 (s, 1H), 3.87 (s, 3H), 3.24 – 3.17 (m, 2H), 3.11 (ddd, *J* = 9.4, 6.1, 2.0 Hz, 2H) 2.29 (s, 3H). ^{13}C NMR (75 MHz, $CDCl_3$) δ 166.32, 155.90, 145.49, 131.08, 127.71, 128.10, 123.63, 112.61, 111.72, 110.01, 105.79, 55.46, 28.28, 24.97, 12.43. HRMS (ESI^+): *m/z* calcd for $C_{15}H_{16}N_2O_2$ $(M)^+$ 256.1212, found 256.1209. HPLC purity 95% (230 to 400 nm).

Synthesis of esters.

Ethyl 2-(5-methoxy-1*H*-indol-3-yl)acetate (1.14).

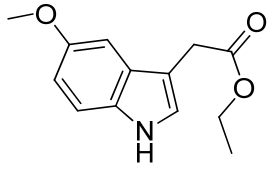

To a solution of acid 2-(5-methoxy-1*H*-indol-3-yl)acetic acid (3.5 g, 17.07 mmol) in 50 mL of EtOH was added 25 drops of concentrated sulfuric acid. The mixture was heated under reflux for 2 h, cooled to room temperature, neutralized with a solution of NaOH 2M, and evaporated in vacuo. The residue was resuspended in water (40 mL) and extracted with

EtOAc (3 x 40 mL). Removal of the solvent under reduced pressure gave **1.14** (3.42 mg, 86%) as a light yellow solid. ^{1}H NMR (300 MHz, DMSO) δ 10.77 (s, 1H), 7.23 (d, *J* = 8.7 Hz, 1H), 7.19 (d, *J* = 2.3 Hz, 1H), 6.98 (d, *J* = 2.4 Hz, 1H), 6.72 (dd, *J* = 8.7, 2.4 Hz, 1H), 4.07 (q, *J* = 7.1 Hz, 2H), 3.74 (s, 3H), 3.68 (s, 2H), 1.18 (t, *J* = 7.1 Hz, 3H). ^{13}C NMR (75 MHz, DMSO) δ 171.52, 153.06, 131.19, 127.38, 124.61, 112.04, 111.19, 106.75, 100.27, 59.98, 55.26, 30.89, 14.14. HPLC-MS (230 to 400 nm) 100% (*m/z*) [MH^{+}] 234.44

Ethyl 3-(5-methoxy-1*H*-indol-3-yl)propanoate (1.15).

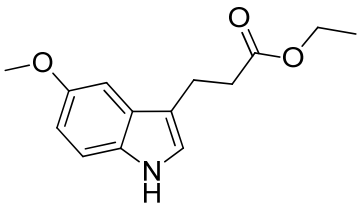

5-methoxy-1*H*-indole (5.0 g, 34 mmol) was placed in a dry flask and dissolved in dichloromethane (DCM, 40 mL) and ethyl acrylate (21.7 mL, 0.2 mol) added. Finally anhydrous $ZrCl_4$ (1.0 g, 4.29 mmol) is added to the solution. The mixture is kept stirring at r.t. for 18h, after which the catalyst is filtered off and the solvent and excess of ethyl acrylate are removed under vacuum and collected in a cold trap. The resulting crude was chromatographed on silica (gradient DCM: MeOH) to afford **1.15** (6.1 g, 71%) as a white pearly solid. ^{1}H NMR (300 MHz, $CDCl_3$) δ 7.88 (s, 1H), 7.24 (d, *J* = 8.8 Hz, 1H), 7.04 (d, *J* = 2.3 Hz, 1H), 6.99 (s, 1H), 6.86 (dd, *J* = 8.8, 2.4 Hz, 1H), 4.15 (q, *J* = 7.1 Hz, 2H), 3.87 (s, 3H), 3.07 (t, *J* = 7.7 Hz, 2H), 2.71 (t, *J* = 7.6 Hz, 2H), 1.25 (t, *J* = 7.1 Hz, 3H). ^{13}C NMR (75 MHz, $CDCl_3$) δ 173.40, 153.93, 131.38, 127.55, 122.12, 114.77, 112.22, 111.77, 100.56, 60.32, 55.92, 34.81, 20.60, 14.19. HPLC-MS (230 to 400 nm) 100% (*m/z*) [MH^{+}] 248.06.

Synthesis of 1,2,4-Oxadiazoles

5-((5-methoxy-1*H*-indol-3-yl)methyl)-3-methyl-1,2,4-oxadiazole (1.16).

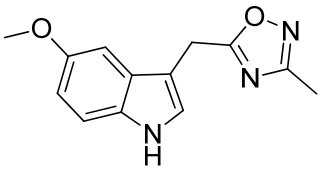

Acetamidoxime (95 mg, 1.3 mmol), 1.5 g of molecular sieves (3Å), and sodium hydride (61 mg, 2.5 mmol) are suspended in anhydrous THF (4 mL) and stirred at 50°. After stirring for 2h, **1.14** (150 mg, 0.64 mmol) is slowly added to the mixture dissolved in 2 mL of THF that is kept with gentle stirring for 18h. The mixture is then filtered and the solids washed with EtOAc (10 mL). The filtrate is evaporated under vacuum and the crude obtained chromatographed on silica (gradient DCM: MeOH) to afford **1.16** (87 mg, 56%) as a brownish solid of mp: 100 – 102°C. ^{1}H NMR (300 MHz, $CDCl_3$) δ 8.01 (s, 1H), 7.30 – 7.23 (m, 1H), 7.20 (d, *J* = 2.6 Hz, 1H), 7.05 (d, *J* = 2.4 Hz, 1H), 6.88 (dd, *J* = 8.8, 2.4 Hz, 1H), 4.31 (s, 2H), 3.86 (s, 3H), 2.37 (s, 3H). ^{13}C NMR (75 MHz, $CDCl_3$) δ 178.23, 167.24, 154.38, 131.23, 127.15, 123.74, 112.89, 112.06, 107.76, 100.33, 55.88, 23.26, 11.60. HRMS (ESI^+): *m/z* calcd for $C_{13}H_{13}N_3O_2$ $(M)^+$ 243.1017, found 243.1008. HPLC purity 100% (230 to 400 nm).

5-(2-(5-methoxy-1*H*-indol-3-yl)ethyl)-3-methyl-1,2,4-oxadiazole (1.17).

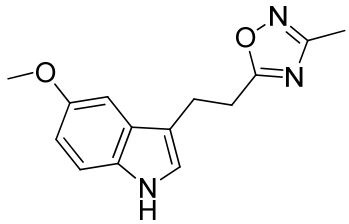

Starting from **1.15** (173 mg, 0.7 mmol), the compound was synthesized according to the procedure described for **1.16,** and thus **1.17** (80 mg, 45%) obtained as an off-white solid of mp: 75 – 76°C. ^{1}H NMR (400 MHz, DMSO) δ 10.66 (s, 1H), 7.21 (d, *J* = 8.7 Hz, 1H), 7.09 (d, *J* = 2.4 Hz, 1H), 6.99 (d, *J* = 2.4 Hz, 1H), 6.71 (dd, *J* = 8.7, 2.4 Hz, 1H), 3.76 (s, 3H), 3.23 (t, *J* = 7.2 Hz, 2H), 3.12 (t, *J* = 7.4 Hz, 2H), 2.30 (s, 3H). ^{13}C NMR (101 MHz, DMSO) δ 180.04, 167.35, 153.71, 131.95, 127.73, 123.90, 112.82, 112.73, 111.95, 100.54, 55.99, 27.40, 22.58, 11.80.

HRMS (ESI$^+$): *m/z* calcd for $C_{14}H_{15}N_3O_2$ $(M)^+$ 257.1164, found 257.1172. HPLC purity 100% (230 to 400 nm).

Synthesis of hydrazides.

2-(5-methoxy-1*H*-indol-3-yl)acetohydrazide (1.18).

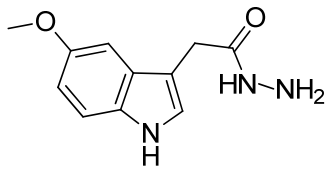

A mixture of **1.14** (1.53 g, 6.5 mmol), and excess of hydrazine hydrate (5 mL) in EtOH (6 mL) was heated to 155°C for 45 min under microwave irradiation. After removing the solvent, the milky crude is resuspended in water (70 mL) and extracted with EtOAc (6 x 50 mL). The extracts were dried over anhydrous magnesium sulfate and solvent removed to give **1.18** (1.40 g, 98%) as a white solid. ^{1}H NMR (300 MHz, DMSO) δ 10.71 – 10.62 (s, 1H), 9.12 – 9.05 (s, 1H), 7.23 – 7.17 (d, *J* = 8.7 Hz, 1H), 7.14 – 7.08 (d, *J* = 2.3 Hz, 1H), 7.08 – 7.04 (d, *J* = 2.3 Hz, 1H), 6.73 – 6.64 (dd, *J* = 8.7, 2.4 Hz, 1H), 4.19 – 4.15 (s, 2H), 3.75 – 3.73 (s, 3H), 3.40 – 3.38 (s, 2H). ^{13}C NMR (75 MHz, DMSO) δ 170.13, 152.94, 131.16, 127.48, 124.31, 111.83, 110.92, 108.41, 100.71, 55.35, 30.74. HPLC-MS (230 to 400 nm) 100% (*m/z*) [MH$^+$] 220.11.

3-(5-methoxy-1*H*-indol-3-yl)propanehydrazide (1.19).

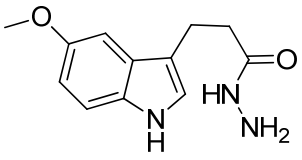

Starting from **1.15** (3.0 g, 12.1 mmol), the compound was synthesized according to the procedure described for **1.18,** and thus **1.19** (2.8 g, 100%) was obtained as an off-white solid. ^{1}H NMR (300 MHz, DMSO) δ 10.59 (s, 1H), 9.00 (s, 1H), 7.20 (d, *J* = 8.7 Hz, 1H), 7.01 (dd, *J* = 17.7, 2.3 Hz, 1H), 6.70 (dd, *J* = 8.7, 2.4 Hz, 1H), 4.18 (s, 2H), 3.76 (s, 3H), 2.87 (t, *J* =

8.1 Hz, 2H), 2.37 (t, *J* = 7.8 Hz, 2H). HPLC-MS (230 to 400 nm) 96% (*m/z*) [MH^+] 234.08.

Synthesis of 1,3,4-Oxadiazoles. General procedure.

The corresponding hydrazide (0.5 mmol) is suspended in an excess of the corresponding orthoester (1 mL) and a catalytic amount of acetic acid (1 drop)is added. The mixture is heated in a microwave system for 1h at 125ºC. Then the excess of the orthoester is rotoevaporated and the crude chromatographed on silica (gradient DCM:MeOH) and thus the corresponding 1,3,4-oxadiazole was obtained.

2-((5-methoxy-1*H*-indol-3-yl)methyl)-5-methyl-1,3,4-oxadiazole (1.20).

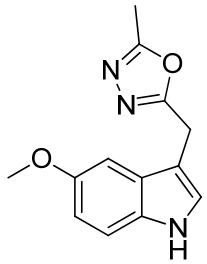

According to the general procedure for the preparation of 1,3,4-oxadiazoles, from **1.18** (100 mg, 0.45 mmol), triethyl orthoacetate (1 mL) and a catalytic amount of acetic acid, **1.20** (71 mg, 64%) is obtained a brownish solid of mp: 139 – 140ºC. ^{1}H NMR (300 MHz, $CDCl_3$) δ 8.33 (s, 1H), 7.25 (d, *J* = 8.8 Hz, 1H), 7.14 (s, 1H), 7.06 (d, *J* = 2.2 Hz, 1H), 6.86 (dd, *J* = 8.8, 2.4 Hz, 1H), 4.27 (s, 2H), 3.84 (s, 3H), 2.44 (s, 3H). ^{13}C NMR (75 MHz, $CDCl_3$) δ 165.95, 163.93, 154.25, 131.26, 127.15, 123.78, 112.75, 112.09, 107.86, 100.24, 55.85, 22.09, 10.94. HRMS (ESI^+): *m/z* calcd for $C_{13}H_{13}N_3O_2$ $(M)^+$ 243.1008, found 243.1017. HPLC purity 100% (230 to 400 nm).

2-(2-(5-methoxy-1*H*-indol-3-yl)ethyl)-5-methyl-1,3,4-oxadiazole (1.21).

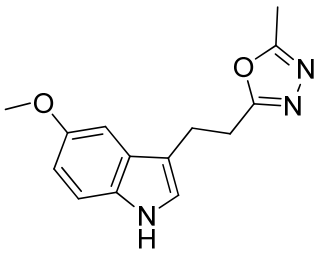

According to the general procedure for the preparation of 1,3,4-oxadiazoles, from **1.19** (405 mg, 1.74 mmol), triethyl orthoacetate (3.5 mL) and a catalytic amount of acetic acid **1.21** (257 mg, 57%) is obtained a brownish solid of mp: 156 – 157°C. ^{1}H NMR (300 MHz, $CDCl_3$) δ 7.91 (s, 1H), 7.26 (d, *J* = 8.8 Hz, 1H), 7.03 (s, 1H), 6.99 (d, *J* = 2.4 Hz, 1H), 6.87 (dd, *J* = 8.8, 2.4 Hz, 1H), 3.87 (s, 3H), 3.24 – 3.20 (m, *J* = 4.7 Hz, 4H), 2.48 (s, 3H). ^{13}C NMR (75 MHz, $CDCl_3$) δ 166.79, 163.64, 154.05, 131.37, 127.39, 122.40, 113.78, 112.34, 111.95, 100.28, 55.93, 26.17, 22.34, 10.90. HRMS (ESI$^+$): *m/z* calcd for $C_{14}H_{15}N_3O_2$ $(M)^+$ 257.1164, found 257.1158. HPLC purity 100% (230 to 400 nm).

2-(2-(5-methoxy-1*H*-indol-3-yl)ethyl)-1,3,4-oxadiazole (1.22).

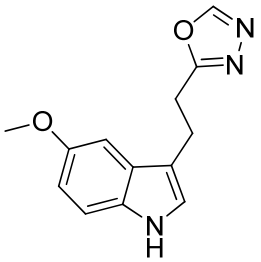

According to the general procedure for the preparation of 1,3,4-oxadiazoles, from **1.19** (120 mg, 0.5 mmol), trimethyl orthoformiate (1 mL) and a catalytic amount of acetic acid **1.22** (41 mg, 34%) is obtained an off-white solid of mp: 148 – 149°C. ^{1}H NMR (300 MHz, DMSO) δ 9.73 (s, 1H), 8.40 (s, 1H), 7.18 (d, *J* = 8.8 Hz, 1H), 6.92 (d, *J* = 2.5 Hz, 1H), 6.87 (d, *J* = 2.5 Hz, 1H), 6.71 (dd, *J* = 8.7, 2.5 Hz, 1H), 3.76 (s, 3H), 3.23 – 3.14 (m, 4H). ^{13}C NMR (75 MHz, DMSO) δ 165.54, 152.51, 152.08, 130.55, 126.06, 121.78, 111.40, 111.15, 110.63, 98.79, 54.71, 24.99, 21.28. HRMS (ESI$^+$): *m/z* calcd for $C_{13}H_{13}N_3O_2$ $(M)^+$ 243.1008, found 243.1014. HPLC purity 98% (230 to 400 nm).

Acyl(thio)semicarbazides. General method.

The corresponding hydrazide (1 mmol) is dissolved in EtOH (10 mL) and then, the corresponding isocyanate or isothiocyanate (1 mmol) is added. The mixture is kept stirring until the reaction is finished, typically after 1h in the case of methylisocyanate. Longer times were needed in the case of ethylisothiocyanate. After the reaction time, solvent is removed and the resulting solid used as such in the next step.

1-(2-(5-methoxy-1*H*-indol-3-yl)acetyl)-4-methylsemicarbazide (1.23).

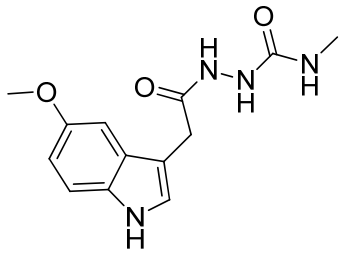

According to the general method for the preparation of acylsemicarbazides, from **1.18** (73 mg, 0.33 mmol) and methylisocyanate (21 µL, 0.33 mmol), after one hour stirring, **1.23** (91 mg, 99%) was obtained as a white solid. HPLC-MS (230 to 400 nm) 97% (*m/z*) [MH^+] 277.37

1-(3-(5-methoxy-1*H*-indol-3-yl)propanoyl)-4-methylsemicarbazide (1.24).

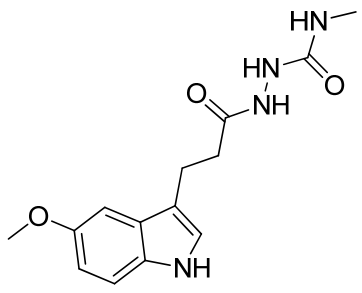

According to the general method for the preparation of acylsemicarbazides, from **1.19** (230 mg, 0.98 mmol) and methylisocyanate (68 µL, 1 mmol), after one hour stirring, **1.24** (290 mg, 100%) was obtained as a white solid. HPLC-MS (230 to 400 nm) 98% (*m/z*) [MH^+] 291.40.

1-(2-(5-methoxy-1*H*-indol-3-yl)acetyl)-4-ethylsemithiocarbazide (1.27).

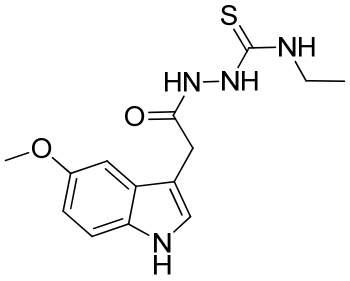

According to the general method for the preparation of acylthiosemicarbazides, from **1.18** (116 mg, 0.5 mmol) and ethylisothiocyanate (44 µL, 0.5 mmol), after 18h stirring, **1.27** (150 mg, 94%) was obtained as a white solid. HPLC-MS (230 to 400 nm) 99% (m/z) [MH+] 307.37.

1-(3-(5-methoxy-1*H*-indol-3-yl)propanoyl)-4-ethylsemithiocarbazide (1.28).

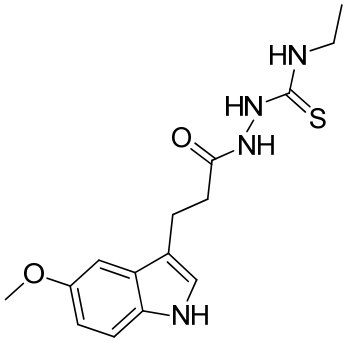

According to the general method for the preparation of acylthiosemicarbazides, from **1.19** (506 mg, 2.17 mmol) and ethylisothiocyanate (190 µL, 2.17 mmol), after 18h stirring, **1.28** (707 mg, 100%) was obtained as a white solid. HPLC-MS (230 to 400 nm) 90% (m/z) [MH+] 321.26.

Synthesis of 1,2,4-triazol-5-(thi)ones. General method.

The corresponding acylsemicarbazide or acylsemithiocarbazide (1 mmol) is dissolved in EtOH (10 mL) and NaOH 2M (7 mL) is added. The mixture is heated under microwave irradiation at 100ºC for 15 min. The solvent is evaporated and the crude redisolved in water. The mixture is progressively acidified to pH 2 with conc. HCl, thus the corresponding triazole precipitates off the solution and is collected by filtration. When necessary, the precipitate was chromatographed in silica (gradient DCM:MeOH) for further purification.

3-((5-methoxy-1*H*-indol-3-yl)methyl)-4-methyl-1*H*-1,2,4-triazol-5(4H)-one (1.25).

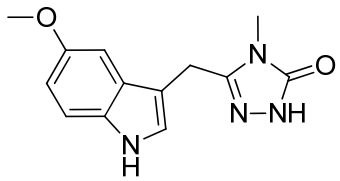

According to the general method for the synthesis of 1,2,4-triazol-5-ones, from **1.23** (82 mg, 0.3 mmol), **1.25** (58 mg, 75%) was obtained as a light orange pearly solid mp: 218 – 219°C. ^{1}H NMR (300 MHz, DMSO) δ 11.41 (s, 1H), 10.82 (s, 1H), 7.25 (d, *J* = 8.8 Hz, 1H), 7.20 (d, *J* = 2.3 Hz, 1H), 7.01 (d, *J* = 2.4 Hz, 1H), 6.74 (dd, *J* = 8.8, 2.4 Hz, 1H), 3.95 (s, 2H), 3.72 (s, 3H), 2.98 (s, 3H). ^{13}C NMR (75 MHz, DMSO) δ 155.65, 153.43, 147.20, 131.77, 127.50, 124.77, 112.51, 111.54, 107.40, 100.68, 55.65, 26.88, 22.86. HRMS (ESI^{+}): *m/z* calcd for $C_{13}H_{14}N_4O_2$ $(M)^{+}$ 258.1117, found 258.1113. HPLC purity 100% (230 to 400 nm).

3-(2-(5-methoxy-1*H*-indol-3-yl)ethyl)-4-methyl-1*H*-1,2,4-triazol-5(4H)-one (1.26).

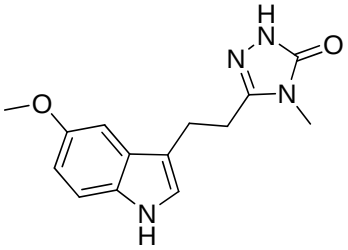

According to the general method for the synthesis of 1,2,4-triazol-5-ones, from **1.26** (290 mg, 1 mmol) and after chromatographic purification on silica, **1.26** (110 mg, 41%) was obtained as a white powder of mp 201 – 202 °C. ^{1}H NMR (500 MHz, DMSO) δ 11.38 (s, 1H), 10.67 (d, *J* = 3.0 Hz, 1H), 7.22 (d, *J* = 8.7 Hz, 1H), 7.12 (d, *J* = 2.4 Hz, 1H), 6.94 (d, *J* = 2.4 Hz, 1H), 6.70 (dd, *J* = 8.7, 2.4 Hz, 1H), 3.75 (s, 3H), 3.01 (s, 3H), 2.98 (t, 2H), 2.82 (t, 2H). ^{13}C NMR (126 MHz, DMSO-d_6) δ 155.65, 153.39, 148.13, 131.70, 127.66, 123.70, 113.24, 112.45, 111.60, 100.26, 55.68, 26.75, 26.73, 21.74. HRMS (ESI^{+}): Calcd. for $C_{14}H_{16}N_4O_2$ $(M)^{+}$ 272.1283, found *m/z* 272.1273. HPLC purity 100% (230 to 400 nm).

4-ethyl-3-((5-methoxy-1*H*-indol-3-yl)methyl)-1*H*-1,2,4-triazole-5(4H)-thione (1.29).

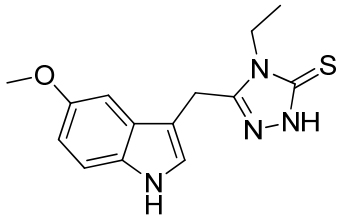

According to the general method for the synthesis of 1,2,4-triazol-5-thiones, from **1.27** (40 mg, 0.13 mmol), **1.29** (30 mg, 80%) was obtained as a shiny brownish solid of mp: 200 - 203 ^{o}C. ^{1}H NMR (300 MHz, DMSO) δ 13.51 (s, 1H), 10.88 (s, 1H), 7.27 (d, *J* = 3.2 Hz, 1H), 7.25 (d, *J* = 3.2 Hz, 1H), 6.99 (d, *J* = 2.3 Hz, 1H), 6.74 (dd, *J* = 8.8, 2.4 Hz, 1H), 4.16 (s, 2H), 3.90 (q, *J* = 7.0 Hz, 2H), 3.72 (s, 3H), 0.94 (t, *J* = 7.1 Hz, 3H). ^{13}C NMR (75 MHz, DMSO) δ 166.63, 153.49, 151.61, 131.74, 127.43, 125.08, 112.60, 111.58, 107.29, 100.64, 55.65, 38.62, 22.22, 13.23. HRMS (ESI^{+}): *m/z* calcd for $C_{14}H_{16}N_4OS$ $(M)^{+}$ 288.1045, found 288.1036. HPLC purity 100% (230 to 400 nm)

4-ethyl-3-(2-(5-methoxy-1*H*-indol-3-yl)ethyl)-1*H*-1,2,4-triazole-5(4H)-thione (1.30).

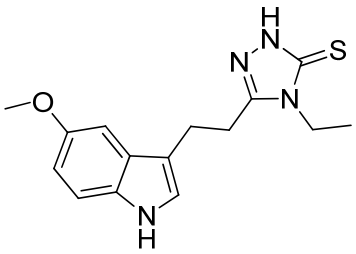

According to the general method for the synthesis of 1,2,4-triazol-5-thiones, from **1.28** (200 mg, 0.62 mmol), and after chromatographic purification on silica **1.30** (140 mg, 84%) was obtained as a white powder of mp: 214 – 217^{o}C. ^{1}H NMR (500 MHz, DMSO) δ 13.52 (s, 1H,), 10.68 (d, *J* = 2.7 Hz, 1H), 7.22 (d, *J* = 8.7 Hz, 1H), 7.14 (d, *J* = 2.4 Hz, 1H), 6.96 (d, *J* = 2.4 Hz, 1H), 6.70 (dd, *J* = 8.7, 2.4 Hz, 1H), 3.91 (q, *J* = 7.2 Hz, 2H), 3.75 (s, 3H), 3.06 – 3.02 (m, 2H), 3.02 – 2.97 (m, 2H), 1.14 (t, *J* = 7.2 Hz, 3H). ^{13}C NMR (126 MHz, DMSO) δ 166.26, 153.42, 152.45, 131.69, 127.60, 123.77, 113.04, 112.48, 111.66, 100.24, 55.69, 38.40, 26.15, 22.05, 13.77. HRMS (ESI^{+}): Calcd for $C_{15}H_{18}N_4OS$ $(M)^{+}$ 302.1201, found *m/z* 302.1207. HPLCMS (230 to 400 nm) 98% (*m/z*) (M^{+}) 303.28

Synthesis of amino-1,3,4-thiadiazol 1.31.

***N*-ethyl-5-((5-methoxy-1*H*-indol-3-yl)methyl)-1,3,4-thiadiazol-2-amine (1.31).**

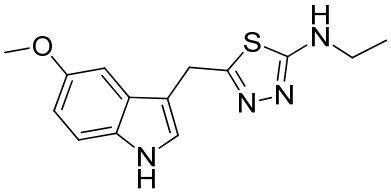

$POCl_3$ (1 mL) was added over **1.27** (92 mg, 0.3 mmol) and the mixture kept stirring at r.t. for 18h. After this time water (10 mL) was carefully added to the mixture and then basified at 0°C to pH 9-10 with NaOH 2M. The mixture was extracted with EtOAc (3 x 20 mL), and the extracts dried over $MgSO_4$. After evaporation of the solvent **1.31** (58 mg, 67%) was recovered as an off-white solid of mp: 136 – 139°C. ^{1}H NMR (500 MHz, DMSO) δ 10.79 (s, 1H), 7.40 (t, *J* = 5.3 Hz, 1H), 7.23 (d, *J* = 8.7 Hz, 1H), 7.21 (d, *J* = 2.5 Hz, 1H), 6.94 (d, *J* = 2.4 Hz, 1H), 6.72 (dd, *J* = 8.7, 2.4 Hz, 1H), 4.19 (s, 2H), 3.70 (s, 3H), 3.18 (qd, *J* = 7.2, 5.3 Hz, 2H), 1.09 (t, *J* = 7.2 Hz, 3H). ^{13}C NMR (126 MHz, DMSO) δ 168.98, 159.10, 153.54, 131.84, 127.39, 124.74, 112.63, 111.64, 110.96, 100.72, 55.76, 39.63, 26.47, 14.74. HRMS (ESI$^+$): Calcd. for $C_{14}H_{16}N_4OS$ $(M)^+$ 288.1045, found *m/z* 288.1050. HPLC-MS (230 to 400 nm) 95% (*m/z*) [MH^+] 289.40.

Synthesis of 1,3,4-oxadiazol-2-(thio)ones

5-((5-methoxy-1*H*-indol-3-yl)methyl)-1,3,4-oxadiazol-2(3H)-one (1.32).

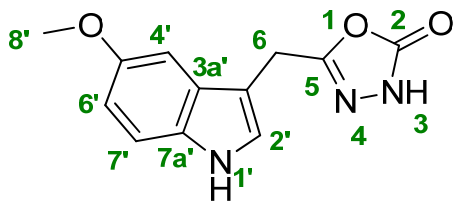

A mixture of **1.18** (86 mg, 0.4 mmol), CDI (76 mg, 0.47 mmol), TEA (0.11 mL, 0.8 mmol) dissolved in THF is heated to 100°C for 15 min. Solvent was evaporated and the residue is resuspended in a small amount of water (2 mL), basified to pH 12-13 with NaOH (conc.) and filtered. The filtrate was collected and acidified with HCl

(conc.) and thus, the compound precipitates. The precipitate was filtered off to afford **1.32** (72 mg, 73%) as a white pearly solid of mp: 140 – 141°C. ^{1}H NMR (300 MHz, DMSO) δ 12.08 (s, 1H, N3), 10.89 (s, 1H, N1′), 7.26 (d, *J* = 6.1 Hz, 1H, H7′), 7.24 (s, 1H, H2′), 7.00 (d, *J* = 2.3 Hz, 1H, H4′), 6.74 (dd, *J* = 8.8, 2.4 Hz, 1H, H6′), 3.97 (s, 2H, H6′), 3.73 (s, 3H, H8′). ^{13}C NMR (75 MHz, DMSO) δ 156.46 (C5), 155.07 (C2), 153.18 (C5′), 131.24 (C7a′), 127.03 (C3a′), 124.78 (C2′), 112.22 (C7′), 111.27 (C6′), 105.87 (C3′), 100.11 (C4′), 55.30 (C8′), 22.54 (C6). HRMS (ESI^{+}): *m/z* calcd for $C_{12}H_{11}N_3O_3$ $(M)^{+}$ 245.0800, found 246.0802. HPLC purity 100% (230 to 400 nm).

5-(2-(5-methoxy-1*H*-indol-3-yl)ethyl)-1,3,4-oxadiazol-2(3H)-one (1.33).

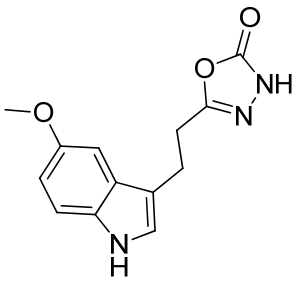

Starting from **1.19** (146 mg, 0.62 mmol), the compound was synthesized according to the procedure described for **1.32,** and thus **1.33** (138 mg, 86%) was obtained as an off-white solid of mp: 140 – 144°C. ^{1}H NMR (400 MHz, DMSO) δ 12.00 (s, 1H), 10.66 (s, 1H), 7.20 (d, *J* = 8.7 Hz, 1H), 7.09 (d, *J* = 2.3 Hz, 1H), 6.95 (d, *J* = 2.4 Hz, 1H), 6.69 (dd, *J* = 8.7, 2.4 Hz, 1H), 3.74 (s, 3H), 2.97 (t, *J* = 7.4 Hz, 2H), 2.85 (t, *J* = 7.7 Hz, 2H). ^{13}C NMR (101 MHz, DMSO) δ 157.65, 155.77, 153.70, 131.92, 127.77, 124.00, 112.76, 112.72, 111.93, 100.36, 55.92, 27.55, 21.54. HRMS (ESI^{+}): *m/z* calcd for $C_{13}H_{13}N_3O_3$ $(M)^{+}$ 259.0957, found 259.0966. HPLC purity 100% (230 to 400 nm).

5-((5-methoxy-1*H*-indol-3-yl)methyl)-1,3,4-oxadiazole-2(3H)-thione (1.34).

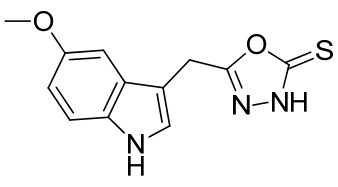

A mixture of **1.18** (83 mg, 0.37 mmol), KOH (70 mg, 1.24 mmol) and an excess of carbon disulfide (1.35 mL, 38 mmol) in EtOH was heated to 155°C

for 10 min under microwave irradiation. Solvent and carbon disulfide excess was evaporated under reduced pressure and the residue resuspended in water. The solution was acidified with conc. HCl and **1.34** (91 mg, 95%) precipitated as a yellow solid that was filtered off. Mp: 171 – 173°C. ^{1}H NMR (300 MHz, DMSO) δ 14.37 – 14.29 (s, 1H), 10.95 – 10.88 (s, 1H), 7.29 – 7.24 (d, *J* = 11.8 Hz, 1H), 7,28—7.27 (s, 1H), 7.02 – 6.99 (d, *J* = 2.3 Hz, 1H), 6.77 – 6.72 (dd, *J* = 8.8, 2.4 Hz, 1H), 4.18 – 4.15 (s, 2H), 3.74 – 3.72 (s, 3H). ^{13}C NMR (75 MHz, DMSO) δ 177.73, 163.44, 153.25, 131.23, 126.94, 125.01, 112.28, 111.38, 105.39, 100.08, 55.31, 21.74. HRMS (ESI^{+}): *m/z* calcd for $C_{12}H_{11}N_3O_2S$ $(M)^{+}$ 261.0572, found 261.0577. HPLC purity 100% (230 to 400 nm).

5-(2-(5-methoxy-1*H*-indol-3-yl)ethyl)-1,3,4-oxadiazole-2(3H)-thione (1.35).

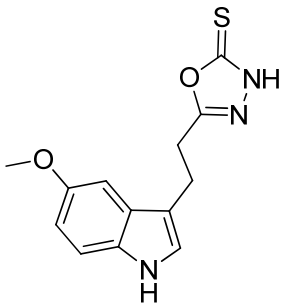

Starting from **1.19** (116 mg, 0.5 mmol), the compound was synthesized according to the procedure described for **1.34,** and thus **1.35** (56 mg, 41%) was obtained as an off-white solid of mp: 99 – 101°C. ^{1}H NMR (400 MHz, DMSO) δ 14.29 (s, 1H), 10.70 (d, *J* = 2.6 Hz, 1H), 7.21 (d, *J* = 8.7 Hz, 1H), 7.11 (d, *J* = 2.4 Hz, 1H), 6.97 (d, *J* = 2.4 Hz, 1H), 6.70 (dd, *J* = 8.7, 2.4 Hz, 1H), 3.76 (s, 3H), 3.10 – 2.97 (m, 4H). ^{13}C NMR (101 MHz, DMSO) δ 177.69, 164.05, 153.08, 131.25, 127.06, 123.38, 112.12, 111.84, 111.37, 99.70, 55.31, 26.14, 21.05. HRMS (ESI^{+}): *m/z* calcd for $C_{13}H_{13}N_3O_2S$ $(M)^{+}$ 275.0728, found 275.0726. HPLC purity 95% (230 to 400 nm).

Assays for MT_1 and MT_2 receptor subtypes. 2-[^{125}I]Iodomelatonin (2200 Ci/mmol) was purchased from NEN (Boston, MA). Other drugs and chemicals were purchased from Sigma–Aldrich (Saint Quentin, France).

2-[^{125}I]Iodomelatonin binding assay conditions were essentially as previously described[64]. Briefly, binding was initiated by addition of membrane preparations from transfected CHO cells stably expressing the human melatonin MT_1 or MT_2 diluted in binding buffer (50 mM Tris–HCl buffer, pH 7.4, containing 5 mM $MgCl_2$) to 2-[^{125}I]iodomelatonin (20 pM for MT_1 and MT_2 receptors expressed in CHO cells) and the tested drug. Non-specific binding was defined in the presence of 1 μM melatonin. After 120 min incubation at 37 °C, reaction was stopped by rapid filtration through GF/B filters presoaked in 0.5% (v/v) polyethylenimine. Filters were washed three times with 1 mL of ice-cold 50 mM Tris–HCl buffer, pH 7.4.

Data from the dose–response curves (seven concentrations in duplicate) were analysed using the program PRISM (Graph Pad Software Inc., San Diego, CA) to yield IC_{50} (inhibitory concentration 50). Results are expressed as K_i with $K_i = IC_{50}/1 + ([L]/K_D)$, where [L] is the concentration of radioligand used in the assay and K_D, the dissociation constant of the radioligand characterizing the membrane preparation.

[^{35}S]GTPγS binding assay was performed according to published methodology[64]. Briefly, membranes from transfected CHO cells expressing MT_1 and MT_2 receptor subtypes and compounds were diluted in binding buffer (20 mM HEPES, pH 7.4, 100 mM NaCl, 3 μM GDP, 3 mM $MgCl_2$, and 20 μg/mL saponin). Incubation was started by the addition of 0.2 nM [^{35}S]GTPγS to membranes (20 μg/mL) and drugs, and further followed for 1 h at room temperature. Reaction was stopped by rapid filtration through GF/B filters followed by three successive washes with ice-cold buffer.

Usual levels of [^{35}S]GTPγS binding (expressed in dpm) were for CHO-MT_2 membranes: 2000 for basal activity, 8000 in the presence of melatonin 1 μM and 180 in the presence of GTPγS 10 μM which defined the non-specific binding. Data from the dose–response curves (seven concentrations in

duplicate) were analyzed by using the program PRISM (Graph Pad Software Inc., San Diego, CA) to yield EC_{50}, with EC_{50} the effective concentration 50%) and E_{max} (maximal effect) for agonists.

Thermodinamic solubility determination.

UV maximums are extracted from recorded UV-spectrum of the compounds in the 270-400 nm range. A 10 mM stock solution of the corresponding compound in DMSO is prepared. A calibration line is built by measuring the absorbance at the corresponding maximum wavelength of sequential dilutions of the stock solution in buffer-MeCN (80:20) mixture in a 96-well plate containing 200 µL per point. The buffers employed are: pH 1.2 KCl 45 mM buffer, pH 7.4 phosphate 45 mM buffer and pH 9.4 NH_4Cl buffer. In order to validate the calibration line, and exclude interferences due to the presence of 5% DMSO, a quality control standard of known concentrations is employed. The calibration line is accepted if $R^2>0.990$, the residual value of each point <15% and the relative error of the quality control standard <15%. The solubility determination is made as follows: 200 µL of buffer solution are added over approximately 1 mg accurately weighted of the corresponding compound in order to achieve a saturated solution. The mixture is kept at room temperature in an orbital stirrer at 320 rpm for 24h and then centrifuged at 135 rpm for 15 min. 160 µL of the supernatant are transferred to a 96-well plate and diluted with 40 µL of a buffer-MeCN (80:20) mixture. The solubility is determinated by extrapolation to the calibration line within the linearity range and expressed in mol/L. The expermients were run in triplicates.

Superimposition computational studies.

Compounds were built with Maestro 9.2[65] and subjected to an energy minimization procedure using the OPLS2005[66] force field to a convergence threshold of 0.05 kJ mol^{-1} $Å^{-1}$. Compounds were superposed to the putative bioactive conformation of melatonin[11] having torsion angles: τ1 (C3a–C3–Cβ–Cα) ≈ -90°; τ2(C3–Cβ–Cα–N) ≈ 180°; τ3(Cβ–Cα–N–CO) ≈ 180°. Superposed atoms are: methoxy oxygens, C3a, C5 and C7 of the benzene ring of indoles and the amide oxygen of melatonin superposed to the N atom within the five-membered cycles.

Bibliography

(1) Zlotos, D. P.; Jockers, R.; Cecon, E.; Rivara, S.; Witt-Enderby, P. a MT1 and MT2 Melatonin Receptors: Ligands, Models, Oligomers, and Therapeutic Potential. *J. Med. Chem.* **2013**, in press.

(2) Pala, D.; Lodola, A.; Bedini, A.; Spadoni, G.; Rivara, S. Homology Models of Melatonin Receptors: Challenges and Recent Advances. *Int. J. Mol. Sci.* **2013**, *14*, 8093–8121.

(3) Maeda, S.; Schertler, G. F. Production of GPCR and GPCR Complexes for Structure Determination. *Curr. Opin. Struct. Biol.* **2013**, *23*, 381–392.

(4) Pala, D.; Beuming, T.; Sherman, W.; Lodola, A.; Rivara, S.; Mor, M. Structure-Based Virtual Screening of MT2 Melatonin Receptor: Influence of Template Choice and Structural Refinement. *J. Chem. Inf. Model.* **2013**, *53*, 821–835.

(5) Dubocovich, M. L.; Delagrange, P.; Krause, D. N.; Sugden, D.; Cardinali, D. P.; Olcese, J. International Union of Basic and Clinical Pharmacology. LXXV. Nomenclature, Classification, and Pharmacology of G Protein-Coupled Melatonin Receptors. *Pharmacol. Rev.* **2010**, *62*, 343–380.

(6) Kokkola, T.; Foord, S. M.; Watson, M.-A.; Vakkuri, O.; Laitinen, J. T. Important Amino Acids for the Function of the Human MT1 Melatonin Receptor. *Biochem. Pharmacol.* **2003**, *65*, 1463–1471.

(7) Conway, S.; Mowat, E. S.; Drew, J. E.; Barrett, P.; Delagrange, P.; Morgan, P. J. Serine Residues 110 and 114 Are Required for Agonist Binding but Not Antagonist Binding to the Melatonin MT1 Receptor. *Biochem. Biophys. Res. Commun.* **2001**, *282*, 1229–1236.

(8) Mazna, P.; Obsilova, V.; Jelinkova, I.; Balik, A.; Berka, K.; Sovova, Z.; Ettrich, R.; Svoboda, P.; Obsil, T.; Teisinger, J. Molecular Modeling of Human MT2 Melatonin Receptor: The Role of Val204, Leu272 and Tyr298 in Ligand Binding. *J. Neurochem.* **2004**, *91*, 836–842.

(9) Mazna, P.; Berka, K.; Jelinkova, I.; Balik, A.; Svoboda, P.; Obsilova, V.; Obsil, T.; Teisinger, J. Ligand Binding to the Human MT2 Melatonin Receptor: The Role of Residues in Transmembrane Domains 3, 6, and 7. *Biochem. Biophys. Res. Commun.* **2005**, *332*, 726–734.

(10) Mor, M.; Rivara, S.; Pala, D.; Bedini, A.; Spadoni, G.; Tarzia, G. Recent Advances in the Development of Melatonin MT(1) and MT(2) Receptor Agonists. *Expert Opin. Ther. Pat.* **2010**, *20*, 1059–1077.

(11) Rivara, S.; Diamantini, G.; Di Giacomo, B.; Lamba, D.; Gatti, G.; Lucini, V.; Pannacci, M.; Mor, M.; Spadoni, G.; Tarzia, G. Reassessing the Melatonin pharmacophore—Enantiomeric Resolution, Pharmacological Activity, Structure Analysis, and Molecular Modeling of a Constrained Chiral Melatonin Analogue. *Bioorg. Med. Chem.* **2006**, *14*, 3383–3391.

(12) Jansen, J. M.; Copinga, S.; Gruppen, G.; Molinari, E. J.; Dubocovich, M. L.; Grol, C. J. The High Affinity Melatonin Binding Site Probed with Conformationally Restricted ligands—I. Pharmacophore and Minireceptor Models. *Bioorg. Med. Chem.* **1996**, *4*, 1321–1332.

(13) Mor, M.; Rivara, S.; Silva, C.; Bordi, F.; Plazzi, P. V; Spadoni, G.; Diamantini, G.; Balsamini, C.; Tarzia, G.; Fraschini, F.; Lucini, V.; Nonno, R.; Stankov, B. M. Melatonin Receptor Ligands: Synthesis of New Melatonin Derivatives and Comprehensive Comparative Molecular Field Analysis (CoMFA) Study. *J. Med. Chem.* **1998**, *41*, 3831–3844.

(14) Descamps-François, C.; Yous, S.; Chavatte, P.; Audinot, V.; Bonnaud, A.; Boutin, J. A.; Delagrange, P.; Bennejean, C.; Renard, P.; Lesieur, D. Design and Synthesis of Naphthalenic Dimers as Selective MT1 Melatoninergic Ligands. *J. Med. Chem.* **2003**, *46*, 1127–1129.

(15) Depreux, P.; Lesieur, D.; Mansour, H. A.; Morgan, P.; Howell, H. E.; Renard, P.; Caignard, D.-H.; Pfeiffer, B.; Delagrange, P. Synthesis and Structure-Activity Relationships of Novel Naphthalenic and Bioisosteric Related Amidic Derivatives as Melatonin Receptor Ligands. *J. Med. Chem.* **1994**, *37*, 3231–3239.

(16) Uchikawa, O.; Fukatsu, K.; Tokunoh, R.; Kawada, M.; Matsumoto, K.; Imai, Y.; Hinuma, S.; Kato, K.; Nishikawa, H.; Hirai, K.; Miyamoto, M.; Ohkawa, S. Synthesis of a Novel Series of Tricyclic Indan Derivatives as Melatonin Receptor Agonists. *J. Med. Chem.* **2002**, *45*, 4222–4239.

(17) Rivara, S.; Lorenzi, S.; Mor, M.; Plazzi, P. V.; Spadoni, G.; Bedini, A.; Tarzia, G. Analysis of Structure-Activity Relationships for MT2 Selective Antagonists by Melatonin MT1 and MT2 Receptor Models. *J. Med. Chem.* **2005**, *48*, 4049–4060.

(18) Dubocovich, M. Luzindole (N-0774): A Novel Melatonin Receptor Antagonist. *J. Pharmacol. Exp. Ther.* **1988**, *246*, 902–910.

(19) Laudon, M.; Zisapel, N. Characterization of Central Melatonin Receptors Using 125I-Melatonin. *FEBS Lett.* **1986**, *197*, 9–12.

(20) Vakkuri, O.; Lämsä, E.; Rahkamaa, E.; Ruotsalainen, H.; Leppäluoto, J. Iodinated Melatonin: Preparation and Characterization of the Molecular Structure by Mass and 1H NMR Spectroscopy. *Anal. Biochem.* **1984**, *142*, 284–289.

(21) Bissantz, C.; Kuhn, B.; Stahl, M. A Medicinal Chemist's Guide to Molecular Interactions. *J. Med. Chem.* **2010**, *53*, 5061–5084.

(22) Waring, M. J. Lipophilicity in Drug Discovery. *Expert Opin. Drug Discov.* **2010**, *5*, 235–248.

(23) Arnott, J. A.; Planey, S. L. The Influence of Lipophilicity in Drug Discovery and Design. *Expert Opin. Drug Discov.* **2012**, *7*, 863–875.

(24) Ritchie, T. J.; Macdonald, S. J. F. The Impact of Aromatic Ring Count on Compound Developability – Are Too Many Aromatic Rings a Liability in Drug Design? *Drug Discov. Today* **2009**, *14*, 1011–1020.

(25) Dubocovich, M. L.; Masana, M. I.; Iacob, S.; Sauri, D. M. Melatonin Receptor Antagonists That Differentiate between the Human Mel1a and Mel1b Recombinant Subtypes Are Used to Assess the Pharmacological Profile of the Rabbit Retina ML1 Presynaptic Heteroreceptor. *Naunyn. Schmiedebergs. Arch. Pharmacol.* **1997**, *355*, 365–375.

(26) Ettaoussi, M.; Sabaouni, A.; Rami, M.; Boutin, J. A.; Delagrange, P.; Renard, P.; Spedding, M.; Caignard, D.-H.; Berthelot, P.; Yous, S. Design, Synthesis and Pharmacological Evaluation of New Series of Naphthalenic Analogues as Melatoninergic (MT1/MT2) and Serotoninergic 5-HT2C Dual Ligands (I). *Eur. J. Med. Chem.* **2012**, *49*, 310–23.

(27) Leclerc, V.; Fourmaintraux, E.; Depreux, P.; Lesieur, D.; Morgan, P.; Howell, H. E.; Renard, P.; Caignard, D. H.; Pfeiffer, B.; Delagrange, P.; Guardiola-Lemaître, B.; Andrieux, J. Synthesis and Structure-Activity Relationships of Novel Naphthalenic and Bioisosteric Related Amidic Derivatives as Melatonin Receptor Ligands. *Bioorg. Med. Chem.* **1998**, *6*, 1875–1887.

(28) Brown, N. *Bioisosteres in Medicinal Chemistry*; Brown, N., Ed.; Wiley-VCH Verlag GmbH & Co. KGaA: Weinheim, Germany, 2012.

(29) Meanwell, N. A. Synopsis of Some Recent Tactical Application of Bioisosteres in Drug Design. *J. Med. Chem.* **2011**, *54*, 2529–2591.

(30) Lima, L. M.; Barreiro, E. J. Bioisosterism: A Useful Strategy for Molecular Modification and Drug Design. *Curr. Med. Chem.* **2005**, *12*, 23–49.

(31) Patani, G. A.; LaVoie, E. J. Bioisosterism: A Rational Approach in Drug Design. *Chem. Rev.* **1996**, *96*, 3147–3176.

(32) Laudon, M. Putative Melatonin Receptors in Benign Human Prostate Tissue. *J. Clin. Endocrinol. Metab.* **1996**, *81*, 1336–1342.

(33) Willis, G. L. The Role of ML-23 and Other Melatonin Analogues in the Treatment and Management of Parkinson's Disease. *Drug News Perspect.* **2005**, *18*, 437–444.

(34) Laudon, M.; Peleg-Shulgman, T. Pyrone-Indole Derivatives and Process for Their Preparation. US 7,635,710 B2, 2009.

(35) He, P.; Ouyang, X.; Zhou, S.; Yin, W.; Tang, C.; Laudon, M.; Tian, S. A Novel Melatonin Agonist Neu-P11 Facilitates Memory Performance and Improves Cognitive Impairment in a Rat Model of Alzheimer' Disease. *Horm. Behav.* **2013**, *64*, 1–7.

(36) Tian, S.; Laudon, M.; Han, L.; Gao, J.; Huang, F.; Yang, Y.; Deng, H. Antidepressant- and Anxiolytic Effects of the Novel Melatonin Agonist Neu-P11 in Rodent Models. *Acta Pharmacol. Sin.* **2010**, *31*, 775–783.

(37) Rami, M.; Landagaray, E.; Ettaoussi, M.; Boukhalfa, K.; Caignard, D.-H.; Delagrange, P.; Berthelot, P.; Yous, S. Novel Conformationally Constrained

Analogues of Agomelatine as New Melatoninergic Ligands. *Molecules* **2012**, *18*, 154–166.

(38) Hardeland, R. Melatonin Metabolism in the Central Nervous System. *Curr. Neuropharmacol.* **2010**, *8*, 168–181.

(39) Ma, X.; Chen, C.; Krausz, K. W.; Idle, J. R.; Gonzalez, F. J. A Metabolomic Perspective of Melatonin Metabolism in the Mouse. *Endocrinology* **2008**, *149*, 1869–1879.

(40) Shen, H.-W.; Jiang, X.-L.; Winter, J. C.; Yu, A.-M. Psychedelic 5-Methoxy-N,N-Dimethyltryptamine: Metabolism, Pharmacokinetics, Drug Interactions, and Pharmacological Actions. *Curr. Drug Metab.* **2010**, *11*, 659–666.

(41) Pauletti, G. Improvement of Oral Peptide Bioavailability: Peptidomimetics and Prodrug Strategies. *Adv. Drug Deliv. Rev.* **1997**, *27*, 235–256.

(42) Choudhary, A.; Raines, R. T. An Evaluation of Peptide-Bond Isosteres. *Chembiochem* **2011**, *12*, 1801–7.

(43) Boström, J.; Hogner, A.; Llinàs, A.; Wellner, E.; Plowright, A. T. Oxadiazoles in Medicinal Chemistry. *J. Med. Chem.* **2011**, *55*, 1817–1830.

(44) Basarab, G. S.; Manchester, J. I.; Bist, S.; Boriack-Sjodin, P. A.; Dangel, B.; Illingworth, R.; Sherer, B. A.; Sriram, S.; Uria-Nickelsen, M.; Eakin, A. E. Fragment-to-Hit-to-Lead Discovery of a Novel Pyridylurea Scaffold of ATP Competitive Dual Targeting Type II Topoisomerase Inhibiting Antibacterial Agents. *J. Med. Chem.* **2002**, *56*, 8712–8735.

(45) Verniest, G.; England, D.; De Kimpe, N.; Padwa, A. Synthesis of Substituted B-Carbolines via gold(III)-Catalyzed Cycloisomerization of N-Propargylamides. *Tetrahedron* **2010**, *66*, 1496–1502.

(46) Verniest, G.; Padwa, A. Gold- and Silver-Mediated Cycloisomerizations of N-Propargylamides. *Org. Lett.* **2008**, *10*, 4379–4382.

(47) Yao, T.; Zhang, X.; Larock, R. C. AuCl3-Catalyzed Synthesis of Highly Substituted Furans from 2-(1-Alkynyl)-2-Alken-1-Ones. *J. Am. Chem. Soc.* **2004**, *126*, 11164–11165.

(48) Kumar, V.; Kaur, S.; Kumar, S. ZrCl4 Catalyzed Highly Selective and Efficient Michael Addition of Heterocyclic Enamines with A,β-Unsaturated Olefins. *Tetrahedron Lett.* **2006**, *47*, 7001–7005.

(49) Saitoh, M.; Kunitomo, J.; Kimura, E.; Iwashita, H.; Uno, Y.; Onishi, T.; Uchiyama, N.; Kawamoto, T.; Tanaka, T.; Mol, C. D.; Dougan, D. R.; Textor, G. P.; Snell, G. P.; Takizawa, M.; Itoh, F.; Kori, M. 2-{3-[4-(Alkylsulfinyl)phenyl]-1-Benzofuran-5-Yl}-5-Methyl-1,3,4-Oxadiazole Derivatives as Novel Inhibitors of Glycogen Synthase Kinase-3β with Good Brain Permeability. *J. Med. Chem.* **2009**, *52*, 6270–6286.

(50) Zoumpoulakis, P.; Camoutsis, C.; Pairas, G.; Soković, M.; Glamočlija, J.; Potamitis, C.; Pitsas, A. Synthesis of Novel Sulfonamide-1,2,4-Triazoles, 1,3,4-Thiadiazoles and 1,3,4-Oxadiazoles, as Potential Antibacterial and Antifungal Agents. Biological Evaluation and Conformational Analysis Studies. *Bioorg. Med. Chem.* **2012**, *20*, 1569–1583.

(51) Erdem, S. S. Synthesis and Electronic Structure of New Aryl-and Alkyl-Substituted 1, 3, 4-Oxadiazole-2-Thione Derivatives. *Turk J Chem* **2002**, *26*, 159–169.

(52) Zubets, I. V.; Vergizov, S. N.; Yakovlev, S. I.; V'yunov, K. A. Basicity and Mechanism of Transmission of Electronic Effects of Substituents in the Series of 2-Amino-5-Aryl-1,3,4-Thiadiazoles. *Chem. Heterocycl. Compd.* **1987**, *23*, 225–228.

(53) Conway, S.; Canning, S. J.; Howell, H. E.; Mowat, E. S.; Barrett, P.; Drew, J. E.; Delagrange, P.; Lesieur, D.; Morgan, P. J. Characterisation of Human Melatonin mt1 and MT2 Receptors by CRE-Luciferase Reporter Assay. *Eur. J. Pharmacol.* **2000**, *390*, 15–24.

(54) Bedini, A.; Lucarini, S.; Spadoni, G.; Tarzia, G.; Scaglione, F.; Dugnani, S.; Pannacci, M.; Lucini, V.; Carmi, C.; Pala, D.; Rivara, S.; Mor, M. Toward the Definition of Stereochemical Requirements for MT2-Selective Antagonists and Partial Agonists by Studying 4-Phenyl-2-Propionamidotetralin Derivatives. *J. Med. Chem.* **2011**, *54*, 8362–72.

(55) Mattson, R. J.; Catt, J. D.; Keavy, D.; Sloan, C. P.; Epperson, J.; Gao, Q.; Hodges, D. B.; Iben, L.; Mahle, C. D.; Ryan, E.; Yocca, F. D. Indanyl Piperazines as Melatonergic MT2 Selective Agents. *Bioorg. Med. Chem. Lett.* **2003**, *13*, 1199–1202.

(56) Durieux, S.; Chanu, A.; Bochu, C.; Audinot, V.; Coumailleau, S.; Boutin, J. A.; Delagrange, P.; Caignard, D. H.; Bennejean, C.; Renard, P.; Lesieur, D.; Berthelot, P.; Yous, S. Design and Synthesis of 3-Phenyltetrahydronaphthalenic Derivatives as New Selective MT2 Melatoninergic Ligands. Part II. *Bioorg. Med. Chem.* **2009**, *17*, 2963–2974.

(57) Sigma-Aldrich Co. LLC.

(58) O'Neil, M. J.; et al. The Merck Index - An Encyclopedia of Chemicals, Drugs, and Biologicals (14th Edition - Version 14.9) **2012**.

(59) Duncan, M. J.; Takahashi, J. S.; Dubocovich, M. L. 2-[125I]iodomelatonin Binding Sites in Hamster Brain Membranes: Pharmacological Characteristics and Regional Distribution. *Endocrinology* **1988**, *122*, 1825–1833.

(60) Glennon, R. A.; Titeler, M.; McKenney, J. D. Evidence for 5-HT2 Involvement in the Mechanism of Action of Hallucinogenic Agents. *Life Sci.* **1984**, *35*, 2505–2511.

(61) Nonaka, R.; Nagai, F.; Ogata, A.; Satoh, K. In Vitro Screening of Psychoactive Drugs by [(35)S]GTPgammaS Binding in Rat Brain Membranes. *Biol. Pharm. Bull.* **2007**, *30*, 2328–2333.

(62) Cagnacci, A.; Krauchi, K.; Wirz-Justice, A.; Volpe, A. Homeostatic versus Circadian Effects of Melatonin on Core Body Temperature in Humans. *J. Biol. Rhythms* **1997**, *12*, 509–517.

(63) Hardeland, R.; Cardinali, D. P.; Srinivasan, V.; Spence, D. W.; Brown, G. M.; Pandi-Perumal, S. R. Melatonin--a Pleiotropic, Orchestrating Regulator Molecule. *Prog. Neurobiol.* **2011**, *93*, 350–384.

(64) Audinot, V.; Mailliet, F.; Lahaye-Brasseur, C.; Bonnaud, A.; Le Gall, A.; Amossé, C.; Dromaint, S.; Rodriguez, M.; Nagel, N.; Galizzi, J.-P.; Malpaux, B.; Guillaumet, G.; Lesieur, D.; Lefoulon, F.; Renard, P.; Delagrange, P.; Boutin, J. A. New Selective Ligands of Human Cloned Melatonin MT1 and MT2 Receptors. *Naunyn. Schmiedebergs. Arch. Pharmacol.* **2003**, *367*, 553–61.

(65) Maestro, Version 9.2 Schrödinger, LLC, New York, NY, 2011.

(66) Jorgensen, W. L.; Maxwell, D. S.; Tirado-Rives, J. Development and Testing of the OPLS All-Atom Force Field on Conformational Energetics and Properties of Organic Liquids. *J. Am. Chem. Soc.* **1996**, *118*, 11225–11236.

Chapter 2

Neurogenesis studies on melatonin analogues

Introduction

The central nervous system of adult mammals has long been considered a complex static structure unable to undergo any regenerative process to refurbish dead nodes. This dogma was challenged by Altman in the 1960s and neuron self-renewal has been demonstrated ever since in many species including primates and humans[1–3]. The neurogenic process implies the proliferation of new cells, migration, cell differentiation, and integration within the neural circuitry. In lower vertebrates the neurogenic process is widely extended in the central nervous system, whereas in animals with higher brain complexity is restricted to a few regions[4]. In adult human brain neurogenesis is vestigial; only two brain region retain a significant continuous neurogenic turnover: the subventricular zone (SVZ) lining the lateral ventricles; and the subgranular zone (SGZ) which is a part of the dentate gyrus of hippocampus.

Hippocampus belongs to the limbic system and plays important roles in the consolidation of information from short-term memory to long-term memory and spatial navigation. Although the relevance of neurogenesis in

adult brain hippocampus remains to be determined, it seems to play a role in certain learning processes and memory consolidation[5]. Neurogenesis in the dentate gyrus is dynamic and responds to physiological, pathological and pharmacological stimuli[6]. Ageing, for instance, is associated with an exponential decrease in hippocampal neurogenesis[5]. Provided the decline in cell proliferation occurring in elder brain, the controlled stimulation of the endogenous neural stem cells from adult brain neurogenic niches might be able to counteract the memory and cognitive deterioration subsequent to age-related neurodegenerative diseases[7,8].

Melatonin plasma levels decline with age in a similar manner as the neurogenic rate does[9]. Whether both phenomena are related or not is still unclear, albeit melatonin has been reported to positively modulate neurogenesis[10]. Exogenous administration of melatonin increases precursor cell survival in hippocampus of mice, and promotes neuronal differentiation of neural precursors *in vitro*[11]. Its chronic administration increases the cell proliferation rate and delays the decline of the neurogenesis in the hippocampus of adult mice[12]. These data are in agreement with previous observations in different mice strains that concluded that exogenous melatonin administration does ameliorate the process of ageing, including a much better cognitive performance, and delays the onset of poor health states prior to death[13]. The term 'methuselah syndrome' was appropriately coined to summarize the health-preserving properties of the pineal neurohormone. Exploitation of these properties opens up a vast therapeutic potential in the development of melatonin-related cognitive-preserving agents and possibly in the field of regenerative medicine. Thus, we have explored the neurogenic potential of a selection of novel melatonin analogues, obtained in the previous chapter, using *in vitro* and *in vivo* experiments. The melatonergic agonists **1.9**, **1.21**, **1.31**, **1.33,** and **1.34** were selected (figure 1), covering different melatonergic profiles and structural features.

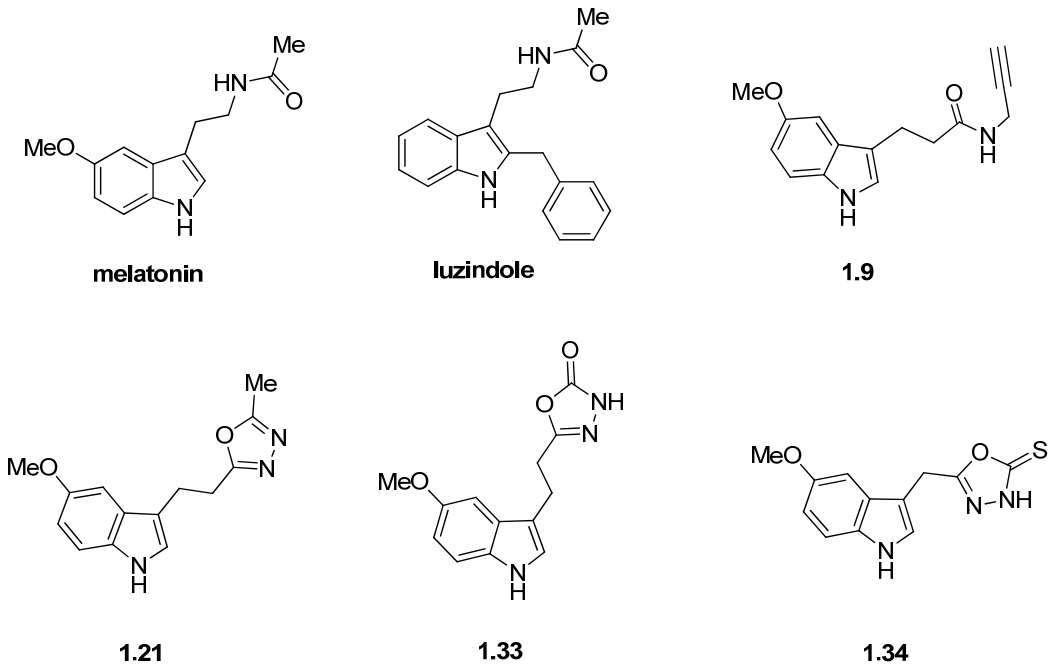

Figure 1. Compounds subject of study.

Results

In vitro neural differentiation and maturation in the presence of different melatonin analogues.

All selected melatonergic agonists (**1.9**, **1.21**, **1.31**, **1.33**, and **1.34**), together with melatonin, were screened at 10 μM in primary neural stem cells, which were obtained from the SGZ of the dentate gyrus of the hippocampus of adult Wistar rats and induced to proliferate as described in the experimental section. Their neurogenic potential of each compound was determined by direct observation of the expression of two immunostained markers, namely human β-tubulin III (Tuj1) and microtubule-associated protein 2 (MAP2). The nucleus of the cells was identified by staining with 4',6-diamidino-2-phenylindole (DAPI). Tuj1 is a structural protein expressed in

neurons of the peripheral and central nervous system (PNS, CNS) that contributes to microtubule stability in neuronal cell bodies and axons and plays a role in axonal transport[14]. Tuj1 is expressed in neural stem cells in the early stages of their differentiation to neurons. MAP2 is a neuronal cytoskeletal protein involved in microtubule stabilization responsible for the maintenance of neuronal morphology which expression is essential in early stages of neurogenesis[15]. Chronologically, Tuj1 is expressed at earlier stages of neural differentiation than MAP2. The expression of MAP2 in neurospheres indicates consolidated neuronal stage (figure 2)[16]. After incubation of SVZ neurospheres with the compounds for 7 days in culture, they were allowed to differentiate for 48h and finally, after immunostaining, the expression of Tuj1 and MAP2 was visualized by confocal microscopy (figures 3 and 4 respectively).

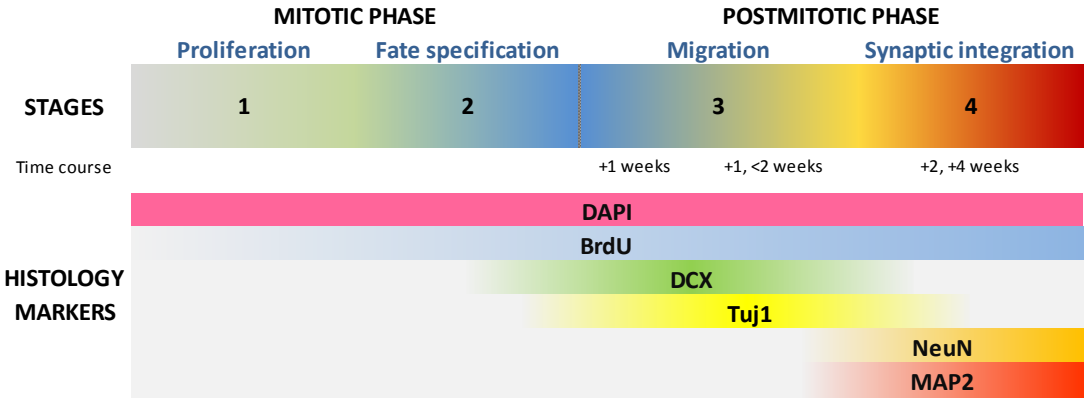

Figure 2. Sequencial phases in neuronal development *in vivo*, along with specific markers employed in this work to determine neural cell life-cycle phase. Adapted from Kempermann et al. 2004[17].

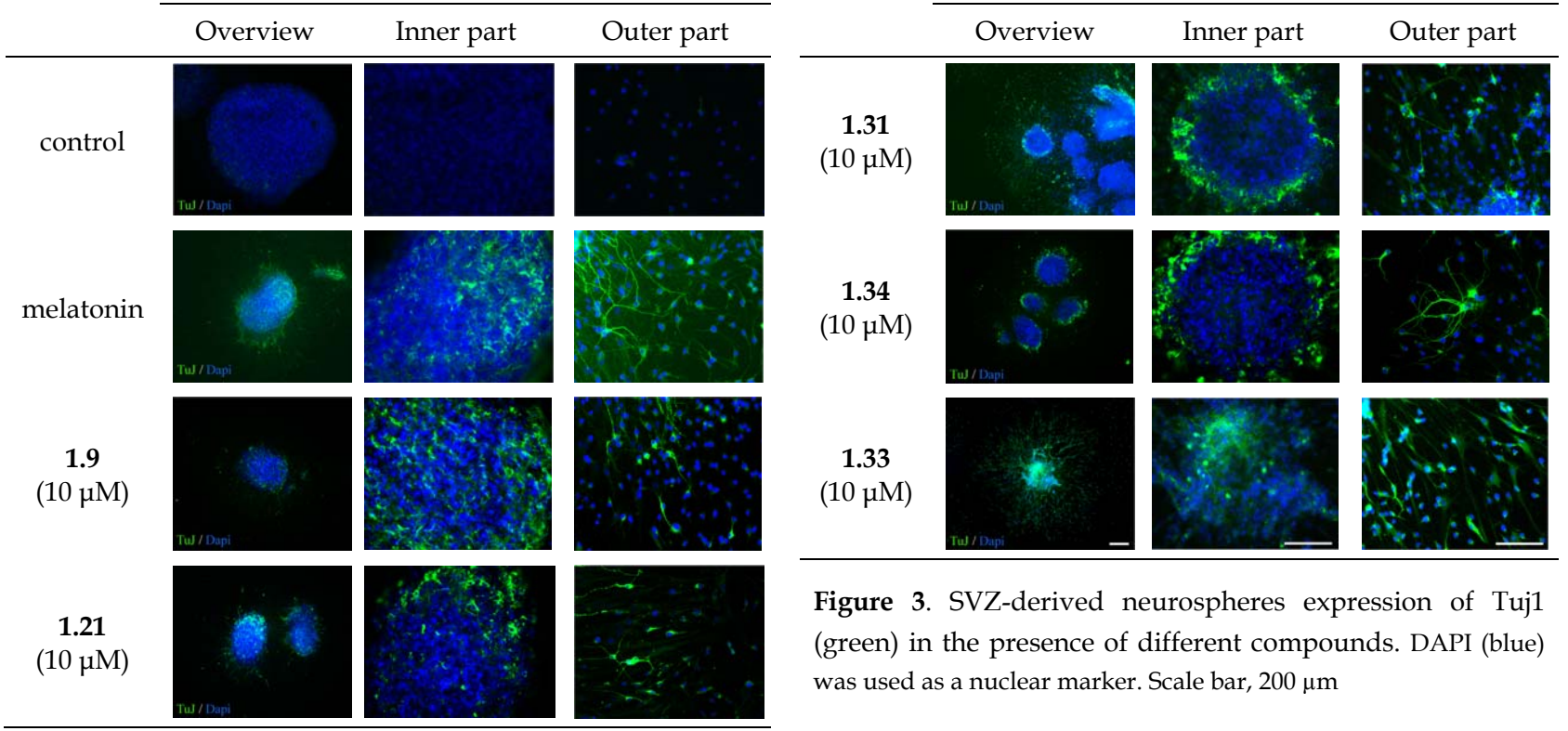

Figure 3. SVZ-derived neurospheres expression of Tuj1 (green) in the presence of different compounds. DAPI (blue) was used as a nuclear marker. Scale bar, 200 µm

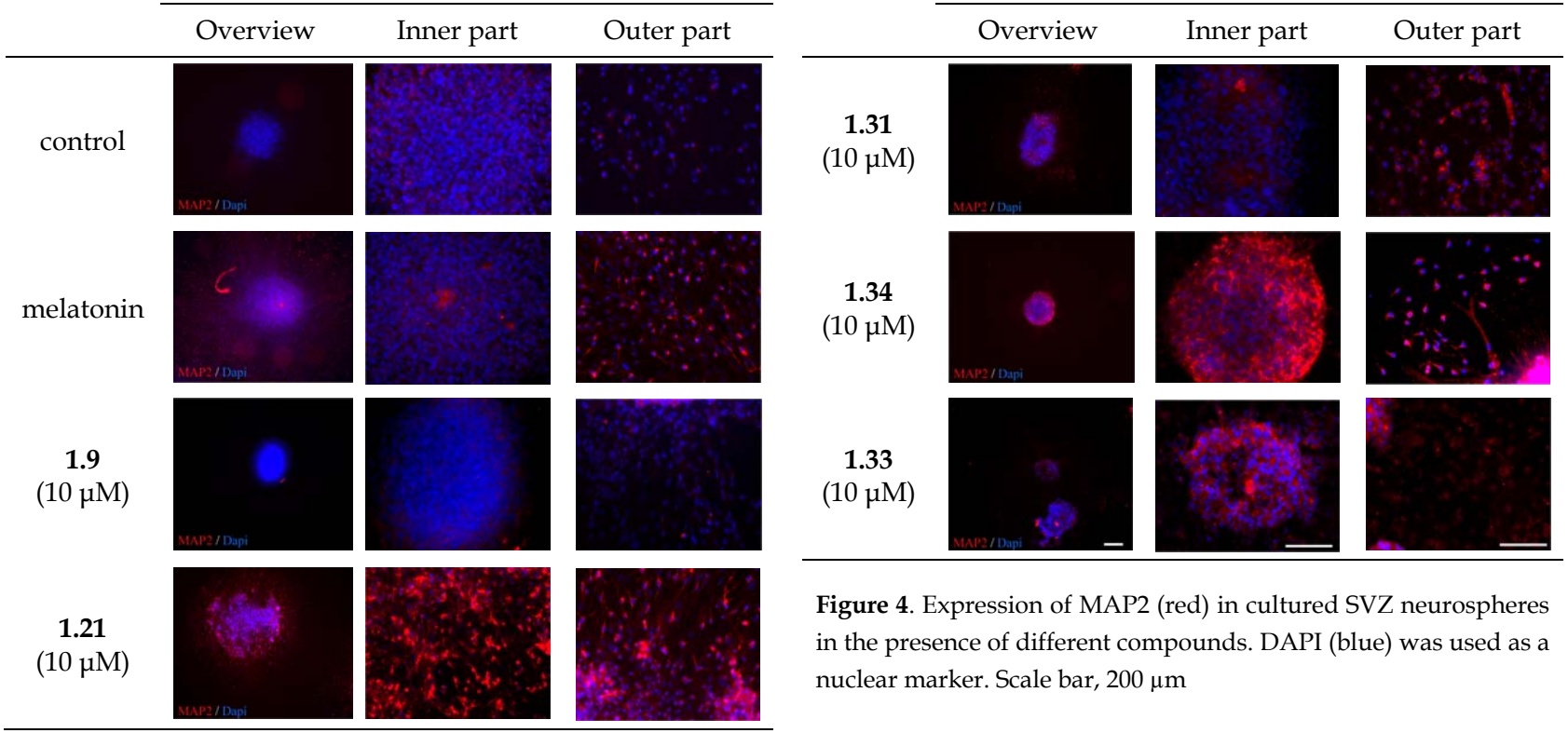

Figure 4. Expression of MAP2 (red) in cultured SVZ neurospheres in the presence of different compounds. DAPI (blue) was used as a nuclear marker. Scale bar, 200 µm

Figures 3 and 4 shows the neurogenic effects of new melatonin-based compounds and melatonin on neural stem cell cultures, compared with the effect of vehicle (basal). As expected, melatonin induced both early neurogenesis and cell maturation. All new melatonergic agonists (**1.9**, **1.21**, **1.34**, **1.33**, and **1.31**) were able to express Tuj1, in most cases better than melatonin, showing also the typical neuronal morphology. Greater differences could be observed in the expression of MAP2. From a qualitative point of view, the 1,3,4-oxadiazole derivatives **1.21**, **1.34**, **1.33** appear to be the most potent compounds at stimulating cell maturation, even more than melatonin itself. However, the propargylic intermediate **1.9** and the 1,3,4-thiadiazole **1.31** did not promote the MAP2 expression.

Compound **1.21** is qualitatively the most potent compound at stimulating the neurogenic response *in vitro* and **1.33** the most potent melatonin agonist able to promote the expression of both Tuj1 and MAP2 (table 1). Both compounds were thus selected for studying their neurogenic effect in the presence of the non-selective melatonergic antagonist luzindole *in vitro*. Neurospheres from rat hippocampus were incubated with **1.21**, **1.33** or melatonin in the presence and absence of luzindole to evaluate the implication of melatonin receptors MT_1 and MT_2 in the expression of the neurogenic markers (figure 5 and 6). Luzindole appeared to reduce the basal expression of Tuj1 compared to the compound-free control. In all three cases luzindole was able to block the expression of both Tuj1 and MAP2 promoted by the tested compounds. The blockade was complete in the case of **1.33**, but in the case of melatonin and **1.21**, luzindole was not able to fully block the expression of Tuj1 and MAP2, and residual expression of both markers could be observed.

Table 1. Summarized affinity and intrinsic activity data at melatonin receptors. Affinity measured as radioligand displacement of 2-[^{125}I]iodomelatonin. Intrinsic activity measured as binding of [^{35}S]GTPγS and referenced to melatonin. All values are accompanied by the SEM. Qualitative central nervous system (CNS) permeability predicted by the parallel artificial membrane permeation assay (PAMPA).

	MT_1			MT_2			PAMPA
Cpd.	K_i (nM)	EC_{50} (nM)	E_{max}(%)	K_i (nM)	EC_{50} (nM)	E_{max}(%)	CNS perm.
Mel.[a]	0.091±0.005	0.098±0.003	100	0.15±0.07	0.069±0.003	100	nd
1.9	5.0±0.9	38±3	106±9	1.0±0.6	3±0.3	99±9	+
1.21	709±10	961±16	19±6	190±8	881±23	32±4	+
1.31	>10000	-	-	17±3	110±25	35±7	-
1.33	35±1	326±30	26±4	4±0.5	29±3	29±3	-
1.34	>10000	-	-	535±30	>10000	agonist[b]	-

[a] Melatonin. [b] A full EC_{50} curve could not be obtained nevertheless agonistic response was observed

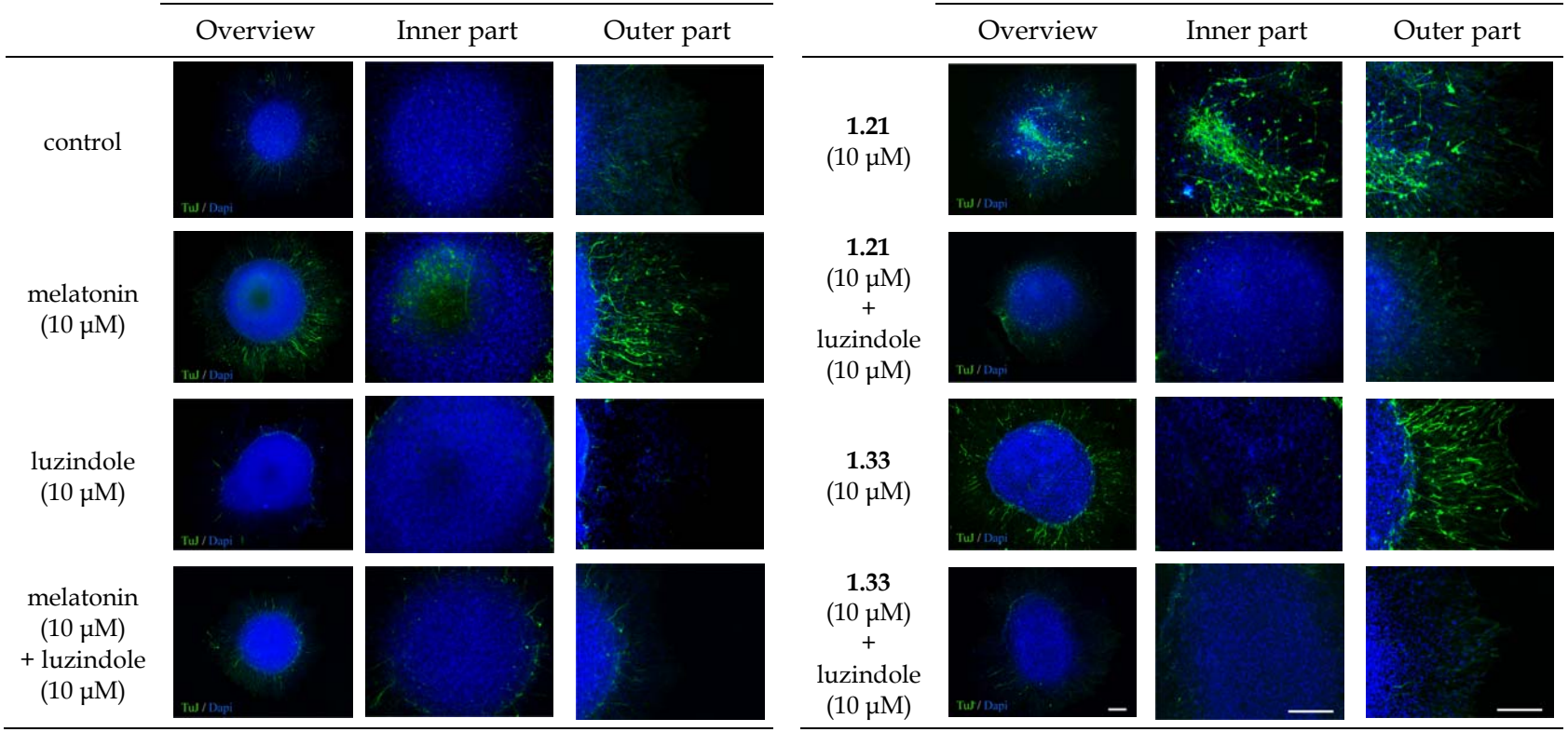

Figure 5. Effect of luzindole on the expression of Tuj1 (green) promoted by melatonin, **1.21** and **1.33** in hippocampal-derived neurospheres. DAPI (blue) was used as a nuclear marker. Scale bar, 200 µm.

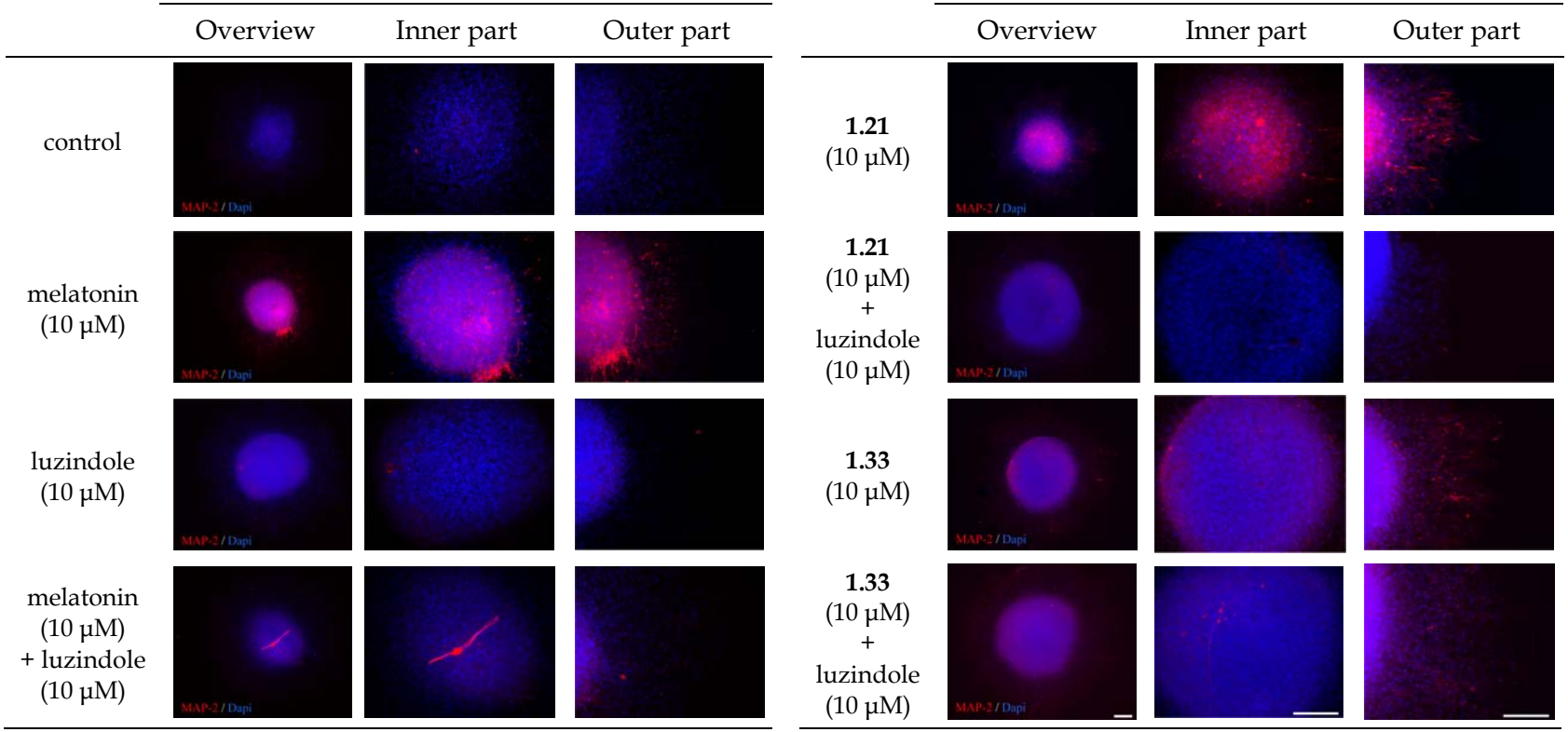

Figure 6. Effect of luzindole on the expression of MAP2 (red) promoted by melatonin, **1.21** and **1.33** in hippocampal-derived neurospheres. DAPI (blue) was used as a nuclear marker. Scale bar, 200 µm.

According to the brain-blood barrier model PAMPA prediction (parallel artificial membrane permeability assay), most of the heterocyclic melatonin are unable to cross the blood-brain barrier via passive diffusion (table 1). This non-cellular assay consists of an artificial membrane that resembles the blood-brain barrier thus permitting a facile high-throughput evaluation of compounds in a simplified yet validated model. Based on the results obtained in the studies performed in neurospheres and its predicted permeability, compound **1.21** was selected for further studies. A dose-response experiment was carried out with compound **1.21** (figure 7). **1.21** probed to be able to stimulate the expression of Tuj1 and MAP2 at all tested concentrations in SVZ-derived neurospheres. Nevertheless at 100 nM the expression of both markers seems mildly diminished compared to **1.21** 1 μM.

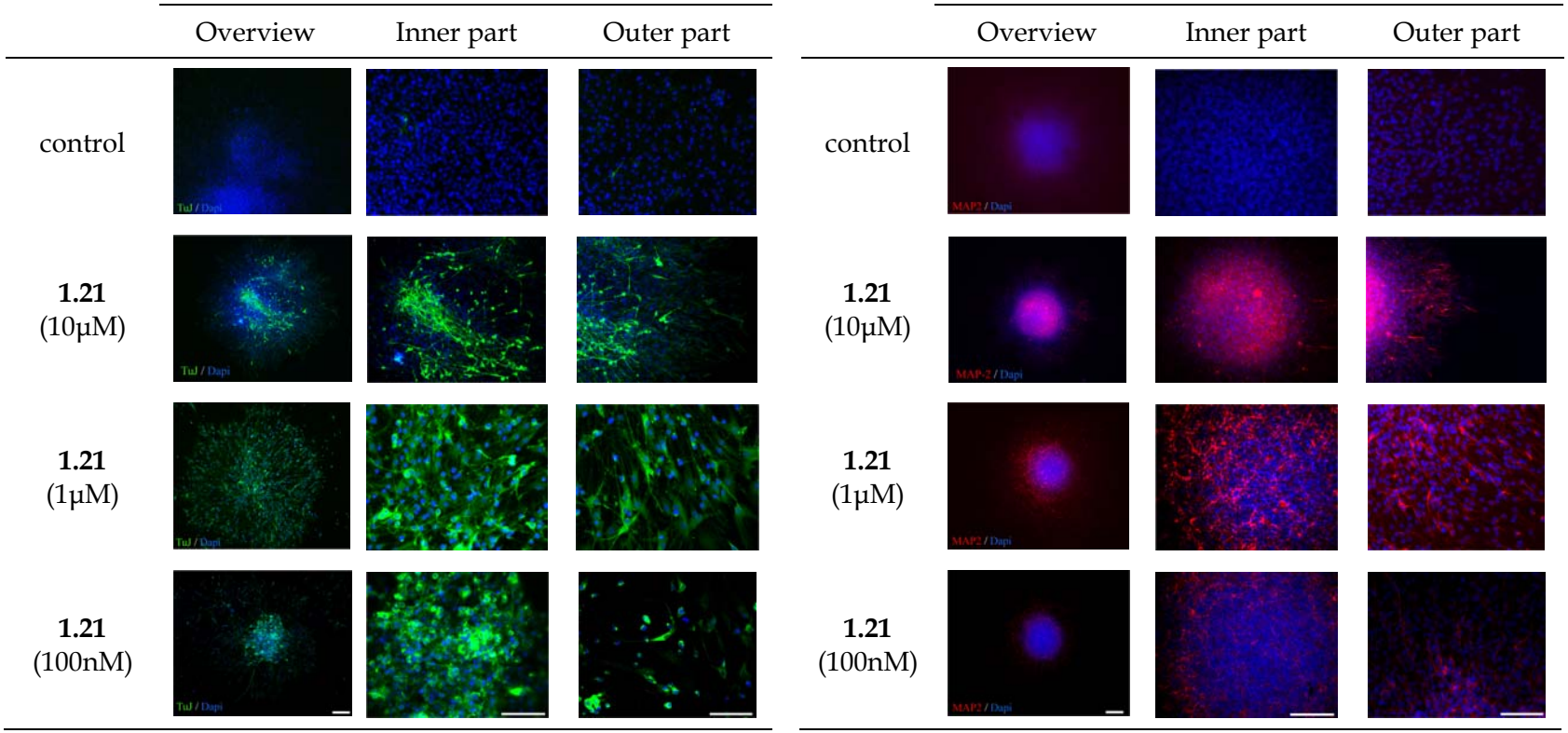

Figure 7. Dose-response effect on the expression of Tuj1 (green) and MAP2 (red) in cultured SVZ-derived neurospheres. DAPI (blue) was used as a nuclear marker. Scale bar, 200 µm.

In vivo neural differentiation and maturation after chronic treatment with **1.21**

1.21 is qualitatively the most potent compound at stimulating the expression of the neurogenic markers Tuj1 and MAP2, apparently even more than melatonin. Being **1.21** also predicted to permeate through the blood-brain barrier according to the PAMPA-BBB model (table 1) it was chosen to be evaluated in an *in vivo* neurogenesis model. Control wild-type C57BL/6 male mice were administered BrdU (50 mg/kg) and treated mice were administered BrdU (50 mg/kg) and **1.21** (500µg/kg) intraperitoneally for 7 days. Cell proliferation was measured as incorporation of BrdU into the DNA, and the identification of neural precursor cells was measured as expression of doublecortin (DCX), a microtubule-associated protein expressed by immature neurons which expression nearly coincides in the same neuronal development stage with Tuj1 (figure 2). The immunostaining of the hippocampus sections revealed that the administration of **1.21** slightly reduces the number of BrdU positive cells in the dentate gyrus of hippocampus (figure 8A). Conversely BrdU/DCX doubled marked nuclei augmented to nearly twice in the treated group compared to control mice ($p<0.05$, Fig. 8B). These results indicate that 7-days administration of **1.21** increases the neural differentiation of progenitor cells without significantly affecting the proliferation rate.

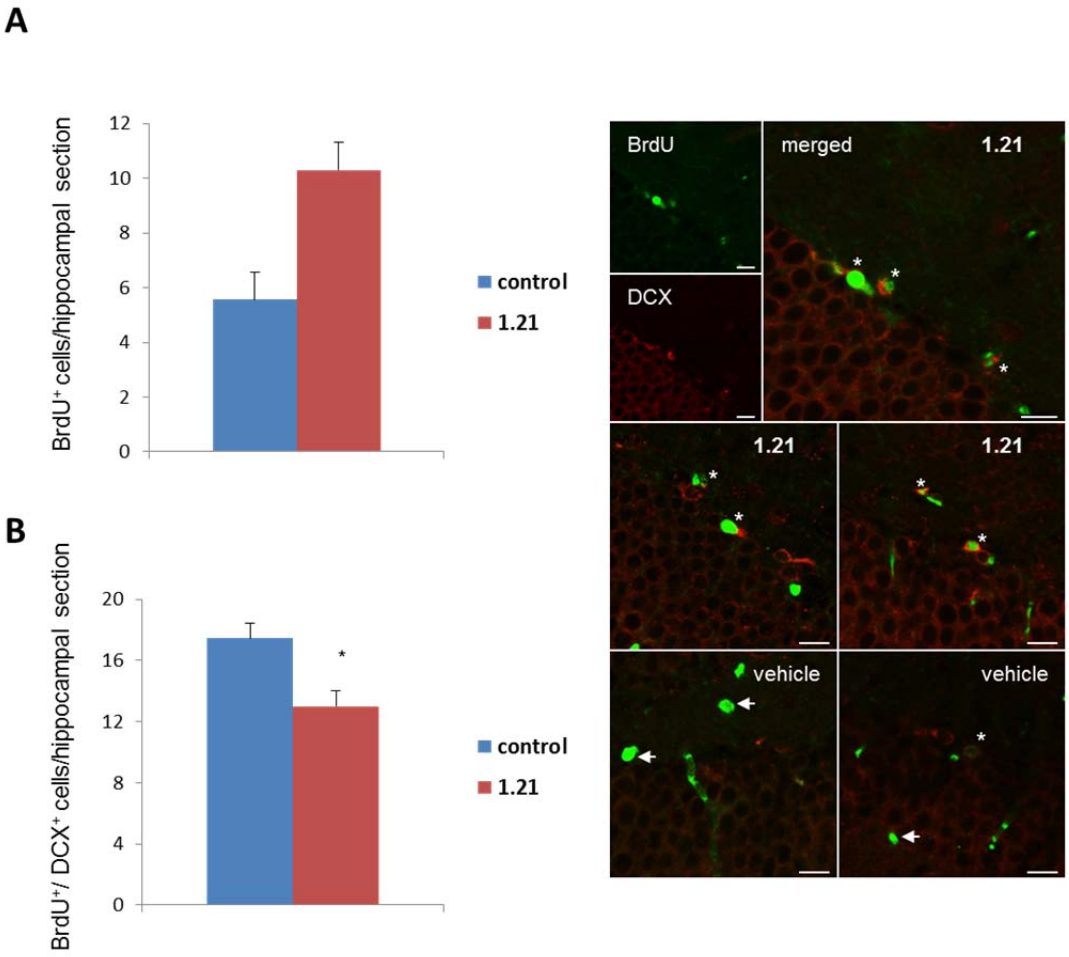

Figure 8. Hippocampal neural precursor cell proliferation and differentiation *in vivo*. (**A**) Number of BrdU⁺ in mice hippocampus in **1.21**-treated group and control (**B**) Number of BrdU⁺/DCX⁺ in hippocampus in **1.21**-treated group and control and representative microimages.

The ability of the new developing neurons to reach the mature state was measured as NeuN expression, a neuronal nuclear antigen typically expressed by neurons that downregulate the expression of DCX when they reach the mature state (figure 2)[18]. An identical protocol as in the case of DCX expression determination was followed in terms of dosage and days of treatment. Rats were sacrificed 21 days after the treatment was finished in order to let newborn neurons reach maturity. No significant differences were

found in the incorporation of BrdU between the treated and the control group (figure 9A). In the previous assay the replication rate of progenitor cells slightly decreased right after treatment was finished. These results show that after sometime the replication rate is recovered. A 6-fold increase in the number of BrdU/NeuN double marked neurons was observed in the treated group (figure 9B), which indicates that the expression of NeuN is greatly enhanced in newborn mature neurons. A virtually unaffected proliferation rate, followed by a net increase in the number of newborn mature neurons, indicated that chronic administration of **1.21** potently enhances hippocampal neurogenesis in mice.

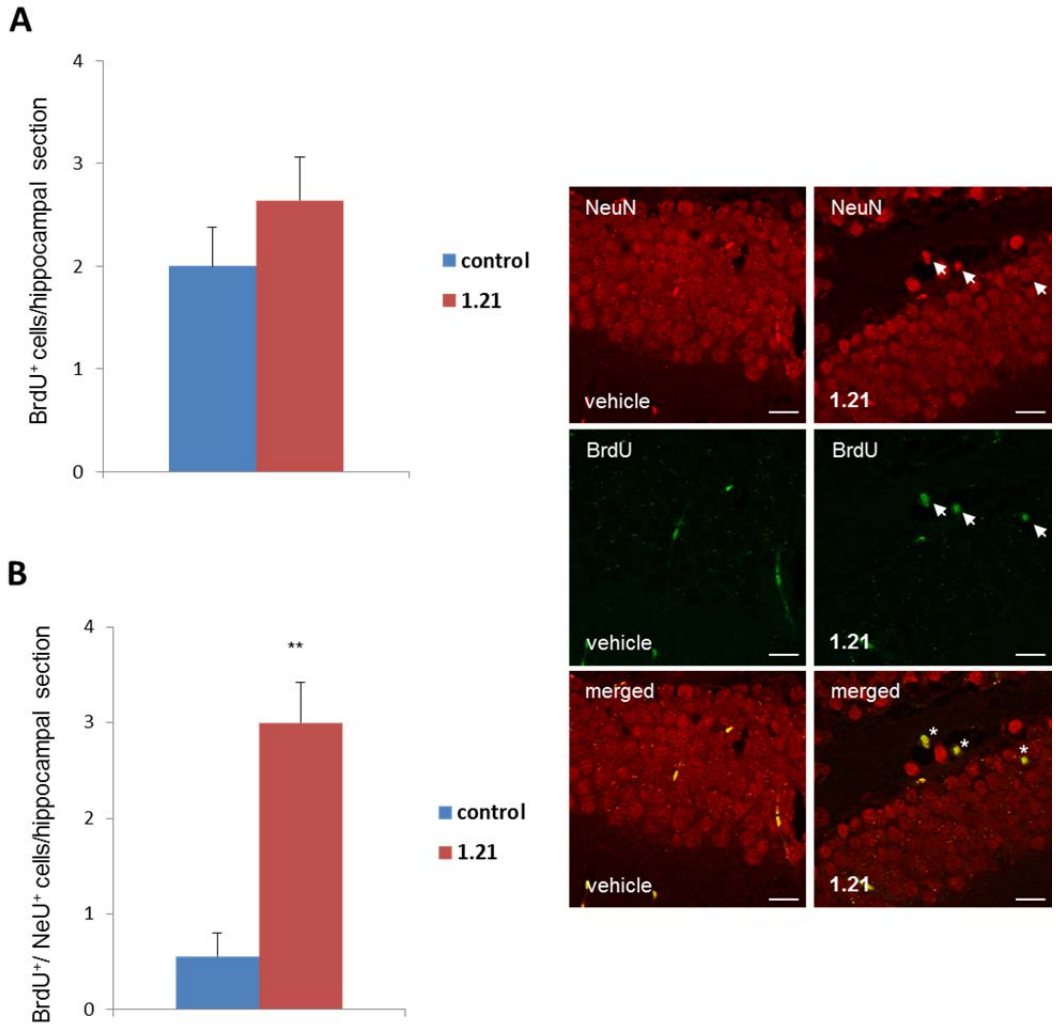

Figure 9. Hippocampal neurogenesis *in vivo*. (**A**) Number of BrdU⁺ in mice hippocampus in **1.21**-treated group and control. (**B**) Number of BrdU⁺/NeuN⁺ in hippocampus in **1.21**-treated group and control and representative microimages.

Discussion

In the present study we first analyzed the neurogenic effects of melatonin and some selected synthetic analogues *in vitro*, and we observed that the degree of potentiation of neural differentiation and maturation of primary neural stem cells did not correlate with their potency at melatonergic

receptors MT_1 and MT_2 (table 1). **1.9** is a full agonist, weaker at both receptor subtypes compared to melatonin, yet the most potent in the series of analogues tested and the only full agonist among them. **1.9** weakly induces neural differentiation whereas is clearly unable to stimulate neural maturation *in vitro*. In this regard, partial agonists **1.21**, **1.33** and **1.31** seem to perform much better. **1.34** intrinsic activity at melatonin receptors could not be studied in concentrations below 10μM, **1.21** is a weak partial agonists, **1.33** is also a weak partial agonist but significantly more potent than **1.21**. **1.31** is a selective MT_2 partial agonist with virtually no effect on MT_1. Nevertheless all three partial agonists were able to promote neural development in levels comparable to melatonin (figures 3 and 4). Despite its poor intrinsic activity and weak potency at melatonergic receptors **1.21** turned out to be the most potent compound at promoting neurogenesis *in vitro,* even more than the reference compound melatonin, in a dose dependent manner.

In order to evaluate whether other receptors and pathways could be involved in the neurogenic effect of **1.21**, the compound was screened at 10 μM concentration in several receptors reportedly related to neurogenesis, namely: glycogen synthase kinase 3β (GSK-3B)[19]; cannabinoid receptors 1 and 2 (CB_1, CB_2)[20]; serotonin receptors subtype 1A, 2A, 2B, 2C (5-HT_{1A}, 5-HT_{2A}, 5-HT_{2B}, 5-HT_{2C})[21]; serotonin transporter (SERT)[22]; RARα and PPARγ[23]. No significant interaction with the abovementioned receptors was observed. MT_1 and/or MT_2 are clearly implicated in the mechanism of action of **1.21**, **1.33** and melatonin, as demonstrated by the blockade of the neurogenic effect exerted by luzindole in neurospheres from hippocampus (figures 5 and 6). In this experiment **1.33** appears to be a weak neuronal maturation inducer, nevertheless the expression pattern of the markers, as well as previous experiments (figure 3 and 4), seem to suggest that longer incubation times might be needed in its case to reach neural maturation *in vitro*.

Luzindole is unable to fully block the neural differentiation *in vitro* elicited by melatonin or **1.21**. This effects have been already been observed in the case of melatonin by Ramírez-Rodríguez et al. (2009)[11]. The residual expression of Tuj1 stimulated by both melatonin and **1.21** in the presence of luzindole could be related to the dose of antagonist employed, perhaps unable to totally block the receptors or to the interaction of both compounds with other systems. López et al. (2010) related the neurogenic properties of melatonin to its intriguing role in mitochondria[10]. Melatonin has also been reported to directly interact with nuclear receptors from the retinoic acid superfamily among others, presumably independent to the signaling pathways mediated by MT_1 and MT_2 membrane receptors[24].

Yet unable to totally counteract the effects of melatonin and **1.21**, interestingly, luzindole blocks the basal neural differentiation below its basal levels as observed in the Tuj1 expression *in vitro* (figure 5). This effect of luzindole has been already reported, and could be related to the nature of luzindole, reportedly a pure antagonist at MT_2, and an inverse agonist at MT_1[11,25]. Both receptor subtypes can be found in the dentate gyrus of rat hippocampus[26]. Luzindole ability to decrease melatonergic intrinsic activity below its constitutive level could in turn negatively interact with other intracellular pathways via cross-talk, blocking or partially blocking them, and as a result, reduce the basal neural differentiation (figure 10A and 10B). The magnitude of this observed effect is rather low at basal levels, nevertheless it could be of relevance in the case of melatonin or **1.21**, which putative neurogenic effects beyond MT_1 and/or MT_2 could be partially masked in this negative cross-talk.

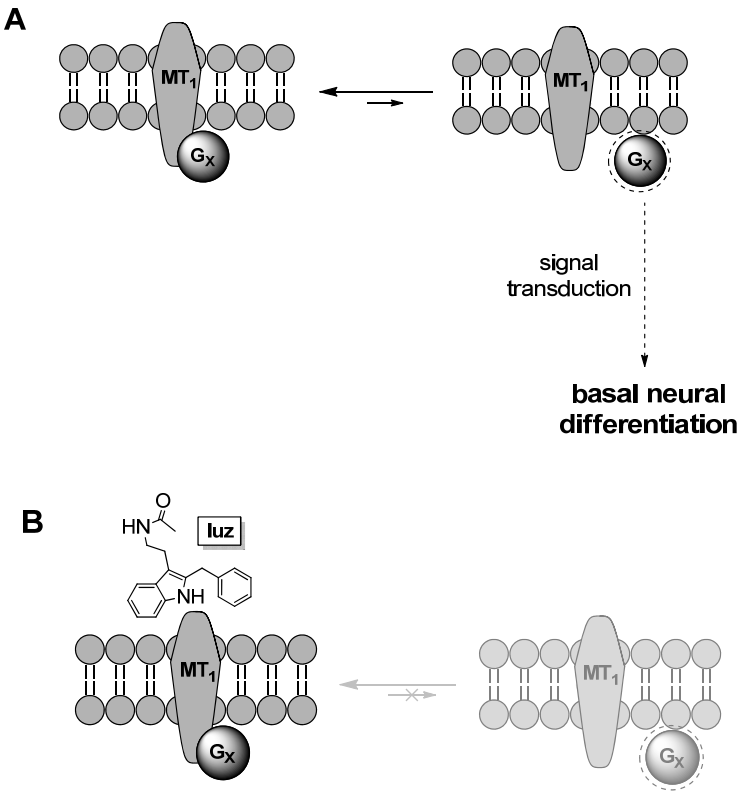

Figure 10. Schematic representation of the constitutive activity of MT_1 in neurospheres from rat hippocampus in absence (**A**) and presence of luzindole (luz) (**B**). The population of transient activated MT_1 receptors is comparably much smaller than the resting conformation, but still able to positively modulate the basal neural differentiation in the absence of any other factors. Conversely, luzindole stabilizes the resting form of the MT_1 receptors keeping the G-protein in its off-state, thus suppressing the basal formation of secondary messengers needed for the neural differentiation.

Chronic treatment with **1.21** *in vivo* increased the number of newborn hippocampal neurons, without major effect on the proliferative rate. Assuming that both **1.21** and melatonin share a common mechanism in their neurogenic effect these results are partially in agreement with those previously reported by Ramírez-Rodríguez et al. (2009) that also observed a slight decrease in the amount of BrdU in C57BL/6 mice treated with 8 mg/kg melatonin for 7 days. A two-fold increase in BrdU/DCX labelled cells was also observed in their model after 14 days of treatment with melatonin. The main

point of divergence is the amount of newborn mature neurons. 14-Days treatment with melatonin did not affect the proportion of new neurons but did increase the number of BrdU cells in the dentate gyrus, giving as a result a net increase in neurogenesis. In our case, even if it is not statistically significative, a mild increase in the amount of BrdU cells was also observed, but followed by a 6-fold increase in the proportion of newborn mature neurons. A plausible interpretation for the observed difference lies in the experiment total time. In our case a 21 days latency time doubles the total time course of the experiment, what could in turn favor delayed expression of NeuN. Nevertheless the treatment duration in our protocol is half, with 16-fold less dosage, what suggests that beyond time differences between both protocols **1.21** could be acting more potently than melatonin at promoting neurogenesis in a similar manner.

The implication of MT_1 and/or MT_2 in their neurogenic actions in hippocampus is beyond doubt in both cases. Whether a certain subtype is more involved in mediating the neurogenic effect than the other is a challenging task beyond the scope of this work. These GPCRs are known to heterodimerize between them and with other membrane receptors[27]. The trend to ascribe differential effects to the stimulation of either subtype is continuously challenged by the complex pharmacology of the melatonergic receptors[24]. Nevertheless, it is still surprising how a weak partial agonist like **1.21,** 10^{-6} fold less potent than melatonin and barely able to stimulate the activation of melatonin receptors (≤30% relative intrinsic activity in the [^{35}S]GTPγS assay), is more potent at potentiating neurogenesis *in vitro,* and *in vivo*. An additional functional assay was carried out with **1.21** in which its intrinsic activity at melatonin receptors was measured as impedance in the case of MT_1 and as decrease of cAMP levels in the case of MT_2. Briefly, MF316 was too weak to elicit any measurable stimulation of the MT_1 receptor whereas it behaved as a full agonists at the MT_2 (EC_{50}, 1.6 μM; E_{max}, 92%). A

plausible hypothesis to explain this behavior is functional selectivity[28]. This phenomenon is quite ubiquitous in GPCRs, and melatonin receptors are known to couple to several G-protein that upon activation could differentially activate parallel pathways[24]. The [^{35}S]GTPγS assay employed for functional characterization is unable to discriminate between different G-proteins. Therefore, in the [^{35}S]GTPγS assay a functional selective agonist that specifically promotes conformational state changes leading to a certain type or types of G-protein activation would in principle return a lower signal compared to a reference agonist that activates the receptor regardless of the G-proteins coupled to it, in this case melatonin (figure 11)[28,29]. The preferential activation of certain MT_2-G-protein populations would provoke the activation on their coupled signaling pathways, and thus only their mediated effects would be observed. The decrease of cAMP levels subsequent to MT_2 stimulation is mediated by $G_{\alpha i}$ protein activation. Therefore, taking into account the lower binding of [^{35}S]GTPγS relative to melatonin elicited by **1.21** via MT_2, and its full-agonistic properties at the same receptor subtype when the decrease of cAMP levels is measured, our main hypothesis is that **1.21** preferentially activate $G_{\alpha i}$-coupled MT_2 receptors. It remains to be determined whether the $G_{\alpha i}$/cAMP pathway is responsible for the neurogenic effect observed.

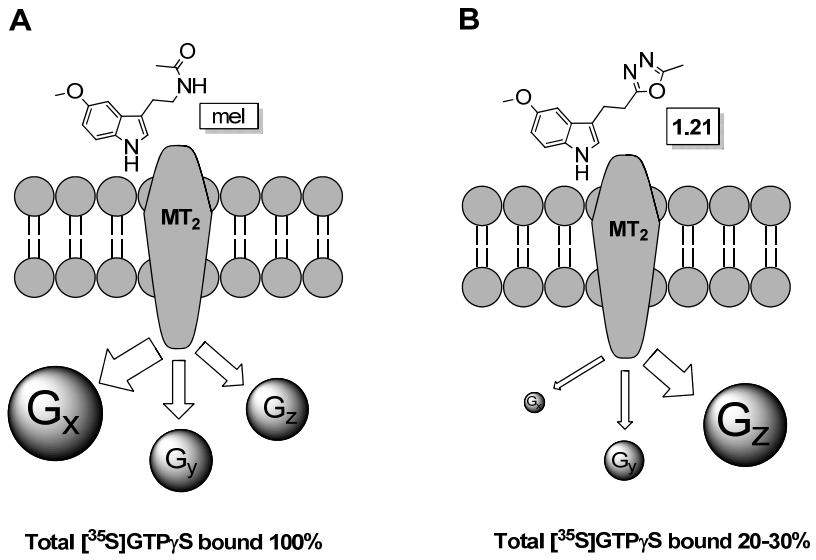

Figure 11. Schematic representation of the functional selectivity hypothesis of **1.21** in MT_2 receptor. (**A**) Melatonin (mel), the reference and natural ligand, binds to melatonergic receptors coupled to G-proteins, that upon activation bind [^{35}S]GTPγS. The amount of G-protein activated is taken arbitrarily as 100%. The size of the G-proteins and arrows represent the relative population of certain activated G-protein isoforms. (**B**) The low binding of [^{35}S]GTPγS upon binding of **1.21** to melatonergic receptor could be indicating the preferential activation of certain populations of MT_x-G_x and thus, only certain signaling pathways are activated.

Conclusions

Herein, we have evaluated the ability of synthetic melatonin analogues potential as neurogenic agents *in vitro*. We have demonstrated that the efficiency at promoting this effect does not correlate with their potency at MT_1 and MT_2 receptors even if both receptors are indeed implicated in mediating their neurogenic effect. This fact could be possibly related to a functional selectivity phenomenon, or to the interaction with additional pathways no directly related to the MT_1 or MT_2 activation but affected by their blockade. Being as it may, we can conclude that **1.21** and related neurogenic azole-containing melatonin analogues are, in classical pharmacological terms, weak melatonergic agonists that, conversely, potentiate neurogenesis *in vitro* with

clear implication of MT_1 and/or MT_2 receptors. Moreover we have demonstrated the ability of **1.21** to potently increase the neurogenesis in mice hippocampus without significantly affecting the proliferation rate after chronic administration. In other words, in terms of orthodox bioisosterism, we can conclude that compound **1.21** that poorly substitutes for melatonin at melatonin receptors, conversely fully behaves as a bioisostere in the promotion of neurogenesis. Therefore, we propose **1.21** as a potential candidate for further development as therapeutic agent in the development of reparative agents for neurodegenerative diseases.

Experimental section

Assays for MT_1 and MT_2 receptor subtypes

The binding and intrinsic activity data was taken from chapter 1. Detailed description of the procedures can be found in the experimental section of the mentioned chapter.

The effect of compound **1.21** on cAMP levels was measured in Chinese Hamster Ovary cells expressing human recombinant MT_2 receptor in a homogeneous time resolved fluorescent assay. Melatonin was used as reference (100% agonist effect). Detailed information on the protocol can be found in www.cerep.fr.

In vitro Blood–Brain Barrier Permeation Assay (PAMPA)

Prediction of the brain penetration was evaluated using a parallel artificial membrane permeation assay (PAMPA-BBB), in a similar manner as previously described[30–32]. Pipetting was performed with a semi-automatic robot (CyBi®-SELMA) and UV reading with a microplate spectrophotometer (Multiskan Spectrum, Thermo Electron Co.). Commercial drugs, phosphate buffered saline solution at pH 7.4 (PBS), and dodecane were purchased from Sigma, Aldrich, Acros, and Fluka. Millex filter units (PVDF membrane, diameter 25 mm, pore size 0.45 µm) were acquired from Millipore. The porcine brain lipid (PBL) was obtained from Avanti Polar Lipids. The donor microplate was a 96-well filter plate (PVDF membrane, pore size 0.45 µm) and the acceptor microplate was an indented 96-well plate, both from Millipore. The acceptor 96-well microplate was filled with 200 µL of PBS : ethanol (70:30) and the filter surface of the donor microplate was impregnated with 4 µL of porcine brain lipid (PBL) in dodecane (20 mg mL^{-1}). Compounds were dissolved in PBS: ethanol (70:30) at 100 µg mL^{-1}, filtered through a Millex

filter, and then added to the donor wells (200 µL). The donor filter plate was carefully put on the acceptor plate to form a sandwich, which was left undisturbed for 240 min at 25 ºC. After incubation, the donor plate is carefully removed and the concentration of compounds in the acceptor wells was determined by UV-Vis spectroscopy. Every sample is analyzed at five wavelengths, in four wells and at least in three independent runs, and the results are given as the mean ± standard deviation. In each experiment, 11 quality control standards of known BBB permeability were included to validate the analysis set.

Neurogenesis studies *in vitro* in the presence of different melatonin analogues

Animals. Adult (8-12 weeks old) male Wistar rats (n = 6 per group), housed in a 12 h light-dark cycle animal facility, were used in this study. All procedures with animals were specifically approved by the Ethics Committee for Animal Experimentation of the CSIC and carried out in accordance with National (normative 1201/2005) and International recommendations (Directive 2010/63 from the European Communities Council). Special care was taken to minimize animal suffering.

Neurosphere culture. Neurospheres (NS) were derived from the subventricular zone (SVZ) and subgranular zone (SGZ) of the dentate gyrus of the hippocampus of adult Wistar rats, which were induced to proliferate using established passaging methods to achieve optimal cellular expansion according to published protocols[33]. Rats were decapitated and brains dissected, obtaining the hippocampus and SVZ as described[34]. Briefly, cell suspension obtained after digestion was separated by centrifugation and later on seeded into 12-well dishes and cultured in Dubecco's Modified Eagle's Medium (DMEM)/F12 (1:1, Invitrogen) containing 10 ng/mL epidermal

growth factor (EGF, Peprotech, London, UK), 10 ng/mL fibroblast growth factor (FGF, Peprotech), and B27 medium (Gibco). After 3 days in culture, when neurospheres (NS) were visible, cultures were treated with the different compounds. Some cultures were pre-treated with luzindole for 2h prior to the addition of the tested compound addition. To determine the ability of compounds to induce differentiation, NS from 10-day old cultures were plated onto 100 µg/mL poly-L-lysine-coated coverslips for 48h in the presence of serum but in the absence of exogenous growth factors.

Immunocytochemistry. After treatment, cells were processed for immunocytochemistry with two types of neurogenesis-associated neuronal markers: anti-β-tubulin antibody (clone Tuj1), associated with early stages of neurogenesis, and MAP-2 (microtubule-associated protein 2), a marker of neuronal maturation. DAPI staining (4',6-diamidino-2-phenylindole) was used as a nuclear marker. Basal values were obtained under the same conditions, but in the absence of any product. Melatonin (endogenous ligand of the melatonergic receptors) and luzindole (melatonergic antagonist) were used as controls. The images were obtained using a Nikon fluorescence microscope 90i that was coupled to a digital camera Qi. The microscope configuration was adjusted to produce the optimum signal-to-noise ratio.

Neurogenesis *in vivo*. MF316 treatment and labelling in adult mice

Animals. Male C57BL/6 mice from our in-house colony (Instituto de Investigacion Hospital 12 de Octubre), were used. Age-matched mice not expressing the transgene were used as wild-type controls. **1.21** (500µg/kg), and BrdU (50 mg/kg) were injected intraperitoneally to each mouse once a day for 7 days, and mice were sacrificed, after deep anesthesia, 24 hours (group 1) or 21 days (group 2)after the last injection of BrdU. All animals were handled and cared for Council Directive 2010/63/UE of 22 September 2010.

Immunohistochemistry. Mice were deeply anesthetized with isoforane, transcardially perfused with 0.9% saline and brains were immediately removed. Next, tissues were fixed in phosphate-buffered 4% paraformaldehyde, pH 7.4, at 4ºC. Fixed brains were cut on a vibratome (Leica Microsystems) at 30 μm, and tissue sections were collected in cold PB 0.1 M, and incubated overnight at 4 °C with mouse anti-BrdU primary antibodies (1:20000, Hybridoma Bank). Additionally goat anti- doublecortin (DCX, 1:500, Santa Cruz Biotechnology) and NeuN (1:500, Millipore) were employed in group 1 (3 animals sacrificed 24h after the last injection of BrdU), and 2 (6 animals sacrificed 21 days after the last injection of BrdU) respectively. After overnight incubation, primary antibody staining was revealed using donkey anti-mouse IgG 488 (FluoProbes®, Interchim) for BrdU, and Texas Red goat anti-rabbit IgG antibody (Jackson Immunoresearch, West Grove) for both DCX and NeuN.

Quantification. The number of BrdU-positive cells in the granule cell and subgranular cell layer of the dentate gyrus were counted to estimate the total number of BrdU-positive cells in the entire dentate gyrus. BrdU-positive were counted in one of every six sections from rostral (2 mm from bregma) to caudal (-4.3 mm from bregma). To determine the fate of dividing cells 100-150 BrdU-positive cells across 4-6 sections per mouse were analyzed by confocal microscopy for co-expressing with DCX (group 1) or NeuN (group 2). Those BrdU-positive nuclei with co-localization of DCX in the cytoplasm were considered as newly born immature neurons, and those BdrU-positive with NeuN co-localization were considered as newly born mature neurons. The number of double-positive cells was expressed as a percentage of BrdU-positive cells in both cases.

Bibliography

(1) Altman, J. Are New Neurons Formed in the Brains of Adult Mammals? *Science.* **1962**, *135*, 1127–1128.

(2) Eriksson, P. S.; Perfilieva, E.; Björk-Eriksson, T.; Alborn, A. M.; Nordborg, C.; Peterson, D. A.; Gage, F. H. Neurogenesis in the Adult Human Hippocampus. *Nat. Med.* **1998**, *4*, 1313–1317.

(3) Gould, E. Neurogenesis in the Neocortex of Adult Primates. *Science.* **1999**, *286*, 548–552.

(4) Kempermann, G.; Wiskott, L.; Gage, F. H. Functional Significance of Adult Neurogenesis. *Curr. Opin. Neurobiol.* **2004**, *14*, 186–191.

(5) Rolando, C.; Taylor, V. Neural Stem Cell of the Hippocampus: Development, Physiology Regulation, and Dysfunction in Disease. *Curr. Top. Dev. Biol.* **2014**, *107*, 183–206.

(6) Duman, R. S.; Malberg, J.; Nakagawa, S. Regulation of Adult Neurogenesis by Psychotropic Drugs and Stress. *J. Pharmacol. Exp. Ther.* **2001**, *299*, 401–407.

(7) Allsopp, T. E.; Bunnage, M. E.; Fish, P. V. Small Molecule Modulation of Stem Cells in Regenerative Medicine: Recent Applications and Future Direction. *Med. Chem. Commun.* **2010**, *1*, 16 – 29.

(8) Rishton, G. M. Small Molecules That Promote Neurogenesis in Vitro. *Recent Pat. CNS Drug Discov.* **2008**, *3*, 200–208.

(9) Iguichi, H.; Kato, K. I.; Ibayashi, H. Age-Dependent Reduction in Serum Melatonin Concentrations in Healthy Human Subjects. *J. Clin. Endocrinol. Metab.* **1982**, *55*, 27–29.

(10) López, L. C.; Escames, G.; López, A.; García, J. A.; Doerrier, C.; Acuña-Castroviejo, D. Melatonin, Neurogenesis, and Aging Brain. *Open Neuroendocr. J* **2010**, *3*, 121–133.

(11) Ramírez-Rodríguez, G.; Klempin, F.; Babu, H.; Benítez-King, G.; Kempermann, G. Melatonin Modulates Cell Survival of New Neurons in the Hippocampus of Adult Mice. *Neuropsychopharmacology* **2009**, *34*, 2180–2191.

(12) Ramírez-Rodríguez, G.; Vega-Rivera, N. M.; Benítez-King, G.; Castro-García, M.; Ortíz-López, L. Melatonin Supplementation Delays the Decline of Adult Hippocampal Neurogenesis during Normal Aging of Mice. *Neurosci. Lett.* **2012**, *530*, 53–58.

(13) Poeggeler, B. Melatonin, Aging, and Age-Related Diseases. *Endocrine* **2005**, *27*, 201–212.

(14) Memberg, S. P.; Hall, A. K. Dividing Neuron Precursors Express Neuron-Specific Tubulin. *J. Neurobiol.* **1995**, *27*, 26–43.

(15) Sánchez, C. Phosphorylation of Microtubule-Associated Protein 2 (MAP2) and Its Relevance for the Regulation of the Neuronal Cytoskeleton Function. *Prog. Neurobiol.* **2000**, *61*, 133–168.

(16) Menezes, J.; Luskin, M. Expression of Neuron-Specific Tubulin Defines a Novel Population in the Proliferative Layers of the Developing Telencephalon. *J. Neurosci.* **1994**, *14*, 5399–5416.

(17) Kempermann, G.; Jessberger, S.; Steiner, B.; Kronenberg, G. Milestones of Neuronal Development in the Adult Hippocampus. *Trends Neurosci.* **2004**, *27*, 447–452.

(18) Brandt, M. D.; Jessberger, S.; Steiner, B.; Kronenberg, G.; Reuter, K.; Bick-Sander, A.; Behrens, W. von der; Kempermann, G. Transient Calretinin Expression Defines Early Postmitotic Step of Neuronal Differentiation in Adult Hippocampal Neurogenesis of Mice. *Mol. Cell. Neurosci.* **2003**, *24*, 603–613.

(19) Lange, C.; Mix, E.; Frahm, J.; Glass, A.; Müller, J.; Schmitt, O.; Schmöle, A.-C.; Klemm, K.; Ortinau, S.; Hübner, R.; Frech, M. J.; Wree, A.; Rolfs, A. Small Molecule GSK-3 Inhibitors Increase Neurogenesis of Human Neural Progenitor Cells. *Neurosci. Lett.* **2011**, *488*, 36–40.

(20) Jiang, W.; Zhang, Y.; Xiao, L.; Van Cleemput, J.; Ji, S.-P.; Bai, G.; Zhang, X. Cannabinoids Promote Embryonic and Adult Hippocampus Neurogenesis and Produce Anxiolytic- and Antidepressant-like Effects. *J. Clin. Invest.* **2005**, *115*, 3104–3116.

(21) Banasr, M.; Hery, M.; Printemps, R.; Daszuta, A. Serotonin-Induced Increases in Adult Cell Proliferation and Neurogenesis Are Mediated through Different and Common 5-HT Receptor Subtypes in the Dentate Gyrus and the Subventricular Zone. *Neuropsychopharmacol. Off. Publ. Am. Coll. Neuropsychopharmacol.* **2004**, *29*, 450–460.

(22) Benninghoff, J.; van der Ven, A.; Schloesser, R. J.; Moessner, R.; Möller, H. J.; Rujescu, D. The Complex Role of the Serotonin Transporter in Adult Neurogenesis and Neuroplasticity. A Critical Review. *World J. Biol. Psychiatry* **2012**, *13*, 240–247.

(23) Yu, S.; Levi, L.; Siegel, R.; Noy, N. Retinoic Acid Induces Neurogenesis by Activating Both Retinoic Acid Receptors (RARs) and Peroxisome Proliferator-Activated Receptor B/δ (PPARβ/δ). *J. Biol. Chem.* **2012**, *287*, 42195–42205.

(24) Hardeland, R. Melatonin: Signaling Mechanisms of a Pleiotropic Agent. *Biofactors* **2009**, *35*, 183–192.

(25) Masana, M. I.; Dubocovich, M. L. Melatonin Receptor Signaling: Finding the Path through the Dark. *Sci. STKE* **2001**, *(2001)*, pe39.

(26) Musshoff, U.; Riewenherm, D.; Berger, E.; Fauteck, J.-D.; Speckmann, E.-J. Melatonin Receptors in Rat Hippocampus: Molecular and Functional Investigations. *Hippocampus* **2002**, *12*, 165–173.

(27) Jockers, R.; Maurice, P.; Boutin, J. A.; Delagrange, P. Melatonin Receptors, Heterodimerization, Signal Transduction and Binding Sites: What's New? *Br. J. Pharmacol.* **2008**, *154*, 1182–1195.

(28) Urban, J. D.; Clarke, W. P.; von Zastrow, M.; Nichols, D. E.; Kobilka, B.; Weinstein, H.; Javitch, J. A.; Roth, B. L.; Christopoulos, A.; Sexton, P. M.; Miller, K. J.; Spedding, M.; Mailman, R. B. Functional Selectivity and Classical Concepts of Quantitative Pharmacology. *J. Pharmacol. Exp. Ther.* **2007**, *320*, 1–13.

(29) Kenakin, T. Ligand-Selective Receptor Conformations Revisited: The Promise and the Problem. *Trends Pharmacol. Sci.* **2003**, *24*, 346–354.

(30) Di, L.; Kerns, E. H.; Fan, K.; McConnell, O. J.; Carter, G. T. High Throughput Artificial Membrane Permeability Assay for Blood–brain Barrier. *Eur. J. Med. Chem.* **2003**, *38*, 223–232.

(31) Rodríguez-Franco, M. I.; Fernández-Bachiller, M. I.; Pérez, C.; Hernández-Ledesma, B.; Bartolomé, B. Novel Tacrine-Melatonin Hybrids as Dual-Acting Drugs for Alzheimer Disease, with Improved Acetylcholinesterase Inhibitory and Antioxidant Properties. *J. Med. Chem.* **2006**, *49*, 459–462.

(32) López-Iglesias, B.; Pérez, C.; Morales-García, J. A.; Alonso-Gil, S.; Pérez-Castillo, A.; Romero, A.; López, M. G.; Villarroya, M.; Conde, S.; Rodríguez-Franco, M. I. New Melatonin-N,N-Dibenzyl(N-Methyl)amine Hybrids: Potent Neurogenic Agents with Antioxidant, Cholinergic, and Neuroprotective Properties as Innovative Drugs for Alzheimer's Disease. *J. Med. Chem.* **2014**, *57*, 3773–85.

(33) Ferrón, S. R.; Andreu-Agulló, C.; Mira, H.; Sánchez, P.; Ángeles Marqués-Torrejón, M.; Fariñas, I. A Combined Ex/in Vivo Assay to Detect Effects of Exogenously Added Factors in Neural Stem Cells. *Nat. Protoc.* **2007**, *2*, 849–859.

(34) Morales-Garcia, J. A.; Luna-Medina, R.; Alfaro-Cervello, C.; Cortes-Canteli, M.; Santos, A.; Garcia-Verdugo, J. M.; Perez-Castillo, A. Peroxisome Proliferator-Activated Receptor Γ Ligands Regulate Neural Stem Cell Proliferation and Differentiation in Vitro and in Vivo. *Glia* **2011**, *59*, 293–307.

Chapter 3

Pinoline pharmacological characterization and development of rigid melatonin-pinoline hybrids with neurogenic potential

Introduction

Pinoline was first isolated from pineal glands in 1978 by Schoemaker[1,2]. It was proposed to be the endogenous ligand of the [^{3}H]imipramine binding site and the factor isolated by Farrell in 1960, named adrenoglomerulotropin, responsible for the pineal regulation of the adrenal gland[3–9]. Pinoline attracted a lot of attention until controversy arouse on its occurrence as an endogenous neurochemical of the pineal gland[10]. Ever since, its interest diminished and at the present time is mostly focused on the study of its antioxidant properties and as a probe for cytochrome activity[11–15]. In recent years, beyond its scientific interests, pinoline has also attracted attention of new age religious groups that ascribe enlightening properties to this molecule, probably due to its structural similarity to *N*,*N*-dimethyltryptamine, nevertheless no reports of its exogenous administration to humans has ever been reported to the best of our knowledge[15,16].

Both melatonin and pinoline are structurally related to serotonin. Pinoline is a methoxylated restricted-analogue of tryptamine. It has often been referred to as the endogenous pineal β-carboline from which it takes its name. According to its β-carboline structure, it is named 6-methoxy-1,2,3,4-tetrahydro-β-carboline (6-MeO-THBC), but it can be also named as a tryptoline: 5-methoxy-tryptoline. The numbering for the methoxy group changes between both systems, and this can be misleading since both names can be found in the literature (figure 1).

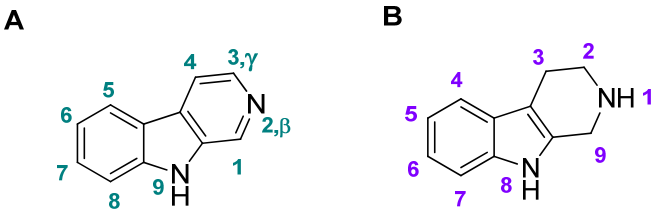

Figure 1. Numbering of the carboline (**A**) and tryptoline (**B**) structures. β-Carboline pyrido nitrogen is in position 2, γ-carboline in position 3. This nomenclature does not apply in the case of tryptolines.

Numerous efforts were done during the 80s to determine the levels of pinoline in different tissues resulting in a wide variety of concentrations that ranged from few ng/g up to 1 µg/g, being the top scoring tissues: brain, pineal and adrenal gland[5,19–22]. Nevertheless criticism may apply in certain early determinations since the analytical procedures require a fine design of the protocol in order to avoid artifact formation[21]. Langer et al. 1985 reported the concentration of pinoline in the pineal gland to be as low as 2 ng/g in rats[4]. Since the synthesis of pinoline by pineal gland appears to be inexistent or at most scant, such levels question the relevance of the pineal production of pinoline. Even if there is no support for an active role of pineal gland in the synthesis of pinoline, however there are reports in the literature that suggest that spontaneous non-enzymatic generation of the β-carboline core could be

feasible from 5-methoxytryptamine in the presence of the superoxide anion in an oxidant environment, or via a spontaneous Pictet-Spengler condensation in the presence of glyoxylate in physiologic conditions followed by enzymatic decarboxylation[22–26]. 5-Methoxytryptamine is synthesized in the pineal gland as a precursor of melatonin, which would in principle support the pineal origin of pinoline[27,28].

Autoradiographic studies with tritiated pinoline reveal that it binds to neural membranes, mitochondria and cell nuclei. It is in nuclei where the largest amount of tracks was located. This intracellular location suggests that pinoline could act as an antioxidant in the nucleus as a direct scavenger, or perhaps exert direct interaction with nuclear receptors and transcription factors like melatonin does[29,30].

The synthesis of 1,2,3,4-tetrahydro-β-carbolines from tryptamines and aldehydes or ketones is straightforward via Pictet-Spengler reaction. This reaction was described as earlier as 1911 by the chemists A. Pictet and T. Spengler in the obtention of 1,2,3,4-tetrahydroisoquinolines[31]. Twenty years later Tatsui obtained 1,2,3,4-tetrahydro-β-carbolines from tryptamine[32]. This skeleton is found in numerous alkaloids and it has been widely studied in the total synthesis of natural products[33]. The importance of this reaction yields also in its occurrence *in vivo*, not only in the biosynthesis of numerous alkaloids by certain plants, but also of endogenous carbolines in superior animals[26]. As abovementioned, previous studies have demonstrated that the reaction is feasible under physiological conditions (buffered solution at 37 ^{o}C and pH 7.4) without the presence of an enzymatic catalyst, especially in the case of 5-methoxytryptamine[24]. Enzymatic-catalysed Pictet-Spengler reactions are also involved in the biosynthesis of alkaloids, among them, morphine and ajmalicine. The enzymes implicated in this transformation are known as Pictet-Spenglerases, and can be found in different plant species[33].

The β-carbolines family, to which pinoline belongs, includes several alkaloids isolated from different plant sources[34–36]. Harmala alkaloids are among them. They receive their name from the plant *Peganum harmala* in which seeds are found, but their occurrence is not limited to *P. harmala*, they are also present in other plant species, like the vine *Banisteriopsis caapi,* the main ingredient of the hallucinogenic beverage Ayahuasca used in Amazonian shamanism[34,36]. There is a wide variety of β-carbolines within the family of harmala alkaloids with different degrees of saturation, bearing or not a methoxy/hydroxy group (figure 2). The essential differences between pinoline and the harmala alkaloids are: the methyl in position 1, and the degree of saturation of the pyrido ring, with the exception of tetrahydroharmine which pyrido ring is fully saturated as well. In the case of harmala alkaloids numerous pharmacological and structure-activity relationship (SAR) studies have been conducted, and there are numerous examples showing how the degree of saturation of the pyrido ring greatly determines the pharmacological profile of these β-carbolines[37–41]. Harmala alkaloids have been more extensively studied than pinoline, therefore, being their structures so closely related, the advances achieved in the understanding of the pharmacology of harmala alkaloids provides hints on the putative role of the so-called pineal β-carboline. Some harmala alkaloids are known to be hallucinogenic *per se*; others act as coadjutant by inhibiting monoaminoxidase A (MAO-A)[16,36,42,43]. Whether pinoline is a hallucinogenic β-carboline in humans remains unknown.

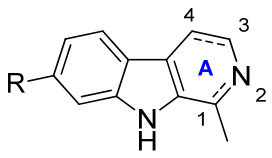

R	Ring A saturation	Common name
-H	Fully unsaturated	Harmane
-OMe	Fully unsaturated	Harmine
-OH	3,4-dihydro	Harmalol
-OMe	3,4-dihydro	Harmaline
-OMe	1,2,3,4-tetrahydro	Tetrahydroharmine

Figure 2. Harmala alkaloids. The numbering on pyrido ring A has been assigned based on the carboline structure.

Approach

Pinoline and melatonin share the 5-methoxyindole ring in their structure, but there are two major structural differences between them: the nature of the non-aromatic nitrogen and the degree of flexibility. Pinoline, like serotonin, is an amine. The basicity of this secondary amine suggests a likely protonated ammonium state at physiologic pH with its corresponding positive charge. Melatonin is a primary amide; this carbamoyl moiety is able to intervene both as a donor and as acceptor in hydrogen bonds, but lacks any absolute charge. With regard on their flexibility, melatonin, like serotonin, has two free-rotation bonds separating the acetamido and heteroaromatic group, thus being able to adopt several energetically equivalent conformations by rotation around its sp^3 carbons. Conversely, the additional methylene present in pinoline that configures the tetrahydropyrido ring limits the conformational freedom of the molecule being the relative spatial disposition constant. The approach employed in our study emerges from multiple ligand design strategies[44]. Taking into account the high structural similarity between pinoline and melatonin we based our design in the merging of the differential

features of both pineal neurochemicals and thus, we aimed for the synthesis and pharmacological characterization of compound **3.3** (figure 3).

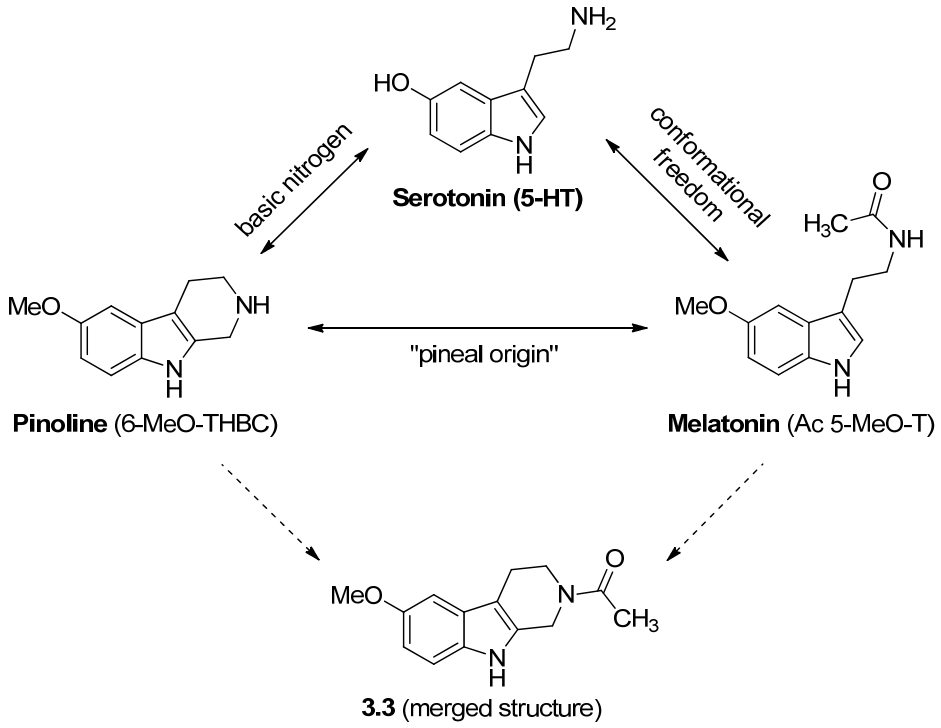

Figure 3. Schematic representation of the approach employed. Filled arrows represent the common features of the depicted structures. Broken arrows represent the hybridization of pinoline and melatonin.

Being **3.3** the target molecule of this project, we have further extended the synthesis to the obtention of position isomers **3.4** and **3.5** and its non-acetylated counterparts **3.1** and **3.2** in order to establish a SAR in the receptors studied, and to compare it to their parent amino compounds (figure 4). The synthesis and characterization of these pinoline isomers (**3.1** and **3.2**) allowed us to gain insights into the structural determinants of the pharmacology and antioxidant properties of methoxy-tetrahydrocarbolines with special interest focused on pinoline. Moreover provided the neurogenic potential of melatonin and our interest in developing new potential brain-repairing

agents, we explored also the neurogenic potential of **3.3** in neural stem cells[45–47].

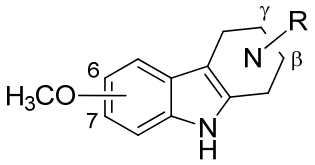

Compound	Methoxy position	Nitrogen position	R
pinoline	6	β	H
3.1	7	β	H
3.2	6	γ	H
3.3	6	β	$COCH_3$
3.4	7	β	$COCH_3$
3.5	6	γ	$COCH_3$

Figure 4. Pinoline isomers, and melatonin – pinoline hybrids obtained in this work

Chemistry

For the synthesis of pinoline and **3.1** an acid-catalysed Pictec-Spengler procedure was employed[48]. The treatment of the appropriate tryptamine with paraformaldehyde in the presence of trifluoroacetic acid (TFA) afforded the corresponding β-carbolines as trifluoroacetate salts in fair yields. The synthesis of the acetylated tetrahydro-β-carbolines **3.3** and **3.4** from the corresponding free bases of the above-mentioned compounds and acetic anhydride proceeded smoothly with excellent yields (scheme 1).

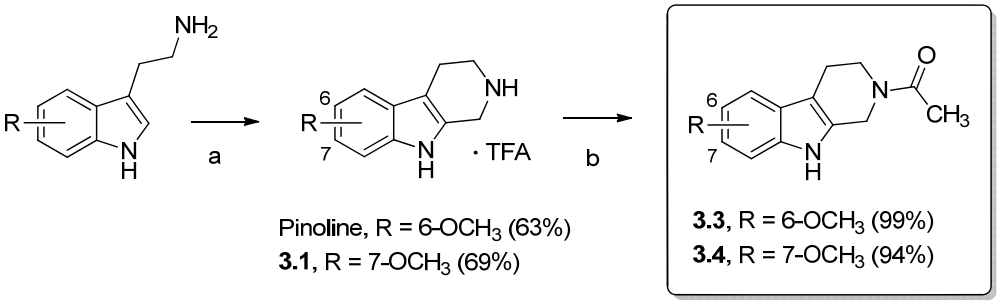

Scheme 1. Synthesis of pinoline and related 1,2,3,4-tetrahydro-β-carbolines **3.1**, **3.3** and **3.4.** *Reagents and conditions*. (a) paraformaldehyde, TFA, DCM, rt, 72h; (b) acetic anhydride, TEA, MeCN, rt, 1h.

The acid-catalysed Pictet-Spengler reaction of tryptamines with keto-derivatives starts with the condensation of the amine with the carbonyl group to form an iminium ion, followed by nucleophilic attack by the pyrrol core and cyclization (scheme 2).

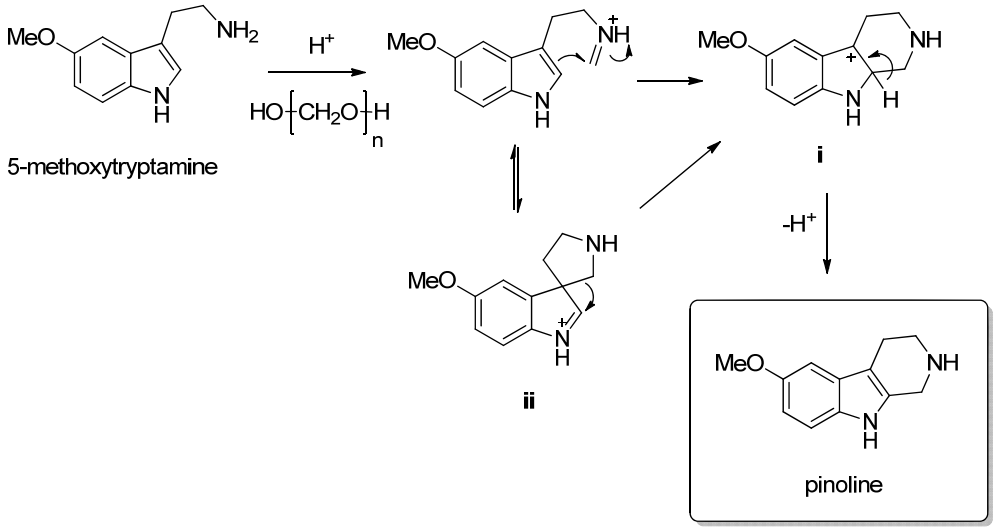

Scheme 2. Proposed mechanism for the synthesis of pinoline from 5-methoxytryptamines *via* Pictet-Spengler reaction. There is evidence of the existence of a spiro intermediate **ii**, which formation is fast and reversible[49]. There is a debate on whether this specie takes part in the whole route as a precursor of the intermediate **i** or not[50].

1,2,3,4-Tetrahydro-γ-carbolines **3.2** and **3.5** were obtained via Fischer indole synthesis starting from (4-methoxyphenyl)hydrazine hydrochloride and the corresponding 4-piperidone using two different methods (scheme 3).

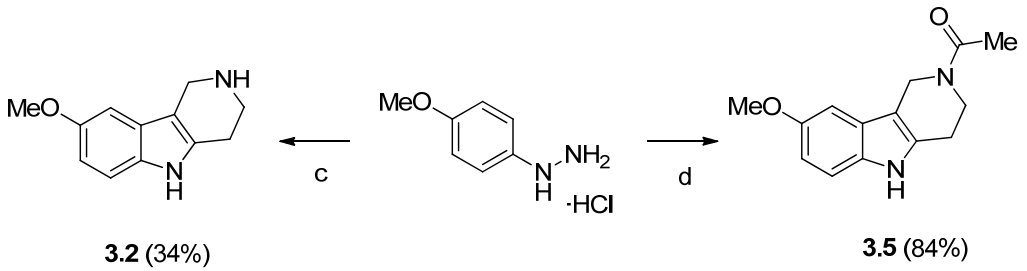

3.2 (34%) **3.5** (84%)

Scheme 3. *Reagents and conditions*. (c) 4-piperidone, EtOH, conc. HCl, 80 °C; (d) 1-acetyl-4-piperidinone, methylurea:tartartic acid (70:30), 80 °C.

In the case of **3.2** a traditional acid-catalysed method was employed: the starting hydrazine chlorhydrate was refluxed with 4-piperidone in a mixture of ethanol and aq. HCl, obtaining **3.2** in low yield[51]. In the synthesis of **3.5** a different acid source was used. Deep eutectic mixtures have proven to be cheap and versatile solvents with similar properties to traditional ionic liquids, with the additional advantage of being greener media and much less toxic to environment and humans. To such extent, that in certain cases they can be employed as cosolvents in biocatalysis[52]. Moreover some natural occurring eutectic mixtures have been proposed to play a role in cell physiology and metabolism[53,54]. In this particular case, following the procedure described by Gore et al., a eutectic mixture of methylurea and tartaric acid (70:30) provided an acidic polar medium able to catalyse Fischer indole synthesis, and thus **3.5** was obtained from (4-methoxyphenyl)hydrazine and 1-acetyl-4-piperidinone in very good yield[55]. The proposed mechanism leading to compounds **3.2** and **3.5** is shown in scheme 4. Condensation of the hydrazine and the corresponding piperidone

forms a hydrazone, that after a [3,3]-sigmatropic rearrangement, formation of a cyclic aminal, and irreversible elimination of ammonia, affords the corresponding γ-carboline.

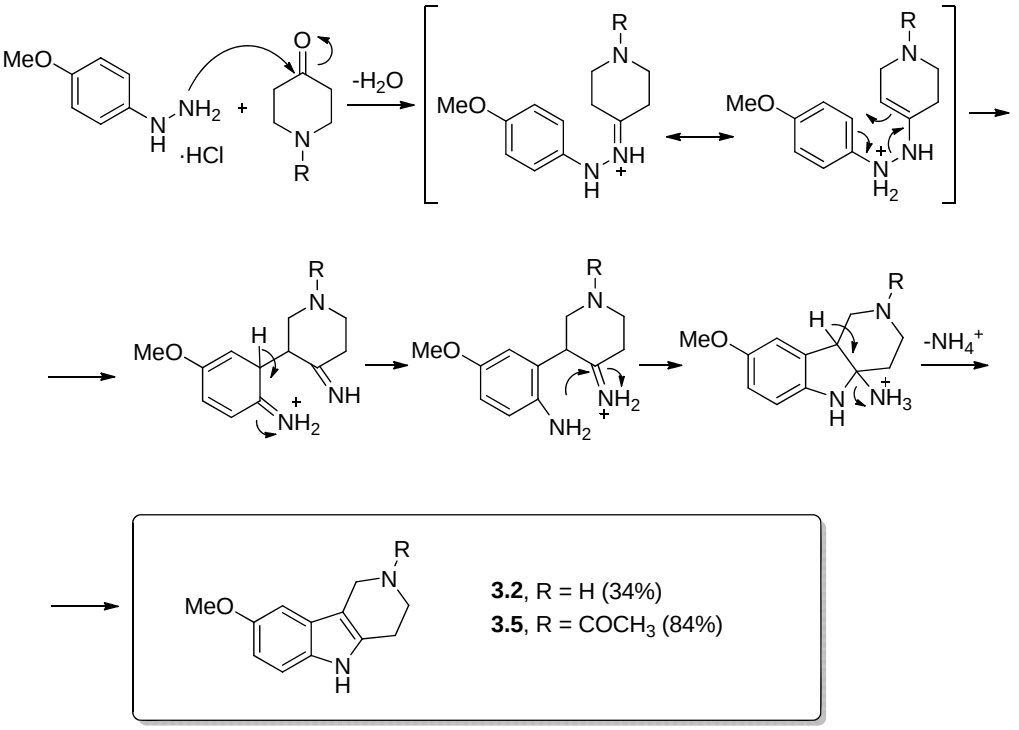

Scheme 4. Adapted mechanism for the synthesis of 1,2,3,4-tetrahydro-γ-carbolines (**3.2** and **3.5**) via Fischer indole synthesis.

Pharmacology

Serotonin receptors and transporter

The binding affinities of the compounds for different serotonin receptors and transporter (5-HT and SERT, respectively) were determined in radioligand displacement studies in transfected cells stably or transiently expressing 5-HT receptors or SERT. The results are summarized in table 1.

Table 1. Binding profiles to 5-HT receptors, and SERT determined by radioligand displacement. K_i, μM (pK_i ± SEM)

Cpd	5-HT$_{1A}$	5-HT$_{1D}$	5-HT$_{2A}$	5-HT$_{2B}$	5-HT$_{2C}$	5-HT$_3$	5-HT$_6$	5-HT$_7$	SERT
pinoline	4.335 (5.36±0.07)	3.714 (5.43±0.03)	2.210 (5.66±0.09)	0.156 (6.81±0.06)	1.503 (5.82±0.06)	4.431 (5.35±0.08)	>10	0.607 (6.22±0.06)	0.172 (6.76±0.05)
3.1	5.797 (5.24±0.08)	>10	2.919 (5.53±0.08)	0.385 (6.41±0.05)	1.258 (5.90±0.07)	>10	>10	1.906 (5.72±0.07)	0.614 (6.21±0.09)
3.2	>10	>10	0.229 (6.64±0.07)	0.194 (6.71±0.08)	0.219 (6.66±0.06)	>10	4.748 (5.32±0.05)	0.938 (6.03±0.06)	>10
3.3	7.305 (5.14±0.08)	>10	3.073 (5.51±0.08)	>10	>10	1.842 (5.73±0.07)	3.063 (5.51±0.06)	>10	>10
3.4	>10	>10	>10	>10	>10	>10	>10	>10	>10
3.5	>10	>10	>10	2.555 (5.59±0.09)	>10	>10	>10	>10	>10

Pinoline and compounds **3.1** and **3.2**, bearing a protonatable amino group, showed more affinity for 5-HT receptors than their acetylated counterparts which lacked significant affinity for most of them. All three protonatable tetrahydrocarbolines showed, however, rather similar binding profiles: K_i values around the low or sub micromolar range for 5-HT_{1A}, 5-HT_{2A}, 5-HT_{2B}, 5-HT_{2C} and 5-HT_7. The similarities are even more obvious in the β-carbolines pinoline and **3.1**, where the relative position of the methoxy group does not appear to be relevant except for 5-HT_{1D} and 5-HT_7 receptors. The relative position of the protonatable nitrogen appears to be more relevant when comparing the γ-carboline **3.2** and pinoline. The nitrogen in γ-position abolishes the binding to 5-HT_{1A} receptors, but increases the affinity for 5-HT_{2A} and 5-HT_{2C} receptors while maintaining the affinity for 5-HT_{2B} and 5-HT_7 unchanged. In the case of the SERT the same SAR applies, being the affinity of the methoxy-regioisomers pinoline and **3.1** nearly identical, whereas the γ-carboline **3.2** lacks significant affinity for this transporter. Among the acetamides, only derivative **3.3** seems to partially retain the affinity profile of its parent compound (pinoline) for the 5-HT_{1A}, 5-HT_{2A} and 5-HT_3 with no significant affinity for any of the other 5-HT_2 subtypes. Additionally it shows improved affinity for the 5-HT_3 and modest affinity for the 5-HT_6 receptor, not observed in any of the other tested compounds. Compound **3.4** showed no affinity for any receptor, and **3.5** only had some significant binding to 5-HT_{2B}.

The intrinsic activity of selected compounds was determined at 5-HT_2 receptors; the results are shown in table 2. The β-carboline derivatives pinoline and **3.1,** showed a very similar qualitative pharmacological profile: partial agonism at the 5-HT_{2A}, antagonism at the 5-HT_{2B} (both in the low micromolar range) and full agonism at the 5-HT_{2C} (in the sub-micromolar range). Pinoline is a relatively potent partial agonist at this subtype (EC_{50}, 33 nM). γ-Carboline **3.2** was unable to activate either receptor subtype.

Table 2. Functional characterization of non-acetylated compounds at 5-HT_2 receptors determined as intracellular calcium mobilization[a].

	5-HT_{2A}			5-HT_{2B}		5-HT_{2C}		
Cpd	EC_{50}	E_{max}	*n*	IC_{50}	*n*	EC_{50}	E_{max}	*n*
pinoline	2.14±0.10	75	1.58	1.12±0.05	1.5	0.033±0.001	95	1.9
3.1	3.28±0.15	57	1.35	3.63±0.17	1.3	0.120±0.005	100	1.7
3.2	–[b]			19.8±0.9	1.4	–[b]		

[a] All EC_{50} or IC_{50} values in μM with ± SEM values. E_{max} is expressed as a percentage of the maximum reponse elicited by 5-HT. *n* represent the Hill coefficient. Experiments are run in duplicates.

[b] **3.2** was unable to activate 5-HT_{2A} nor 5-HT_{2C} receptors.

Inhibition of monoamine-oxidase isoforms A and B

Table 3 summarizes the ability of tested compound to inhibit monoamineoxidase A (MAO-A) and B (MAO-B). Only basic tetrahydro-β-carbolines showed significant inhibition of the MAO-A isoform, being the inhibition elicited by pinoline ~25-fold lower than that of **3.1**.

Table 3. Pharmacological characterization of compounds: inhibition of the MAO isoforms, radioligand displacement studies at MT_1 and MT_2 receptors, and CNS predicted permeability determined by the PAMPA-BBB model

	IC_{50}, μM ± SEM		K_i, μM ± SEM		PAMPA CNS perm.
Cpd	MAO-A	MAO-B	MT_1	MT_2	
pinoline	41.5 ± 6.3	>100	>10	>10	+
3.1	1.3 ± 0.3	>100	>10	>10	+
3.2	>100	>100	>10	>10	+
3.3	>100	>100	0.685±0.025	0.330±0.010	+
3.4	>100	>100	>10	>10	+
3.5	>100	>100	>10	>10	+

Affinity and intrinsic activity at melatonin receptors

The affinity of the different compounds was determined by displacement of the radiolabelled ligand [^{125}I]iodomelatonin; the results are summarized in table 3. Out of the six compounds tested only **3.3** showed significant binding activity for the melatonin receptors, being the affinity for MT_2 two-fold higher than for MT_1. None of its position isomers (**3.5** or **3.4**) showed any significant activity. Neither did any of the parent amino compounds: pinoline or its isomers (**3.1** and **3.2**).

Compound **3.3** was functionally characterized at MT_1 and MT_2 receptor subtypes in the [^{35}S]GTPγS binding assay (table 4). Derivative **3.3** is a partial

agonist at both receptor subtypes, being slightly more potent at the MT_2 subtype.

Table 4. Functional characterization of compound **3.3** at MT_1 and MT_2 receptors[a].

	MT_1		MT_2	
Cpd	EC_{50}	E_{max}	EC_{50},	E_{max}
3.3	338±275	70%	141±70	77%

[a] EC_{50} values in nM scale with ± SEM values. E_{max} is expressed as a percentage of the maximum reponse elicited by melatonin. Experiments are run in duplicates.

Blood-brain barrier permeability

According to the brain-blood barrier model PAMPA (parallel artificial membrane permeability assay), all tested compounds showed positive permeability in this model (table 3). In the case of pinoline, these results are in agreement with previous reports in which radiolabelled pinoline was able to reach the brain after intraperitoneal or intravenous administration to mice, even if its ability to do so was limited[18,30].

***In vitro* antioxidant potential**

Table 5 shows the antioxidant properties of all compounds determined in the oxygen radical absorbance capacity (ORAC) assay. Trolox, the aromatic part of vitamin E and the part that is responsible for radical capturing, was used as an internal standard to which the unit value is arbitrarily given, ORAC (trolox) = 1. Thus, results were expressed as trolox equivalents

(micromoles of trolox/micromoles of tested compounds) on a comparative scale that shows if the products are better (ORAC > 1) or worse than trolox (ORAC < 1). Some indoles and indoleamines were included for comparison purposes to establish a subtractive structure-activity relationship between the different moieties. Among tested molecules, pinoline showed the highest antioxidant capacity equivalent to 3-fold trolox activity, followed by **3.1** with a value identical to that melatonin. γ-Carboline **3.2** showed the lowest value among the non-acetylated carbolines. On the other hand, its antioxidant potential is maintained when acetylated (**3.5**), unlike pinoline or **3.1**. Amides **3.3** and **3.4** antioxidant potential diminishes in up to one equivalent compared to parent compounds. Melatonin, equivalent to nearly 2.5 units of trolox, showed the highest ORAC value within the indoles and indoleamines included in the assay, followed by 5-methoxytryptamine (0.5 eq. difference) and 5-methoxyindole (1 eq. difference). Non-substituted indole showed significant antioxidant activity similar to that of trolox, whereas 1-methylindole was totally devoid of it.

Table 5. Antioxidant properties of compounds and references determined in the ORAC assay.

Cpd	eq. trolox ±SEM
melatonin	2.43±0.05
5-methoxytryptamine	1.95±0.04
5-methoxyindole	1.60±0.03
indole	1.2±0.02
1-methylindole	Not antiox at 10µM
pinoline	3.07±0.25
3.1	2.39±0.26
3.2	1.83±0.08
3.3	2.07±0.19
3.4	1.38±0.08
3.5	1.67±0.12

Neurogenesis studies *in vitro*

The neurogenic potential of melatonin and **3.3** was determined in an *in vitro* model of neural stem cells from adult rat subventricular zone (SVZ). Both melatonin and **3.3** were able to promote neurogenesis in the model employed, whereas the melatonergic antagonist luzindole did not show any differences compared to control. **3.3**-treated SVZ neurospheres appear to qualitatively express more Tuj1 (neuron-specific class III beta-tubulin, figure 5A) and MAP2 (microtubule-associated protein 2, figure 5B) than those treated with melatonin. Melatonin-promoted Tuj1 expression occurred mainly in the outer

part of the neurospheres in cells spreading out of the formation whereas the total expression of MAP2 was diffuse within the neurosphere, and occurred mostly surrounding the nuclei. Tuj1 expression pattern of **3.3**-treated SVZ neurospheres seemed to correspond to that of melatonin, more abundant in the outer parts and in cells spreading out of the neurosphere, but the density of expression appeared to be comparatively higher. The expression of MAP2 was dense and homogeneous both in the inner and the outer parts of the neurospheres treated with **3.3**. Comparing the expression pattern of MAP2 there were clear differences between melatonin and **3.3**. The expression of MAP2 elicited by the latter was not limited to the surrounding of the nuclei but irradiated throughout the cell bodies.

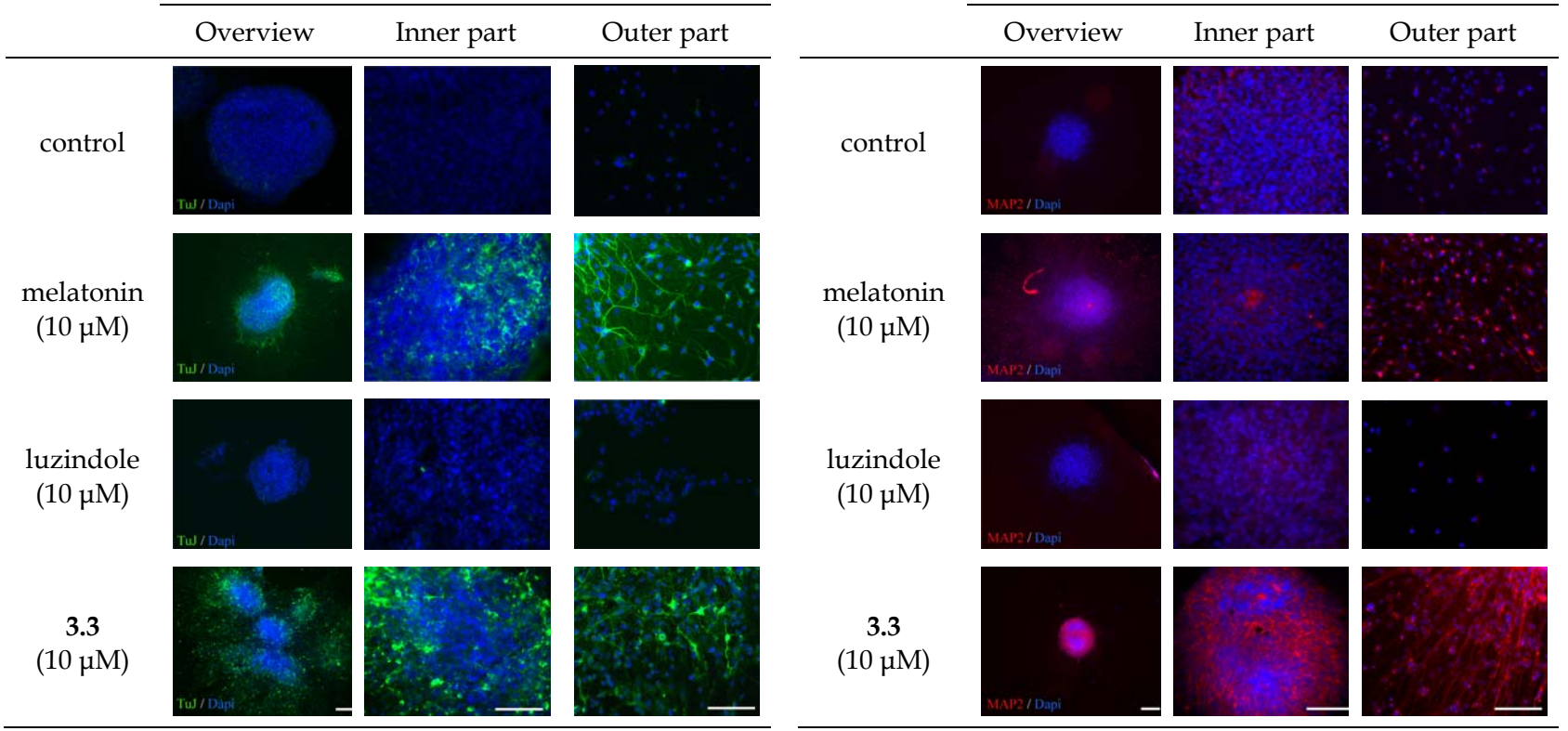

Figure 5. Immunostaining of neurogenic markers Tuj1 (green) and MAP2 (red) in SVZ neurospheres in the presence of different compounds. DAPI (blue) was used as nuclear marker. Scale bar, 200 µm.

In a second assay the neurogenic properties of pinoline were also evaluated *in vitro* in the same model. At 10 µM pinoline potently promotes the irradiated expression of both Tuj1 and MAP2 showing a pattern similar to that of **3.3** (figures 6). Pinoline was also evaluated at 10 nM as a preliminar study of its intrinsic neurogenic potential at a concentration comparable to the trace presence of pinoline reported by Langer et al. (1985)[4]. The expression of Tuj1 appears unaffected by the concentration of pinoline, whereas the density of MAP2 clearly diminished at 10 nM being mostly located around the nuclei.

The implication of melatonin receptors in the neurogenic properties of **3.3** was studied *in vitro.* When SVZ neurospheres were preincubated in the presence of the non-selective melatonin antagonist luzindole, the expression of both Tuj1 and MAP2 was blocked. The blockade was complete in the case of MAP2, but some minor expression of Tuj1 remained despite the presence of the antagonist (figure 7).

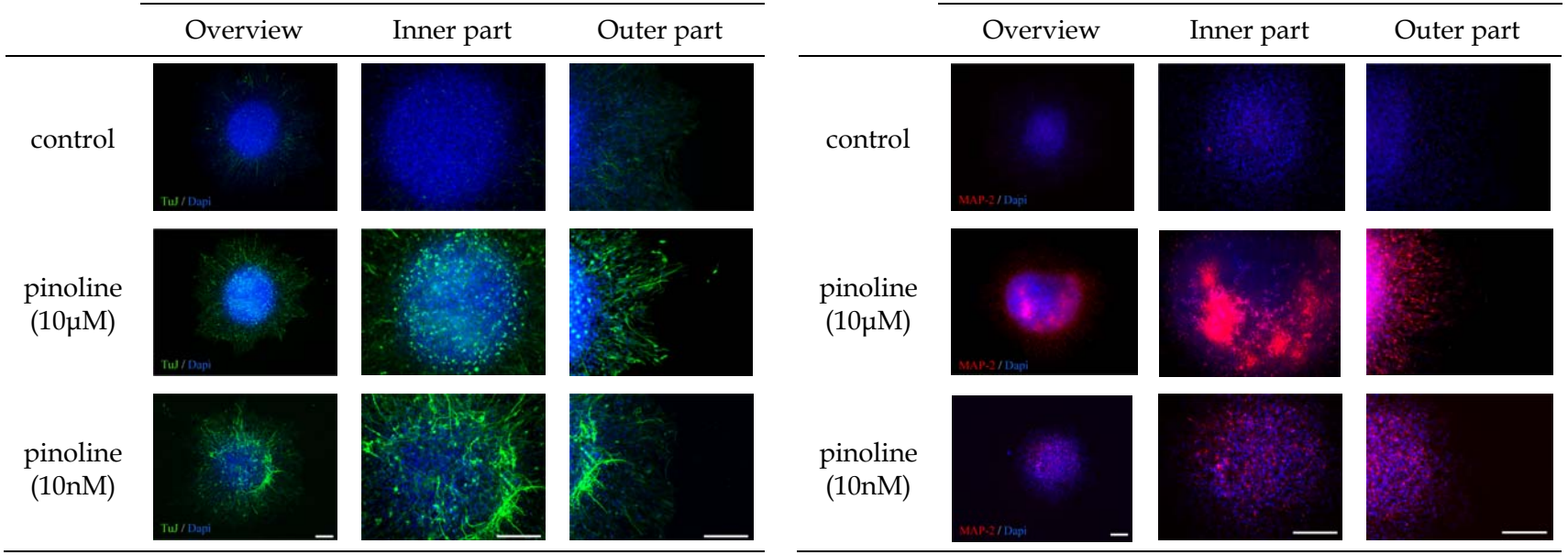

Figure 6. Immunostaining of neurogenic markers Tuj1 (green) and MAP2 (red) in SVZ neurospheres in the presence of pinoline at different concentrations. DAPI (blue) was used as nuclear marker in all cases. Scale bar, 200 µm.

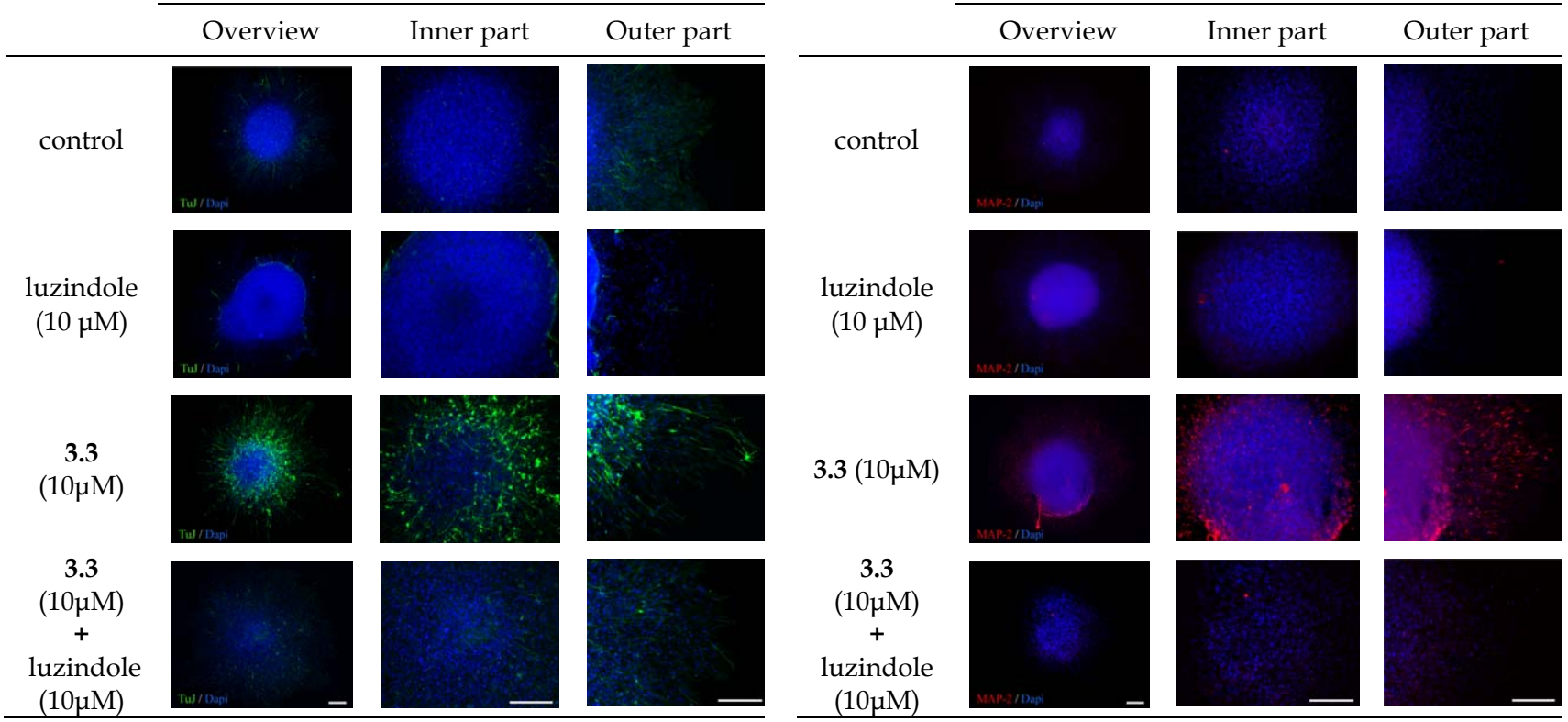

Figure 7. Effect of luzindole on the expression of neurogenic markers promoted by **3.3** Tuj1 (green) and MAP2 (red) in SVZ neurospheres. DAPI (blue) was used as nuclear marker. Scale bar, 200 µm.

Discussion

To the best of our knowledge it is the first time that pinoline intrinsic activity has been characterized in 5-HT_2 receptors even though direct 5-HT receptor stimulation has long been speculated[18,56–58]. Binding properties of pinoline and compound **3.1** were already studied by Glennon et al. (2000)[38]. The affinities of both compounds, together with other β-carbolines, were characterized in rat 5-HT_{1A}, 5-HT_{2A} and 5-HT_{2C} receptors. Significant differences with their reported values were found only in the 5-HT_{2C} receptor. [^{3}H]Mesulergine was the radioligand employed in both cases but in our studies both pinoline and **3.1** showed more affinity for the human 5-HT_{2C} receptor than for the rat receptor in Glennon's report, being the difference around one order of magnitude.

It should be noted that binding properties of pinoline at the 5-HT_{2C} were determined by displacement of the antagonist radioligand [^{3}H]mesulergine. Being pinoline a full agonist at this receptor subtype, the differences found between the K_i and the EC_{50} obtained may be attributable to the difference between the intrinsic activities of radiolabelled ligand and tested compound. The same disparities are observed in the case of **3.1** at the same receptor subtype. Conversely, in the case of 5-HT_{2A}, being the case analogous, no significant differences were observed between the values. Comparing pinoline and **3.1** we can conclude that the relative position of the methoxy group barely affects the affinity or the intrinsic activity of both β-carbolines at 5-HT_2 receptors whereas the relative position of the basic nitrogen does; γ-carboline **3.2** is an antagonist.

Pinoline and **3.1** are both partial agonists at the 5-HT_{2A} receptor within the low micromolar range what to the best of our knowledge represents the first time that direct agonism is reported at the 5-HT_{2A} , not only for the particular case of this two compounds, but also for the whole family of β-

carbolines including harmala alkaloids. Since Glennon et al. (2000) studied some selected hallucinogenic β-carbolines, among them harmaline and harmine, at the 5-HT_{2A} receptor and found no IP_3 (inositol-1,4,5-triphosphate) accumulation, the classification of harmala alkaloids as classical hallucinogens turned troublesome[38]. The inclusion in this category implies: hallucinogenic effect in humans, agonism or partial agonism at the 5-HT_{2A}, and appropriate response in rats trained to discriminate DOM (2,5-dimethoxy-4-methylamphetamine) or LSD (lysergic acid diethylamide) from vehicle[59]. Agonism or partial agonism at 5-HT_{2A} is needed to elicit psychedelic effects exerted by classical hallucinogens; nevertheless not all agonists at this subtype possess hallucinogenic properties. The hallucinogenic effects of harmala alkaloids has been proved in humans, and even though they bind to 5-HT_{2A} receptor with affinities ranging from good to modest, they were reported to be unable to activate the 5-HT_{2A}[16,38,42]. The ability of hallucinogenic harmala alkaloids and pinoline to substitute for LSD in LSD-trained rats is rather low, however harmaline showed some similarity of effect with DOM in harmaline-trained rat[38,57,60–62].

5-HT_{2A} is a G-protein coupled receptor (GPCR) that activates phospholipase C (PLC). The activated PLC hydrolyses membrane lipids generating diacyl glycerol (DAG) and IP_3, being the latter the responsible for the release of Ca^{2+} from intracellular stores. The lack of correlation between the IP_3 production and subsequent Ca^{2+} release with the hallucinogenic potential arose doubts about the exclusivity of this signaling cascade and indeed 5-HT_{2A}-activated additional pathways have been described: phospholipase A_2-arachidonic acid (PLA_2-AA) and phospholipase D (PLD)[59,63]. Interestingly, some hallucinogenic phenylalkylamine compounds, have demonstrated functional selectivity by differentially stimulating the PLC-IP_3 or the PLA_2-AA pathways[64]. In this report the ability of pinoline and **3.1** to promote intracellular Ca^{2+} release via 5-HT_{2A} has been studied, an effect

mediated by IP3 production. Both measurable components correspond to the same signaling cascade subsequent to PLC activation. To the best of our knowledge, the 5-HT_{2A}-mediated activation of additional signaling cascades has never been studied in the case of pinoline or harmala alkaloids. Recently, Briereley and Davidson (2012) found that the increase in electrically-evoked dopamine efflux provoked by harmine was effectively blocked by ketanserin, a 5-HT_{2A} antagonist, suggesting dependence on 5-HT_{2A} agonism for such effect[60]. Our results with pinoline and **3.1** do not prove that the β-carbolines found in *P. harmala* are 5-HT_{2A} agonists, however, the gathered data suggest that the pharmacology of harmala alkaloids at the 5-HT_{2A} receptor might need an update and perhaps, other events, like additional signaling pathways or receptor heterodimerization should be considered[65]. Further studies would be needed to determine to what extent the tetrahydro-β-carbolines **3.1** and pinoline converge or diverge on their pharmacology profile with hallucinogenic harmala alkaloids in the central nervous system stimulation of 5-HT_{2A} receptors. The hallucinogenic properties of pinoline and **3.1** remain unknown to the best of our knowledge[16]. Even if its ability to substitute LSD in trained rats is scant, this is a shared feature with hallucinogenic harmala alkaloids[57,58,66]. Unlike other β-carbolines, pinoline toxicity is rather low (LD_{50} 112 mg/kg i.v. in mice) compared to harmala alkaloids like harmine (LD_{50} 38 mg/kg i.v. in mice), however it has never been reported to be tested in humans[12,67].

Pinoline is a weak MAO-A inhibitor. This inhibition could be of relevance at pharmacological doses but not if pinoline occurs in trace amounts under physiological conditions.–The inhibitory effect in MAO-A is more pronounced in the nor-isomer of tetrahidroharmine: **3.1.** Both **3.1** and tetrahidroharmine show a similar IC_{50} in the micromolar range[40,68].

With regard on MAO inhibition, a few words should be addressed to the imidazoline-2 binding site (I_2-BS). There is evidence that the I_2-BS is indeed

two different biding sites within the monoaminoxidase: a low affinity binding site involved in competitive inhibition, and a high affinity allosteric site. Potent I_2-BS ligands like 2-(2-benzofuranyl)-2-imidazoline (2BFI; K_i, 10 nM) are known to inhibit the MAO-A (IC_{50}, 12 μM) and MAO-B (IC_{50}, 43 μM) with a much lower potency[69]. The same behavior is observed in the cases of pinoline and **3.1** (K_i of 1.6 μM and 0.012 μM respectively for I_2-BS), their potency at inhibiting MAO-A (IC_{50} 41.5 μM and 1.3 μM respectively) compared to their binding affinities to rat I_2-BS is 25 and 100 fold lower[39].

To what extent these results could be of relevance in endogenous occurring pinoline remains unknown, in the same way the presence of endogenous pinoline is still controversial. Exogenous origin cannot be excluded, several β-carbolines have been reported to be present in food stuff[70]. Regardless of the origin of the pinoline found on the pineal gland, such low levels could still be of a certain relevance in the stimulation of 5-HT_{2C} receptor since its potency is close to the concentration found, at least, in the pineal gland (2 ng/g ≈ 10 nM pinoline in pineal gland, EC_{50}(5-HT_{2C}) = 33 nM)[4,17]. Previous studies revealed the presence of radiolabelled pinoline in neuronal membranes where 5-HT receptors and SERT are located[30]. The careful determination of pinoline concentration employed by Langer et al. (1985) in pineal gland has never been performed in adrenal gland to the best of our knowledge, but previous reports reveal a much higher concentration of pinoline in this gland than in the pineal body[2,22]. This fact allows us to speculate that, even if the concentration observed is above its real levels due to the formation of artifacts, accumulation could occur in the adrenal gland and the levels achieved to some degree could be of relevance in the endocrine system. The effect of exogenous administration of pinoline in the hypothalamic-pituitary-adrenal axis has already been previously studied, and this effect has been associated to the stimulation of 5-HT receptors.[66,71,72]

There are several reports that link the effects of pinoline to serotoninergic modulation[73]. Our results in the serotoninergic system call for a revision of the behavioral effects resulting from exogenous administration of pinoline; effects generally attributed to its inhibitory action of SERT and MAO-A[74,75]. The effects elicited by pinoline are more likely to be additive, if not synergic.

The effects elicited by pinoline after intraperitoneal administration to rats resemble those of tricyclic antidepressants, together with some anxiogenic-like effects[66]. Some β-carboline compounds related to harmala alkaloids are antagonists or inverse agonists at the benzodiazepine (BZD) binding site producing anxiogenic effects. According to previous reports pinoline lacks any affinity for the BZD binding site or the convulsive potential associated to its antagonism[37,41]. Anxiogenic effects are also observed after stimulation of 5-HT_{2C} receptors, what suggests that such anxiogenic-like effects mediated by pinoline could be elicited via 5-HT_{2C} receptor[76,77]. Its activation could result both from direct interaction of pinoline with the 5-HT_{2C} subtype and a net increase of serotonin levels in the synapse subsequent to SERT and MAO-A inhibition.

With regard on the radical scavenging properties of the studied compounds, the comparison between pinoline and its isomer **3.1** results in the ORAC assay reveals that the relative position of the methoxy group seems to play a key role in the antioxidant potential of tetrahydro-β-carbolines. The observed difference is probably due to the differential radical/charge stabilization contribution of the lone pairs of the methoxy group during the oxidation process. Comparing pinoline and 5-methoxytryptamine, the antioxidant potential of the latter is 1 trolox eq. lower. 5-Methoxytryptamine is essentially an open-ring pinoline what suggests that the plausible ring opening of the tetrahydropyrido cycle in the presence of oxidant species confers the tricyclic molecule added antioxidant potential compared to the 5-

methoxytryptamine. The same structural analogy can be made between melatonin and **3.3**, but with inverted results, being melatonin antioxidant potential slightly higher. This difference could be possibly related to the nature of the nitrogen in both pairs: amine, in the case of 5-methoxytryptamine/pinoline; and amide, in the case of melatonin/**3.3**. The acetylation results in a dramatic reduction of the antioxidant potential of tetrahydro-β-carbolines (pinoline/**3.3**, **3.1**/**3.4**) but not in the case tetrahydro-γ-carbolines (**3.2**/**3.5**). The only amine-amide pair in which acetylation results in improved antioxidant potential is in the case of 5-methoxytryptamine-melatonin. Kynuramines are metabolites formed as the result of oxidative degradation of melatonin[78–81]. Their structure suggests that melatonin's antioxidant hotspot is located between position C2 and C3 within the 5-methoxyindole (scheme 5). Even though it does not seem obvious looking at the structure of such compounds, these data suggest that the acetamido group of melatonin must play a role in the oxidative degradation, or in later phases of the scavenging cascade. Removal of the ethyl-acetamido group in melatonin or the tetrahydropyrido ring in pinoline leaves the bare 5-methoxyindole, the common heteroaromatic core of both compounds. This small scaffold is able to retain a significant antioxidant potential, of which nearly one third is attributable to the 5-methoxy group substitution, by comparison with the non-substituted indole. The contribution of the proton in position 1 seems to be even greater, being the 1-methylindole totally devoid of any antioxidant activity at 10 μM.

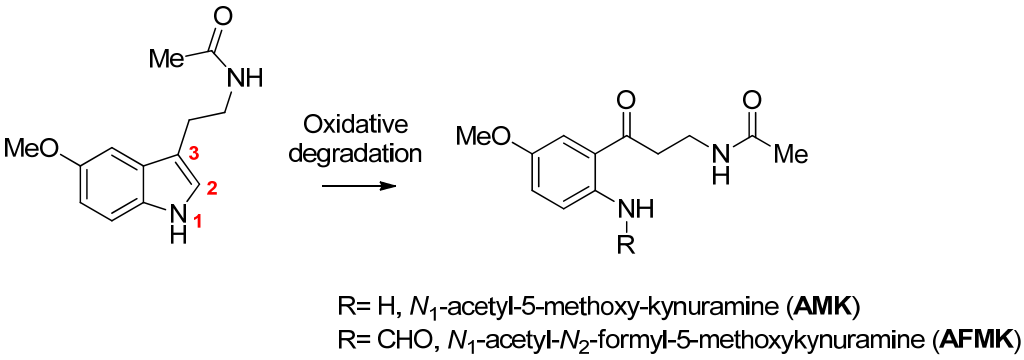

Scheme 5. Structure of kynuramines resulting from the oxidative degradation of melatonin.

Out of this subtractive antioxidant SAR no structural conclusions can be drawn to determine which fragments are best to enhance the reactivity in the presence of oxidant species. Acetylation clearly represents an upgrade in the case of melatonin compared to its precursor 5-methoxytryptamine, but not in the case of pinoline. Cyclization seems to be the key feature responsible for the high antioxidant potential of pinoline, but in the case of melatonin, when comparing it against **3.3**, such cyclization penalizes the reactivity in nearly half an equivalent. Compound **3.3** seems to retain some of the pharmacological properties of the parent compounds, pinoline and melatonin, in the receptors tested in this study, but in this case, the returned value by this synthetic hybrid is not in between, but below both of them. Therefore, we could conclude that the antioxidant nature of pinoline and melatonin cannot be simply attributed to the reactivity of the 5-methoxyindole nucleus, nor envisioned as the result of a combination of chemical fragments that contribute separately to the whole antioxidant potential; instead, it suggests a more complex and optimized interaction between the moieties integrated in the heteroaromatic indole scaffold.

ORAC assay is able to measure the reactivity of a certain molecule against reactive oxygen species (ROS), but it is important to mention that *in*

vivo other radicals are present as well, such as reactive nitrogen species (NOS) for which this model it is not valid. Moreover molecules like melatonin, and presumably pinoline, can mediate antioxidant responses within the cell via membrane receptors, interaction with transcription factors or by other mechanisms not directly related to the reactivity of the molecule. The contribution of melatonin's chemical structure to the antioxidant properties observed *in vivo* is a controversial topic. High levels of the molecule would be needed, and these levels could only be achieved locally in certain tissues or at pharmacological doses[82]. In the case of pinoline, it has been proposed to have a direct role as DNA protecting agent against oxidative damage, and indeed some β-carbolines with antitumoral properties have demonstrated to bind to it[12,37]. As abovementioned, radiolabelled pinoline was found to bind significantly to mitochondria, where an eventual malfunction in the respiratory chain can result in the production of oxidative species. Here we have demonstrated that the chemical structures of both pinoline and melatonin intrinsically possess a certain degree of reactivity that in both cases confers them an optimized antioxidant profile when compared with their simplified structures (5-methoxytryptamine, 5-methoxyindole) or with structural isomers in the case of pinoline (**3.1**, **3.2**).

Derivatives **3.3**, **3.4** and **3.5** are conformationally restricted melatonin analogues. The only compound that shows significant affinity and activity at the melatonin receptor is the structurally orthodox melatonin-pinoline hybrid **3.3**. Compared to melatonin's subnanomolar affinity for MT_1 and MT_2 receptors (table 1, chapter 1), **3.3** affinity is penalized by three orders of magnitude. Conformational restriction is an "all or nothing" approach. Freezing the conformation of a flexible ligand can greatly enhance the affinity since the entropic penalty associated to the accommodation of flexible ligands within the binding site decreases. However, the rigidified ligand ability to adapt itself to the receptor topography is extremely limited, and thus, the

relative spatial disposition of the functional groups involved in the molecular recognition by the receptor needs to be finely tuned. Unlike some previously reported melatonin restricted analogues, in our case the rigidification through a secondary amide renders impossible a captodative hydrogen bond (figure 5)[83,84]. This interaction of the amide group with the receptor appears to be relevant at least for the MT_1 subtype[85]. β-Carboline **3.3** is a partial agonist at both receptors; its ability to activate both MT_1 and MT_2 suggests in principle that the union of **3.3** to melatonin receptors should occur in an analogous way to that of melatonin. None of the other melatonin restricted analogues reported in this work showed any activity at the melatonergic receptors; thus it is important to stress out that the orthodox structural hybrid of pinoline and melatonin **3.3** should be the only compound able to exert agonism at MT_1/MT_2 receptors.

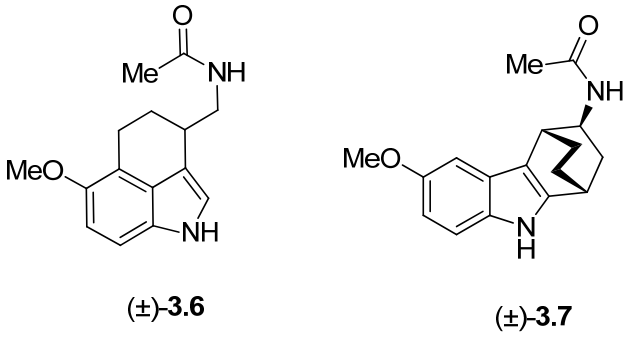

Figure 5. Previously conformationally restrained melatonin analogues reported by Spadoni et al. (1997)[84] and Zefirova et al. (2011)[83] that display low nanomolar for melatonergic receptors.

Compound **3.3** has also demonstrated its ability to stimulate early neurogenesis and maturation in adult rat SVZ neural stem cells. The blockade of the expression of neurogenic markers exerted by luzindole, together with its demonstrated agonistic properties at the melatonin receptors allow us to infer that the neurogenic effect of **3.3** is mediated by MT_1 and MT_2 receptors.

Taking into account its predicted ability to permeate through the blood-brain barrier, further studies *in vivo* will be required to determine if its potent neurogenic properties are also observed in the original cell niche. Both melatonin and pinoline, the two compounds embedded within the structural hybrid **3.3** demonstrated their *in vitro* neurogenic properties. In the case of melatonin its neurogenic effect can be effectively blocked likewise by luzindole (chapter 2, figures 5 and 6). Pinoline does not interact with MT_1 or MT_2 receptor, but is qualitative as potent as **3.3** and melatonin at the same concentration (10 μM). The stimulation of serotonin receptors 5-HT_{1A} and 5-HT_2 is known to increase the neurogenesis rate in adult rat brain[86]. Pinoline is able to evoke agonistic response in the 5-HT_{2C} subtype in the nanomolar concentration range, whether the sole stimulation of this subtype is able to elicit the neurogenic effect described at low concentrations of pinoline requires further studies, but so far taking into account the serotoninergic pharmacological profile of pinoline we hypothesize that its neurogenic effect could be at least partially mediated by serotonin receptors.

Conclusions

We have synthesized and studied the SAR of a series of pinoline isomers and pinoline-melatonin hybrids able to penetrate the central nervous system. We have characterized their pharmacological profile and compared it to their parent amino compounds in different enzymes and receptor systems. This systematic study has allowed us to identify **3.1** and pinoline as full agonists at the 5-HT_{2C} and partial agonists at the 5-HT_{2A}. To the best of our knowledge, this represent the first report of β-carbolines resembling hallucinogenic harmala alkaloids exerting direct agonism at the 5-HT_{2A}. Pinoline has been long known to be both a SERT and MAO-A inhibitor; our results demonstrate that it indeed binds to the serotonin transporter, and that

it weakly inhibits MAO-A. Thus, the contribution of MAO-A inhibition to the observed behavioral effects of pinoline might have been overrated, and be more likely due to a broader interaction with the serotoninergic system.

We have further studied the potential of melatonin and pinoline to act as direct radical scavengers in the presence of oxidant species. The results obtained reveal that both pinoline and melatonin are optimized antioxidant structures that cannot be envisioned as the sum of different moieties added over the 5-methoxyindole nucleus.

We have synthesized and characterized **3.3** as a structural and pharmacological hybrid between melatonin and pinoline, able to partially retain the activity of melatonin over the MT_1 and MT_2, the affinity of pinoline for 5-HT_{1A} and 5-HT_{2A} receptors and to a lesser extent their direct scavenging properties *in vitro*. Moreover we have demonstrated its neurogenic potential *in vitro*; an effect unequivocally mediated by melatonergic receptors and qualitatively superior to that of melatonin. Further studies will be required to establish whether its administration elicits the same effect *in vivo*.

Additionally we have demonstrated that pinoline is able to stimulate neurogenesis *in vitro* at low nanomolar concentration; an effect that could be, at least partially, mediated by its agonistic properties at serotoninergic receptors. Be as it may, trace endogenous neurochemical, dietary β-carboline or myth, pinoline neurogenic properties underscore its ability to potently interact with biological systems at very low concentrations, and allows to this intriguing β-carboline to retain some of the research interest it once had.

Experimental section

Chemistry. **General Methods.** Equipment descriptions and general methods and are detailed in the experimental section of chapter 1.

Pictect-Spengler reaction. General procedure. Trifluoroacetic acid (TFA, 60 μL) and dichloromethane (DCM, 3 mL) were added to a mixture of the corresponding tryptamine (1 mmol) and paraformaldehyde (1 mmol), and the mixture was stirred at room temperature (rt) for 72h. The TFA salt of the corresponding β-carboline was collected by filtration.

6-Methoxy-1,2,3,4-tetrahydro-β-carboline trifluoroacetate (**pinoline**).

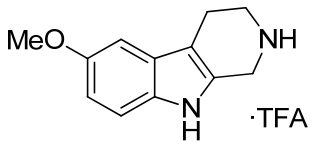

Obtained from 5-methoxytryptamine in 63% yield as a white-yellow powder of mp 180-185ºC. HPLC-MS (230-400nm) 100% (*m/z*) (MH^+) 203.47. ^1H NMR (500 MHz, DMSO) δ 10.51 (s, 1H), 7.16 (d, *J* = 7.5 Hz, 1H), 6.80 (d, *J* = 1.5 Hz, 1H), 6.78 (dd, *J* = 7.5, 1.5 Hz, 1H), 3.87 (s, 2H), 3.80 (s, 3H), 2.94 (t, *J* = 6.0 Hz, 2H), 2.61 (t, *J* = 5.9 Hz, 2H). The compound was used as such for the next reaction. The compound employed for pharmacology assays was purchased from Sigma-Aldrich.

7-Methoxy-1,2,3,4-tetrahydro-β-carboline trifluoroacetate (**3.1**).

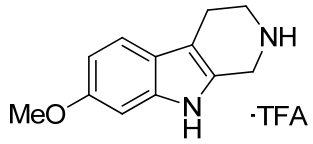

Obtained from 6-methoxytryptamine in 69% yield as a white fine powder of mp 171 – 173ºC. ^1H NMR (300 MHz, DMSO) δ 10.84 (s, 1H), 7.32 (d, *J* = 8.6 Hz, 1H), 6.88 (d, *J* = 2.0 Hz, 1H), 6.67 (dd, *J* = 8.5, 2.4 Hz,

1H), 4.28 (s, 2H), 3.76 (s, 3H), 3.41 (t, *J* = 6.0 Hz, 2H), 2.87 (t, *J* = 5.9 Hz, 2H). ^{13}C NMR (75 MHz, DMSO) δ 156.13, 137.22, 125.84, 120.71, 118.73, 109.09, 105.77, 95.10, 55.54, 42.03, 40.91, 18.74. Anal. ($C_{14}H_{15}F_3N_2O_3$) C,H,N

Acetylation. General procedure. The corresponding TFA salt (1 mmol) was disolved in acetonitrile (MeCN, 3 mL) and triethylamine (TEA, 2.2 mmol) was slowly added. Finally acetic anhydride (1.1 mmol) is added. After 1 hour at rt the reaction is finished and forming a suspension. The TFA ·TEA salt is filtered off and the filtrate evaporated. Washing the evaporated solid with water yielded the corresponding acetylated-β-carboline.

2-Acetyl-6-methoxy-1,2,3,4-tetrahydro-β-carboline (**3.3**).

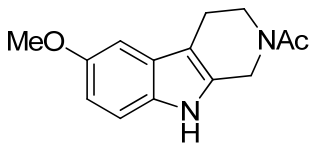

Obtained from **pinoline** in 100% yield as a beige solid of mp: 183 – 187°C. ^{1}H NMR (300 MHz, DMSO) δ 10.66 (s, 1H), 7.17 (d, *J* = 8.7 Hz, 1H), 6.88 (d, *J* = 2.0 Hz, 2H), 6.66 (dd, *J* = 8.7, 2.2 Hz, 2H), 4.62 (s, 3H), 3.86 – 3.61 (m, 9H), 2.71 (t, *J* = 5.4 Hz, 3H), 2.11 (s, 3H). ^{13}C NMR (75 MHz, DMSO) δ 168.90, 153.07, 131.99, 130.91, 126.88, 111.54, 110.28, 106.44, 99.81, 55.29, 44.09, 39.65, 21.52, 21.37. HRMS (ESI$^+$): *m/z* calcd for $C_{14}H_{16}N_2O_2$ $(M)^+$ 244.1212, found 244.1217. HPLC purity 100% (230 to 400 nm).

2-Acetyl-7-methoxy-1,2,3,4-tetrahydro-β-carboline (**3.4**).

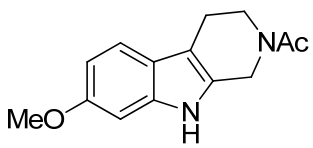

Obtained from **3.1** in 94% yield as a white solid of mp: 169 – 173°C. ^{1}H NMR (400 MHz, DMSO) δ 10.65 (s, 1H), 7.25 (d, *J* = 8.5 Hz, 1H), 6.82 (d, *J* = 2.2 Hz, 1H), 6.62 (dd, *J* = 8.5, 2.3 Hz, 1H), 4.61 (s, 2H), 3.86 –

3.60 (m, 5H), 2.71 (t, *J* = 5.6 Hz, 2H), 2.12 (s, 3H). ^{13}C NMR (101 MHz, DMSO) δ 169.60, 155.92, 137.34, 130.48, 121.62, 118.67, 108.79, 107.10, 95.35, 55.83, 44.75, 40.27, 22.20, 22.11. HRMS (ESI$^+$): *m/z* calcd for $C_{14}H_{16}N_2O_2$ $(M)^+$ 244.1212, found 244.1212. HPLC purity 100% (230 to 400 nm).

6-Methoxy-1,2,3,4-tetrahydro-γ-carboline (**3.2**).

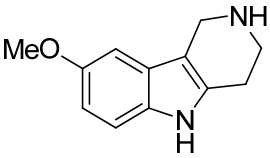

(4-methoxy-phenyl)hydrazine hydrochloride (150 mg, 0.86 mmol) and 4-piperidone (85 mg, 0.86 mmol) were dissolved in ethanol (EtOH, 5 mL) and aq. HCl (2M, 150 μL) was added. The reaction was refluxed for 3h after which solvent was removed and the resulting solid chromatographed on silica (gradient DCM:MeOH, TEA 1%) to afford **3.2** (61 mg, 34%) as an off white solid of mp: 174 – 179^{o}C. ^{1}H NMR (500 MHz, DMSO) δ 10.52 (s, 1H), 7.13 (dd, *J* = 8.6, 0.6 Hz, 1H), 6.81 (d, *J* = 2.5 Hz, 1H), 6.62 (dd, *J* = 8.7, 2.5 Hz, 1H), 3.83 (s, 2H), 3.72 (s, 3H), 3.02 (t, *J* = 5.7 Hz, 2H), 2.65 (t, *J* = 5.6 Hz, 2H). ^{13}C NMR (126 MHz, DMSO) δ 152.87, 133.89, 130.42, 125.91, 111.18, 109.55, 107.82, 99.57, 55.30, 42.97, 41.70, 24.06. Anal. ($C_{12}H_{14}N_2O$) C,H,N.

3-Acetyl-6-methoxy-1,2,3,4-tetrahydro-γ-carboline (**3.5**).

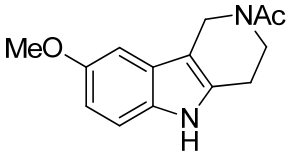

A eutectic mixture of methylurea (MU) and tartaric acid (TA) was prepared (70:30) and melted at 80^{o}C. Over the heated mixture (4-methoxy-phenyl)hydrazine hydrochloride (171 mg, 1 mmol) and 1-acetyl-4-piperidone (141 mg, 1 mmol) were added. After 1.5 h stirring at 80^{o}C reaction reached completion. While still hot water was added and the mixture allowed cooling. A white precipitate formed that was filtered off and rinsed with water to afford **3.5** (204 mg, 84%) as a white solid of mp: 199 –

200°C. ^{1}H NMR (400 MHz, DMSO) δ 10.72 (s, 1H), 7.17 (d, *J* = 8.7 Hz, 1H), 6.93 (d, *J* = 2.4 Hz, 1H), 6.66 (dd, *J* = 8.6, 2.5 Hz, 1H), 4.59 (s, 2H), 3.82 (t, *J* = 5.8 Hz, 2H), 3.74 (s, 3H), 2.84 (d, *J* = 5.6 Hz, 2H), 2.12 (s, 3H). ^{13}C NMR (101 MHz, cdcl$_3$) δ 168.74, 153.09, 133.02, 130.81, 125.61, 111.50, 110.29, 105.79, 99.48, 55.28, 43.46, 38.49, 23.79, 21.58. HRMS (ESI$^+$): *m/z* calcd for $C_{14}H_{16}N_2O_2$ $(M)^+$ 244.1212, found 244.1204. HPLC purity 97% (230 to 400 nm).

Assays for 5-HT receptors and 5-HT transporter

K_i determinations, agonist and antagonist functional data was generously provided by the National Institute of Mental Health's Psychoactive Drug Screening Program, Contract # HHSN-271-2013-00017-C (NIMH PDSP). The NIMH PDSP is Directed by Bryan L. Roth MD, PhD at the University of North Carolina at Chapel Hill and Project Officer Jamie Driscol at NIMH, Bethesda MD, USA.

Radioligands and cell lines employed for determining binding affinities: [^{3}H]8-OH-DPAT in CHO (chineses ovary hamster) cells stably expressing 5-HT$_{1A}$, [^{3}H]GR125743 in HEKT (human embryonic kidney) cells transiently expressing 5-HT$_{1D}$, [^{3}H]Ketanserin in HEKT cells transiently expressing 5-HT$_{2A}$, [^{3}H]LSD in HEKT cells stably expressing 5-HT$_{2B}$, [^{3}H]Mesulergine in Flp-IN HEKT cells stably expressing 5-HT$_{2C}$, [^{3}H]LY278584 in HEKT cells stably expressing 5-HT$_3$, [^{3}H]LSD in HEKT cells stably expressing 5-HT$_6$ or 5-HT$_7$ and [^{3}H]Citalopram in HEKT cells stably expressing SERT.

Functional characterization of compounds in 5-HT$_{2A}$, 5-HT$_{2B}$ and 5-HT$_{2C}$ was performed in transfected Flp-In HEK cells stably expressing the corresponding receptor subtype in the calcium mobilization FLIPR^{TETRA} assay.

Detailed experimental protocols are described in the PDSP web site http://pdsp.med.unc.edu/.

Determination of MAO isoform activity

The potential effects of the test drugs on hMAO activity were investigated by measuring their effects on the production of hydrogen peroxide from *p*-tyramine (a common substrate for both hMAO-A and hMAO-B), using the Amplex® Red MAO assay kit (Molecular Probes, Inc., Eugene, Oregon, USA) and microsomal MAO isoforms prepared from insect cells (BTI-TN-5B1-4) infected with recombinant baculovirus containing cDNA inserts for hMAO-A or hMAO-B (Sigma-Aldrich Química S.A., Alcobendas, Spain).

The production of H_2O_2 catalysed by MAO isoforms can be detected using 10-acetyl-3,7-dihydroxyphenoxazine (Amplex® Red reagent), a non-fluorescent, highly sensitive and stable probe that reacts with H_2O_2 in the presence of horseradish peroxidase to produce a fluorescent product: resorufin. In this study hMAO activity was evaluated using the above method following the general procedure described previously by us[87].

Briefly, 0.1 ml of sodium phosphate buffer (0.05 M, pH 7.4) containing various concentrations of the test drugs (new compounds or reference inhibitors) and adequate amounts of recombinant hMAO-A or hMAO-B required to obtain in our experimental conditions the same reaction velocity, i.e., to oxidize (in the control group) the same concentration of substrate: 165 pmol of *p*-tyramine/min (hMAO-A: 1.1 μg; specific activity: 150 nmol of *p*-tyramine oxidized to *p*-hydroxyphenylacetaldehyde/min/mg protein; hMAO-B: 7.5 μg; specific activity: 22 nmol of *p*-tyramine transformed/min/mg protein) were incubated for 15 min at 37ºC in a flat-black-bottom 96-well microtiter (microtest™ plate, BD Biosciences, Franklin Lakes, NJ, USA) placed in the dark fluorimeter chamber. After this incubation period, the reaction was started by adding (final concentrations) 200 μM Amplex® Red reagent, 1 U/ml horseradish peroxidase and 1 mM *p*-tyramine. The production of H_2O_2 and,

consequently, of resorufin was quantified at 37 °C in a Multi-Detection microplate fluorescence reader (Fluostar Optima, BMG Labtech GmbH, Offenburg, Germany) based on the fluorescence generated (excitation, 545 nm, emission, 590 nm) over a 15 min period, in which the fluorescence increased linearly.

Control experiments were carried out simultaneously by replacing the test drugs (new compounds and reference inhibitors) with appropriate dilutions of the vehicles. In addition, the possible capacity of the above test drugs to modify the fluorescence generated in the reaction mixture due to non-enzymatic inhibition (e.g., for directly reacting with Amplex® Red reagent) was determined by adding these drugs to solutions containing only the Amplex® Red reagent in a sodium phosphate buffer.

The specific fluorescence emission (used to obtain the final results) was calculated after subtraction of the background activity, which was determined from vials containing all components except the MAO isoforms, which were replaced by a sodium phosphate buffer solution.

Assays for MT_1 and MT_2 Receptor Subtypes

Detailed description of the affinity and intrinsic activity studies are included in the experimental section of chapter 1.

***In Vitro* Blood–Brain Barrier Permeation Assay by PAMPA method**

The PAMPA assay was carried out according to the procedures described in the experimental section of chapter 2.

Oxygen Radical Absorbance Capacity Assay. The ORAC-FL method was followed[88], using a Polarstar Galaxy plate reader (BMG Labtechnologies GmbH, Offenburg, Germany) with 485-P excitation and 520-P emission filters. The equipment was controlled by Fluorostar Galaxy software (version 4.11-0) for fluorescence measurement. 2,2'-Azobis-(amidinopropane) dihydrochloride (AAPH), (±)-6-hydroxy-2,5,7,8-tetramethylchromane-2-carboxylic acid (trolox) and fluorescein (FL) were purchased from Sigma-Aldrich. The reaction was carried out in 75 mM phosphate buffer (pH 7.4) and the final reaction mixture was 200 μL. Antioxidant (20 μL) and FL (120 μL; 70 mM, final concentration) solutions were placed in a black 96-well microplate (96F untreat, Nunc™). The mixture was pre-incubated for 15 min at 37 ºC and then, AAPH solution (60 μL, 12 mM, final concentration) was added rapidly using a multichannel pipette. The microplate was immediately placed in the reader and the fluorescence recorded every minute for 80 min. The microplate was automatically shaken prior each reading. Samples were measured at eight different concentrations (0.1-1μM). A blank (FL + AAPH in phosphate buffer) instead of the sample solution and eight calibration solutions using trolox (1-8 μM) were also carried out in each assay. All the reaction mixtures were prepared in duplicate, and at least three independent assays were performed for each sample. Raw data were exported from the Fluostar Galaxy Software to an Excel sheet for further calculations. Antioxidant curves (fluorescence *vs.* time) were first normalized to the curve of the blank corresponding to the same assay, and the area under the fluorescence decay curve (AUC) was calculated. The net AUC corresponding to a sample was calculated by subtracting the AUC corresponding to the blank. Regression equations between net AUC and antioxidant concentration were calculated for all the samples. ORAC-FL values were expressed as trolox equivalents by using the standard curve calculated for each assay, where the ORAC-FL value of trolox was taken as 1.0.

Neurogenesis studies *in vitro* in the presence of different melatonin analogues.

Detailed descriptions of the procedures employed for the evaluation of the expression of neurogenic markers in the presence of different compounds in the presence or absence of luzindole can be found in the experimental section of chapter 2.

Bibliography

(1) Shoemaker, D. W.; Cummins, J. T.; Bidder, T. G. Beta-Carbolines in Rat Arcuate Nucleus. *Neuroscience* **1978**, *3*, 233–239.

(2) Barker, S. A.; Harrison, R. E. W.; Monti, J. A.; Brown, G. B.; Christian, S. T. Identification and Quantification of 1,2,3,4-Tetrahydro-B-Carboline, 2-Methyl-1,2,3,4-Tetrahydro-B-Carboline, and 6-Methoxy-1,2,3,4-Tetrahydro-B-Carboline as in Vivo Constituents of Rat Brain and Adrenal Gland. *Biochem. Pharmacol.* **1981**, *30*, 9–17.

(3) Segonzac, A.; Schoemaker, H.; Tateishi, T.; Langer, S. Z. 5-Methoxytryptoline, a Competitive Endocoid Acting at [3H]imipramine Recognition Sites in Human Platelets. *J. Neurochem.* **1985**, *45*, 249–256.

(4) Langer, S. Z.; Lee, C. R.; Schoemaker, H.; Segonzac, A.; Esnaud, H. 5-Methoxytryptoline and Close Analogs as Candidates for the Endogenous Ligand of the 3H-Imipramine Recognition Site. *Prog. Clin. Biol. Res.* **1985**, *192*, 441–455.

(5) Barbaccia, M. L.; Melloni, P.; Pozzi, O.; Costa, E. [3H]imipramine Displacement and 5HT Uptake Inhibition by Tryptoline Derivatives: In Rat Brain 5-Methoxytryptoline Is Not the Autacoid for [3H]imipramine Recognition Sites. *Eur. J. Pharmacol.* **1986**, *123*, 45–52.

(6) Farrell, G. Adrenoglomerulotropin. *Circulation* **1960**, *21*, 1009–1015.

(7) Airaksinen, M. M.; Sainio, E. L.; Leppäluoto, J.; Kari, I. 6-Methoxy-Tetrahydro-Beta-Carboline (pinoline): Effects on Plasma Renin Activity and Aldosterone, TSH, LH and Beta-Endorphin Levels in Rats. *Acta Endocrinol. (Copenh).* **1984**, *107*, 525–530.

(8) Sejian, V.; Srivastava, R. S.; Varshney, V. P. Pineal-Adrenal Relationship: Modulating Effects of Glucocorticoids on Pineal Function to Ameliorate Thermal-Stress in Goats. *J. Physiol. Biochem.* **2008**, *66*, 339–349.

(9) Farrell, G.; McIsaac, M.; Taylor, N. Neurohumoral Factors from the Brainstem and Epiphysis. *Horm. Steroids Biochem. Pharmacol. Ther.* **1964**, *1*, 141–147.

(10) Pähkla, R.; Rägo, L.; Callaway, J. J.; Airaksinen, M. M. Binding of Pinoline on the 5-Hydroxytryptamine Transporter: Competitive Interaction with [3H] Citalopram. *Pharmacol. Toxicol.* **1997**, *80*, 122–126.

(11) Tang, G. Y.; Ip, A. K.; Siu, A. W. Pinoline and N-Acetylserotonin Reduce Glutamate-Induced Lipid Peroxidation in Retinal Homogenates. *Neurosci. Lett.* **2007**, *412*, 191–194.

(12) García, J. J.; Martínez-Ballarín, E.; Robinson, M.; Allué, J. L.; Reiter, R. J.; Osuna, C.; Acuña-Castroviejo, D. Protective Effect of Beta-Carbolines and Other Antioxidants on Lipid Peroxidation due to Hydrogen Peroxide in Rat Brain Homogenates. *Neurosci. Lett.* **2000**, *294*, 1–4.

(13) Siu, A. W.; Reiter, R. J.; To, C. H. Pineal Indoleamines and Vitamin E Reduce Nitric Oxide-Induced Lipid Peroxidation in Rat Retinal Homogenates. *J. Pineal Res.* **1999**, *27*, 122–128.

(14) Pähkla, R.; Zilmer, M.; Kullisaar, T.; Rägo, L. Comparison of the Antioxidant Activity of Melatonin and Pinoline in Vitro. *J. Pineal Res.* **1998**, *24*, 96–101.

(15) Jiang, X.-L.; Shen, H.-W.; Yu, A.-M. Pinoline May Be Used as a Probe for CYP2D6 Activity. *Drug Metab. Dispos.* **2009**, *37*, 443–446.

(16) Shulgin, A. A. *Tihkal: The Continuation*; Transform Press (CA), 1997; p. 804.

(17) Langer, S. Z.; Galzin, A. M.; Lee, C. R.; Schoemaker, H. Antidepressant-Binding Sites in Brain and Platelets. *Ciba Found. Symp.* **1986**, *123*, 3–29.

(18) Leino, M.; Airaksinen, M. M.; Antikainen, R.; Gynther, J.; Kari, E.; Kari, I.; Peura, P. Distribution of 1,2,3,4-Tetrahydro-Beta-Carboline and 6-Methoxy-1,2,3,4-Tetrahydro-Beta-Carboline in Mice. *Acta Pharmacol. Toxicol. (Copenh).* **1984**, *54*, 361–371.

(19) Kari, I. 6-Methoxy-1,2,3,4-Tetrahydro-Beta-Carboline in Pineal Gland of Chicken and Cock. *FEBS Lett.* **1981**, *127*, 277–280.

(20) Langer, S. Z.; Lee, C. R.; Segonzac, A.; Tateishi, T.; Esnaud, H.; Schoemaker, H.; Winblad, B. Possible Endocrine Role of the Pineal Gland for 6-Methoxytetrahydro-Beta-Carboline, a Putative Endogenous Neuromodulator of the [3H]imipramine Recognition Site. *Eur. J. Pharmacol.* **1984**, *102*, 379–380.

(21) Bosin, T. R.; Holmstedt, B.; Lundman, A.; Beck, O. Presence of Formaldehyde in Biological Media and Organic Solvents: Artifactual Formation of Tetrahydro-B-Carbolines. *Anal. Biochem.* **1983**, *128*, 287–293.

(22) Susilo, R.; Rommelspacher, H. Formation of 1-Methyl-B-Carbolines in Rats from Their Possible Carboxylic Acid Precursor. *Naunyn. Schmiedebergs. Arch. Pharmacol.* **1988**, *337*, 566–571.

(23) Uemura, T.; Kanashiro, M.; Yamano, T.; Hirai, K.; Miyazaki, N. Isolation, Structure, and Properties of the Beta-Carboline Formed from 5-Hydroxytryptamine by the Superoxide Anion-Generating System. *J. Neurochem.* **1988**, *51*, 710–717.

(24) Callaway, J. C.; Gynther, J.; Poso, A.; Vepsäläinen, J.; Airaksinen, M. M.; Gyntber, J. The Pictet-Spengler Reaction and Biogenic Tryptamines: Formation of Tetrahydro-B-Carbolines at Physiological pH. *J. Heterocycl. Chem.* **1994**, *31*, 431–435.

(25) Fekkes, D.; Tuiten, A.; Bom, I.; Pepplinkhuizen, L. *Tryptophan: A Precursor for the Endogenous Synthesis of Norharman in Man*; 2001; Vol. 303, pp. 145–148.

(26) Rommelspacher, H.; Wernicke, C.; Lehmann, J. B-Carbolines: Occurrence, Biosynthesis, and Biodegradation. *Curr. Top. Neurotox.* **2012**, *1*, 105–113.

(27) Galzin, A. M.; Eon, M. T.; Esnaud, H.; Lee, C. R.; Pevet, P.; Langer, S. Z. Day-Night Rhythm of 5-Methoxytryptamine Biosynthesis in the Pineal Gland of the Golden Hamster (Mesocricetus Auratus). *J. Endocrinol.* **1988**, *118*, 389–397.

(28) Klein, D. C.; Moore, R. Y. Pineal N-Acetyltransferase and Hydroxyindole-O-Methyl-Transferase: Control by the Retinohypothalamic Tract and the Suprachiasmatic Nucleus. *Brain Res.* **1979**, *174*, 245–262.

(29) Luchetti, F.; Canonico, B.; Betti, M.; Arcangeletti, M.; Pilolli, F.; Piroddi, M.; Canesi, L.; Papa, S.; Galli, F. Melatonin Signaling and Cell Protection Function. *FASEB J.* **2010**, *24*, 3603–3624.

(30) Pähkla, R.; Masso, R.; Zilmer, M.; Rägo, L.; Airaksinen, M. M. Autoradiographic Localization of [3H]-Pinoline Binding Sites in Mouse Tissues. *Methods Find. Exp. Clin. Pharmacol.* **1996**, *18*, 359–366.

(31) Pictet, A.; Spengler, T. Über Die Bildung von Isochinolin-Derivaten Durch Einwirkung von Methylal Auf Phenyl-Äthylamin, Phenyl-Alanin Und Tyrosin. *Berichte der Dtsch. Chem. Gesellschaft* **1911**, *44*, 2030–2036.

(32) Tatsui, G. T. -. *J. Pharm. Soc. Jpn.* **1928**, *48*, 92.

(33) Stöckigt, J.; Antonchick, A. P.; Wu, F.; Waldmann, H. The Pictet–Spengler Reaction in Nature and in Organic Chemistry. *Angew. Chemie Int. Ed.* **2011**, *50*, 8538–8564.

(34) Callaway, J. C.; Brito, G. S.; Neves, E. S. Phytochemical Analyses of Banisteriopsis Caapi and Psychotria Viridis. *J. Psychoactive Drugs* **2005**, *37*, 145–150.

(35) Cassady, J. M.; Blair, G. E.; Raffauf, R. F.; Tyler, V. E. The Isolation of 6-Methoxyharmalan and 6-Methoxyharman from Virola Cuspidata. *Lloydia* **1971**, *34*, 161–162.

(36) Herraiz, T.; González, D.; Ancín-Azpilicueta, C.; Arán, V. J.; Guillén, H. B-Carboline Alkaloids in Peganum Harmala and Inhibition of Human Monoamine Oxidase (MAO). *Food Chem. Toxicol.* **2010**, *48*, 839–845.

(37) Cao, R.; Peng, W.; Wang, Z.; Xu, A. Beta-Carboline Alkaloids: Biochemical and Pharmacological Functions. *Curr. Med. Chem.* **2007**, *14*, 479–500.

(38) Glennon, R. A.; Dukat, M.; Grella, B.; Hong, S.; Costantino, L.; Teitler, M.; Smith, C.; Egan, C.; Davis, K.; Mattson, M. V Binding of Beta-Carbolines and Related Agents at Serotonin (5-HT(2) and 5-HT(1A)), Dopamine (D(2)) and Benzodiazepine Receptors. *Drug Alcohol Depend.* **2000**, *60*, 121–132.

(39) Glennon, R. A.; Grella, B.; Tyacke, R. J.; Lau, A.; Westaway, J.; Hudson, A. L. Binding of Beta-Carbolines at Imidazoline I2 Receptors: A Structure-Affinity Investigation. *Bioorg. Med. Chem. Lett.* **2004**, *14*, 999–1002.

(40) Fernández de Arriba, A.; Lizcano, J. M.; Balsa, M. D.; Unzeta, M. Inhibition of Monoamine Oxidase from Bovine Retina by Beta-Carbolines. *J. Pharm. Pharmacol.* **1994**, *46*, 809–813.

(41) Cain, M.; Weber, R. W.; Guzman, F.; Cook, J. M.; Barker, S. A.; Rice, K. C.; Crawley, J. N.; Paul, S. M.; Skolnick, P. Beta-Carbolines: Synthesis and Neurochemical and Pharmacological Actions on Brain Benzodiazepine Receptors. *J. Med. Chem.* **1982**, *25*, 1081–1091.

(42) Naranjo, C. Ayahuasca, Caapi, Yage. Psychotropic Properties of the Harmala Alkaloids. *Psychopharmacol. Bull.* **1967**, *4*, 16–17.

(43) Riba, J.; Valle, M.; Urbano, G.; Yritia, M.; Morte, A.; Barbanoj, M. J. Human Pharmacology of Ayahuasca: Subjective and Cardiovascular Effects, Monoamine Metabolite Excretion, and Pharmacokinetics. *J. Pharmacol. Exp. Ther.* **2003**, *306*, 73–83.

(44) Morphy, R.; Rankovic, Z. Designed Multiple Ligands. An Emerging Drug Discovery Paradigm. *J. Med. Chem.* **2005**, *48*, 6523–6543.

(45) Manda, K.; Reiter, R. J. Melatonin Maintains Adult Hippocampal Neurogenesis and Cognitive Functions after Irradiation. *Prog. Neurobiol.* **2010**, *90*, 60–68.

(46) Liu, J.; Somera-Molina, K. C.; Hudson, R. L.; Dubocovich, M. L. Melatonin Potentiates Running Wheel-Induced Neurogenesis in the Dentate Gyrus of Adult C3H/HeN Mice Hippocampus. *J. Pineal Res.* **2013**, *54*, 222–231.

(47) Rennie, K.; De Butte, M.; Pappas, B. A. Melatonin Promotes Neurogenesis in Dentate Gyrus in the Pinealectomized Rat. *J. Pineal Res.* **2009**, *47*, 313–317.

(48) Jiang, W.; Zhang, X.; Sui, Z. Potassium Superoxide as an Alternative Reagent for Winterfeldt Oxidation of B-Carbolines. *Org. Lett.* **2002**, *5*, 43–46.

(49) Bailey, P. D. Direct Proof of the Involvement of a Spiro Intermediate in the Pictect-Spengler Reaction. *J. Chem. Res. - S* **1987**, 202–203.

(50) Czerwinski, K. M.; Deng, L.; Cook, J. M. Mechanism Driven Trans Stereospecificity in the Pictet-Spengler Reaction. Stereospecific Formation of Trans-1,2,3-Trisubstituted-Tetrahydro B- Carbolines by Condensation of Nb-Diphenylmethyl Tryptophan Isopropyl Esters Wtm Aldehydes. *Tetrahedron Lett.* **1992**, *33*, 4721–4724.

(51) Bridoux, A.; Goossens, L.; Houssin, R.; Héanichart, J.-P. Synthesis of 8-Substituted Tetrahydro-Γ-Carbolines. *J. Heterocycl. Chem.* **2006**, *43*, 571–578.

(52) Lindberg, D.; de la Fuente Revenga, M.; Widersten, M. Deep Eutectic Solvents (DESs) Are Viable Cosolvents for Enzyme-Catalyzed Epoxide Hydrolysis. *J. Biotechnol.* **2010**, *147*, 169–171.

(53) Choi, Y. H.; van Spronsen, J.; Dai, Y.; Verberne, M.; Hollmann, F.; Arends, I. W. C. E.; Witkamp, G.-J.; Verpoorte, R. Are Natural Deep

Eutectic Solvents the Missing Link in Understanding Cellular Metabolism and Physiology? *Plant Physiol.* **2011**, *156*, 1701–1705.

(54) Dai, Y.; van Spronsen, J.; Witkamp, G.-J.; Verpoorte, R.; Choi, Y. H. Natural Deep Eutectic Solvents as New Potential Media for Green Technology. *Anal. Chim. Acta* **2013**, *766*, 61–68.

(55) Gore, S.; Baskaran, S.; König, B. Fischer Indole Synthesis in Low Melting Mixtures. *Org. Lett.* **2012**, *14*, 4568–4571.

(56) Schechter, M. D. Serotonergic Mediation of Tetrahydro-Beta-Carboline. *Pharmacol. Biochem. Behav.* **1986**, *24*, 1209–1213.

(57) Nielsen, E. B.; White, F. J.; Holohean, A. M.; Callahan, P. M.; Appel, J. B. Behavioral and Biochemical Evidence for Serotonergic Actions of Tetrahydro-Beta-Carbolines. *Life Sci.* **1982**, *31*, 2433–2439.

(58) Nistico, G.; De Sarro, G. B.; Langer, S. Z. Behavioural and Electrocortical Power Spectrum Effects of 5-Methoxytryptoline and Other Analogs after Intraventricular Administration in Rats. *Eur. J. Pharmacol.* **1987**, *142*, 121–128.

(59) Nichols, D. E. Hallucinogens. *Pharmacol. Ther.* **2004**, *101*, 131–181.

(60) Brierley, D. I.; Davidson, C. Developments in Harmine Pharmacology--Implications for Ayahuasca Use and Drug-Dependence Treatment. *Prog. Neuropsychopharmacol. Biol. Psychiatry* **2012**, *39*, 263–272.

(61) Helsley, S.; Fiorella, D.; Rabin, R. A.; Winter, J. C. A Comparison of N,N-Dimethyltryptamine, Harmaline, and Selected Congeners in Rats Trained with LSD as a Discriminative Stimulus. *Prog. Neuropsychopharmacol. Biol. Psychiatry* **1998**, *22*, 649–663.

(62) Glennon, R. A.; Young, R.; Jacyno, J. M.; Slusher, M.; Rosecrans, J. A. DOM-Stimulus Generalization to LSD and Other Hallucinogenic Indolealkylamines. *Eur. J. Pharmacol.* **1983**, *86*, 453–459.

(63) Rabin, R. A.; Regina, M.; Doat, M.; Winter, J. C. 5-HT2A Receptor-Stimulated Phosphoinositide Hydrolysis in the Stimulus Effects of Hallucinogens. *Pharmacol. Biochem. Behav.* **2002**, *72*, 29–37.

(64) Moya, P. R.; Berg, K. A.; Gutiérrez-Hernandez, M. A.; Sáez-Briones, P.; Reyes-Parada, M.; Cassels, B. K.; Clarke, W. P. Functional Selectivity of Hallucinogenic Phenethylamine and Phenylisopropylamine Derivatives

at Human 5-Hydroxytryptamine (5-HT)2A and 5-HT2C Receptors. *J. Pharmacol. Exp. Ther.* **2007**, *321*, 1054–1061.

(65) Moreno, J. L.; Holloway, T.; Albizu, L.; Sealfon, S. C.; González-Maeso, J. Metabotropic Glutamate mGlu2 Receptor Is Necessary for the Pharmacological and Behavioral Effects Induced by Hallucinogenic 5-HT2A Receptor Agonists. *Neurosci. Lett.* **2011**, *493*, 76–79.

(66) Pähkla, R.; Harro, J.; Rägo, L. Behavioural Effects of Pinoline in the Rat Forced Swimming, Open Field and Elevated plus-Maze Tests. *Pharmacol. Res.* **1996**, *34*, 73–78.

(67) O'Neil, M. J.; et al. The Merck Index - An Encyclopedia of Chemicals, Drugs, and Biologicals (14th Edition - Version 14.9) **2012**.

(68) McKenna, D. J.; Towers, G. H.; Abbott, F. Monoamine Oxidase Inhibitors in South American Hallucinogenic Plants: Tryptamine and Beta-Carboline Constituents of Ayahuasca. *J. Ethnopharmacol.* **1984**, *10*, 195–223.

(69) Paterson, L. M.; Tyacke, R. J.; Robinson, E. S. J.; Nutt, D. J.; Hudson, A. L. In Vitro and in Vivo Effect of BU99006 (5-Isothiocyanato-2-Benzofuranyl-2-Imidazoline) on I2 Binding in Relation to MAO: Evidence for Two Distinct I2 Binding Sites. *Neuropharmacology* **2007**, *52*, 395–404.

(70) Agüí, L.; Peña-Farfal, C.; Yáñez-Sedeño, P.; Pingarrón, J. M. Determination of Beta-Carboline Alkaloids in Foods and Beverages by High-Performance Liquid Chromatography with Electrochemical Detection at a Glassy Carbon Electrode Modified with Carbon Nanotubes. *Anal. Chim. Acta* **2007**, *585*, 323–330.

(71) Jørgensen, H. S. Studies on the Neuroendocrine Role of Serotonin. *Dan. Med. Bull.* **2007**, *54*, 266–288.

(72) Airaksinen, M. M.; Ho, B. T.; An, R.; Taylor, D. Major Pharmacological Effects of 6-Methoxytetrahydro-Beta-Carboline, a Drug Elevating the Tissue 5-Hydroxytryptamine Level. *Arzneimittelforschung.* **1978**, *28*, 42–46.

(73) Pahkla, R.; Rago, L. Pinoline: Formation, Distribution, and Effects. *Melatonin Promot. Heal.* **1998**, 163.

(74) Komulainen, H.; Tuomisto, J.; Airaksinen, M. M.; Kari, I.; Peura, P.; Pollari, L. Tetrahydro-Beta-Carbolines and Corresponding Tryptamines: In Vitro Inhibition of Serotonin, Dopamine and Noradrenaline Uptake in Rat Brain Synaptosomes. *Acta Pharmacol. Toxicol. (Copenh).* **1980**, *46*, 299–307.

(75) Sparks, D. L.; Buckholtz, N. S. 6-Methoxy-1,2,3,4-Tetrahydro-Beta-Carboline: A Specific Monoamine Oxidase-A Inhibitor in CF-1 Mouse Brain. *Neurosci. Lett.* **1980**, *20*, 73–78.

(76) Heisler, L. K.; Zhou, L.; Bajwa, P.; Hsu, J.; Tecott, L. H. Serotonin 5-HT(2C) Receptors Regulate Anxiety-like Behavior. *Genes. Brain. Behav.* **2007**, *6*, 491–496.

(77) Millan, M. J. Serotonin 5-HT2C Receptors as a Target for the Treatment of Depressive and Anxious States: Focus on Novel Therapeutic Strategies. *Therapie* **2005**, *60*, 441–460.

(78) Hardeland, R.; Tan, D.-X.; Reiter, R. J. Kynuramines, Metabolites of Melatonin and Other Indoles: The Resurrection of an Almost Forgotten Class of Biogenic Amines. *J. Pineal Res.* **2009**, *47*, 109–126.

(79) Ressmeyer, A.-R.; Mayo, J. C.; Zelosko, V.; Sáinz, R. M.; Tan, D.-X.; Poeggeler, B.; Antolín, I.; Zsizsik, B. K.; Reiter, R. J.; Hardeland, R. Antioxidant Properties of the Melatonin Metabolite N1-Acetyl-5-Methoxykynuramine (AMK): Scavenging of Free Radicals and Prevention of Protein Destruction. *Redox Rep.* **2003**, *8*, 205–213.

(80) Poeggeler, B.; Thuermann, S.; Dose, A.; Schoenke, M.; Burkhardt, S.; Hardeland, R. Melatonin's Unique Radical Scavenging Properties - Roles of Its Functional Substituents as Revealed by a Comparison with Its Structural Analogs. *J. Pineal Res.* **2002**, *33*, 20–30.

(81) Tan, D. X.; Manchester, L. C.; Reiter, R. J.; Plummer, B. F.; Limson, J.; Weintraub, S. T.; Qi, W. Melatonin Directly Scavenges Hydrogen Peroxide: A Potentially New Metabolic Pathway of Melatonin Biotransformation. *Free Radic. Biol. Med.* **2000**, *29*, 1177–1185.

(82) Wolfler, A. Questionable Benefit of Melatonin for Antioxidant Pharmacologic Therapy. *J. Clin. Oncol.* **2002**, *20*, 4127–4129.

(83) Zefirova, O. N.; Baranova, T. Y.; Ivanova, A. A.; Ivanov, A. A.; Zefirov, N. S. Application of the Bridgehead Fragments for the Design of

Conformationally Restricted Melatonin Analogues. *Bioorg. Chem.* **2011**, *39*, 67–72.

(84) Spadoni, G.; Balsamini, C.; Diamantini, G.; Di Giacomo, B.; Tarzia, G.; Mor, M.; Plazzi, P. V; Rivara, S.; Lucini, V.; Nonno, R.; Pannacci, M.; Fraschini, F.; Stankov, B. M. Conformationally Restrained Melatonin Analogues: Synthesis, Binding Affinity for the Melatonin Receptor, Evaluation of the Biological Activity, and Molecular Modeling Study. *J. Med. Chem.* **1997**, *40*, 1990–2002.

(85) Farce, A.; Chugunov, A. O.; Logé, C.; Sabaouni, A.; Yous, S.; Dilly, S.; Renault, N.; Vergoten, G.; Efremov, R. G.; Lesieur, D.; Chavatte, P. Homology Modeling of MT1 and MT2 Receptors. *Eur. J. Med. Chem.* **2008**, *43*, 1926–1944.

(86) Banasr, M.; Hery, M.; Printemps, R.; Daszuta, A. Serotonin-Induced Increases in Adult Cell Proliferation and Neurogenesis Are Mediated through Different and Common 5-HT Receptor Subtypes in the Dentate Gyrus and the Subventricular Zone. *Neuropsychopharmacol. Off. Publ. Am. Coll. Neuropsychopharmacol.* **2004**, *29*, 450–460.

(87) Yáñez, M.; Fraiz, N.; Cano, E.; Orallo, F. Inhibitory Effects of Cis- and Trans-Resveratrol on Noradrenaline and 5-Hydroxytryptamine Uptake and on Monoamine Oxidase Activity. *Biochem. Biophys. Res. Commun.* **2006**, *344*, 688–695.

(88) Dávalos, A.; Gómez-Cordovés, C.; Bartolomé, B. Extending Applicability of the Oxygen Radical Absorbance Capacity (ORAC-Fluorescein) Assay. *J. Agric. Food Chem.* **2004**, *52*, 48–54.

Chapter 4

Conformationally restrained carbamoylcholine analogues and bioisosteres. Design, synthesis and pharmacology at nicotinic acetylcholine receptors (nAChRs)

Introduction

Acetylcholine (ACh) is one of the most important neurotransmitters in the central nervous system (CNS) and peripheral nervous system (PNS). Presence of ACh is ubiquitous among all levels of life complexity, and has gained relevance along evolution[1]. In the nervous system its actions are mediated through two types of acetylcholine receptors (AChRs): the metabotropic G protein-coupled muscarinic AChRs (mAChRs) and the ligand-gated ion channel nicotinic AChRs (nAChRs). Neuronal nAChR are located at presynaptic and postsynaptic neuron terminals where they modulate functions of major neurotransmitter systems, and thereby influence numerous brain functions[2–4]. There is wide evidence that nAChRs play a role in a broad range of neurodegenerative and psychiatric disorders such as Alzheimer's

disease, Parkinson's disease, epilepsy, schizophrenia, anxiety, and depression[5–17]. These implications provide support to the development of potential treatments for neurological and neurodegenerative diseases based on the direct intervention in the cholinergic system[5–7,18]. To date the only marketed drug targeting nAChR is varenicline, for smoking cessation[19].

The nAChR complex consists of five subunits embedded in the cell membrane symmetrically arranged forming the channel pore (figure 1A). The architecture of nAChRs is similar in CNS and PNS, but in contrast to muscle receptors, neuronal receptors only contain α (α_2-α_{10}) and β (β_2-β_4) subunits[20]. Among all the possible receptor combinations, in the CNS the vast majority of the nAChRs are heteromeric receptors containing α_4 and β_2 subunits and α_7 homomeric receptors, whereas in the PNS the most prevalent are α_3 and β_3 heteromers (figure 1B)[21]. The orthosteric binding site of ACh binds is situated in the interface of neighboring α subunits and between α and β subunits in the heteromeric receptors[22–24].

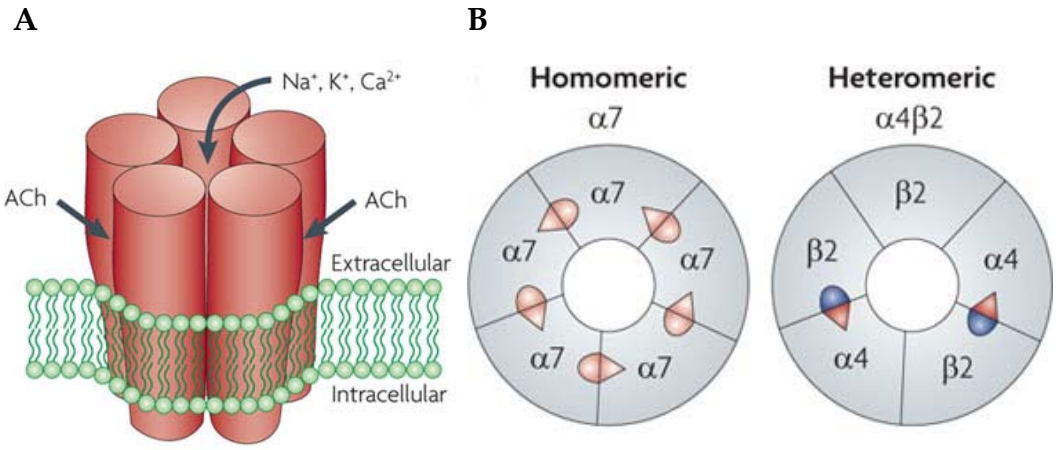

Figure 1. (**A**) Structure of a generic nicotinic receptor embedded in the cell membrane; the five transmembrane domains configure the ion channel. (**B**) Schematic representation of the subunit arrangement in α_7 and $\alpha_4\beta_2$ nAChRs as examples of homomeric and heteromeric receptors. The drop-like coloured shape found in the interfaces of the subunits α_7 and α_4-β_2 represents the ACh orthosteric binding site. Pictures adapted from Changeaux (2010)[25].

In order to achieve a better understanding of nAChR physiological and pathophysiological roles within the complexity of neurotransmission and neurological processes, and the eventual exploitation of their potential as therapeutic targets for the above-mentioned disorders, the development of tools capable to distinguish between the different nAChR subtype recognition is needed[21,26]. This process is not trivial since the orthosteric binding site is a highly conserved region within the family of nAChRs[27].

Recently Frølund's group at University of Copenhagen synthesized and studied the structure-activity relationship (SAR) of a wide set of carbamoylcholine (CCh) analogues that led to the discovery of potent nAChR agonists with high affinity and very good selectivity for $\alpha_4\beta_2$ subtypes. Some selected structures are depicted in figure 2[28–30].

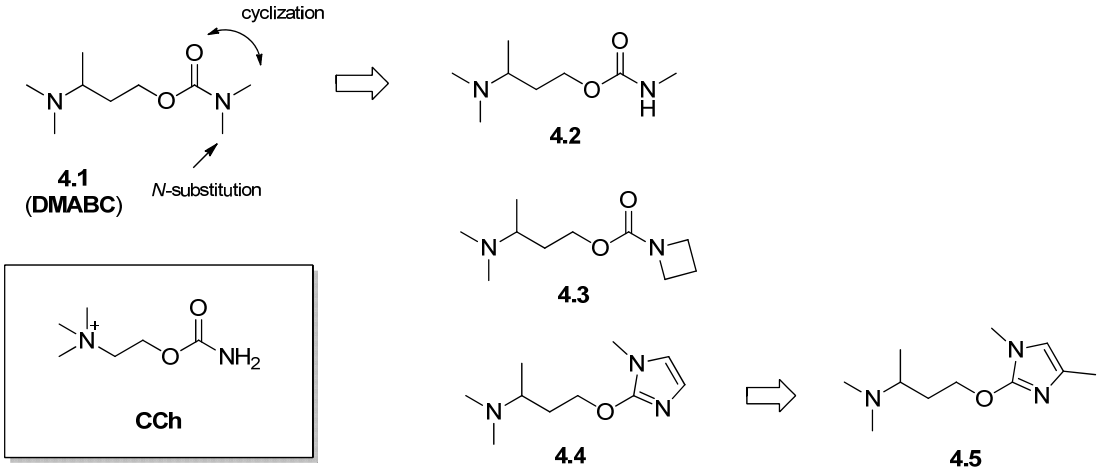

Figure 2. Structures of **CCh** (carbamoylcholine), **4.1** (DMABC, 3-(dimethylamino)butyl dimethylcarbamate) and selected analogues in which the carbamate moiety has been modified: **4.2** (3-(dimethylamino)butyl methylcarbamate), **4.3** (3-(dimethylamino)butyl azetidine-1-carboxylate), **4.4** [4-(1-methyl-1*H*-imidazol-2-yloxy)but-2-yl]-*N*,*N*-dimethylamine and **4.5** [4-(1,4-dimethyl-1*H*-imidazol-2-yloxy)but-2-yl]-*N*,*N*-dimethylamine.

CCh analogues **4.1** and **4.2** exhibit a high degree of selectivity for nicotinic over muscarinic receptors[28]. Additionally, compounds **4.2-4.5** display a pronounced degree of selectivity towards nAChRs subtypes containing β_2 subunits when both their potencies and binding affinities for $\alpha_4\beta_2$, $\alpha_3\beta_4$, $\alpha_4\beta_4$ and α_7 nAChRs are compared[30,31]. Initially, these CCh analogues were thought to bind to the nAChRs in a linear conformation similar to that determined by X-ray crystallography for acetylcholine ACh and CCh co-crystalised with *Lymnaea stagnalis* ACh binding protein (*Ls*-AChBP), a widely used nAChR model[32]. This putative binding pose was further supported by docking studies and the ability of compound **4.1** to superimpose to the epibatidine bound conformation in *Ls*-AChBP [30]. Later crystallographic studies demonstrated that **4.1** and **4.4** bind to *Ls*-AChBP in a folded conformation favored by a likely intramolecular hydrogen bond established between the protonated

dimethylamino group and the ester-like oxygen of these compounds (figure 3)[31].

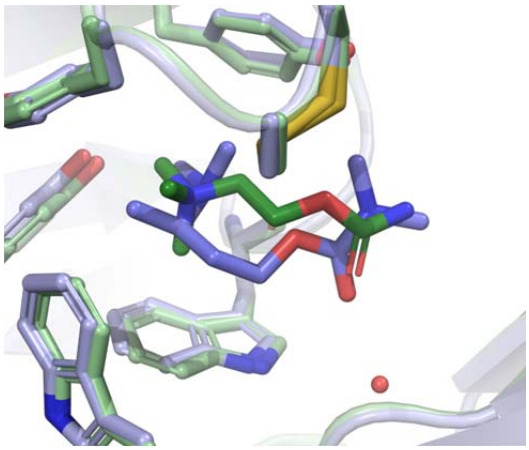

Figure 3. Superimposition of the bound conformation of **CCh** (green, linear) and *R*-DMABC (*R*)-**4.1** (blue, folded), both determined by X-ray structure in *Ls*-AChBP binding site. The carbonyl of (*R*)-**4.1** forms a hydrogen bond with a water molecule (red ball) in the binding site. The ester-like oxygen is within hydrogen bond distance to the presumably protonated dimethylamino group (3.0 Å).

As abovementioned, the binding of ACh to the nAChRs occurs in the interface between two subunits, with at least one α subunit involved. The putative union of CCh, DMABC (**4.1)** and related compounds to the nAChRs is suggested to resemble that of ACh with the dimethyl ammonium group covered by the C-loop of the α subunit whilst the other end faces the complementary subunit. The most important interaction proposed with the complementary subunit is a hydrogen bond established between the carbonyl in the carbamate series or N3 in the imidazole, and a water molecule close to the subunit interface. This interaction has been observed in **4.1** and **4.4** bound to *Ls*-AChBP and it is considered a determinant contact for optimal binding to nAChR (figure 4)[30,31,33].

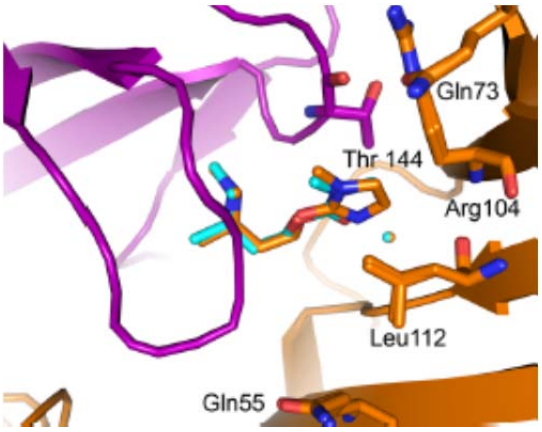

Figure 4. Superimposition of (*R*)-**4.1** (cyan), and (*R*)-**4.4** (orange) co-crystalised in *Ls*-AChBP. The alkyl-ammonium part of both molecules appears covered in the primary subunit (purple) by the C-loop (big purple loop on the right) whereas the carbamate of **4.1**, and the imidazole of **4.4** are found in the interface of both subunits interacting with a water molecule of the complementary subunit (blue and yellow ball). Relevant amino acid side-chains are shown. Figure adapted from Rohde et al. (2012)[33].

Besides this proposed hydrogen-bond interaction with the complementary subunit, the carbamate/azole part of the ligand is considered to be determinant for the observed subtype selectivity profiles. Plausible steric clashes against the complementary subunit are thought to be the most relevant interaction regarding nAChR subtype discrimination. To such extent in the case of imidazoles that $\alpha_4\beta_2$ nAChRs subtype stoichiometry selectivity can be achieved[31].

Approach

The carbamate moiety was extensively studied and high affinity selective ligands were developed. The alkyl-amino end of **4.1** was also studied by means of chain elongation, resolution of the enantiomers, alpha-methyl suppression or alkyl substitution, among others[30]. Some cyclic structures were also studied before but herein, we proposed the first systematic introduction

of different cycles representing various degrees of constriction within the structure of the flexible ligand **4.1** aiming to diminish the degrees of freedom of the original scaffold[29,34]. The main structural features of **4.1**, the carbamoyl moiety and the protonatable amine at physiologic pH, were embedded in different cyclic structures (figure 5). The main purpose of this approach was to push the formation of the putative intramolecular hydrogen bond described above in the crystal structure of **4.1** in *Ls*-AChBP in order to verify the folded conformation of the bound ligand. For this purpose, a cyclopropyl moiety was included within the structure of **4.1** and **4.2**. Additionally, the main structural features of **4.1** were progressively embedded in bigger synthetically-accessible cycles in order to gain insights on the ability of different scaffolds showing different degrees of bulkiness and flexibility to fit within the ACh binding site and presumably potentiate the ligand selectivity. Thus, several urea and thiourea analogues were prepared. Piperazine or homopiperazine have been widely exploited in the development of nicotinic ligands previously[35].

Additionally, in a continuation of Frølund's group efforts to study the interactions of nicotinic ligands with the complementary subunit of the receptor, we utilized two oxadiazole isomers in the bioisosteric replacement of the carbamate moiety of compound **4.1** whilst the flexible amino-alkyl scaffold was kept intact (figure 5).

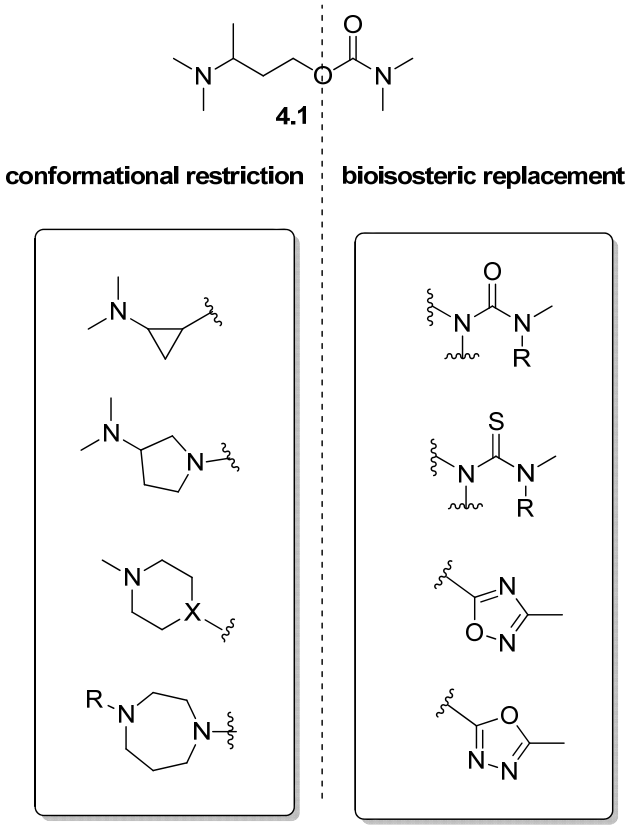

Figure 5. Schematic representation of the modifications performed in the structure of **4.1.**

Chemistry

Synthesis of restricted analogues of DMABC (4.1)

The synthetic route that led to target compounds *trans*-**4.17** - *cis*-**4.20** is outlined in scheme 1. *Trans*-**4.6** was synthesized via enzymatic hydrolysis of the meso diester diethyl *trans*-1,2-cyclopropanedicarboxylate by pig liver esterase (PLE)[36,37]. This procedure transformed the water-insoluble diethyl *trans*-1,2-cyclopropanedicarboxylate into the corresponding soluble mono-hydrolysis product, which was easily extracted from the buffer with ethyl acetate, thus rendering *trans*-**4.6** in excellent yield. This method is reportedly

also valid for diethyl *cis*-1,2-cyclopropanedicarboxylate, however for the synthesis of *cis*-**4.7** alcoholysis of the inexpensive 1,2-cyclopropanedicarboxylic anhydride was chosen instead affording the mono-ester in very good yield[38].

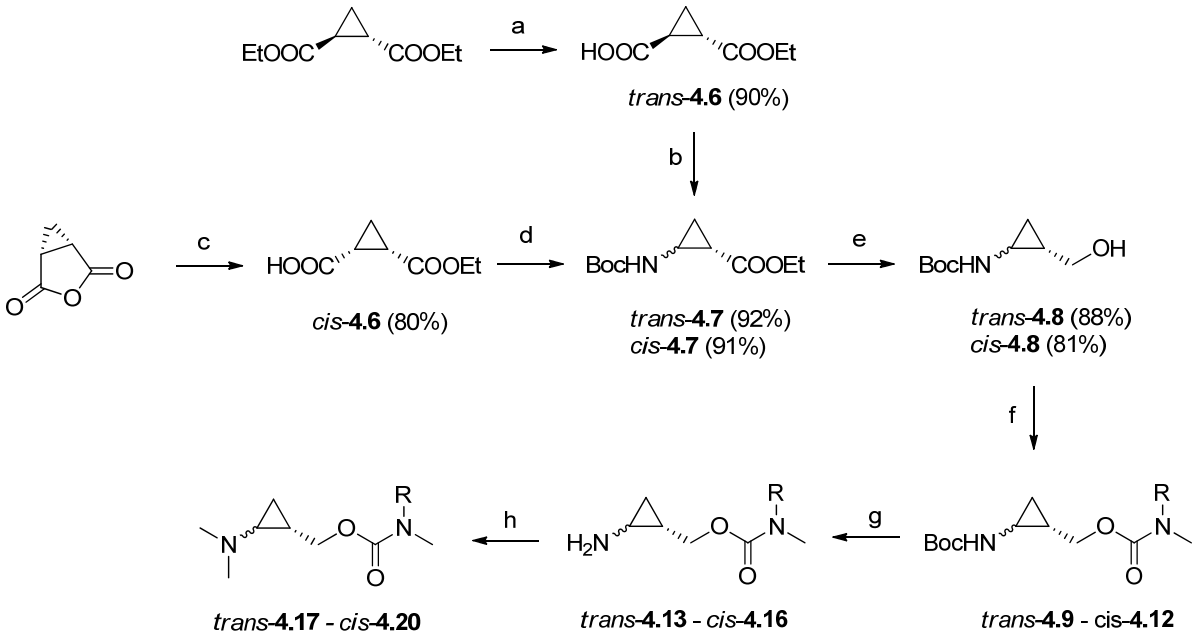

Cpd.	R	Yield(%)	Cpd.	R	Yield(%)
trans-**4.9**	Me	83	*cis*-**4.15**	Me	65
trans-**4.10**	H	78	*cis*-**4.16**	H	70
cis-**4.11**	Me	76	*trans*-**4.17**	Me	65
cis-**4.12**	H	75	*trans*-**4.18**	H	95
trans-**4.13**	Me	77	*cis*-**4.19**	Me	94
trans-**4.14**	H	56	*cis*-**4.20**	H	90

Scheme 1. *Reagents and conditions* (a) PLE, pH 7, 0.1M K_2HPO_3 buffer, rt, 3h; (b) DPPA, TEA, ^{t}BuOH, toluene, 80^{o}C, 24h; (c) DIBAL, toluene, -78^{o}C, 4h; (d) (1) CDI, DMAP (cat.), toluene, rt, 3h; (2) RMeNH 33% EtOH, rt, 1h; (e) TFA, CH_2Cl_2, rt, 0.5h ; (f) $NaCNBH_3$, CH_2O, H_2O-MeCN, rt, 1h.; (g) EtOH, pyr, reflux, 18h; (h) DPPA, TEA, ^{t}BuOH, toluene, 55^{o}C, 24h.

The Curtius rearrangement of acids *trans*-**4.6** and *cis*-**4.6** mediated by diphenhylphosphoryl azide (DPPA) rendered both *trans*-**4.7** and *cis*-**4.7** in excellent yields. An adapted mechanism for the synthesis of *cis*-**4.7** is shown in

scheme 2. DPPA transfers the azido group to the carboxylic acid thus forming an acyl azide stabilized by resonance. Upon heating, the acyl azide decomposes through a concerted mechanism releasing molecular nitrogen and forming an isocyanate. Finally, attack of *tert*-butanol over the electrophilic isocyanate forms the carbamate *cis*-**4.7**. The heating was milder in the synthesis of *cis*-**4.6** in order to avoid isomerization. Nevertheless, unlike Csuk et al. reported previously, no isomerization of the *cis*-isomer was observed at all in NMR[39–41].

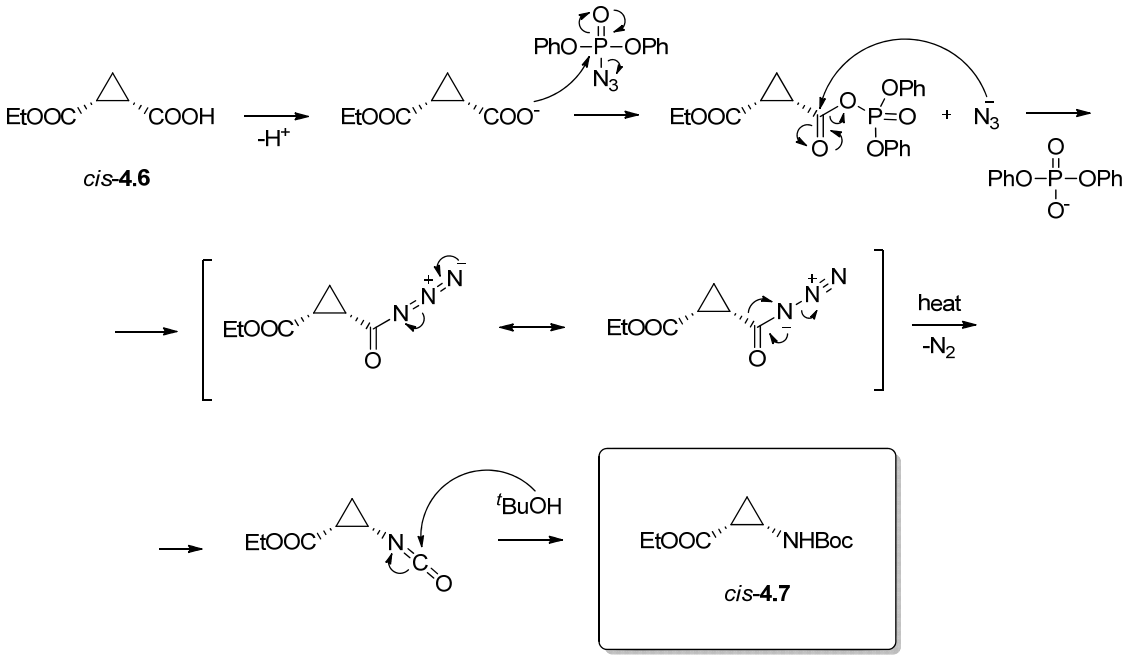

Scheme 2. Suggested mechanism for the DPPA-mediated Curtius rearrangement adapted to the synthesis of *cis*-**4.7.**

Trans-**4.7** and *cis*-**4.7** were chemoselectively reduced to the corresponding alcohols *trans*-**4.8** and *cis*-**4.8** with diisobuthylaluminium hydride (DIBAL) in excellent yield. Different reducing agents ($LiBH_4$, $LiAlH_4$ and DIBAL) were tested to selectively reduce the carbonyl group of the

ethylcarboxylate to the corresponding alcohol; out of the three tested reducing agents, DIBAL provided the best yields[37].

Boc-protected methyl- and dimethylcarbamates *trans*-**4.9**, *trans*-**4.10**, *cis*-**4.11** and *cis*-**4.12** were obtained in good yields in a two-step synthesis. First, addition of carbonyldiimidazole (CDI) over the corresponding alcohol (*trans*-**4.8** or *cis*-**4.8**) formed the corresponding imidazolylcarboxylate. Then, dimethylamine or methylamine was added. The nucleophilic amine attacked the electrophilic imidazolylcarboxylate forming the corresponding carbamate. In each step of the reaction imidazole was released to the medium (scheme 3).

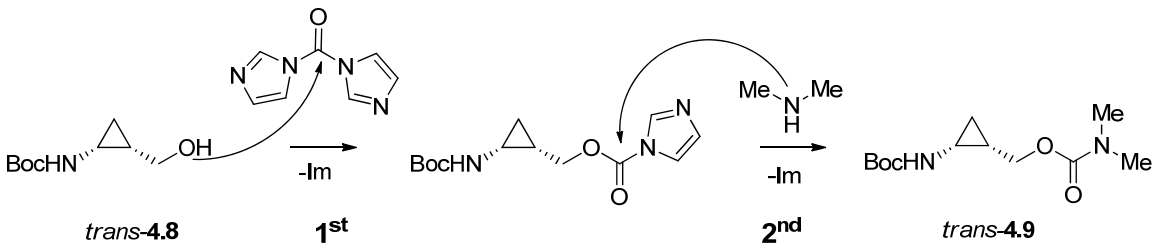

Scheme 3. Schematic representation of the two steps leading to the formation of carbamate *trans*-**4.9** from *trans*-**4.8** (Im: imidazole).

The Boc group was cleaved from compounds *trans*-**4.9**, *trans*-**4.10**, *cis*-**4.11** and *cis*-**4.12** using a mixture of trifluoroacetic acid and dichloromethane[42]. The yields of the free primary amines *trans*-**4.13**, *trans*-**4.14**, *cis*-**4.15** and *cis*-**4.16** ranged from fair to good. During the work-up the process of extraction of the corresponding free amine from a basified solution of the salt was tedious and required continuous liquid-liquid extraction with dichloromethane. The reductive alkylation of the primary amines with formaline and sodium cyanoborohydride afforded the demethylated derivatives *trans*-**4.17**, *trans*-**4.18**, *cis*-**4.19** and *cis*-**4.20** in excellent yields[43]. Both primary and dimethylated amines were tested as oxalate salts.

Addition of dimethylcarbamyl chloride to 3-dimethylaminopyrrolidine afforded compound **4.21** in fair yield. Compounds **4.22-4.24** were synthesised by addition of ethylisocyanate, methylisothiocyanate, or ethylisothiocyanate to a solution of 3-dimethylaminopyrrolidine in ether. The corresponding ureas and thioureas were obtained in various yields (scheme 4). Compounds **4.25-4.27** were obtained from 1-methylpiperazine, 1-methylhomopiperazine and 1-Boc-homopiperazine and dimethylcarbamyl chloride. Compounds **4.28-4.35** were obtained by addition of the corresponding isocyanate or isothiocyanate to 1-methylpiperazine, 1-methylhomopiperazine and 1-Boc-homopiperazine. The ureas and thioureas generally precipitated off the solvent and were obtained in high yields and good purity (scheme 5).

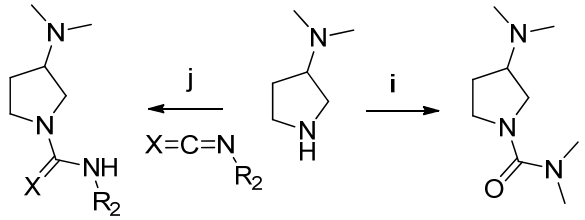

Cpd	X	R_2	yield(%)
4.21	-	-	55
4.22	O	Et	62
4.23	S	Me	7
4.24	S	Et	63

Scheme 4. *Reagents and conditions*. (i) Dimethylcarbamoyl chloride, TEA, THF (anh.) rt, 2h; (j) Et_2O, rt, 1h.

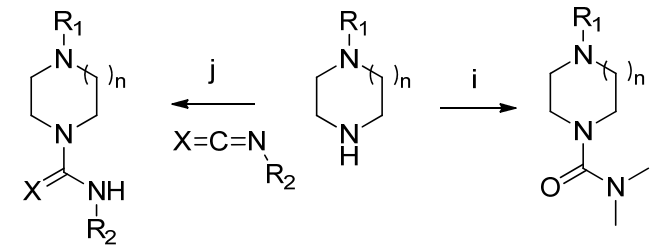

4.28 - 4.35 **4.25 - 4.27**

Cpd	n	X	R_1	R_2	yield(%)
4.25	1	-	-	Me	65
4.26	2	-	-	Me	67
4.27	2	-	-	Boc	100
4.28	1	O	Me	Et	100
4.29	2	O	Me	Et	98
4.30	1	S	Me	Me	100
4.31	2	S	Me	Me	100
4.32	1	S	Me	Et	98
4.33	2	S	Me	Et	98
4.34	2	S	Boc	Me	98
4.35	2	S	Boc	Et	99

Scheme 5. *Reagents and conditions*. (i) Dimethylcarbamoyl chloride, TEA, THF (anh.) rt, 2h; (j) Et_2O, rt, 1h.

Amide **4.36** was synthesized from 1-Boc piperidine-4-carboxylic acid via carbonyldiimidazole coupling with dimethylamine in good yield. Additon of bromhydric acid to amide **4.36** cleaved the protecting group and formed the hydrobromide salt **4.37** in fair yield after recrystallization. This procedure was also employed in the synthesis of compounds **4.38**, **4.39** and **4.40** which hydrobromide salts were isolated in good and very good yield respectively (scheme 6).

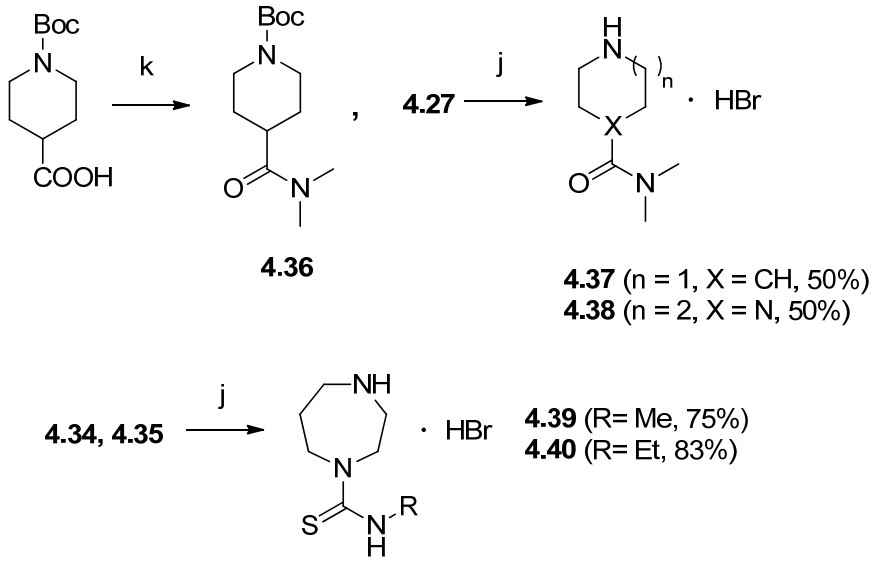

Scheme 6. *Reagents and conditions.*(k) CDI, THF, TEA, DMA, 18h; (l) HBr (aq.), rt, 0.5h.

Synthesis of oxadiazole-containing DMABC analogues.

Compounds **4.42** and **4.45** were both synthesized starting from ethyl levulinate (scheme 7). Ethyl levulinate underwent a microwave-assisted cyclocondensation with acetamidoxime to afford **4.41** in very good yield. Reductive alkylation of **4.41** with dimethylamine and sodium cyanoborohydride afforded the 1,2,4 oxadiazole **4.42** in poor yield. Direct reductive alkylation of ethyl levulinate with dimethylamine and hydrogen in Pd/C afforded the aminoester **4.43** in fair yield. The microwave-irradiated hydrazinolisis of **4.43** quantitatively gave the corresponding hydrazide **4.44**. Cyclocondensation of **4.44** with ethyl orthoacetate afforded the 1,3,4-oxadiazole **4.45** in poor yield.

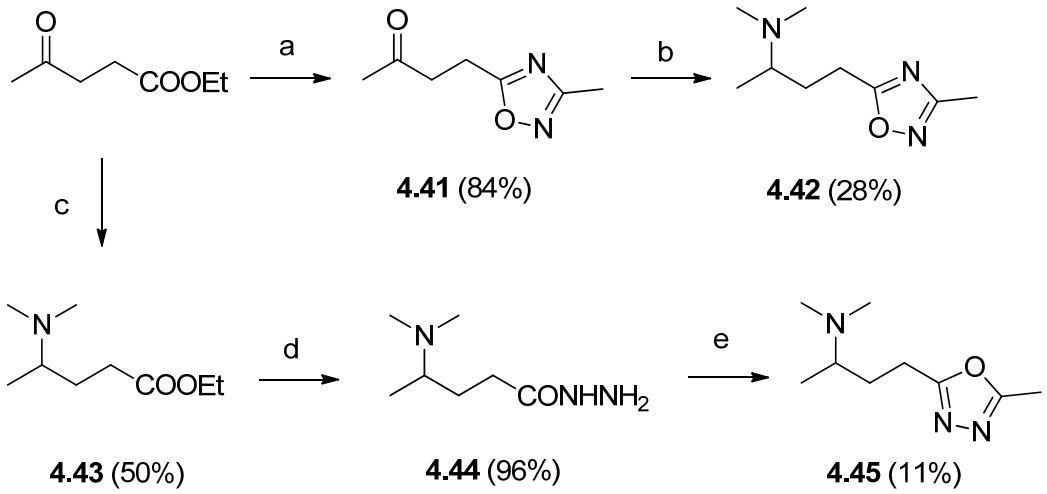

Scheme 7. *Reagents and conditions*. (a) Acetamidoxime, K_2CO_3, MeCN, 180°C (mw), 1h; (b) dimethylamine hydrochloride, dimethylamine (aq.), MeOH, $Na(CN)BH_3$, rt, 18h; (c) dimethylamine (aq.), EtOH, AcOH, H_2, Pd/C, 1 atm, rt, 48h; (e) ethyl orthoacetate, 125°C (mw), 1h.

Pharmacology

Binding at recombinant nAChRs

The binding affinities of the compounds were determined at recombinant heteromeric rat $\alpha_4\beta_2$, $\alpha_4\beta_4$ and $\alpha_3\beta_4$ receptors. The summarized results of radioligand displacement binding studies of compounds showing significant affinity for either receptor are shown in table 2 and 3. None of the synthetic cyclic or oxadiazolic analogues of DMABC (**4.1**) was able to achieve its high affinity for $\alpha_4\beta_2$ nAChR subtype (20 nM)[28].

Table 2. Competition binding, K_i (μM) [pK_i ± S.E.M], of a selection of restricted analogues of DMABC at various nAChRs.

Series	Cpd	$\alpha_4\beta_2$	$\alpha_4\beta_4$	$\alpha_3\beta_4$
	(*S*)nicotine	0.013 [7.85 ± 0.07]	0.072 [7.14 ± 0.09]	0.29 [6.54 ± 0.07]
	4.1[30]	0.02 [7.7 ± 0.04]	0.15 [7.7 ± 0.04]	0.42 [7.7 ± 0.04]
	4.2[28]	0.013 [7.9]	2.6 [5.0]	10 [5.0]
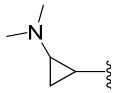	*trans*-**4.17**	~100 [~4.0]	~1000 [~3.0]	~1000 [~3.0]
	trans-**4.18**	~300 [~3.5]	~1000 [~3.0]	>1000 [<3.0]
	cis-**4.19**	1.5 [5.82 ± 0.08]	14 [4.84 ± 0.07]	14 [4.87 ± 0.08]
	cis-**4.20**	2.1 [5.67 ± 0.05]	~30 [~4.5][a]	~50 [~4.3][a]
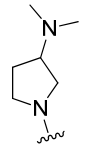	**4.21**	6.4 [5.19 ± 0.05]	2.3 [5.64 ± 0.07]	6.4 [5.19 ± 0.11]
	4.22	5.7 [5.25 ± 0.08]	~30 [~4.5][a]	~30 [~4.5][a]
	4.23	2.3 [5.63 ± 0.09]	~100 [~4.0][a]	~300 [~3.5][a]
	4.24	1.2 [5.93 ± 0.04]	~300 [~3.5][a]	>1000 [<3.0]
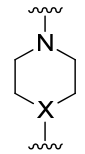	**4.25**	~30 [~4.5][a]	~50 [~4.3][a]	~50 [~4.3][a]
	4.28	10 [5.00 ± 0.05]	~100 [~4.0][a]	~100 [~4.0][a]
	4.30	19 [4.72 ± 0.08]	~500 [~3.3][a]	>1000 [<3.0]
	4.32	5.8 [5.23 ± 0.07]	~300 [~3.5][a]	>1000 [<3.0]
	4.37	>1000 [<3.0]	>1000 [<3.0]	>1000 [<3.0]
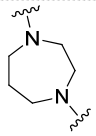	**4.26**	~50 [~4.3][a]	~300 [~3.5][a]	~300 [~3.5][a]
	4.38	11 [4.94 ± 0.11]	~50 [~4.3][a]	~300 [~3.5][a]

[a] Since a complete concentration-inhibition curve could not be obtained for the compound in the concentration ranges tested the IC_{50} value given is an estimate. nd, not determined.

Table 3. Competition binding, K_i (μM) [pK_i ± S.E.M], of oxadiazole analogues of DMABC at various nAChRs.

Series	Cpd	$\alpha_4\beta_2$	$\alpha_4\beta_4$	$\alpha_3\beta_4$
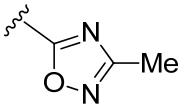	**4.42**	1.7 [5.76 ± 0.06]	~50 [~4.3][a]	~300 [~3.5][a]
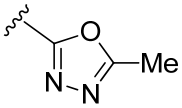	**4.45**	18 [4.73 ± 0.05]	~100 [~4.0][a]	~300 [~3.5][a]

[a] Since a complete concentration-inhibition curve could not be obtained for the compound in the concentration ranges tested the IC_{50} value given is an estimate. nd, not determined.

Among the cyclopropane series the relative position of the substituents on the cycle is essential for receptor recognition, being the *trans* series totally devoid of affinity for any tested nAChRs. Conversely, the *cis* series, if still on a 60-fold decrease in affinity constant compared to **4.1**, showed a selectivity pattern similar to that of the reference compounds **4.1** and **4.2**, being the dimethylaminocarbamate *cis*-**4.19** slightly less selective than the monomethylcarbamate *cis*-**4.20** for the $\alpha_4\beta_2$ subtype than for the $\alpha_3\beta_4$ or the $\alpha_4\beta_4$.

All dimethylaminopyrrolidine representatives showed similar low micromolar binding affinities. Dimethyl urea derivative **4.21** showed no selectivity for any of the tested nAChRs. Replacement for a monoethyl urea (**4.22**) slightly increased the degree of selectivity (both $\alpha_4\beta_4/\alpha_4\beta_2$, $\alpha_3\beta_4/\alpha_4\beta_2$ ~5 fold). Monosubstituted thioureas **4.23** and **4.24** maintained the micromolar affinity with improved selectivity: ethylthiourea **4.24** was the most selective compound of the whole set ($\alpha_4\beta_4/\alpha_4\beta_2$ ~250 fold, $\alpha_3\beta_4/\alpha_4\beta_2$ >800 fold) with a selectivity profile identical to that of **4.2** ($\alpha_4\beta_4/\alpha_4\beta_2$ 220 fold, $\alpha_3\beta_4/\alpha_4\beta_2$ 770 fold). In this series, *N*-mono-substituted ureas and thioureas showed a greater

ability to discriminate between the different tested nAChR with clear preference for the $\alpha_4\beta_2$ subtype than the *N,N*-disubsituted **4.21**.

Very few urea and thiourea analogues with larger cycles reached affinity constant values below 10 μM for the $\alpha_4\beta_2$ nAChR except for piperazines **4.28** and **4.32**. A mild selectivity for $\alpha_4\beta_2$ receptors was observed in all the *N*-monosubstituted ureas and thioureas that showed significant affinity. Even if a full displacement curve could not be obtained for the *N,N*-dimethylurea **4.25**, this compound appears to lack selectivity for any subtype. Deletion of the *N*-methyl substituent, and replacement of the sp^2 nitrogen of **4.25** for a sp^3 carbon gave the inactive compound **4.37**. The homopiperazine family was totally inactive, with the only exception of the secondary amine **4.38**. None of 1-methyl homopiperazines was able to significantly bind to the receptor.

The affinity of compound **4.42** for the $\alpha_4\beta_2$ nAChR resulted 75-fold lower than that of compound **4.1**. In the case of **4.45** the affinity drops an additional order of magnitude for the same receptor subtype (750-fold). The carbamate substitution of **4.1** for either methyl-oxadiazole isomer (3-methyl-1,2,4-oxadiazole and 2-methyl-1,3,4-oxadiazole) provoked a loss of affinity, more pronounced in the case of the 1,3,4-oxadiazole **4.45**. It is worth noting that despite the penalty in affinity, the selectivity profile of compound **4.42** is similar to that of compound **4.1**: greater ability to discriminate between the $\alpha_3\beta_4/\alpha_4\beta_2$ than the $\alpha_4\beta_4/\alpha_4\beta_2$ pair.

Functional characterization at recombinant nAChRs

Only selected compounds were functionally characterized in $\alpha_4\beta_2$ and the $\alpha_3\beta_4$ in the Fluorescent Imaging Plate Reader Membrane Potential Blue (FLIPR-FMP) assay (table 4). Several cycle-containing compounds proved to

be agonists but unfortunately EC_{50} could not be determined due to its weak potency except for **4.21**. This compound, as a racemic mixture, was as potent as other high affinity DMABC analogues like **4.3** (EC_{50} 7.1 μM) at the $\alpha_4\beta_2$ subtype but lacking any selectivity over $\alpha_3\beta_4$ (only 3 fold)[30]. In the same assay the oxadiazole **4.42** was characterized as $\alpha_4\beta_2$ antagonist (table 5).

Table 4. Functional characteristics of the selected compounds at $\alpha_4\beta_2$ and $\alpha_3\beta_4$ nAChRs in the FMP agonist assay, EC_{50} (μM) [pEC_{50} ± S.E.M].

Series	Cpd	$\alpha_4\beta_2$	$\alpha_3\beta_4$
	(*S*)nicotine	0.72 [6.14 ± 0.08]	1.5 [5.82 ± 0.07]
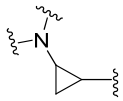	*cis*-**4.15**	agonist[a]	agonist[a]
	cis-**4.19**	agonist[a]	agonist[a]
	cis-**4.20**	agonist[a]	agonist[a]
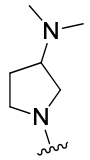	**4.21**	10 [5.01 ± 0.06]	32 [4.49 ± 0.08]
	4.22	agonist[a]	agonist[a]
	4.23	agonist[a]	agonist[a]
	4.24	agonist[a]	agonist[a]
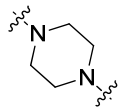	**4.28**	agonist[a]	agonist[a]
	4.32	agonist[a]	agonist[a]

[a] A complete concentration-inhibition curve could not be obtained for the compound in the concentration ranges. The compound elicited significant agonist responses at 300 μM. [b] Weak agonist response at 1 mM. [b] *n* represents the number of members in the ring

Table 5. Functional characteristics of compound **4.42** at $\alpha_4\beta_2$ and $\alpha_3\beta_4$ nAChRs in the FMP antagonist assay, EC_{50} (μM) [$pEC_{50} \pm$ S.E.M].

Series	Cpd	$\alpha_4\beta_2$	$\alpha_3\beta_4$
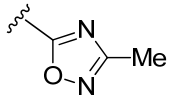	**4.42**	4.2 μM [5.37 ± 0.09]	>300 μM [<3.5]

Molecular modelling. Docking studies

The compounds were docked into *Ls*-AChBP co-crystalised with (*R*)-**4.1** and the top-scoring poses visually evaluated based on its ability to superimpose to the crystal structure of (*R*)-**4.1**. In the case of cyclopropane-containing compounds, the automated docking agreed with the binding results and clearly discriminated between the *trans* and *cis*-isomers. The binding conformation of compound *cis*-**4.19** docked into the binding site of *Ls*-AChBP corresponds with the folded crystalised structure of (*R*)-**4.1** (figure 6A).

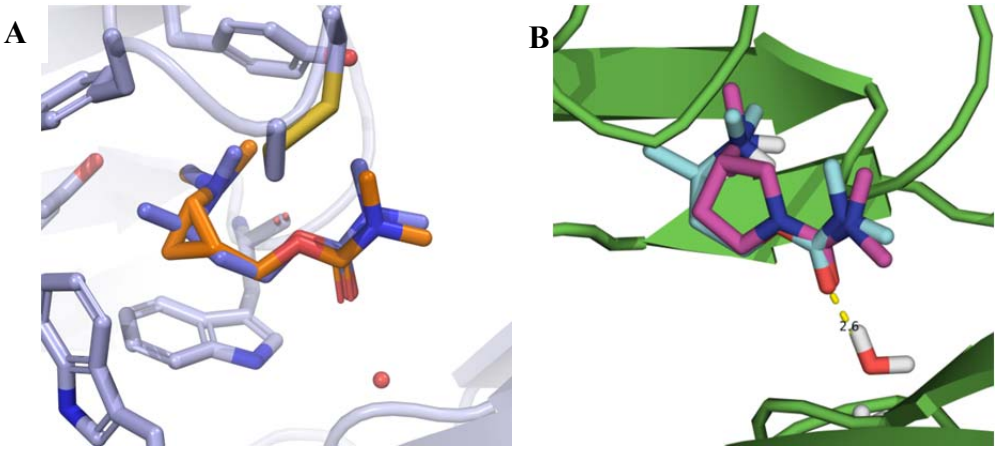

Figure 6. (**A**) Superimposition of (*R*)-**4.1** (blue) and compound *cis*-(1*R*,2*S*)-**4.19** (orange) and (**B**) compound (*S*)-**4.21** (pink) docked into the same binding site (purple) with Schrödinger/Glide.

The dimethylammonium moiety of *cis*-**4.19** rightly overlaps with that of (*R*)-**4.1**, maintaining also the hydrogen-bond distance between the proton held over the charged nitrogen and the ester-like oxygen of the carbamate (figure 6B). Another important feature maintained is the distance between the carbonyl group and the water molecule buried in the binding pocket. Even if the main structural features of *cis*-**4.19** spatially correspond with those of (*R*)-**4.1** crystal structure, the cyclopropyl edge is pointing in a different relative angle compared to the methyl substituent of (*R*)-**4.1.** The distinct geometry of *cis*-**4.19** could involve steric clashes against the wall of the binding pocket and in turn, undermine its affinity.

In the case of the docked conformation of dimethylaminopyrrolidine (*S*)-**4.21**, both the cationic center and the carbonyl group fairly overlap spatially with the folded structure of (*R*)-**4.1**, but the *N*,*N*-dimethyl substituents attached to ammonium nitrogen do not. The intramolecular hydrogen bond proposed in the case of both (*R*)-**4.1** and *cis*-**4.19**, in the case of (*S*)-**4.3** does not seem feasible due to the boat conformation of the pyrrolidine ring and the urea nature of the compound. The urea nitrogen that replaces for

the ester-like oxygen of compounds (*R*)-**4.1** has a single lone pair in a *p* orbital conjugated with the urea carbonyl, what would weaken its availability for establishing hydrogen-bond interactions.

None of the series of compounds synthesized in this work showed a selectivity profile attributable to the cycle used as scaffold. Conversely all series reinforced the hypothesis that the determinant feature for the selectivity displayed by **4.1** and its analogues is the substitution of the *N*-carbamoyl moiety regardless of the scaffold employed. The structural observations suggest that the interactions with the complementary subunit that putatively permit compound **4.2** to discriminate between different nAChR subtypes better than **4.1** are clearly present in the case of the *cis*-**4.19** - *cis*-**4.20** pair.

The agreement found in the *N*-carbamate substitution-selectivity relationship between dimethylaminobutyl flexible ligands (**4.1** and **4.2**) and the *cis*-cyclopropane and dimethylaminopyrrolidine series further support that the binding to the nicotinic receptors of the latter should occur in a similar manner.

Docking of compound (*R*)-**4.42** revealed that the oxadiazole ring could virtually intervene in the same contacts as **4.1** does (figure 7). The alkyl-ammonium ends of both compounds reasonably overlap. Additionally the oxygen within the oxadiazole ring is at hydrogen-bond distance from the dimethylammonium group. The nitrogen in position 4 within the oxadiazole ring replaces for the carbonyl oxygen in (*R*)-**4.1** while keeping the methyl group in position 3 in a rather similar pose. Taking into account the importance of the *N*-carbamate substitution in subtype discrimination, the relative position of this methyl attached to the oxadiazole ring could justify the similar selectivity profile shared between **4.1** and **4.42**.

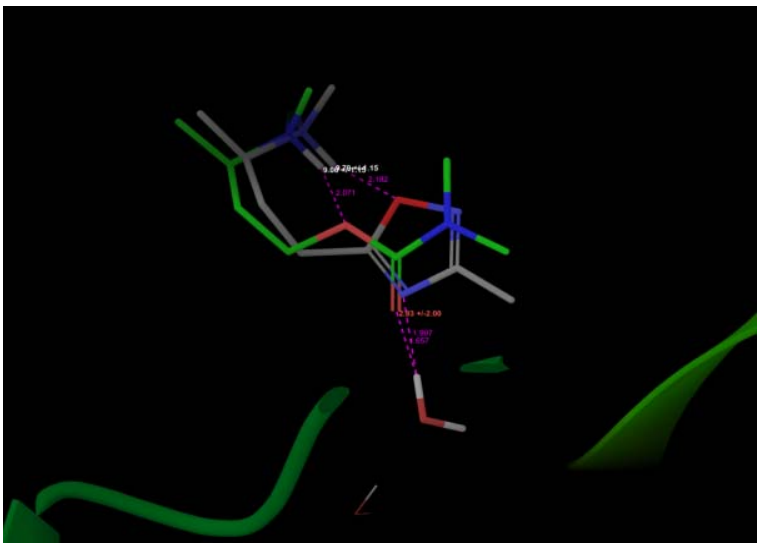

Figure 7. Superimposition of (*R*)-**4.1** (green) and compound **4.42** (gray) docked into *Ls*-AChBP co-crystalised with (*R*)-**4.1** with Schrödinger/Glide.

The structure-function relationship that determines the ability of nAChRs ligands to promote the activation of the receptor remains elusive. Numerous efforts have been made in order to rationalize the mechanistic determinants behind the effect of agonists. The closure of the C-loop of the primary subunit *Ls*-AChBP, as $\alpha_4\beta_2$ surrogate, has been associated with the efficacy of partial agonists.[44,45] More recently, it has been proposed that the C-loop closure determines mostly the binding affinity whereas the efficacy of ligands relies on their ability to stabilize a strong intersubunit bridge between the interfaces of the α subunit and the complementary subunit[33,46]. Accordingly, even if an EC_{50} could not be obtained for most of the compounds prepared in this work, all cyclic-analogues of **4.1** which functional profile was characterized were agonists at the $\alpha_4\beta_2$ subtype regardless of the cyclic scaffold employed. An agonism more likely to be attributable to the ureas and thioureas than to the amino-alkylic core. Following the same hypothesis, the substitution of the carbamate of **4.1** for 3-methyl-1,2,4-oxadiazole ring (**4.42**) could represent the opposite case. The original 3-dimethylaminobutyl scaffold

has been maintained intact, but the oxadiazole replacement possibly blocks the contacts that could lead to the activation of the $\alpha_4\beta_2$ receptor.

Conclusions

A series of cyclic DMABC (**4.1**) analogues have been synthesized and pharmacologically characterized in different nAChRs subtypes. Summarizing the general results, in the context of this work, the smaller the cycle employed, the better affinity achieved. The conformational restriction approach used in this work has failed to provide potent and selective $\alpha_4\beta_2$ nAChR ligands. The compounds showing the highest affinity belong to the aminocyclopropane and aminopyrrolidine series, but the poor activity results obtained cannot clearly confirm the folded disposition of compound **4.1** as the preferred conformation upon binding to the $\alpha_4\beta_2$ nAChR. Nevertheless the results obtained in this work reinforce the importance of the *N*-carbamate substitution in the structure-selectivity relationship of CCh derivatives, and show how substituted urea and thiourea can partially replace for such moiety. Derivative **4.21** proved to be functionally as potent as other studied ligands within the flexible analogues series. Further biostructural studies would be needed, and the pharmacology profile of both possible enantiomers established. Furthermore, our efforts to broaden up the family of DMABC azolic analogues have demonstrated how the bioisiosteric replacement of the carbamate of **4.1** for a 3-methyl-1,2,4-oxadiazole (**4.42**) leads to a reversion of the intrinsic activity while still maintaining the selectivity profile of the reference compound. Therefore, further exploitation of the bioisosteric replacement of the carbamate moiety could be an interesting strategy for the development of differential pharmacological profiles.

Experimental section

Chemistry. General procedures. All reactions involving air sensitive reagents were performed under a N_2 atmosphere using syringe-septum cap techniques and glassware was flame-dried *in vacuo* prior to use. Unless otherwise noted, all materials were obtained from commercial suppliers and used without further purification. When dry solvents were used, THF was distilled and stored over molecular sieves (4Å and toluene was purchased from a commercial source and stored over molecular sieves (4Å). ^{1}H NMR and ^{13}C NMR spectra were obtained on a Varian Gemini 2000 (300 MHz) or Varian Mercury Plus (300 MHz). Analytical thin-layer chromatography (TLC) was carried out using Merck silica gel 60 F254 plates, and the compounds were visualized using either $KMnO_4$ spraying reagent or phosphomolybdic acid 10% wt. in ethanol. Elemental analyses were performed by J. Theiner at Department of Physical Chemistry, University of Vienna, Austria. Melting points were determined in open capillary tubes and are uncorrected. Liquid chromatography was performed on a Waters analytical LC-MS equipped with a SunFire C18 4.6 x 50 mm column and a cuadrupole mass spectrometer (Micromass ZQ).

General procedure for oxalate salt formation: To the free base of the amine (1 equiv.) was added a solution of oxalic acid (1.0 – 1.3 equiv.) dissolved in warm acetone, the mixture was cooled to force crystallization. In the cases were this was not sufficient, after the evaporation of the solvent, the mixture was recrystallized from EtOH:Et_2O.

Method A. *N,N*,4-Trimethylpiperazine-1-carboxamide oxalate (4.25).

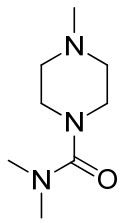

1-methylpiperazine (221 mg, 2.21 mmol) was added carefully over a solution of dimethylcarbamyl chloride (236 mg, 2.21 mmol) and triethylamine (637 μL, 4.42 mmol) dissolved in anhydrous THF (10 mL). The evolution was followed by TLC. After 2 h stirring at room temperature a fine white precipitate was formed that was filtered off, and the filtrate was evaporated to give a light brown oil that was resuspended in water made basic with NaOH 2M (pH 11-12). The aqueous suspension was subjected to liquid-liquid continuous extraction with EtOAc that after, drying over $MgSO_4$, and evaporation of the solvent gave the free base (**4.25**) (245 mg, 65%) as a slightly yellow oil. ^{1}H NMR (400 MHz, $CDCl_3$) δ 3.26 (t, *J* = 5.0 Hz, 4H), 2.76 (s, 6H), 2.42 (t, *J* = 4.8 Hz, 4H), 2.29 (s, 3H). The free base was crystalised as an oxalate according to the general method and thus (**4.25**) was obtained as a white solid. Mp: 112-114ºC. ^{1}H NMR (400 MHz, D_2O) δ 3.83 (d, *J* = 13.2 Hz, 2H), 3.55 (d, *J* = 11.0 Hz, 2H), 3.27 – 3.11 (m, 4H), 2.95 (s, 3H), 2.90 (s, 6H). ^{13}C NMR (101 MHz, $CDCl_3$) δ 167.14, 55.54, 46.17, 45.50, 40.20. HPLCMS (*m/z*) [MH^+] 172.1 (free base). Anal. ($C_8H_{117}N_3O \cdot 1.3\ C_2H_2O_4$) C, H, N.

Method B. ***N,N*-Dimethylpiperidine-4-carboxamide hydrobromide (4.37).**

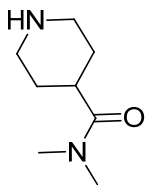

4.36 was dissolved in EtOH (4 mL) and a solution of HBr 62% aq. (0.3 mL) was added. The mixture was kept stirring overnight, solvent removed and the resulting solid was recrystalised from EtOH:Et_2O to yield **4.37** (81 mg, 50%) as a white solid. Mp: 178-180ºC. ^{1}H NMR (400 MHz, DMSO) δ 8.38 (s, 1H), 8.04 (s, 1H), 3.27 (d, *J* = 12.5 Hz, 2H), 3.02 (s, 3H), 3.00 – 2.93 (m, 3H), 2.80 (s, 3H), 1.82 – 1.62 (m, 4H). ^{13}C NMR (101 MHz, DMSO) δ 172.74, 42.42, 36.58, 34.96, 34.70,

24.88. HPLCMS (*m/z*) [MH^+] 157.2 (free base). Anal. ($C_8H_{16}N_2O \cdot 1.6HBr$) C, H, N.

Method C. *N*-Ethyl-4-methylpiperazine-1-carboxamide oxalate (**4.28**).

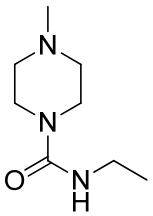

1-homopiperazine (79 mg, 0.78 mmol) was dissolved in 1 mL of Et_2O and ethyl isocyanate (68 µL, 0.86 mmol) was then added. The evolution of the reaction was followed by TLC. After 0.5 h stirring at room temperature, the solvent was removed and the free base **4.28** (134 mg, 100%) was recovered as an oil that crystalised upon standing. ^1H NMR (400 MHz, $CDCl_3$) δ 4.39 (s, 1H), 3.34 (t, *J* = 5.1 Hz, 4H), 3.20 (qd, *J* = 7.2, 5.3 Hz, 2H), 2.37 (t, *J* = 5.1 Hz, 4H), 2.27 (s, 3H), 1.07 (t, *J* = 7.2 Hz, 3H).The free base was converted to the oxalate salt according to the general procedure to obtain a white solid. Mp: 164-165ºC. ^1H NMR (400 MHz, D_2O) δ 4.05 (d, *J* = 14.5 Hz, 2H), 3.47 (d, *J* = 12.4 Hz, 2H), 3.20 – 3.14 (m, 2H), 3.11 (q, *J* = 7.3 Hz, 2H), 3.00 (td, *J* = 12.4, 2.9 Hz, 2H), 2.86 (s, 3H), 1.02 (t, *J* = 7.2 Hz, 3H). ^{13}C NMR (101 MHz, D_2O) δ 165.76, 52.85, 42.89, 40.90, 35.56, 14.39.LCMS (*m/z*) [MH^+] 172.2 (free base). Anal. ($C_8H_{17}N_3O \cdot C_2H_2O_4$) C, H, N.

trans-**2-(Ethoxycarbonyl)cyclopropanecarboxylic acid (*trans*-4.6).**

A suspension of *trans*-1,2-cyclopropanedicarboxylate (8.33 g, 44.7 mmol) in K_2HPO_4 buffer at pH 7.0 (250 mL) and room temperature is stirred gently and a suspension of PLE (412 mg, 7000 units, Sigma Aldrich) previously soaked for 2 h at room temperature in the same buffer (250 mL) is added over the mixture. The pH is maintained at pH 7.0 – 7.2 by manual addition of NaOH 35% wt dropwise. No pH change was observed after 1 hour, nevertheless the stirring was maintained for 16 h. The

mixture was filtrated to remove the protein aggregates, acidified (pH 1-2) by addition of HCl 4M and extracted with diethyl ether (4 x 100 mL). The combined organic phases were dried ($MgSO_4$) and the solvent removed. The remaining oil crystallized upon standing at room temperature to afford *trans*-**4.6** (6.4 g, 90%) as brownish crystals. Mp: 49.8-52.3ºC. ^{1}H NMR (300 MHz, $CDCl_3$) δ 4.23 – 4.08 (q, *J* = 7.1 Hz, 2H), 2.29 – 2.08 (dddd, *J* = 17.8, 8.6, 6.0, 3.8 Hz, 2H), 1.56 – 1.41 (m, 2H), 1.33 – 1.23 (t, *J* = 7.1 Hz, 3H). ^{13}C NMR (75 MHz, $CDCl_3$) δ 178.04, 171.49, 61.52, 23.30, 22.34, 16.13, 14.45.

trans-**Ethyl-2-((*tert*-butoxycarbonyl)amino)cyclopropanecarboxylate (*trans*-4.7).**

To a stirred solution of *trans*-**4.6** (5.59 g, 32.5 mmol) in dry toluene (50 mL), dry triethylamine (3.49 g, 34.6 mmol) and dry *tert*-butanol (13.27 g, 179 mmol) diphenyl-phosphorylazide (8.94 g, 32.5 mmol) is added. The solution is heated to 80ºC under nitrogen and stirred for 20 h. After cooling to room temperature the solvent and the excess of *tert*-butanol were removed under reduced pressure and the remaining oil resuspended in citric acid 10% (50 mL) and extracted with EtOAc (20 mL x 4). The combined organics were then washed with $NaHCO_3$ sat. (40 mL) and brine (40 mL), dried ($MgSO_4$) and solvent evaporated to afford *trans*-**4.7** (6.9 g, 92%) as a brownish oil that crystallized upon standing at room temperature and that was used as such for the next step. Mp: 58.5-59.5ºC. ^{1}H NMR (300 MHz, $CDCl_3$) δ 4.76 – 4.67 (br s, 1H), 4.23 – 4.07 (m, 2H), 3.15 – 2.90 (m, 1H), 1.78 – 1.68 (ddd, *J* = 8.8, 5.7, 2.7 Hz, 1H), 1.49 – 1.43 (s, 9H), 1.44 – 1.35 (dt, *J* = 7.7, 5.7 Hz, 1H), 1.33 – 1.22 (t, *J* = 7.1 Hz, 3H), 1.15 – 1.06 (dt, *J* = 9.1, 5.1 Hz, 1H). ^{13}C NMR (75 MHz, $CDCl_3$) δ 172.34, 155.93, 80.20, 60.94, 32.19, 28.57, 22.79, 15.99, 14.53. IR(cm^{-1}): 3337, 2980, 2930, 1721, 1688, 1514, 1163.

cis-**2-(Ethoxycarbonyl)cyclopropanecarboxylic acid (***cis*-**4.6).**

1,2-Cyclopropanedicarboxylic anhydride (4 g, 35 mmol) was dissolved in a mixture of EtOH (7 mL) and pyridine (4.5 mL) and heated to 100ºC. The mixture was stirred for 18 h after which the solvents were evaporated at reduced pressure. The remaining oil was resuspended in H_2O (30 mL), acidified with conc. aqueous HCl (pH 1-2) and extracted with Et_2O (20 mL x 5). The combined ethereal extracts were dried ($MgSO_4$) and solvent evaporated to afford *cis*-**4.6** (4.4 g, 80%) as white crystals. ^{1}H NMR (300 MHz, $CDCl_3$) δ 8.50 – 7.94 (br s, 1H), 4.42 – 3.88 (q, *J* = 7.1 Hz, 2H), 2.17 – 2.00 (m, 2H), 1.73 – 1.61 (td, *J* = 6.7, 5.0 Hz, 1H), 1.36 – 1.27 (td, *J* = 8.5, 5.1 Hz, 1H), 1.27 – 1.21 (m,1H; t, *J* = 7.1 3H), 1.19 – 1.11 (q, *J* = 5.9 Hz, 1H). ^{13}C NMR (75 MHz, $CDCl_3$) δ 175.62, 170.18, 61.61, 22.77, 21.63, 14.34, 12.77.

cis-**Ethyl 2-((***tert***-butoxycarbonyl)amino)cyclopropanecarboxylate (***cis*-**4.7).**

To a stirred solution of *cis*-**4.6** (4.3 g, 27.4 mmol) in dry toluene (30 mL), dry triethylamine (2.7 g, 27.4mmol) and dry *tert*-butanol (25.7 g, 347 mmol) diphenyl-phosphorylazide (7.52 g, 27.4 mmol) is added. The solution is heated to 55ºC under nitrogen and stirred for 24 h. After cooling to room temperature the solvent and the excess of *tert*-butanol were removed under reduced pressure, the remaining oil resuspended in EtOAc (40 mL) and washed with citric acid 10% (2 x 30 mL). The acidic washings were extracted with EtOAc (20 mL). The combined organics were then washed with $NaHCO_3$ sat. (30 mL) and brine (30 mL), dried ($MgSO_4$) and solvent evaporated to afford *cis*-**4.7** (5.71 g, 91%) as a white crystals. Mp: 53-55ºC. ^{1}H NMR (300 MHz, $CDCl_3$) δ 5.55 – 5.08 (s, 1H), 4.30 – 3.98 (qd, *J* = 7.1, 1.1 Hz, 2H), 3.45 – 3.20 (m, 1H), 1.93 – 1.76 (q, *J* = 7.7 Hz, 1H),

1.46 – 1.39 (s, 9H), 1.31 – 1.24 (t, *J* = 7.1 Hz, 4H), 1.19 – 1.11 (q, *J* = 5.9 Hz, 1H). ^{13}C NMR (75 MHz, $CDCl_3$) δ 172.12, 156.19, 79.85, 61.05, 31.70, 28.70, 19.36, 14.57, 14.31. IR (cm^{-1}): 3361, 2980, 2935, 1710, 1512, 1183, 1155.

trans-tert-**Butyl (2-(hydroxymethyl)cyclopropyl)carbamate (***trans*-**4.8).**

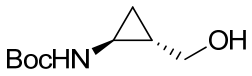

DIBAL (30.5 mL, 1M in toluene) was cooled to -78°C under nitrogen. A solution of *trans*-**4.7** (2 g, 8.73 mmol) was slowly added in THF with an automated system over 40 min. Stirring at -78°C was kept for 4 h, after which the reaction was quenched by slow addition of Na_2SO_4 soaked in H_2O. The mixture was allowed to reach room temperature and stirred for 1 h after which the precipitate was filtered off and washed with EtOAc (4 x 20 mL). The filtrate and the washings were combined, washed with brine (30 mL), dried ($MgSO_4$) and solvent removed to afford *trans*-**4.8** (1.45g, 88%) as a dark yellow oil. ^{1}H NMR (300 MHz, $CDCl_3$) δ 4.92 – 4.83 (br s, 1H), 3.91 – 3.72 (m, 1H), 3.21 – 3.01 (t, *J* = 9.8 Hz, 1H), 2.96 – 2.84 (s, 1H), 2.33 – 2.30 (dd, *J* = 4.5, 2.8 Hz, 1H), 1.51 – 1.41 (s, 9H), 1.36 – 1.14 (td, *J* = 9.2, 5.9 Hz, 1H), 0.87 – 0.76 (td, *J* = 9.5, 4.6 Hz, 1H), 0.76 – 0.66 (dt, *J* = 7.5, 5.9 Hz, 1H). ^{13}C NMR (75 MHz, $CDCl_3$) δ 156.71, 80.16, 65.07, 29.96, 28.61, 24.24, 11.55. IR (cm^{-1}): 3330, 2925, 2854, 1686, 1513, 1165.

cis-tert-**Butyl (2-(hydroxymethyl)cyclopropyl)carbamate (***cis*-**4.8).**

According to the preparation of *trans*-**4.8,** from *cis*-**4.7** (3.22 g, 14.06 mmol) *cis*-**4.8** (2.10 g, 81%) was obtained as colorless oil that crystallized upon standing. Mp: 63.5-64.8. ^{1}H NMR (300 MHz, $CDCl_3$) δ 4.90 – 4.82 (br s, 1H), 3.98 – 3.89 (td, *J* = 11.5, 3.7 Hz, 1H), 3.52 – 3.48 (d, *J* = 11.2 Hz, 1H), 3.19 – 3.09 (t, *J* = 11.1 Hz, 1H), 2.65 – 2.58 (td, *J* = 6.9, 4.2 Hz, 1H), 1.47 – 1.46 (s, 9H), 1.42 – 1.32 (m, 1H), 0.96 – 0.88 (ddd, *J* = 9.2, 7.2,

5.7 Hz, 1H), 0.27 – 0.20 (td, *J* = 6.2, 4.3 Hz, 2H). ^{13}C NMR (75 MHz, $CDCl_3$) δ 158.52, 80.83, 61.74, 28.58, 26.94, 21.31, 9.43. IR (cm^{-1}): 3370, 2951, 1689, 1508, 1163.

trans-**(2-((*tert*-Butoxycarbonyl)amino)cyclopropyl)methyl dimethylcarbamate (*trans*-4.9).**

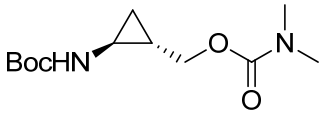

To a solution of *trans*-**4.8** (704 mg, 3.76 mmol) in a mixture anhydrous toluene (11 mL) and anhydrous THF (3 mL) carbonyldiimizadole (914 mg, 5.64 mmol) and a catalytic amount of 4-dimethylaminopyridine were added. After stirring at room temperature for 2.5 h a solution of dimethylamine 33% in EtOH was added (18.8 mL) and stirred for an additional hour. The reaction was monitored on TLC. The solvent was eliminated under vacuum and the resulting oil dissolved in EtOAc (30 mL). The solution was washed with citric acid 10% in H_2O until the pH stays acidic after washing, then NaOH 1 M (2 x 10 mL), brine (10mL), dried ($MgSO_4$) and solvent evaporated to afford *trans*-**4.9** (800 mg, 83%) as a colorless oil. ^{1}H NMR (300 MHz, $CDCl_3$) δ 4.88 – 4.75 (br s, 1H), 3.99 – 3.90 (m, 2H), 2.88 – 2.85 (d, *J* = 0.9 Hz, 6H), 2.48 – 2.41 (m, 1H), 1.42 – 1.38 (s, 9H), 1.31 – 1.16 (m, 1H), 0.77 – 0.70 (dd, *J* = 8.1, 5.2 Hz, 1H). ^{13}C NMR (75 MHz, $CDCl_3$) δ 156.61, 156.34, 79.61, 66.95, 36.61, 36.13, 28.60, 28.33, 19.81, 12.37. IR (cm^{-1}): 3332, 2976, 2932, 1686, 1498, 1163.

trans-tert-**Butyl (2-((methylcarbamoyl)oxy)methyl)cyclopropyl)carbamate (*trans*-4.10).**

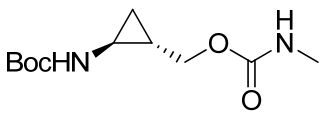

According to the preparation of *trans*-**4.9,** from *trans*-**4.8** (1.45 g, 7.75 mmol), employing

methylamine 33% in EtOH instead (3.6 mL), *trans*-**4.10** (1.48 g, 78%) was obtained as a white solid. Mp: 94.7-95.2°C. ^{1}H NMR (300 MHz, $CDCl_3$) δ 4.70 – 4.64 (br s, 2H), 4.00 – 3.90 (d, *J* = 8.3 Hz, 2H), 2.82 – 2.77 (d, *J* = 4.2 Hz, 3H), 2.50 – 2.45 (s, 1H), 1.47 – 1.42 (s, 9H), 1.30 – 1.22 (m, 1H), 0.82 – 0.72 (m, 1H). ^{13}C NMR (75 MHz, $CDCl_3$) δ 157.24, 156.37, 79.81, 66.72, 28.66, 28.47, 27.82, 19.87, 12.43. IR (cm^{-1}): 3338, 2977, 1693, 1524, 1253, 1167.

(2-((*tert*-Butoxycarbonyl)amino)cyclopropyl)methyl dimethylcarbamate (*cis*-4.11).

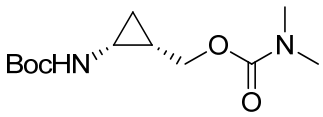

According to the preparation of *trans*-**4.9,** from *cis*-**4.8** (1.12 g, 6.01 mmol) *cis*-**4.11** (1.19 g, 76%) was obtained as white crystal. Mp: 84.5-87.0°C.^{1}H NMR (300 MHz, $CDCl_3$) δ 5.72 – 5.67 (br s, 1H), 4.30 – 4.22 (dd, *J* = 11.9, 4.6 Hz, 1H), 4.01 – 3.92 (dd, *J* = 11.9, 9.4 Hz, 1H), 2.92 – 2.90 (s, 6H), 2.70 – 2.57 (m, 1H), 1.44 – 1.43 (s, 9H), 1.30 – 1.17 (m, 1H), 1.04 – 0.96 (dt, *J* = 12.4, 5.8 Hz, 1H), 0.43 – 0.36 (td, *J* = 6.1, 4.2 Hz, 1H). ^{13}C NMR (75 MHz, $CDCl_3$) δ 157.52, 157.13, 79.48, 64.40, 36.80, 36.28, 28.67, 27.58, 17.01, 11.02. IR(cm^{-1}): 3326, 2977, 2933, 1685, 1500, 1387, 1365, 1165.

cis-tert-**Butyl(2-(((methylcarbamoyl)oxy)methyl)cyclopropyl)carbamate (*cis*-4.12).**

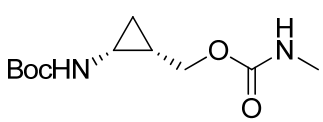

According to the preparation of *trans*-**4.9,** from *cis*-**4.8** (885 mg, 4.73 mmol), employing methylamine 33% in EtOH (3.4 mL) *cis*-**4.12** (866 mg, 75%) was obtained as white crystal. Mp: 92.8-95.2°C. IR(cm^{-1}): 3327, 2977, 1689, 1514, 1253, 1164. ^{1}H NMR (300 MHz, $CDCl_3$) δ 5.60 – 5.49 (br s, 1H), 4.81 – 4.72 (br s, 1H), 4.29 – 4.19 (dd, *J* = 11.8, 4.9 Hz, 2H), 4.01 – 3.89 (t, *J* = 10.6 Hz,

1H), 2.83 – 2.76 (d, *J* = 5.4 Hz, 3H), 2.67 – 2.59 (m, 1H), 1.45 – 1.43 (s, 9H), 1.30 – 1.17 (m, 1H), 1.04 – 0.96 (m, 1H), 0.44 – 0.38 (td, *J* = 6.1, 4.2 Hz, 1H). ^{13}C NMR (75 MHz, $CDCl_3$) δ 157.50, 157.09, 79.59, 64.13, 28.70, 27.84, 27.53, 16.89, 11.16.

trans-**(2-Aminocyclopropyl)methyl dimethylcarbamate oxalate (***trans*-**4.13 oxalate).**

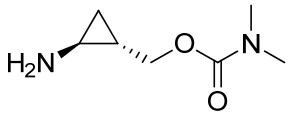

A solution of *trans*-**4.9** (688 mg, 2.68 mmol) in CH_2Cl_2 (10 mL) and TFA (10 mL) was stirred at room temperature for 30 min after which solvent was evaporated to afford the corresponding trifluoroacetic salt as a crude. ^{1}H NMR (300 MHz, D_2O) δ 3.85 – 3.78 (dd, *J*=12.2, 6.6 Hz, 1H), 3.69 – 3.62 (dd, *J*=12.2, 8.1 Hz, 1H), 2.66 – 2.65 (s, 6H), 2.48 – 2.41 (dt, *J* = 7.6, 3.6 Hz, 1H), 1.47 – 1.34 (dddd, *J* = 13.6, 9.8, 6.4, 3.2 Hz, 1H), 0.89 – 0.81 (ddd, *J* = 9.9, 6.9, 4.2 Hz, 1H), 0.76 – 0.69 (q, J=9.3 Hz, 1H). The reaction crude was dissolved in H_2O (20 mL) and basified with conc. NaOH. The free amine was extracted from the solution through continuous liquid-liquid extraction with CH_2Cl_2. The solvent was dried ($MgSO_4$) and evaporated to afford *trans*-**4.13** (326 mg, 77%) as a yellow oil. ^{1}H NMR (300 MHz, $CDCl_3$) δ 3.95 – 3.79 (qd, *J* = 11.5, 7.2 Hz, 2H), 2.91 – 2.89 (s, 6H), 2.71 – 2.68 (s, 2H), 2.34 – 2.29 (m, 1H), 1.27 – 1.12 (m, 1H), 0.71 – 0.62 (ddd, *J* = 9.2, 5.3, 4.0 Hz, 1H), 0.59 – 0.49 (dt, *J* = 7.1, 5.4 Hz, 1H). ^{13}C NMR (75 MHz, $CDCl_3$) δ 156.83, 67.75, 36.66, 36.19, 30.04, 20.58, 12.80. IR(cm^{-1}): 3393, 2941, 1698,1459, 1390, 1185. The oxalate salt was formed according to the general method and thus from *trans*-**4.13** (131 mg, 0.83 mmol), *trans*-**4.13 oxalate** (97 mg, 47%) was obtained as white crystals. Mp: 129.1-130.2^{o}C ^{1}H NMR (300 MHz, D_2O) δ 3.96 – 3.83 (dd, *J* = 11.6, 6.2 Hz, 1H), 3.83 – 3.69 (dd, *J* = 11.6, 7.4 Hz, 1H), 2.84 – 2.63 (s, 6H), 2.60 – 2.47 (dt, *J* = 7.4, 3.6 Hz, 1H), 1.56 – 1.41 (dtt, *J* = 13.8, 7.1, 3.6 Hz, 1H), 1.00 – 0.88 (ddd, *J* = 10.1, 6.8, 4.2 Hz, 1H),

0.88 – 0.75 (q, *J* = 7.0 Hz, 1H). HPLCMS (*m/z*) [MH^+] 159.32 (free base). Anal. ($C_7H_{14}N_2O_2 \cdot 1.25\ C_2H_2O_4$) C, H, N.

***trans*-(2-Aminocyclopropyl)methyl methylcarbamate oxalate (*trans*-4.14 oxalate).**

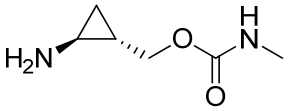

According to the preparation of *trans*-**4.13,** from *trans*-**4.10** (1.32 g, 5.4 mmol) *trans*-**4.14** (432 mg, 56%) was obtained as a colourless oil. ^{1}H NMR (300 MHz, $CDCl_3$) δ 4.72 – 4.56 (br s, 1H), 3.95 – 3.77 (m, 2H), 2.83 – 2.76 (d, *J* = 4.9 Hz, 3H), 2.32 – 2.25 (dt, *J* = 6.9, 3.4 Hz, 1H), 1.74 – 1.71 (s, 2H), 1.16 – 1.06 (m, 1H), 0.66 – 0.57 (ddd, *J* = 9.0, 5.1, 3.9 Hz, 1H), 0.54 – 0.46 (dt, *J* = 6.9, 5.3 Hz, 1H). ^{13}C NMR (75 MHz, $CDCl_3$) δ 157.83, 66.75, 29.05, 27.82, 19.95, 12.24. IR (cm^{-1}): 3350, 2956, 1693, 1536, 1265, 1139. The oxalate salt was formed according to the general method and thus from *trans*-**4.14** (180 mg, 1.25 mmol) *trans*-**4.14 oxalate** (175 mg, 57%) was obtained as white crystals. Mp: 115.8-116.5°C. ^{1}H NMR (300 MHz, D_2O) δ 3.91 – 3.82 (dd, *J* = 11.9, 6.6 Hz, 1H), 3.73 – 3.65 (dd, *J* = 11.9, 8.0 Hz, 1H), 2.54 – 2.45 (s, 3H; m 1H), 1.49 – 1.37 (m, 1H), 0.94 – 0.86 (ddd, *J* = 10.1, 6.9, 4.5 Hz, 1H), 0.81 – 0.73 (q, *J* = 7.1 Hz, 1H). HPLCMS (*m/z*) [MH^+] 145.29 (free base). Anal. ($C_6H_{12}N_2O_2 \cdot 1.3\ C_2H_2O_4$) C found 38.78, calcd 39.54; H found, 6.15 calcd 5.63; N found 11.71, calcd 10.72.

***cis*-(2-Aminocyclopropyl)methyl dimethylcarbamate oxalate (*cis*-4.15 oxalate).**

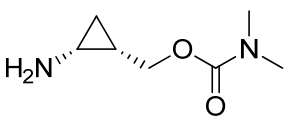

According to the preparation of *trans*-**4.13,** from *cis*-**4.11** (1.15 g, 4.5 mmol) *cis*-**4.15** (460 mg, 65%) was obtained as an orange oil. ^{1}H NMR (300 MHz, $CDCl_3$) δ 4.43 – 4.34 (dd, *J* = 11.4, 5.5 Hz, 1H), 4.16 – 4.05 (dd, *J* = 11.3, 9.2 Hz, 1H), 2.94

– 2.90 (s, 6H), 2.55 – 2.46 (td, *J* = 6.9, 4.1 Hz, 1H), 1.77 – 1.69 (s, 2H), 1.17 – 1.01 (ddd, 12.5, 6.3, 3.4 Hz, 1H), 0.82 – 0.71 (ddd, *J* = 9.1, 6.8, 5.2 Hz, 1H), 0.31 – 0.22 (dt, *J* = 5.7, 4.2 Hz, 1H). ^{13}C NMR (75 MHz, $CDCl_3$) δ 156.99, 64.82, 36.64, 36.24, 28.59, 17.31, 12.32. IR (cm^{-1}): 3378, 2937, 1686, 1408, 1187. The oxalate salt was formed according to the general method and thus from *cis*-**4.15** (138 mg, 0.87 mmol) *cis*-**4.15 oxalate** (88 mg, 40%) was obtained as white crystals. Mp: 117.2-118.5ºC. ^{1}H NMR (300 MHz, D_2O) δ 4.33 – 4.26 (dd, *J* = 12.5, 5.5 Hz, 1H), 3.85 – 3.74 (dd, *J* = 12.5, 9.9 Hz, 1H), 2.77 – 2.69 (d, *J* = 11.4 Hz, 8H), 2.66 – 2.56 (td, *J* = 7.3, 4.6 Hz, 1H), 1.47 – 1.31 (qd, *J* = 9.7, 4.2 Hz, 1H), 1.05 – 0.95 (dt, *J* = 10.7, 7.8 Hz, 1H), 0.67 – 0.58 (dt, *J* = 6.8, 4.6 Hz, 1H). HPLCMS (*m/z*) [MH^+] 159.20 (free base). Anal. ($C_7H_{14}N_2O_2 \cdot 1\ C_2H_2O_4$) N found 11.89, calcd 11.29.

cis-**(2-Aminocyclopropyl)methyl methylcarbamate (*cis*-4.16).**

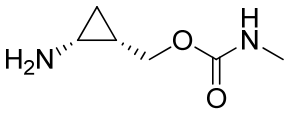

According to the preparation of *trans*-**4.13,** from *cis*-**4.12** (826 mg, 3.38 mmol) *cis*-**4.16** (340 mg, 70%) was obtained as a colourless oil. ^{1}H NMR (300 MHz, $CDCl_3$) δ 4.72 – 4.63 (br s, 1H), 4.43 – 4.35 (dd, *J* = 11.3, 5.5 Hz, 1H), 4.12 – 4.03 (dd, *J* = 11.3, 9.1 Hz, 1H), 2.81 – 2.78 (d, *J* = 4.9 Hz, 3H), 2.53 – 2.46 (td, *J* = 6.8, 4.1 Hz, 1H), 1.73 – 1.69 (s, 2H), 1.17 – 0.99 (m, 1H), 0.80 – 0.71 (ddd, *J* = 9.0, 6.8, 5.2 Hz, 1H), 0.28 – 0.21 (td, *J* = 5.6, 4.1 Hz, 1H). ^{13}C NMR (75 MHz, $CDCl_3$) δ 157.51, 64.42, 28.55, 27.85, 17.22, 12.25. IR (cm^{-1}): 3341, 2924, 1692, 1535, 1259, 1135. All the attempts to precipitate *cis*-**4.16 oxalate** according to the general method previously described were unsuccessful.

trans-**(2-(Dimethylamino)cyclopropyl)methyl dimethylcarbamate oxalate (*trans*-4.17 oxalate)).**

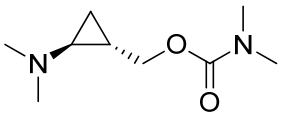

To a solution of *trans*-**4.13** (133 mg, 0.85 mmol) in H_2O (4 mL) AcCN (5 mL) formaldehyde 37% in H_2O (670 µL) $NaCNBH_3$ (165 mg, 2.66 mmol) was added. The pH was adjusted and maintained at 6 by addition of glacial AcOH and the mixture stirred at room temperature for 1 h. The reaction mixture was quenched with few drops of conc. HCl and washed with EtOAc (2 x 10 mL). The pH was then turned basic by addition of conc. NaOH and extracted with CH_2Cl_2 (4 x 10 mL). The organic layer was dried ($MgSO_4$) and solvent evaporated to afford *trans*-**4.17** (127 mg, 65%) as a colourless oil. ^{1}H NMR (300 MHz, $CDCl_3$) δ 4.13 – 4.05 (dd, *J* = 11.4, 6.1 Hz, 1H), 3.72 – 3.63 (dd, *J* = 11.4, 8.7 Hz, 1H), 2.94 – 2.91 (s, 6H), 2.36 – 2.33 (s, 6H), 1.60 – 1.54 (dt, *J* = 6.9, 3.5 Hz, 1H), 1.25 – 1.17 (ddd, *J* = 8.8, 5.9, 3.0 Hz, 1H), 0.78 – 0.70 (dt, *J* = 9.2, 4.5 Hz, 1H), 0.58 – 0.50 (dt, *J* = 6.8, 5.3 Hz, 1H). ^{13}C NMR (75 MHz, $CDCl_3$) δ 156.75, 67.76, 45.87, 45.15, 36.65, 36.13, 19.85, 12.21. IR (cm^{-1}): 3393, 2940, 1908, 1459, 1390, 1185. The oxalate salt was formed according to the general method and thus from *trans*-**4.17** (103 mg, 0.55 mmol) *trans*-**4.17 oxalate** (101 mg, 66%) was obtained as white crystals. Mp: 109.6 -110.5°C. ^{1}H NMR (300 MHz, D_2O) δ 4.07 – 3.99 (dd, *J* = 11.6, 5.8 Hz, 1H), 3.63 – 3.55 (dd, *J* = 11.6, 8.3 Hz, 1H), 2.81 – 2.79 (s, 6H), 2.76 – 2.70 (m, 6H; dd, *J* = 7.6, 3.5 Hz, 1H), 1.69 – 1.55 (ttd, *J* = 11.7, 6.2, 3.5 Hz, 1H), 1.14 – 1.06 (ddd, *J* = 10.5, 7.3, 4.3 Hz, 1H), 0.98 – 0.90 (dd, *J* = 7.3, 7.5 Hz, 1H). HPLCMS (*m/z*) [MH^+] 187.32 (free base). Anal. ($C_9H_{18}N_2O_2 \cdot 0.95\ C_2H_2O_4$) C, H, N.

trans-**(2-(Dimethylamino)cyclopropyl)methyl methylcarbamate oxalate ((±)-*trans*-4.18 oxalate).**

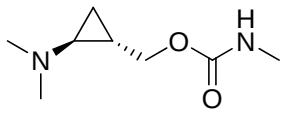

According to the preparation of *trans*-**4.17,** from *trans*-**4.14** (250 mg, 3.38 mmol) *trans*-**4.18** (284 mg, 95%) was obtained as a colourless oil. ^{1}H NMR (300 MHz, $CDCl_3$) δ 4.72 – 4.54 (br s, 1H), 4.03 – 3.91 (dd, *J* = 11.5, 6.6 Hz, 1H), 3.84 – 3.72 (dd, *J* = 11.3, 8.1 Hz, 1H), 2.84 – 2.76 (d, *J* = 4.9 Hz, 3H), 2.42 – 2.32 (s, 6H), 1.68 – 1.57 (dt, *J* = 6.7, 3.3 Hz, 1H), 1.32 – 1.16 (m, 1H), 0.83 – 0.74 (m, 1H), 0.60 – 0.50 (q, *J* = 5.7 Hz, 1H). ^{13}C NMR (75 MHz, $CDCl_3$) δ 156.84, 67.23, 45.88, 45.15, 27.86, 19.72, 12.01. IR (cm^{-1}): 3336, 2949, 1694, 1534, 1421, 1263, 1059. The oxalate salt was formed according to the general method and thus from *trans*-**4.18** (299 mg, 1.74 mmol) *trans*-**4.18 oxalate** (324 mg, 71%) was obtained as white crystals. Mp: 125.4-126.4°C. ^{1}H NMR (300 MHz, D_2O) δ 4.02 – 3.88 (dd, *J* = 11.7, 6.0 Hz, 1H), 3.63 – 3.55 (dd, *J* = 11.8, 8.1 Hz, 1H), 2.79 – 2.78 (s, 6H; m, 1H), 2.53 – 2.51 (s, 3H), 1.66 – 1.49 (m, 1H), 1.14 – 1.00 (m, 1H), 0.98 – 0.82 (m, 1H). HPLCMS (*m/z*) [MH^+] 173.29 (free base). Anal. ($C_8H_{16}N_2O_2 \cdot 1.1\ C_2H_2O_4$) C found 44.28, calcd 45.16; N found 11.13, calcd 10.33.

cis-**(2-(Dimethylamino)cyclopropyl)methyl dimethylcarbamate oxalate (*cis*-4.19 oxalate).**

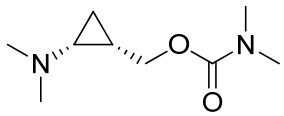

According to the preparation of *trans*-**4.17,** from *cis*-**4.15** (293 mg, 1.85 mmol) *cis*-**4.19** (325 mg, 94%) was obtained as a bright yellow oil. ^{1}H NMR (300 MHz, $CDCl_3$) δ 4.73 – 4.62 (s, 1H), 4.40 – 4.33 (dd, *J* = 11.2, 6.6 Hz, 1H), 4.11 – 3.94 (dd, *J* = 11.2, 8.8 Hz, 1H), 2.92 (s, 6H), 2.33 – 2.33 (s, 6H), 1.77 – 1.70 (td, *J* = 6.8, 4.4 Hz, 1H), 1.27 – 1.14 (tdd, *J* = 12.6, 7.5, 4.6 Hz, 1H), 0.78 – 0.68 (ddd, *J* = 9.0, 6.8, 5.2 Hz, 1H), 0.36 – 0.28 (dt, *J* = 5.7, 4.7 Hz, 1H). ^{13}C NMR (75 MHz, $CDCl_3$) δ 156.39, 65.20, 45.87, 44.90, 36.71, 36.31, 18.24, 10.26. IR (cm^{-1}): 3372, 2942,

1681, 1457, 1190, 1056. The oxalate salt was formed according to the general method and thus from *cis*-**4.19** (320 mg, 1.72 mmol) *cis*-**4.19 oxalate** (233 mg, 84%) was obtained as white crystals. Mp: 84.7-85.6. ^{1}H NMR (300 MHz, D_2O) δ 4.53 – 4.44 (dd, *J* = 12.6, 5.6 Hz, 1H), 3.74 – 3.65 (dd, *J* = 12.4, 10.6 Hz, 1H), 2.89 – 2.85 (s, 6H), 2.82 – 2.70 (m, 1H; m 6H), 1.66 – 1.52 (dtd, *J* = 13.2, 9.9, 6.9 Hz, 1H), 1.17 – 1.07 (qd, *J* = 7.5, 3.8 Hz, 1H), 0.77 – 0.69 (td, *J* = 7.1, 5.0 Hz, 1H). HPLCMS (*m/z*) [MH$^+$] 187.39 (free base). Anal. ($C_9H_{18}N_2O_2 \cdot 1.55\ C_2H_2O_4$) C found 42.46, calcd 44.61; N found 10.93 calcd 8.6.

cis-**(2-(Dimethylamino)cyclopropyl)methyl methylcarbamate oxalate (***cis*-**4.20 oxalate).**

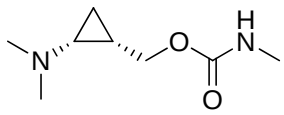

According to the preparation of *trans*-**4.17,** from *cis*-**4.15** (199 mg, 1.38 mmol) *cis*-**4.20** (211 mg, 90%) was obtained as a yellow oil. ^{1}H NMR (300 MHz, $CDCl_3$) δ 4.72 – 4.62 (s, 1H), 4.32 – 4.23 (dd, *J* = 11.0, 6.3 Hz, 1H), 4.13 – 4.06 (dd, *J* = 11.1, 8.3 Hz, 1H), 2.82 – 2.77 (d, *J* = 4.9 Hz, 3H), 2.30 – 2.28 (s, 6H), 1.74 – 1.65 (td, *J* = 6.8, 4.3 Hz, 1H), 1.21 – 1.09 (m, 1H), 0.77 – 0.65 (ddd, *J* = 8.9, 6.8, 5.1 Hz, 1H), 0.32 – 0.23 (dt, *J* = 6.0, 4.6 Hz, 1H). ^{13}C NMR (75 MHz, $CDCl_3$) δ 157.57, 64.86, 45.91, 44.71, 27.84, 18.14, 10.50. IR (cm^{-1}): 3339, 2945, 1694, 1534, 1459, 1260, 1139. The oxalate salt was formed according to the general method and thus from *cis*-**4.20** (210 mg, 1.28 mmol) *cis*-**4.20 oxalate** (187 mg, 56%) was obtained as white crystals. Mp: 103.5-104.8°C. ^{1}H NMR (300 MHz, D_2O) δ 4.53 – 4.45 (dd, *J* = 12.6, 5.4 Hz, 1H), 3.75 – 3.65 (dd, *J* = 12.5, 10.0 Hz, 1H), 2.90 – 2.83 (s, 6H; m, 1H), 2.55 – 2.50 (s, 3H), 1.63 – 1.48 (m, 1H), 1.16 – 1.06 (dt, *J* = 9.3, 7.3 Hz, 1H), 0.78 – 0.69 (td, *J* = 7.2, 4.9 Hz, 1H). HPLCMS (*m/z*) [MH$^+$] 173.17 (free base). Anal. ($C_8H_{16}N_2O_2 \cdot 1.15\ C_2H_2O_4$) C found 43.71, calcd 44.86; H found 6.72, calcd 6.69; N found 38.42, calcd 38.29.

3-(Dimethylamino)-*N,N*-dimethylpyrrolidine-1-carboxamide oxalate (**4.21**).

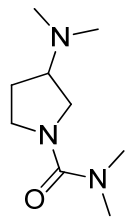

Following method A, from 3-(dimethylamino)pyrrolidine (89 mg, 0.78 mmol), the free base **4.21.** ^{1}H NMR (400 MHz, $CDCl_3$) δ 3.58 – 3.39 (m, 3H), 3.22 (dd, *J* = 10.0, 8.7 Hz, 1H), 2.82 (s, 6H), 2.63 (tt, *J* = 8.7, 6.3 Hz, 1H), 2.27 (s, 6H), 2.12 – 2.00 (m, 1H), 1.74 (dtd, *J* = 11.9, 10.3, 8.6 Hz, 1H). was obtained as an orange oil that was converted to the oxalate salt according to the general procedure to yield a white powder (153 mg, 55%, two steps). Mp: 113-116°C. ^{1}H NMR (400 MHz, D_2O) δ 3.93 (p, *J* = 7.5, 7.0 Hz, 1H), 3.83 (dd, *J* = 11.3, 7.2 Hz, 1H), 3.63 (dt, *J* = 10.6, 5.9 Hz, 2H), 3.59 – 3.48 (m, 1H), 2.97 (s, 3H), 2.96 (s, 3H), 2.89 (s, 6H), 2.52 – 2.40 (m, 1H), 2.15 (dq, *J* = 13.1, 8.4 Hz, 1H). ^{13}C NMR (101 MHz, D_2O) δ 165.62, 163.62, 64.62, 48.80, 46.62, 42.00, 41.54, 37.62, 26.94. HPLCMS (*m/z*) [MH^+] 186.2. Anal. ($C_9H_{19}N_3O \cdot 1.05\ C_2H_2O_4$) C, H, N.

3-(Dimethylamino)-*N*-ethylpyrrolidine-1-carboxamide (**4.22**).

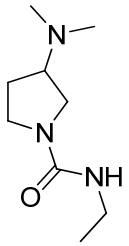

Following method B, from 3- (dimethylamino)pyrrolidine (89 mg, 0.78 mmol), and ethyl isocyanate (71 µL, 0.87 mmol), **4.22** precipitated as a white solid that was filtered off and washed with cold Et_2O (91 mg, 62%). Mp: 74-76°C. ^{1}H NMR (400 MHz, $CDCl_3$) δ 4.07 (dd, *J* = 11.0, 4.9 Hz, 1H), 3.56 (t, *J* = 9.0 Hz, 1H), 3.45 (td, *J* = 9.4, 1.7 Hz, 1H), 3.28 – 3.15 (m, 3H), 3.03 (t, *J* = 8.9 Hz, 1H), 2.63 (dtd, *J* = 10.0, 8.5, 6.8 Hz, 1H), 2.20 (s, 6H), 2.13 – 1.99 (m, 1H), 1.75 (dtd, *J* = 12.1, 10.2, 8.8 Hz, 1H), 1.07 (t, *J* = 7.2 Hz, 3H). ^{13}C NMR (101 MHz, $CDCl_3$) δ 156.83, 65.51, 50.09, 44.76, 44.42, 35.57, 30.55, 15.97. HPLCMS (*m/z*) [MH^+] 186.2. Anal. ($C_9H_{19}N_3O$) H calcd 10.34, found 9.52; N calcd 22.68, found 21.80.

3-(Dimethylamino)-*N*-methylpyrrolidine-1-carbothioamide (**4.23**).

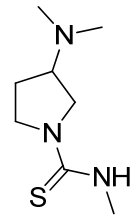

Following method B, from 3- (dimethylamino)pyrrolidine (89 mg, 0.78 mmol), and methyl isothiocyanate (63 mg, 0.87 mmol), **4.23** precipitated as a white solid that was filtered off and washed with cold Et_2O (recovered 11 mg, 7%.). Mp: 97-99°C. ^{1}H NMR (400 MHz, $CDCl_3$) δ 5.32 – 5.09 (m, 1H), 4.00 – 3.81 (m, 1H), 3.81 – 3.61 (m, 1H), 3.52 – 3.36 (m, 1H), 3.36 – 3.19 (m, 1H), 3.08 (d, *J* = 4.5 Hz, 3H), 2.73 (p, *J* = 7.6 Hz, 1H), 2.22 (s, 6H), 2.17 – 2.09 (m, 1H), 1.86 (q, *J* = 10.4 Hz, 1H). ^{13}C NMR (101 MHz, $CDCl_3$) δ 179.98, 65.20 53.63, 48.10, 44.07, 32.40, 30.21. HPLCMS (*m/z*) [MH^+] 188.1. Anal. ($C_8H_{17}N_3S$) C; H; N found 21.69, calcd 22.43; S found 15.55 calcd 17.12.

3-(Dimethylamino)-*N*-ethylpyrrolidine-1-carbothioamide oxalate (**4.24**).

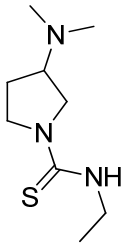

Following method B, from 3-(dimethylamino)pyrrolidine (89 mg, 0.78 mmol), and ethyl isothiocyanate (77 µL, 0.89 mmol), the free base **4.24**. ^{1}H NMR (400 MHz, $CDCl_3$) δ 5.05 (s, 1H), 4.00 – 3.66 (m, 2H), 3.61 (qd, *J* = 7.2, 5.2 Hz, 2H), 3.33 – 3.20 (m, 1H), 2.71 (dt, *J* = 15.7, 7.2 Hz, 1H), 2.22 (s, 6H), 2.12 (dt, *J* = 11.7, 5.8 Hz, 2H), 1.83 (p, *J* = 10.3 Hz, 1H), 1.17 (t, *J* = 7.2 Hz, 3H) was obtained as a yellowish oil that was converted to the oxalate salt according to the general procedure to yield a white powder (184 mg, 63%, two steps). Mp: 175-177°C. ^{1}H NMR (400 MHz, D_2O) δ 4.18 (dd, *J* = 11.6, 7.4 Hz, 1H), 4.05 (p, *J* = 7.1 Hz, 1H), 3.96 – 3.76 (m, 2H), 3.62 – 3.53 (m, 3H), 2.97 (s, 6H), 2.61 (ddd, *J* = 19.1, 7.4, 4.4 Hz, 1H), 2.33 (dq, *J* = 16.6, 8.3 Hz, 1H), 1.18 (t, *J* = 7.2 Hz, 3H). ^{13}C NMR (101 MHz, D_2O) δ 176.21, 165.56, 63.91, 50.78, 46.87, 41.95, 41.27, 40.39, 26.66, 13.91. HPLCMS (*m/z*) [MH^+] 202.2 (free base). Anal. ($C_9H_{19}N_3S \cdot 1.05\ C_2H_2O_4$) C, H, N, S.

***N,N*,4-Trimethylpiperazine-1-carboxamide oxalate** (**4.25**)**.** The synthesis and characterization of compound **4.25** is described in Method A.

***N,N*,4-Trimethyl-1,4-diazepane-1-carboxamide oxalate** (**4.26**).

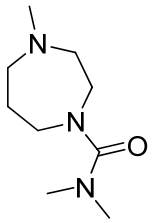

Following method A, starting from 1-methylhomopiperazine (180 mg, 1.6 mmol), the free base **4.26** (200 mg, 67%) was obtained as a yellowish oil. ^{1}H NMR (400 MHz, $CDCl_3$) δ 3.42 (t, *J* = 4.8 Hz, 1H), 3.37 (t, *J* = 6.1 Hz, 1H), 2.71 (s, 6H), 2.67 (t, *J* = 4.8 Hz, 1H), 2.57 (t, *J* = 5.2 Hz, 1H), 2.33 (s, 1H), 1.90 (q, *J* = 6.0 Hz, 1H). The free base was converted to the oxalate salt according to the general procedure to obtain white crystals. Mp: 84-87°C. ^{1}H NMR (400 MHz, D_2O) δ 3.65 (dd, *J* = 15.9, 4.7 Hz, 1H), 3.57 – 3.24 (m, 8H), 3.16 (t, *J* = 11.8 Hz, 1H), 2.86 (s, 3H), 2.75 (s, 6H), 2.21 – 1.99 (m, 2H). ^{13}C NMR (101 MHz, D_2O) δ 164.29, 56.82, 55.82, 47.51, 43.96, 42.85, 38.10, 24.39. HPLCMS (*m/z*) [MH^+] 186.2 (free base). Anal. ($C_9H_{19}N_3O \cdot 1.6\ C_2H_2O_4$) C, H, N.

***tert*-Butyl 4-(dimethylcarbamoyl)-1,4-diazepane-1-carboxylate** (**4.27**).

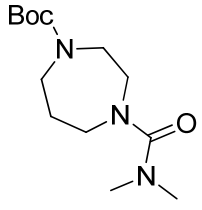

Following method A, starting from 1-*tert*-butoxycarbonyl-homopiperazine (200 mg, 1 mmol), **4.27** (206 mg, 100%) was obtained as a colourless oil. ^{1}H NMR (400 MHz, $CDCl_3$) δ 3.55 – 3.39 (m, 6H), 3.34 (t, *J* = 5.8 Hz, 2H), 2.81 (s, 6H), 1.90 (m, 2H), 1.46 (s, 9H).

***N*-Ethyl-4-methylpiperazine-1-carboxamide oxalate** (**4.28**). The synthesis and characterization of compound **4.28** is described in Method C.

***N*-Ethyl-4-methyl-1,4-diazepane-1-carboxamide** (**4.29**).

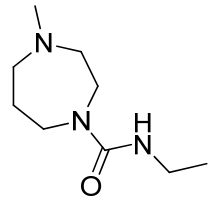

Following method C, starting from 1-methyl-homopiperazine (100 μL, 0.80 mmol) and ethyl isocyanate (68 μL, 0.86 mmol), **4.29** (146 mg, 98%) as a white powder. Mp: 69-70°C. ^{1}H NMR (400 MHz, $CDCl_3$) δ 4.29 (s, 1H), 3.59 (t, *J* = 4.7 Hz, 2H), 3.43 (t, *J* = 6.2 Hz, 2H), 3.26 (qd, *J* = 7.2, 5.4 Hz, 2H), 2.67 – 2.57 (m, 4H), 2.38 (s, 3H), 1.95 (dt, *J* = 11.4, 6.1 Hz, 2H), 1.13 (t, *J* = 7.2 Hz, 3H). ^{13}C NMR (101 MHz, $CDCl_3$) δ 157.95, 59.10, 57.80, 46.71, 45.47, 44.94, 35.85, 27.88, 15.80. HPLCMS (*m/z*) [MH^+] 186.2 (free base). Anal. ($C_9H_{19}N_3O$) C calcd 58.35, found 59.85; H calcd 10.34, found 9.41; N.

***N*,4-Dimethylpiperazine-1-carbothioamide oxalate** (**4.30**).

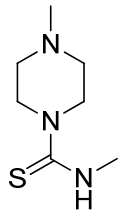

Following method C, from 1-methyl piperazine (97 μL, 0.87 mmol), and methyl isothiocyanate (70 mg, 0.96 mmol) the free base **4.30** (140 mg, 100%) was obtained as a yellow oil. ^{1}H NMR (400 MHz, $CDCl_3$) δ 5.52 (s, 1H), 3.76 (t, *J* = 5.3 Hz, 4H), 3.10 (d, *J* = 4.5 Hz, 3H), 2.38 (t, *J* = 4.8 Hz, 4H), 2.25 (s, 3H). The free base was converted to the oxalate salt according to the general procedure to obtain the oxalate salt as a white solid. Mp: 157-158°C. ^{1}H NMR (400 MHz, D_2O) δ 4.70 – 4.59 (m, 2H), 3.53 (d, *J* = 12.5 Hz, 2H), 3.38 (t, *J* = 13.5 Hz, 2H), 3.08 (t, *J* = 12.4 Hz, 2H), 2.99 (s, 3H), 2.88 (s, 3H). ^{13}C NMR (101 MHz, D_2O) δ 181.19, 165.54, 52.58, 44.40, 42.76, 32.59. HPLCMS (*m/z*) [MH^+] 174.1 (free base). Anal. ($C_7H_{15}N_3S \cdot C_2H_2O_4 \cdot 0.1H_2O$) C, H, N, S.

***N*,4-Dimethyl-1,4-diazepane-1-carbothioamide fumarate** (**4.31**).

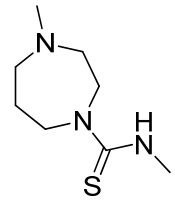

Following method C, from 1-methyl-homopiperazine (100 µL, 0.80 mmol), and methyl isothiocyanate (64 mg, 0.88 mmol), the free base **4.31** (158 mg, 100%) was obtained as a yellow oil. ^{1}H NMR (400 MHz, $CDCl_3$) δ 5.48 (s, 1H), 4.16 – 4.08 (m, 2H), 3.74 (t, *J* = 5.9 Hz, 2H), 3.17 (d, *J* = 4.4 Hz, 3H), 2.76 (t, *J* = 4.6 Hz, 2H), 2.62 (t, *J* = 5.6 Hz, 2H), 2.40 (s, 3H), 2.04 (q, *J* = 6.1, 5.7 Hz, 2H). Attempts to convert the free base **4.31** (110 mg, 0.58 mmol) to its oxalate salt failed and the fumarate was formed instead by the same procedure (122 mg, 62%, white solid). Mp: 148-150°C. ^{1}H NMR (400 MHz, D_2O) δ 6.67 (s, 2H), 4.68 – 4.58 (m, 1H), 3.86 – 3.71 (m, 1H), 3.71 – 3.45 (m, 4H), 3.32 – 3.13 (m, 2H), 2.98 (s, 3H), 2.88 (s, 3H), 2.31 – 2.14 (m, 2H). ^{13}C NMR (101 MHz, D_2O) δ 180.74, 170.79, 134.52, 56.89, 55.86, 47.50, 45.20, 43.91, 32.57, 23.74. HPLCMS (*m/z*) [MH^+] 168.2 (free base). Anal. ($C_8H_{17}N_3S \cdot 1.55\ C_4H_4O_4$) C; H; N calcd 11.44, found 11.94; S calcd 8.73, found 9.25.

***N*-Ethyl-4-methylpiperazine-1-carbothioamide oxalate** (**4.32**).

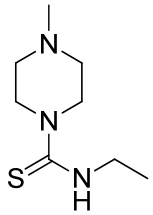

Following method C, from 1-methyl-piperazine (100 µL, 0.90 mmol), and ethyl isothiocyanate (87 µL, 1 mmol), the free base **4.32** (165 mg, 98%) was obtained as a yellowish oil. ^{1}H NMR (400 MHz, $CDCl_3$) δ 5.55 (s, 1H), 3.88 (t, *J* = 4.9 Hz, 4H), 3.70 (qd, *J* = 7.2, 4.9 Hz, 2H), 2.53 (t, *J* = 5.3 Hz, 4H), 2.37 (s, 3H), 1.24 (t, *J* = 7.3 Hz, 3H). The free base was converted to the oxalate salt according to the general procedure to obtain a white solid. Mp: 166-167°C. ^{1}H NMR (400 MHz, D_2O) δ 4.90 – 4.82 (m, 2H), 3.71 – 3.55 (m, 4H), 3.46 (t, *J* = 13.6 Hz, 2H), 3.17 (dd, *J* = 17.5, 7.4 Hz, 2H), 2.97 (s, 3H), 1.20 (t, *J* = 7.2 Hz, 3H). ^{13}C NMR (101 MHz, D_2O) δ 180.10, 165.55, 52.61, 44.42, 42.75, 41.20, 13.46. HPLCMS (*m/z*) [MH^+] 188.1 (free base). Anal. ($C_8H_{17}N_3S \cdot 1.05\ C_2H_2O_4$) C, H, N, S.

***N*-Ethyl-4-methyl-1,4-diazepane-1-carbothioamide oxalate** (**4.33**).

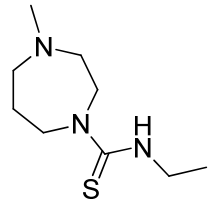

Following method C, from 1-methyl-homopiperazine (100 µL, 0.80 mmol), and ethyl isothiocyanate (77 µL, 0.88 mmol), the free base **4.33** (159 mg, 98%) was obtained as a yellow oil. ^{1}H NMR (400 MHz, $CDCl_3$) δ 5.34 (s, 1H), 4.18 – 4.05 (m, 2H), 3.78 – 3.60 (m, 4H), 2.78 (t, *J* = 4.7 Hz, 2H), 2.65 (t, *J* = 5.3 Hz, 2H), 2.41 (s, 3H), 2.07 (dt, *J* = 11.2, 6.0 Hz, 2H), 1.24 (t, *J* = 7.3 Hz, 3H). The free base was converted to the oxalate salt according to the general procedure to obtain a white solid. Mp: 131-133ºC. ^{1}H NMR (400 MHz, D_2O) δ 4.69 – 4.61 (m, 1H), 3.77 (dd, *J* = 16.9, 9.4 Hz, 1H), 3.72 – 3.47 (m, 6H), 3.32 – 3.13 (m, 2H), 2.88 (s, 3H), 2.34 – 2.11 (m, 2H), 1.11 (t, *J* = 7.3 Hz, 3H). ^{13}C NMR (101 MHz, D_2O) δ 179.63, 165.69, 56.95, 55.85, 47.50, 45.15, 43.91, 41.05, 23.73, 13.77. HPLCMS (*m/z*) [MH^+] 202.1 (free base). Anal. ($C_9H_{19}N_3S \cdot 1.05\ C_2H_2O_4$) C, H, N, S.

***tert*-Butyl 4-(methylcarbamothioyl)-1,4-diazepane-1-carboxylate** (**4.34**).

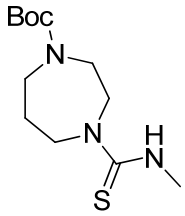

Following method C, from 1-*tert*-butoxycarbonyl-homopiperazine (200 mg, 1 mmol) and methyl isothiocyanate (74 mg, 1 mmol), **4.34** (268 mg, 98%) was obtained as a yellowish oil. ^{1}H NMR (400 MHz, $CDCl_3$) δ 5.48 (s, 1H), 4.03 – 3.94 (m, 1H), 3.90 – 3.74 (m, 2H), 3.60 (t, *J* = 6.1 Hz, 1H), 3.57 – 3.47 (m, 2H), 3.37 – 3.23 (m, 2H), 3.08 (s, 3H), 1.88 (dt, *J* = 13.8, 6.4 Hz, 2H), 1.39 (s, 9H).

***tert*-Butyl 4-(ethylcarbamothioyl)-1,4-diazepane-1-carboxylate** (**4.35**).

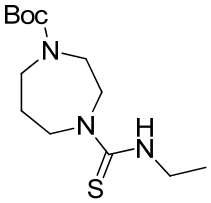

Following method C, from 1-*tert*-butoxycarbonyl-homopiperazine (200 mg, 1 mmol) and ethyl isothiocyanate (87 µL, 1 mmol), **4.35** (281 mg, 99%) was obtained as a yellowish oil. ^{1}H NMR (400 MHz, $CDCl_3$) δ 5.30 (s, 1H), 4.02 – 3.94 (m, 1H), 3.88 – 3.74 (m, 2H), 3.69 – 3.56 (m, 3H), 3.56 – 3.48 (m, 2H), 3.37 – 3.22 (m, 2H), 1.88 (p, *J* = 6.3, 5.8 Hz, 2H), 1.39 (s, 9H), 1.17 (t, *J* = 7.2 Hz, 3H).

***tert*-Butyl 4-(dimethylcarbamoyl)piperidine-1-carboxylate** (**4.36**).

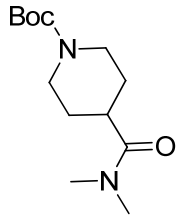

1-(*tert*-butoxycarbonyl) piperidine-4-carboxylic acid (**4.27**) (229 mg, 1 mmol) was dissolved in anhydrous THF (4 mL), 1,1'-carbonyldiimidazole (190 mg, 1.10 mmol) and triethylamine (154 µL, 1.10 mmol) were added to the solution. After 0.5 h at 50°C a solution of dimethylamine 2M in THF (802 µL) were added. The reaction was kept at room temperature overnight. In order to remove the imidazole NaOH 2M was added to the mixture and then extracted with EtOAc , the organic extracts were pooled together, dried over $MgSO_4$, and evaporated to give **4.36** (128 mg, 77%) as a clear oil. ^{1}H NMR (400 MHz, $CDCl_3$) δ 4.08 (dt, *J* = 14.3, 3.6 Hz, 2H), 2.97 (s, 3H), 2.90 (s, 3H), 2.69 (ddd, *J* = 13.3, 11.1, 4.0 Hz, 2H), 2.57 (td, *J* = 10.3, 4.8 Hz, 1H), 1.73 – 1.56 (m, 4H), 1.39 (s, 9H).

***N,N*-Dimethylpiperidine-4-carboxamide hydrobromide (4.37).**The synthesis and characterization of compound **4.37** is described in Method B.

***N*,*N*-Dimethyl-1,4-diazepane-1-carboxamide dihydrobromide** (**4.38**).

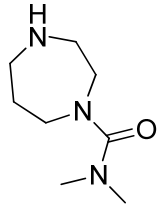

Following method B, starting from **4.26** (206 mg, 0.76 mmol), **4.38** (128 mg, 50%) was obtained as a white solid. Mp: 174-175°C. ^{1}H NMR (400 MHz, DMSO) δ 8.77 (s, 2H), 3.48 – 3.44 (m, 2H), 3.35 (t, *J* = 6.0 Hz, 2H), 3.21 (p, *J* = 4.9 Hz, 2H), 3.13 (dt, *J* = 8.9, 5.2 Hz, 2H), 2.70 (s, 3H), 1.99 (dt, *J* = 11.4, 6.0 Hz, 2H). ^{13}C NMR (101 MHz, DMSO) δ 163.96, 47.26, 45.79, 44.67, 43.87, 38.50, 25.19.HPLCMS (*m/z*) [MH^{+}] 172.2 (free base). Anal. ($C_8H_{17}N_3O \cdot 2HBr \cdot 0.5H_2O$) C, H, N.

***N*-Methyl-1,4-diazepane-1-carbothioamide hydrobromide** (**4.39**).

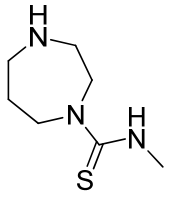

Following method B, from **4.34** (268 mg, 0.98 mmol), **4.39** (190 mg, 75%) was obtained as a white powder. Mp: 200-201°C. ^{1}H NMR (400 MHz, DMSO) δ 4.25 (t, *J* = 5.5 Hz, 2H), 3.80 (t, *J* = 6.2 Hz, 2H), 3.39 (t, *J* = 5.3 Hz, 2H), 3.29 (ddd, *J* = 5.9, 3.9, 2.2 Hz, 2H), 3.04 (s, 3H), 2.23 – 2.12 (m, 2H). ^{13}C NMR (101 MHz, DMSO) δ 181.35, 46.28, 45.15, 44.77, 43.97, 30.67, 23.43. HPLCMS (*m/z*) [MH^{+}] 174.24 (free base). Anal. ($C_7H_{15}N_3S \cdot 1.35\ HBr \cdot 0.25\ C_2H_7O$) C, H, N, S.

***N*-Ethyl-1,4-diazepane-1-carbothioamide hydrobromide** (**4.40**).

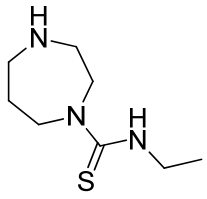

Following method B, from **4.35** (281 mg, 0.99 mmol), **4.40** (224 mg, 83%) was obtained as a white powder. Mp: 154-155°C. ^{1}H NMR (400 MHz, DMSO) δ 4.24 (t, *J* = 5.2 Hz, 2H), 3.80 (t, *J* = 6.2 Hz, 2H), 3.63 (q, *J* = 7.2 Hz, 2H), 3.39 (t, *J* = 5.2 Hz, 2H), 3.32 – 3.24 (m, 2H), 2.23 – 2.12 (m, 2H), 1.17 (t, *J* = 7.2 Hz, 3H). ^{13}C NMR (101 MHz, DMSO) δ 180.40, 46.20, 45.10, 44.87, 44.00, 39.23, 23.40,

12.14. HPLCMS (*m/z*) [MH^+] 188.33 (free base). Anal. ($C_8H_{17}N_3S \cdot 1.2\ HBr \cdot 0.2\ C_2H_7O$) C, H, N, S.

4-(3-Methyl-1,2,4-oxadiazol-5-yl)butan-2-one (**4.41**).

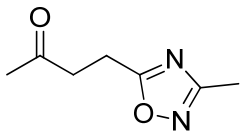

ethyl levulinate (494 µL, 4.0 mmol), acetamidoxime (354 mg, 4.8 mmol), K_2CO_3 (552 mg , 4.0 mmol) were suspended in 2 mL of MeCN, and the mixture was heated to 180ºC for 1h under microwave irradiation. The mixture was filtered through a short silica plug, washed with EtOAc and thus **4.41** (520 mg, 84%) was recovered as a brown oil.^{1}H NMR (300 MHz, $CDCl_3$) δ 3.16 – 3.08 (m, 2H), 3.07 – 2.98 (m, 2H), 2.37 (s, 3H), 2.25 (s, 3H). HPLCMS (m/z) [MH^+] 155.25.

***N,N*-Dimethyl-4-(3-methyl-1,2,4-oxadiazol-5-yl)butan-2-amine oxalate** (**4.42**).

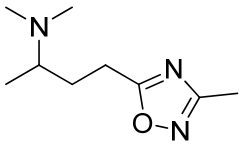

$Na(CN)BH_3$ (130 mg, 2.1 mmol) was added over a solution of **4.41** (107 mg, 0.69 mmol), an aq. solution of dimethylamine 33% (0.3 mL), dimethylamine hydrochloride (562 mg, 6.9 mmol) in MeOH (3 mL). The mixture is kept at rt. for 18 h, then solvent removed. The evaporated mass is resuspended in a sat. aq. K_2CO_3 solution and extracted with EtOAc (x2) and the free base **4.42** (61 mg, 48%) is obtained as a brownish oil, 1H NMR (400 MHz, CDCl3) δ 2.90 – 2.69 (m, 2H), 2.54 (dq, J = 13.0, 6.3 Hz, 1H), 2.42 (s, 3H), 2.15 (s, 6H), 1.92 – 1.80 (m, 1H), 1.76 – 1.63 (m, 1H), 0.91 (d, J = 6.5 Hz, 3H), HPLCMS (m/z) [MH^+] 184.33, that was converted to the oxalate salt according to the general procedure to give **4.42** (53 mg, 28% both steps) as a yellow powder.Mp: 124-125ºC. ^{1}H NMR (400 MHz, DMSO) δ 3.35 (dqd, J = 10.4, 6.6, 3.9 Hz, 1H), 3.08 – 2.90 (m, 2H), 2.66 (s, 6H), 2.31 (s, 3H), 2.20 (dddd, J = 13.6, 10.2, 6.6, 3.9 Hz, 1H), 1.88 (dtd, J = 13.3, 9.7, 5.8 Hz, 1H), 1.23 (d, J = 6.6

Hz, 3H). ^{13}C NMR (101 MHz, DMSO) δ 179.20, 167.42, 165.14, 165.13, 60.19, 27.40, 23.00, 13.26, 11.78. HPLCMS (m/z) [MH^+] 184.30 (free base. Anal. ($C_{11}H_{19}N_3O_5$) C, H, N.

Ethyl 4-(dimethylamino)pentanoate (**4.43**).

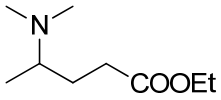

ethyl levulinate (1 mL, 9.87 mmol) is dissolved in EtOH (4 mL), glacial AcOH (1.2 mL) and hydrogenated (Pd/C, 10%, 300 mg) at 1 atm H_2 and rt. for 48h. Then Pd/C was filtered off, the solvent was evaporated and the residue resuspended in H_2O, acidified to pH 2 with HCl 2 M and the water phase was washed with DCM (x2). The aqueous solution was then basified to pH 10 with NaOH 2M and extracted with DCM (x3). The extracts were dried over $MgSO_4$, and solvent evaporated, to give **4.43** (857 mg, 50%) of a yellowish oil.^1H NMR (400 MHz, $CDCl_3$) δ 4.06 (q, J = 7.1 Hz, 2H), 2.52 (p, J = 6.8 Hz, 1H), 2.29 (t, J = 7.6 Hz, 2H), 2.19 (s, 6H), 1.78 (ddd, J = 14.3, 7.9, 6.6 Hz, 1H), 1.53 (dq, J = 13.8, 7.4 Hz, 1H), 1.19 (t, J = 7.1 Hz, 3H), 0.92 (d, J = 6.5 Hz, 3H).

4-(Dimethylamino)pentanehydrazide (**4.44**).

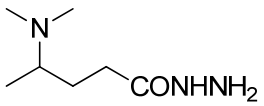

4.43 (121 mg, 0.7 mmol) was subjected to hydrazinolysis with microwave heating with hydrazine hydrate (0.52 mL, 10 mmol), and EtOH (1 mL) at 155ºC for 45 min. Then the solvent and hydrazine excess was evaporated to give **4.44** (95 mg, 85%) as a colourless oil, ^1H NMR (400 MHz, D_2O) δ 2.49 (dqd, *J* = 13.2, 6.6, 3.9 Hz, 1H), 2.27 – 2.07 (m, 9H), 1.80 (dddd, *J* = 13.4, 10.5, 7.0, 4.2 Hz, 2H), 1.51 (ddt, *J* = 13.2, 9.0, 4.6 Hz, 2H), 0.96 (d, *J* = 6.6 Hz, 3H).

***N,N*-Dimethyl-4-(5-methyl-1,3,4-oxadiazol-2-yl)butan-2-amine oxalate** (**4.45**).

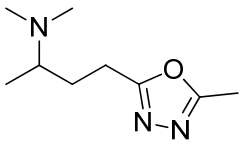

4.44 (95 mg, 0.60 mmol) were suspended in ethyl orthoacetate (1.5 mL) and the mixture heated to 125°C for 1h. The excess of ethyl orthoacetate was removed by evaporation and the residue suspended in H_2O, acidified to pH 2 with HCl 2 M and the water phase was washed with DCM (x2). The aqueous solution was then basified to pH 10 with NaOH 2M and extracted with EtOAc several times.The EtOAc extracts were dried over $MgSO_4$, and solvent evaporated to give the free base **4.45** (30 mg, 27%) as a yellow oil ^{1}H NMR (400 MHz, $CDCl_3$) δ 2.94 – 2.70 (m, 2H), 2.59 (dq, *J* = 13.0, 6.3 Hz, 1H), 2.46 (s, 3H), 2.19 (s, 6H), 1.96 – 1.84 (m, 1H), 1.82 – 1.66 (m, 1H), 0.95 (d, *J* = 6.5 Hz, 3H) that was then converted to the oxalate salt according to the general procedure to give **4.45** (31 mg, 11% both steps) as a white powder. Mp: 118-119°C. ^{1}H NMR (400 MHz, DMSO) δ 3.47 (dtt, J = 10.1, 6.4, 3.2 Hz, 1H), 3.04 – 2.84 (m, 2H), 2.79 (s, 6H), 2.46 (s, 3H), 2.31 – 2.20 (m, 1H), 2.04 – 1.90 (m, 1H), 1.33 (d, J = 6.7 Hz, 3H). ^{13}C NMR (101 MHz, DMSO) δ 164.78, 163.65, 163.51, 59.50, 36.97, 25.50, 19.86, 10.30, 7.85. HPLCMS (m/z) [MH^+] 184.30 (free base). Anal. ($C_{11}H_{19}N_3O_5 \cdot 0.25\ C_2H_2O_4$) C, H, N.

Radioligand binding assays.

The [^{3}H]epibatidine binding experiments using membranes from HEK293 cell lines stably expressing rat $\alpha_4\beta_2$, $\alpha_3\beta_4$, and $\alpha_4\beta_4$ nAChRs.

In the [^{3}H]epibatidine binding experiments, the stable HEK293 cell lines were harvested at 80–90% confluency and scraped into assay buffer [140 mM NaCl, 1.5 mM KCl, 2 mM $CaCl_2$, 1 mM Mg_2SO_4, 25 mM HEPES (pH 7.4)], homogenized using a Polytron for 10 s, and centrifuged for 20 min at 50000*g*. Cell pellets were resuspended in fresh assay buffer, homogenized, and

centrifuged at 50000*g* for another 20 min. Then the cell pellets were resuspended in the assay buffer, and the cell membranes were incubated with 25 pM [^{3}H]epibatidine in the presence of various concentrations of compounds in a total assay volume of 1500 µL. Nonspecific binding was determined in reactions with 5 mM (*S*)-nicotine. The mixtures were incubated for 4 h at room temperature while shaking.

FLIPR membrane potential (FMP) blue assay.

Selected compounds were characterized functionally at the $\alpha_4\beta_2$ and $\alpha_3\beta_4$-HEK293 cell lines in the FMP assay essentially as previously described[28,29]. In brief, cells were split into poly-D-lysine-coated 96-well black Opti-plates (BD Biosciences, Bedford, MA) in Dulbecco's modified Eagle medium supplemented with penicillin (100 U/mL), streptomycin (100 µg/mL), and 10% fetal calf serum, supplemented with 0.7 mg/mL G-418. At 16–24 h later the medium was aspirated, and the cells were washed with 100 µL of Krebs buffer [140 mM NaCl, 4.7 mM KCl, 2.5 mM $CaCl_2$, 1.2 mM $MgCl_2$, 11 mM HEPES, 10 mM D-glucose, pH 7.4]. Then 50 µL of Krebs buffer was added to the wells (in the antagonist experiments, various concentrations of the antagonist were dissolved in the buffer), and then an additional 50 µL of Krebs buffer supplemented with the FMP assay dye (1 mg/mL) was added to each well. Then the plate was incubated at 37 °C in a humidified 5% CO_2 incubator for 30 min and assayed in a NOVOstar plate reader (BMG Labtechnologies, Offenburg, Germany) measuring emission (in fluorescence units, FU) at 560 nm caused by excitation at 530 nm before and up to 1 min after addition of 33 µL of agonist solution. The experiments were performed in duplicate at least three times for each compound at the receptor.

Molecular modelling. Docking studies.

The Ls-AChBP structure co-crystalized with compound 4.1 was obtained from the PDB (3ZDG)[31]. The structure was imported into the Schrödinger Maestro Version 9.3.026 and processed with the Protein Preparation Wizard module. The tested ligands were processed with the program Epik prior to docking with Glide. Post-docking minimization was carried out and the most relevant contacts of the docked ligands measured and visually studied.

Bibliography

(1) Horiuchi, Y.; Kimura, R.; Kato, N.; Fujii, T.; Seki, M.; Endo, T.; Kato, T.; Kawashima, K. Evolutional Study on Acetylcholine Expression. *Life Sci.* **2003**, *72*, 1745–1756.

(2) Singer, S.; Rossi, S.; Verzosa, S.; Hashim, A.; Lonow, R.; Cooper, T.; Sershen, H.; Lajtha, A. Nicotine-Induced Changes in Neurotransmitter Levels in Brain Areas Associated with Cognitive Function. *Neurochem. Res.* **2004**, *29*, 1779–1792.

(3) Paterson, D.; Nordberg, A. Neuronal Nicotinic Receptors in the Human Brain. *Prog. Neurobiol.* **2000**, *61*, 75–111.

(4) Engelman, H. S.; MacDermott, A. B. Presynaptic Ionotropic Receptors and Control of Transmitter Release. *Nat. Rev. Neurosci.* **2004**, *5*, 135–145.

(5) Taly, A.; Corringer, P.-J.; Guedin, D.; Lestage, P.; Changeux, J.-P. Nicotinic Receptors: Allosteric Transitions and Therapeutic Targets in the Nervous System. *Nat. Rev. Drug Discov.* **2009**, *8*, 733–750.

(6) Jensen, A. A.; Frølund, B.; Liljefors, T.; Krogsgaard-Larsen, P. Neuronal Nicotinic Acetylcholine Receptors: Structural Revelations, Target Identifications, and Therapeutic Inspirations. *J. Med. Chem.* **2005**, *48*, 4705–4745.

(7) Romanelli, M. N.; Gratteri, P.; Guandalini, L.; Martini, E.; Bonaccini, C.; Gualtieri, F. Central Nicotinic Receptors: Structure, Function, Ligands, and Therapeutic Potential. *ChemMedChem* **2007**, *2*, 746–767.

(8) Kawamata, J.; Suzuki, S.; Shimohama, S. Enhancement of Nicotinic Receptors Alleviates Cytotoxicity in Neurological Disease Models. *Ther. Adv. Chronic Dis.* **2011**, *2*, 197–208.

(9) Oddo, S.; LaFerla, F. M. The Role of Nicotinic Acetylcholine Receptors in Alzheimer's Disease. *J. Physiol. Paris* **2006**, *99*, 172–179.

(10) Parri, H. R.; Hernandez, C. M.; Dineley, K. T. Research Update: Alpha7 Nicotinic Acetylcholine Receptor Mechanisms in Alzheimer's Disease. *Biochem. Pharmacol.* **2011**, *82*, 931–942.

(11) Mangialasche, F.; Solomon, A.; Winblad, B.; Mecocci, P.; Kivipelto, M. Alzheimer's Disease: Clinical Trials and Drug Development. *Lancet Neurol.* **2010**, *9*, 702–716.

(12) Jürgensen, S.; Ferreira, S. T. Nicotinic Receptors, Amyloid-Beta, and Synaptic Failure in Alzheimer's Disease. *J. Mol. Neurosci.* **2010**, *40*, 221–229.

(13) Quik, M.; Bordia, T.; Huang, L.; Perez, X. Targeting Nicotinic Receptors for Parkinson's Disease Therapy. *CNS Neurol. Disord. Drug Targets* **2011**, *10*, 651–658.

(14) Fujita, M.; Ichise, M.; Zoghbi, S. S.; Liow, J.-S.; Ghose, S.; Vines, D. C.; Sangare, J.; Lu, J.-Q.; Cropley, V. L.; Iida, H.; Kim, K. M.; Cohen, R. M.; Bara-Jimenez, W.; Ravina, B.; Innis, R. B. Widespread Decrease of Nicotinic Acetylcholine Receptors in Parkinson's Disease. *Ann. Neurol.* **2006**, *59*, 174–177.

(15) Kulak, J. M.; Fan, H.; Schneider, J. S. Beta2* and beta4* Nicotinic Acetylcholine Receptor Expression Changes with Progressive Parkinsonism in Non-Human Primates. *Neurobiol. Dis.* **2007**, *27*, 312–319.

(16) Marini, C.; Guerrini, R. The Role of the Nicotinic Acetylcholine Receptors in Sleep-Related Epilepsy. *Biochem. Pharmacol.* **2007**, *74*, 1308–1314.

(17) Hajós, M.; Rogers, B. N. Targeting alpha7 Nicotinic Acetylcholine Receptors in the Treatment of Schizophrenia. *Curr. Pharm. Des.* **2010**, *16*, 538–554.

(18) Gotti, C.; Riganti, L.; Vailati, S.; Clementi, F. Brain Neuronal Nicotinic Receptors as New Targets for Drug Discovery. *Curr. Pharm. Des.* **2006**, *12*, 407–428.

(19) Rollema, H.; Coe, J. W.; Chambers, L. K.; Hurst, R. S.; Stahl, S. M.; Williams, K. E. Rationale, Pharmacology and Clinical Efficacy of Partial Agonists of alpha4beta2 nACh Receptors for Smoking Cessation. *Trends Pharmacol. Sci.* **2007**, *28*, 316–325.

(20) Changeux, J.; Edelstein, S. J. Allosteric Mechanisms in Normal and Pathological Nicotinic Acetylcholine Receptors. *Curr. Opin. Neurobiol.* **2001**, *11*, 369–377.

(21) Bunnelle, W. H.; Dart, M. J.; Schrimpf, M. R. Design of Ligands for the Nicotinic Acetylcholine Receptors: The Quest for Selectivity. *Curr. Top. Med. Chem.* **2004**, *4*, 299–334.

(22) Karlin, A. Emerging Structure of the Nicotinic Acetylcholine Receptors. *Nat. Rev. Neurosci.* **2002**, *3*, 102–114.

(23) Dellisanti, C. D.; Yao, Y.; Stroud, J. C.; Wang, Z.-Z.; Chen, L. Crystal Structure of the Extracellular Domain of nAChR alpha1 Bound to Alpha-Bungarotoxin at 1.94 A Resolution. *Nat. Neurosci.* **2007**, *10*, 953–962.

(24) Li, S.-X.; Huang, S.; Bren, N.; Noridomi, K.; Dellisanti, C. D.; Sine, S. M.; Chen, L. Ligand-Binding Domain of an α7-Nicotinic Receptor Chimera and Its Complex with Agonist. *Nat. Neurosci.* **2011**, *14*, 1253–1259.

(25) Changeux, J.-P. Nicotine Addiction and Nicotinic Receptors: Lessons from Genetically Modified Mice. *Nat. Rev. Neurosci.* **2010**, *11*, 389–401.

(26) Arneric, S. P.; Holladay, M.; Williams, M. Neuronal Nicotinic Receptors: A Perspective on Two Decades of Drug Discovery Research. *Biochem. Pharmacol.* **2007**, *74*, 1092–1101.

(27) Brejc, K.; van Dijk, W. J.; Klaassen, R. V; Schuurmans, M.; van Der Oost, J.; Smit, A. B.; Sixma, T. K. Crystal Structure of an ACh-Binding Protein Reveals the Ligand-Binding Domain of Nicotinic Receptors. *Nature* **2001**, *411*, 269–276.

(28) Jensen, A. A.; Mikkelsen, I.; Frølund, B.; Bräuner-Osborne, H.; Falch, E.; Krogsgaard-Larsen, P. Carbamoylcholine Homologs: Novel and Potent Agonists at Neuronal Nicotinic Acetylcholine Receptors. *Mol. Pharmacol.* **2003**, *64*, 865–875.

(29) Jensen, A. A.; Mikkelsen, I.; Frølund, B.; Frydenvang, K.; Brehm, L.; Jaroszewski, J. W.; Bräuner-Osborne, H.; Falch, E.; Krogsgaard-Larsen, P. Carbamoylcholine Homologs: Synthesis and Pharmacology at Nicotinic Acetylcholine Receptors. *Eur. J. Pharmacol.* **2004**, *497*, 125–137.

(30) Hansen, C. P.; Jensen, A. A.; Christensen, J. K.; Balle, T.; Liljefors, T.; Frølund, B. Novel Acetylcholine and Carbamoylcholine Analogues: Development of a Functionally Selective alpha4beta2 Nicotinic Acetylcholine Receptor Agonist. *J. Med. Chem.* **2008**, *51*, 7380–7395.

(31) Ussing, C. A.; Hansen, C. P.; Petersen, J. G.; Jensen, A. A.; Rohde, L. A. H.; Ahring, P. K.; Nielsen, E. Ø.; Kastrup, J. S.; Gajhede, M.; Frølund, B.; Balle, T. Synthesis, Pharmacology, and Biostructural Characterization of Novel α4β2 Nicotinic Acetylcholine Receptor Agonists. *J. Med. Chem.* **2013**, *56*, 940–951.

(32) Celie, P. H. N.; van Rossum-Fikkert, S. E.; van Dijk, W. J.; Brejc, K.; Smit, A. B.; Sixma, T. K. Nicotine and Carbamylcholine Binding to Nicotinic Acetylcholine Receptors as Studied in AChBP Crystal Structures. *Neuron* **2004**, *41*, 907–914.

(33) Rohde, L. A. H.; Ahring, P. K.; Jensen, M. L.; Nielsen, E. Ø.; Peters, D.; Helgstrand, C.; Krintel, C.; Harpsøe, K.; Gajhede, M.; Kastrup, J. S.; Balle, T. Intersubunit Bridge Formation Governs Agonist Efficacy at Nicotinic Acetylcholine α4β2 Receptors: Unique Role of Halogen Bonding Revealed. *J. Biol. Chem.* **2012**, *287*, 4248–4259.

(34) Søkilde, B.; Mikkelsen, I.; Stensbøl, T. B.; Andersen, B.; Ebdrup, S.; Krogsgaard-Larsen, P.; Falch, E. Analogues of Carbacholine: Synthesis and Relationship between Structure and Affinity for Muscarinic and Nicotinic Acetylcholine Receptors. *Arch. Pharm. (Weinheim).* **1996**, *329*, 95–104.

(35) Nielsen, S. F.; Nielsen, E. O.; Olsen, G. M.; Liljefors, T.; Peters, D. Novel Potent Ligands for the Central Nicotinic Acetylcholine Receptor: Synthesis, Receptor Binding, and 3D-QSAR Analysis. *J. Med. Chem.* **2000**, *43*, 2217–2226.

(36) Sabbioni, G.; Jones, J. B. Enzymes in Organic Synthesis. 39. Preparations of Chiral Cyclic Acid-Esters and Bicyclic Lactones via Stereoselective Pig Liver Esterase Catalyzed Hydrolyses of Cyclic Meso Diesters. *J. Org. Chem.* **1987**, *52*, 4565–4570.

(37) Csuk, R.; von Scholz, Y.; Drone, A. A. Synthesis of Cyclopropyl Carbocyclic Nucleosides. *Tetrahedron* **1994**, *50*, 10431–10442.

(38) Ninomiya, K.; Shioiri, T.; Yamada, S. Phosphorus in Organic synthesis—VII. *Tetrahedron* **1974**, *30*, 2151–2157.

(39) Csuk, R.; Göthe, G. Synthesis of Cyclopropanoid 2-Epi-Muramyldipeptide Analogues as Potential Immunostimulants. *Tetrahedron* **2004**, *60*, 2191–2199.

(40) Csuk, R.; von Scholz, Y. Enantiomerically Pure Cyclopropanoid Nucleoside Analogues: Synthesis and Analysis. *Tetrahedron* **1996**, *52*, 6383–6396.

(41) Csuk, R.; von Scholz, Y. Synthesis of Racemic Carbocyclic Cyclopropanoid Nucleoside Analogues. *Tetrahedron* **1995**, *51*, 7193–7206.

(42) Shendage, D. M.; Fröhlich, R.; Haufe, G. Highly Efficient Stereoconservative Amidation and Deamidation of Alpha-Amino Acids. *Org. Lett.* **2004**, *6*, 3675–3678.

(43) Ang, S.-G.; Williamson, M. P.; Williams, D. H. Structure Elucidation of a Glycopeptide Antibiotic, OA-7653. *J. Chem. Soc. Perkin Trans. 1* **1988**, 1949–1956.

(44) Hibbs, R. E.; Sulzenbacher, G.; Shi, J.; Talley, T. T.; Conrod, S.; Kem, W. R.; Taylor, P.; Marchot, P.; Bourne, Y. Structural Determinants for Interaction of Partial Agonists with Acetylcholine Binding Protein and Neuronal α7 Nicotinic Acetylcholine Receptor. *EMBO J.* **2009**, *28*, 3040–3051.

(45) Brams, M.; Pandya, A.; Kuzmin, D.; Van Elk, R.; Krijnen, L.; Yakel, J. L.; Tsetlin, V.; Smit, A. B.; Ulens, C. A Structural and Mutagenic Blueprint for Molecular Recognition of Strychnine and D-Tubocurarine by Different Cys-Loop Receptors. *PLoS Biol.* **2011**, *9*, e1001034.

(46) Harpsøe, K.; Hald, H.; Timmermann, D. B.; Jensen, M. L.; Dyhring, T.; Nielsen, E. Ø.; Peters, D.; Balle, T.; Gajhede, M.; Kastrup, J. S.; Ahring, P. K. Molecular Determinants of Subtype-Selective Efficacies of Cytisine and the Novel Compound NS3861 at Heteromeric Nicotinic Acetylcholine Receptors. *J. Biol. Chem.* **2013**, *288*, 2559–2570.

Epilogue

Concluding remarks

In each chapter detailed discussions have been made and prospective analysis and specific conclusions have been drawn. Being interrelated in some aspects and divergent in others this epilogue may serve as the common juncture of the chapters contained in this thesis. The purpose of this epilogue is to offer a general overview on how this work was elaborated, why, what was learnt along the way, and thus, somehow, place this thesis work within the context of the current academic practice of medicinal chemistry, and prospectively, in drug discovery. In the previous pages it has been shown what the PhD candidate has done for medicinal chemistry. In this section, it will be presented how medicinal chemistry has been approached by the student, but more importantly, it will be outlined what such approach has taught to the trainee beyond the practice of the discipline. The ideas that appear in the forthcoming paragraphs might sound obvious to a senior investigator, but the learning and realization of most of them have been determining milestones in the course of this work.

Bibliographic review and synthetic ease have been the main driving forces in the design of target compounds. Extensive review of previous reports on the

development of synthetic analogues was the key tool that provided the starting point for the design of compounds. Bibliographic research was what shaped the project and provided the context: which were the main challenges and what gaps were missing in the field of study, what strategies and approaches were attempted before, continued or abandoned in order to fill in those gaps. It was during this process where the main structural clues are revealed: how a new molecular entity should look, "fit", and behave.

Both conformational restriction and bioisosteric replacement are old-school medicinal chemistry strategies within every beginner's reach. With the exception of the synthesis of DMABC restricted analogues in chapter four, no computional-aided design was initially made. Only traditional ligand-based approaches intervened in the design of target molecules for the melatoninergic system and the bioisosteres of DMABC (chapter 4, compound **4.1**).

With regard on the chemical approach, very few reactions were optimized and the obtaining of pure products in sufficient quantities was prioritized over the neatness of the reactions. More products than those described in this thesis were synthesised, some just as reactivity tests, some were just the result of a why-not? approach. Nevertheless, in order to keep this work consistent and systematic they were excluded in this report. As abovementioned, synthetic ease was a major wheel in the design. Being organic synthesis the source for novel molecular entities, in this thesis it was utilized in the most pragmatic way. In order to maximise the synthetic output in the minimum time, we prioritized the generation of as many analogues as a synthetic route could afford over the preparation of complex entities through long synthetic routes. Thus, the pharmacological feedback readily available from a good set of compounds provided a good starting point for rationalization and re-design. The application of chemistry to biological systems is where organic chemistry turns into medicinal chemistry, and therefore pharmacology was what has defined the course of the projects and subprojects included in this manuscript. All synthesised compounds were characterized in as many systems as they could be rationally addressed.

Those were the means employed that yielded the results described and discussed in the different chapters. Nevertheless, during the course of their application a lot of personal reflections and additional insights, not necessarily scientific, came along. It is likely that these revelations would not have been possible without an essential factor: the freedom I have enjoyed throughout the course of this thesis project, from the early design to the rationalization of the results. I am extremely grateful to my supervisor, María Isabel Rodríguez Franco, for letting me take over the whole project. Both for good and bad. Getting deeply involved provoked an exacerbated perception of both the small achievements and the slap-in-the-face results could get to be sometimes. Additionally, it greatly increased the feeling of empowerment and control over the project, what triggered the necessity of finding my very own solutions to the problems that appeared along the way, and turned out to be the most gratifying and fruitful experience of the whole work. It may serve as an example the evolution of this thesis project right from its beginning. In its genesis it was initially conceived for the development of novel positive allosteric modulators of the α7 nicotinic receptor, but the issues that appeared along the way, little by little, reshaped till it became what it is contained in these pages.

And with regard on the nicotinic receptor, it has been of major importance my time in Copenhagen under the supervision of Bente Frølund, both professionally and personally. Even if the synthesis has not been able to return super potent and selective ligands for the $\alpha_4\beta_2$-nicotinic receptor, the nearly-year I spent in the department of Drug Design and Pharmacology of Copenhagen University, offered me much more than a lab bench. Loads of ideas for new projects not directly related with cholinergic system and upgrades for the previous ones, emerged there. A side-project in the synthesis of fluorescent analogues of melatonin that is not contained in this work for intellectual property issues was born during that time. I also had the chance to share and witness how medicinal chemistry is envisioned from different perspectives, and somehow maturate what it is contained in these lines.

In my opinion a thesis in medicinal chemistry not only represents an attempt to apply the scientific method to broaden up knowledge in the field, but it also implies a responsibility. Acquisition of knowledge does not need a justification or revenue.

Knowledge is a goal by itself. And that shall be the main driving force in the design of an academic PhD project. Beyond epistemological considerations, pragmatism applies in medicinal chemistry as well. Independently of the approach employed or the stage of development, the ultimate goal of the whole process is to, at least try, to acquire new knowledge that could be useful from a preventive, therapeutic or diagnostic point of view.

There are different ways to envision the therapeutic potential from a PhD student. The naïve impression of a beginner fresh out of pre-grad school, as I was at the time this thesis period started, is somehow a pipeline that "just" needs to be fulfilled --knowledge is in the books, so putting the things in order and some labwork will do the rest--. The goals seem to be around the corner. But reality little by little slowly puts things in place, and unrest emerges together with the realization that the pipeline to reach the market is infinite. Beyond the everlasting chemical pursuit of the highest affinity/potency/selectivity and novelty there are a million issues i.e. solubility, ADME properties, cardiovascular effects, toxicity, expensive production, lack of venture capitalist… that can lead a hit to nowhere.

Another great feeling of despair comes from the let's-play-like-big-pharma-does pretention. This delusion of grandeur is rather common in academia but in my opinion, academia and industry use the same ball, but they play different games. The tiniest contact with the industry will let you guess how much of a nothing most academic research groups are compared to the gigantic proportions of the industry, in terms of amount of information and data management, efficiency and productivity. Someone that attempts to play the "big pharma" game on its own it is not a David seeking to defeat Goliath, it is a fool. The pharma giant is busy with its own stuff. The stuff that sounds relevant, ultimately, where the money is. But the giant is extremely annoyed, because despite its gigantic proportions is unable to find the panacea. Moreover, it is spending loads of money in the pursuit, and gets nothing back. Upon attendance to any mid-to-large sized medicinal chemistry congress, it is common to find within the programme a certain guy, or several, from a certain pharmaceutical company (which slogan repeats the word "innovation" as a mantra) giving a lecture on how a brand-new translational-multidisciplinary-high-throughput-integrated

approach, developed by them of course, is going to take drug discovery out of the draught. And we all hope they will. Because they are the people who have the money and the means to care about the enormous pipeline. That pipeline is not suitable for an academic PhD. In my opinion an academic PhD must forget about the pipeline, recall the pursuit of knowledge, and focus on all those fields the big pharma is not interested in. Not because they are not interesting, relevant or important, but hard to trade with. Briefly, more medicinal chemistry and less drug discovery, but of course, keeping them both present.

My PhD thesis is professionally the most thrilling project I ever embarked on. And as a project, I consider that it should be envisioned from a holistic point of view, always keeping in mind which are the sole points in you can actually intervene in. These might be seen as a limitation but those points are the actual mines where your gold, the knowledge, is. Bioisosterism and conformational restriction are very classical strategies within every medicinal chemist reach. What defines how conservative or ground-breaking the approach is depends on its application not in the strategy itself. Pharmacological assays are in most cases the scales that are going to weight the relevance of your outputs. And that is a big point, because novelty shall be sought at all possible levels. Biological systems are not just mysterious black boxes. Pharmacology works much differently than organic chemistry does, but there is a lot more than just nanomolar constants. An obsessive seeking of a certain selectivity or pharmacological profile will probably make you miss loads of interesting roads that might appear along the way. If your beloved target feels nausea of your compounds, that is a clear clue that something failed. And that of course should be the first issue to address in the following steps… But it might not be your compounds last word; there is nothing embarrassing in rationally seeking for a different target your failed compounds can fit in. That is what medicinal chemistry is about, not about telling if the chicken or the egg came first. The "medicinal chemist" that invented the superpowerful "utopiate"[1] *soma,* Aldoux Huxley, stated "we can only love what we know, and we can never know completely what we do not love"[2]. In the present case reconciling with pharmacology provided a higher feeling of control in the research, and aroused questions we felt eager to answer. Medicinal chemistry is nothing without chemistry and pharmacology. The cleft between both is perfectly exemplified

by the nature of the matter chemistry and pharmacology work with: inert matter and alive matter. That qualitative leap is what results fascinating in the practice of medicinal chemistry. The more one gets to know about either world, the more likely it will be to feel haunted by the intersection between them. And the broadening of that intersection will be the greatest achievement.

For an organic chemist an amide coupling is for "kids", but if it leads to the ligand you were looking for... who cares? There are loads of clichés that should be disregarded. Click chemistry is "cool", but is it really useful for your purposes or just a pointless way to move away the mainstream? There are plenty of questions that should be answered to decide whether "the trends" represent an added value in your project, or if they are just buzz-words. We went for two humble traditional approaches just because we considered them potentially useful. One should question everything. Science cannot be dogmatic. Most of the paradigms that were well established a decade ago in medicinal chemistry and drug discovery have been challenged; a lot of concepts have been proved wrong whereas others have evolved. Neat selectivity, potency and specificity have been long pursued as "guarantee" of efficacy and safety in the development of drug candidates. That pursuit has lost a great share of support if we take into account phenomena, like compensatory effects, that challenge the reductionism of focusing on a single node within the complexity of biological systems[3]. Phenomena that could also explain the high degree of attrition in clinical trials. Most of old and new marketed drugs interact with dozens of receptors, a fact has been commercially exploited for drug repurposing[4]. Even the very concept of target-based Drug Discovery has been questioned[5]. Old principles are renewed and complemented by emerging ones or by other concepts that regain relevance. The traditional pharmacological ligand-receptor-response paradigm is continuously being enriched with concepts like residence time[6], functional selectivity[7], receptor homo- and heterodimerization[8].

Medicinal chemistry is alive, it is continuously evolving, and the only way to keep track of its constant update is reading. In my opinion, it cannot be emphasised enough how important reading is. Not only to keep oneself updated but also to avoid dead-end alley hidden right behind a certain line. A clear example of this could be

found in this thesis. During the development of the pinoline-melatonin hybrids project, that intriguing and putatively endogenous neurochemical named pinoline evoked into me not only a scientific interest but some kind of fascination too. Especially as an endogenous neurochemical --melatonin's ignored little brother--. There were many hypothesis surrounding the role and relevance of this β-carboline: schizophrenia, the visual content of the dreams[9]… some of them bordering esotericism. This fascination lasted for quite a while, until the molecule revealed itself as nearly a myth according to the studies of Langer and Barbaccia in the 80s[10,11]. Perhaps not even the pineal-relating name of the molecule is justified. Those papers were found when the project was already ongoing, and the report had to be rewritten and the perspective totally redirected. Notwithstanding with that blow, further reading revealed that the agonistic properties of pinoline and its isomer **3.1** at the 5-HT_{2A} receptor could be of relevance, not as an endogenous chemical anymore, but in the pharmacology of harmala alkaloids. A topic, we are currently working on, as fascinating, or even more than pinoline was at the beginning. Reading is the only way a dead-end can turn into a new road stretching to the horizon. In the particular case of the synthetic melatonin analogue **1.21** there are good perspectives for this candidate for further development of its potential. Nevertheless, careful and well-founded observations during its development have arisen many intriguing questions on its mechanism of action, that could result even more intriguing than its development as a therapeutically tool for neurodegenerative diseases.

These are hard times for drug development in neurodegenerative diseases. Loads of clinical trials have been carried out, billions spent, and no candidates have become approved drugs for curing or disease-modifying treatments. There are several clinical trials ongoing in the field, but there is little support for optimism. Several pharmaceutical companies are giving up in such unfruitful field and closing up their Alzheimer disease (AD) drug discovery programmes, a company seeks benefit an perhaps, from an economical point of view, "it is just not worth it"[12]. Current treatments are merely palliative and only effective during early stages of clinically manifested AD. Disease-modifying treatments have been long sought, but none of the candidates have succeeded[13]. The underlying reasons that have led to such awful scenario are found in the very nature of the disease. When AD becomes clinically

manifested, its pathogenic mechanisms have been previously ongoing for a long time. The loss of neuronal tissue is enormous before the AD can be clinically diagnosed. Therefore potential effectiveness of a disease-modifying therapy is compromised by the great degree deterioration present in the patient brain when the treatment starts. Hope rests upon early detection of the disease[14]. Detection of AD on its earlier stages would permit a better comprehension of the declining process and therefore, would open up doors to intervention with conservative and restorative therapies at that pathophysiological level, like for instance, the ambitious neurogenesis potentiation approach. This approach not only attempts to stop the progression of the disease, but also to restore the cognitive functions. It is important to note that neurogenesis is not just restricted to the appearance of new neurons; its relevance relies in the ability of the new neurons to become integrated in the neural circuitry[15]. If we compare the neurogenesis rate of sharks and humans, settling in of new neurons in the most evolved brains of then the animal kingdom during adult stages appears to be manifestly unfavourable. Evolution is clearly discouraging at this point and the remaining neurogenesis in adults appears to be a just a vestigial process. The precise role of naturally occurring hippocampal neurogenesis in adult mammals is unclear, and the contribution of the natural-occurring process to cognitive performance in adults limited[15,16]. Neural renewal might sound as a conceptually science-fictional approach in drug discovery, and additionally, it deserves careful handling, since uncontrolled potentiation of the neural proliferation could easily lead to a neuroma, but it definitely needs to be given a chance. Moreover the characterization of the process should be compelling enough to justify the time and money spent. There are loads of questions surrounding the process in terms of relevance, function, contribution to the cognitive processes, and ultimately therapeutical potential, which deserve to be answered.

The future of neurodegenerative diseases is grim. AD prevalence grows to such extent that it is predicted to become epidemic in some years, but as abovementioned, the biggest issue is that we do not have effective weapons against it[17]. Is it a fair war we are in attempting to defeat it? The classical medical paradigm and the common perception establish that behind the pathology there must be an etiology. This may not be as simplistic in the case of many highly prevalent metabolic

and neurodegenerative diseases like AD. Numerous longitudinal studies have determined what risk and protective factors contribute to a greater or lesser incidence of AD[18]. Some genes have been identified as determinant in certain cases of familial AD but the greatest known risk for developing AD is age[19]. It sounds as strikingly obvious and despairing as saying that the main risk factor for dying is ageing. The older a population gets, the more likely it is to develop AD. We could fantasize with the idea of diminishing the deterioration associated to the process of ageing, but we cannot just simply fight against ageing. Therefore it would be a huge leap in medicine just to be able to slow down the progression of the disease but, as abovementioned, that recalls for early detection of the disease. Furthermore taking into account the characteristics of the disease one might wonder if the pursuit of a cure for AD is not just a chimera.

The nature of AD is revealing. Post-mortem histologic analysis of the patient brains shows that the main affected area by this dementia is the cortex, the structure responsible for superior cognitive functions[20]. If something characterizes the *Homo sapiens* is the ability to perform complex cognitive processes, and this ability is inherently related to the high degree of development achieved by its brain; the most evolved brain in the course of evolution. This machinery is enormously complex and precise; it has been adapted and optimized by evolution throughout hundreds of thousands of years. A robust and reliable machine set up to last, at least, as much as the individual would stay alive. That meant, on average, 31 years globally and less than 50 years in developed countries in the beginning of the 20th century[21]. But the 20th century did make a difference in the course of history. Last century witnessed the greatest technological and scientific progress made by humanity ever since the dawn of civilization. Progress that permeated throughout all levels, and that permitted during the turn of the millennium to witness the achievement of the highest degree of development humanity ever knew. As a result, many indicator boosted, among them, life expectancy[22]. And one might wonder how the organism can adapt itself to such sudden changes. Evolutionary changes occur in periods of hundreds of thousands of years and during a single century humanity has globally nearly doubled its life expectancy, surpassing the 80 years in many developed countries[23]. And such extension of the life expectancy cannot be explained without assuming that such

sudden changes have had an enormous impact in our physiology and pathophysiology. The causes of death and disease have greatly changed along the past century, and nowadays metabolic and neurodegenerative diseases are peaking at both.

And people die, and always will. It could be seen as death and disease always finding its way despite the great progresses made by humanity in hygiene, surgery, medicine… but it is precisely the other way around. Longer lifespan permits certain pathologies to become visible. Pathologies, like AD, that are rather common these days were rare in the old times, just because a 19th century average lifetime would not generally be enough for it to show up. Taking into account these type of dementia mostly appear in populations at stages of life in which their reproductive period is over, not even natural selection would make a strong effort in eradicating them[24]. The homeostatic-guarantee period of the soma has been extended, but it has an expiring date, and that expiring date in the case of the central nervous system, the most complex system in our physiology, is manifested as neurodegenerative diseases. When looked from that point of view, it results extremely pretentious, nearly foolish, to embark on the pursuit of a small molecule able to re-adapt a system that would need thousands of lifetimes to do so. But again, just finding out a way to slow down the progression of the disease would be a ground-breaking therapeutical revolution.

If ask whether I am confident that in the near future a treatment for AD will be discovered, I would say no, not at all. But I am looking forward to taking part in whatever comes next to defeat it.

Bibliography

(1) Portmanteau of utopia and opiate coined by Richard H. Blum of Stanford University in 1964.

(2) Huxley, A. *The Perennial Philosophy*; Chatto and Windus: London, 1946.

(3) Merino, A.; Bronowska, A. K.; Jackson, D. B.; Cahill, D. J. Drug Profiling: Knowing Where It Hits. *Drug Discov. Today* **2010**, *15*, 749–756.

(4) Medina-Franco, J. L.; Giulianotti, M. A.; Welmaker, G. S.; Houghten, R. A. Shifting from the Single to the Multitarget Paradigm in Drug Discovery. *Drug Discov. Today* **2013**, *18*, 495–501.

(5) Sams-Dodd, F. Target-Based Drug Discovery: Is Something Wrong? *Drug Discov. Today* **2005**, *10*, 139–147.

(6) Copeland, R. A.; Pompliano, D. L.; Meek, T. D. Drug–target Residence Time and Its Implications for Lead Optimization. *Nat. Rev. Drug Discov.* **2006**, *5*, 730–739.

(7) Urban, J. D.; Clarke, W. P.; von Zastrow, M.; Nichols, D. E.; Kobilka, B.; Weinstein, H.; Javitch, J. A.; Roth, B. L.; Christopoulos, A.; Sexton, P. M.; Miller, K. J.; Spedding, M.; Mailman, R. B. Functional Selectivity and Classical Concepts of Quantitative Pharmacology. *J. Pharmacol. Exp. Ther.* **2007**, *320*, 1–13.

(8) Milligan, G. G-Protein-Coupled Receptor Heterodimers: Pharmacology, Function and Relevance to Drug Discovery. *Drug Discov. Today* **2006**, *11*, 541–549.

(9) Callaway, J. C.; Hidalgo Olea, I. A Proposed Mechanism for the Visions of Dream Sleep. *Med. Hypotheses* **1988**, *26*, 119–124.

(10) Langer, S. Z.; Lee, C. R.; Schoemaker, H.; Segonzac, A.; Esnaud, H. 5-Methoxytryptoline and Close Analogs as Candidates for the Endogenous Ligand of the 3H-Imipramine Recognition Site. *Prog. Clin. Biol. Res.* **1985**, *192*, 441–455.

(11) Barbaccia, M. L.; Melloni, P.; Pozzi, O.; Costa, E. [3H]imipramine Displacement and 5HT Uptake Inhibition by Tryptoline Derivatives: In Rat Brain 5-Methoxytryptoline Is Not the Autacoid for [3H]imipramine Recognition Sites. *Eur. J. Pharmacol.* **1986**, *123*, 45–52.

(12) Bartfai, T.; Lees, G. V *The Future of Drug Discovery*; Elsevier, 2013; pp. 1–9.

(13) Chiang, K.; Koo, E. H. Emerging Therapeutics for Alzheimer's Disease. *Annu. Rev. Pharmacol. Toxicol.* **2014**, *54*, 381–405.

(14) Opar, A. Hope Builds for Earlier Detection of Alzheimer's Disease. *Nat. Rev. Drug Discov.* **2010**, *9*, 579–581.

(15) Kempermann, G.; Wiskott, L.; Gage, F. H. Functional Significance of Adult Neurogenesis. *Curr. Opin. Neurobiol.* **2004**, *14*, 186–191.

(16) Drapeau, E.; Mayo, W.; Aurousseau, C.; Le Moal, M.; Piazza, P.-V.; Abrous, D. N. Spatial Memory Performances of Aged Rats in the Water Maze Predict Levels of Hippocampal Neurogenesis. *Proc. Natl. Acad. Sci. U. S. A.* **2003**, *100*, 14385–1490.

(17) Mount, C.; Downton, C. Alzheimer Disease: Progress or Profit? *Nat. Med.* **2006**, *12*, 780–784.

(18) Lindsay, J. Risk Factors for Alzheimer's Disease: A Prospective Analysis from the Canadian Study of Health and Aging. *Am. J. Epidemiol.* **2002**, *156*, 445–453.

(19) Corder, E.; Saunders, A.; Strittmatter, W.; Schmechel, D.; Gaskell, P.; Small, G.; Roses, A.; Haines, J.; Pericak-Vance, M. Gene Dose of Apolipoprotein E Type 4 Allele and the Risk of Alzheimer's Disease in Late Onset Families. *Science (80-.).* **1993**, *261*, 921–923.

(20) Terry, R. D. Neuropathological Changes in Alzheimer Disease. *Prog. Brain Res.* **1994**, *101*, 383.

(21) Kannisto, V.; Lauritsen, J.; Thatcher, A. R.; Vaupel, J. W. Reductions in Mortality at Advanced Ages: Several Decades of Evidence from 27 Countries. *Popul. Dev. Rev.* **1994**, *20*, 793–810.

(22) Olshansky, S. J. Prospects for Human Longevity. *Science (80-.).* **2001**, *291*, 1491–1492.

(23) CIA. The World Factbook (accessed April 2014).

(24) Holliday, R. Aging Is No Longer an Unsolved Problem in Biology. *Ann. N. Y. Acad. Sci.* **2006**, *1067*, 1–9.

Abstract

Bioisosterism and conformational restriction: ligand-based design in the development of nicotinic ligands and melatonin analogues with neurogenic properties

Introduction

Neurodegenerative diseases lack determinant causes or specific conditions for their onset. Therefore, the most intuitive approach, the targeting of an etiological agent, is not suitable in their case. Another common characteristic of these widespread diseases is the complexity of their neuropathophysiology. From the very molecular basis of the disease to the cognitive abilities of the patient there are several pathognomonic abnormalities interrelated at all biological levels. In the case of Alzheimer's disease (AD), addressing such complex scenario led to a scientific consensus that required several hypothesis to cover all the characteristic signs of this neurodegenerative process. The most accepted

hypotheses in the case of AD are: the cholinergic deficit, the β-amiloid accumulation and the τ-protein hyperphosporilation. The cholinergic hypothesis, the oldest of the three, has as therapeutic potential merely palliative. Despite this limited potential it is the only therapeutic approach that has been able to provide effective drugs for the treatment of AD with the sole exception of the *N*-methyl-D-aspartate receptor inhibitor memantine. The pharmacodynamics of approved cholinergic based-treatments are essentially based on the inhibiton of the enzyme acetylcholinesterase. This inhibiton results in an indiscriminate net increase of the levels of acetycholine in the central nervous system. This increase compensates for the loss of cholinergic neurons resulting from the neurodegenerative process. During the last two decades, efforts were made in order to achieve a more precise and specific stimulation of the cholinergic system via direct stimulation of acetylcholine receptors, specially nicotinic receptors, by synthetic ligands. This unfinished work requires new pharmacological tools are needed both for a better understanding of the cholinergic system, and for exploiting its therapeutic potential.

Melatonin is a neurohormone secreted by the pineal gland in the absence of light whose main role in the body is the control of the circadian cycles. Recent studies ascribe many other physiological functions to this intriguing molecule. Melatonin modulates the immune system, protects mitochondria from oxidative damage, acts as a neuroprotective agent and interestingly participates in the development of nicotinic receptor. Experiments in mice revealed that chronic treatment with melatonin did not extend the lifespan of the individuals; however, the treated group enjoyed a much healthier aging that includes better performance at cognitive tests. Beyond melatonin neuroprotective properties, in the recent years, melatonin has also demonstrated its ability to stimulate neurogenesis in rodents. Taking into account the neural death that occurs in

neurodegenerative processes this ability could be of special interest in the field of regenerative medicine applied to these types of dementia.

Objectives

In this thesis work we aimed to develop new ligands for both the melatonergic and cholinergic system. For this purpose, we have systematically applied two traditional ligand-based design approaches, bioisosterism and conformational restriction. The compounds thus designed were synthesized and their structures and pharmacological profile characterized. Preliminar studies in biological assays in order to assess their potential as therapeutic tools were carried out for selected compounds.

Results

The *N*-acetyl group of melatonin was replaced for different azolic heterocycles and reversed amides following the principles of bioisosterism. We have set up an efficient synthetic method that permits the generation of a wide variety of azolic compounds that were unequivocally characterized. Those compounds that could exist in a tautomeric equilibrium were found to be present in a single tautomeric form in DMSO. The acidic nature of some of these azoles was confirmed indirectly in a solubility assay at different pH. The ability of the analogues to bioisosterically substitute for melatonin was measured in functional and radioligand displacement experiments in melatonergic receptors. The results obtained revealed that the retroamides and azoles utilized in this work can partially replace for the *N*-acetyl group of melatonin in terms of MT_1 and MT_2 receptor recognition. We have rationalized the results based on the ability of

active compounds to superimpose to the bioactive conformation of melatonin (chapter 1).

Selected melatonin analogues demonstrated their ability to promote the expression of neurogenic markers in neurospheres cultured from rat neural precursors. Their ability to cross the brain-blood barrier was determined *in vitro*. The *in vitro* neurogenic effect of the most potent compounds was effectively blocked by the melatonin antagonist luzindole, and in the case of compound **1.21** the neurogenic results were confirmed *in vivo* (chapter 2).

The putatively pineal β-carboline pinoline was chosen as the skeletal structure in the design of melatonin restricted analogues. A small series of tricyclic compounds with varying relative positions of their amines or amides and methoxy substituent was synthesized and their pharmacological profiles studied in several receptors. Additionally, a structure-antioxidant activity relationship study was carried out, and the neurogenic potential of selected compounds was studied *in vitro*. The fusion of the structures of pinoline and melatonin in the development of conformationally restrained analogues of melatonin was clearly detrimental in terms of melatonergic receptor recognition. Only one compound, **3.3**, retained significant activity at the melatoninergic receptors. With regard on the neurogenesis assay, both compound **3.3** and pinoline demonstrated their ability to stimulate neurogenesis *in vitro*. In the case of compound **3.3** its neurogenic effect was counteracted by luzindole. Pinoline proved to be rather potent at eliciting the expression of neurogenic markers even at nanomolar concentrations (chapter 3).

The structure of DMABC (3-dimethylaminobutyl dimethylcarbamate), an analogue of carbamylcholine with an interesting selectivity profile in nicotinic receptors was embedded in different cycles with varying degrees of

conformational restriction. Out of the four families of compounds prepared only *cis*-dimethylaminocyclopropyl and dimethylaminopyrrolidine series displayed significant affinity for the tested nicotinic receptors. The bioisosteric replacement of the carbamate of DMABC for oxadiazole retained some affinity for some nicotinic receptors, but resulted in antagonism (chapter 4).

Conclusions

We have systematically applied and re-validated two ligand-based drug design strategies in the genesis of novel melatonin and DMABC analogues. The molecular entities resulting from the application of both approaches have been pharmacologically characterized. Beyond their reported activity in the corresponding receptors, this work has also provided several structures suitable to be employed as pharmacological tools in the study of the mechanisms behind the melatoninergic-driven neurogenesis process.

Resumen

Bioisosterismo y restricción conformacional: diseño basado en el ligando aplicado al estudio de la selectividad en receptores nicotínicos y al desarrollo de análogos de melatonina con propiedades neurogénicas

Introducción

Las enfermedades neurodegenerativas carecen de causas o condiciones específicas que desencadenen la instauración de la patología. Por tanto, la estrategia terapéutica más intuitiva consistente en neutralizar los agentes etiológicos no es aplicable en su caso. Otra de las características comunes de estas enfermedades es la complejidad de su neurofisiopatología. Desde la base molecular de la enfermedad hasta el cuadro clínico cognitivo del paciente hay un buen número de signos patognomónicos interrelacionados a todos los niveles biológicos. En el caso de la enfermedad de Alzheimer (EA), entre otras,

enfrentarse a este escenario tan complejo requirió de un consenso científico que necesariamente incluía varias hipótesis para poder así cubrir todos los signos característicos de este proceso neurodegenerativo. Las hipótesis más aceptadas en el caso de la EA son: el déficit colinérgico, la acumulación del péptido β-amiloide y la hiperfosforilación de la proteína τ. La hipótesis colinérgica, la más antigua de las tres, tiene la limitación de que su potencial terapéutico es meramente paliativo. A pesar de ello, es la única aproximación terapéutica capaz de producir fármacos efectivos en el tratamiento de la EA con la única excepción de la memantina (inhibidor del receptor de *N*-metil-D-aspartato). La farmacodinamia de los tratamientos vigentes basados en el sistema colinérgico se basa esencialmente en la inhibición de la enzima acetilcolinesterasa. Dicha inhibición produce un aumento indiscriminado de los niveles de acetilcolina en el sistema nervioso central. Este incremento compensa la pérdida de neuronas colinérgicas que se produce como resultado del proceso neurodegenerativo. En las dos últimas décadas se han realizado grandes esfuerzos con el objetivo de alcanzar una estimulación más precisa y específica del sistema colinérgico mediante ligandos sintéticos, especialmente de los receptores nicotínicos. Este trabajo inacabado requiere de nuevas herramientas farmacológicas tanto para alcanzar un mayor conocimiento del sistema colinérgico, como para explorar su potencial terapéutico.

La melatonina es una neurohormona secretada por la glándula pineal en ausencia de luz cuyo rol principal en el organismo es el control de los ciclos circadianos. Estudios recientes atribuyen a esta fascinante molécula muchas otras funciones fisiológicas. La melatonina modula el sistema inmune, protege a la mitocondria frente al daño oxidativo, actúa como agente neuroprotector y curiosamente también contribuye al desarrollo de los receptores nicotínicos. Experimentos realizados con ratones tratados con melatonina de forma crónica

demostraron que, si bien no se consiguió aumentar la esperanza de vida de los individuos, los animales tratados disfrutaron de un proceso de envejecimiento en mejores condiciones de salud, incluyendo mejores resultados en pruebas cognitivas. Más allá de las propiedades neuroprotectoras de la melatonina, en los últimos años, la melatonina también ha demostrado su capacidad de estimular la neurogénesis en roedores. Teniendo en cuenta la muerte neuronal que se produce como consecuencia de los procesos neurodegenerativos, esta capacidad puede ser de especial interés en el campo de la medicina regenerativa aplicada a este tipo de demencias.

Objetivos

En esta tesis se ha propuesto el desarrollo de nuevos ligandos para los sistemas melatonérgico y colinérgico. Para este propósito se han aplicado de forma sistemática dos aproximaciones tradicionales en el diseño basado en el ligando: bioisosterismo y restricción conformacional. Los compuestos así diseñados fueron sintetizados, y sus estructuras y farmacología caracterizadas. Algunos compuestos fueron seleccionados para el estudio en diferentes ensayos biológicos de su potencial como herramientas terapéuticas.

Resultados

El grupo *N*-acetilo de la melatonina fue reemplazado por diferentes heterociclos azólicos y retro-amidas siguiendo los principios del bioisosterismo. Se puso a punto un método sintético que permitió la generación de una gran variedad de análogos azólicos de forma eficiente. Compuestos que una vez sintetizados fueron caracterizados de forma inequívoca, especialmente en el caso de aquellos susceptibles de existir en un equilibrio tautomérico. Se determinó que

solo uno de los posibles tautómeros estaba presente en disolución en DMSO. La naturaleza acídica de algunos compuestos azólicos se confirmó de forma indirecta en un ensayo de solubilidad a diferentes pH. La capacidad de dichos análogos para sustituir como bioisósteros a la melatonina se evaluó en ensayos funcionales y de desplazamiento de radioligando en receptores melatonérgicos. Los resultados obtenidos revelan que las retroamidas y azoles preparados en este trabajo pueden ser parcialmente reconocidos por los receptores MT_1 y MT_2 de forma análoga al grupo *N*-acetilo de la melatonina. Dichos resultados se racionalizaron basándose en la capacidad de los compuestos activos para ser superpuestos sobre la conformación bioactiva de la melatonina (capítulo 1).

Algunos análogos de melatonina seleccionados demostraron su capacidad para promover la expresión de marcadores neurogénicos en neuroesferas cultivadas de precursores neurales de cerebro de rata. Se determinó su habilidad para permear a través de la barrera hematoencefálica por difusión pasiva *in vitro*. El antagonista de melatonina luzindol bloqueó de forma efectiva el efecto neurogénico de los compuestos más potentes *in vitro*; y en el caso del compuesto **1.21** los resultados de neurogénesis fueron confirmados *in vivo* (capítulo 2).

La pinolina, una β-carbolina supuestamente producida por la glándula pineal, se eligió como esqueleto estructural en el diseño de análogos rígidos de melatonina. Se sintetizó y estudió en diferentes receptores una serie de compuestos tricíclicos con diferentes posiciones relativas de sus grupos amida o amina y metoxilo. Además se llevó a cabo un análisis relacionando la estructura de los compuestos con su actividad antioxidante, y se estudió su potencial neurogénico *in vitro*. La fusión de las estructuras de pinolina y melatonina no resultó favorable para la interacción con los receptores de melatonina. Solo el compuesto **3.3** fue capaz de mantener una actividad significativa en los receptores

melatonérgicos. En el ensayo de neurogénesis, tanto la pinolina como el compuesto **3.3** demostraron su capacidad para promover la neurogénesis *in vitro*. En el caso del compuesto **3.3** su efecto neurogénico fue neutralizado en presencia de luzindol. La pinolina demostró ser capaz de promover la expresión de marcadores neurogénicos incluso a concentraciones en el rango nanomolar (capítulo 3).

La estructura de DMABC (3-dimetilaminobutil dimetilcarbamato), un agonista análogo de carbamilcolina con un interesante perfil de selectividad en receptores nicotínicos, fue integrada en diferentes ciclos con diversos grados de restricción conformacional. De las cuatro familias de compuestos que se prepararon, tan solo la series de *cis*-dimetilamnociclopropilo y dimetilaminopirrolidina mostraron una afinidad significativa por los receptores nicotínicos en los que fueron ensayados. El reemplazo del carbamato de DMABC por oxadiazol también mantuvo una cierta afinidad por los receptores nicotínicos, pero en este caso el compuesto resulto ser un antagonista.

Conclusiones

En este trabajo se han aplicado de forma sistemática, y revalidado, dos estrategias de diseño basado en el ligando para la génesis de nuevos análogos de melatonina y DMABC. Se han caracterizado las propiedades farmacológicas de las entidades moleculares resultantes de la aplicación de ambas aproximaciones. Y más allá de las actividades descritas en sus correspondientes receptores, este trabajo ha proporcionado diversas estructuras susceptibles de ser empleadas como herramientas farmacológicas en el estudio de los mecanismos subyacentes en la capacidad de promoción de la neurogénesis de la melatonina.